MIRNAS AND HORMONAL PATHWAYS REGULATING POSTEMBRYONIC DEVELOPMENT IN INSECTS

Marijke GIJBELS

Supervisor:
Prof. Dr. Jozef Vanden Broeck

Members of the Examination Committee:
Prof. Dr. Robby Stoks
Prof. Dr. Roger Huybrechts
Prof. Dr. Liesbet Temmerman
Dr. José Luis Maestro
Dr. Elisabeth Marchal
Dr. Heleen Verlinden
Dr. Pieter Van Wielendaele

Dissertation presented in partial fulfilment of the requirements for the degree of Doctor of Science (PhD): Biology

December 2020

© 2020 MARIJKE GIJBELS
Uitgegeven in eigen beheer, MARIJKE GIJBELS, 3930 Hamont-Achel, BELGIUM

Alle rechten voorbehouden. Niets uit deze uitgave mag worden vermenigvuldigd en/of openbaar gemaakt worden door middel van druk, fotokopie, microfilm, elektronisch of op welke andere wijze ook zonder voorafgaandelijke schriftelijke toestemming van de uitgever en haar promotor.

All rights reserved. No part of the publication may be reproduced in any form by print, photoprint, microfilm, electronic or any other means without written permission from the publisher and her supervisor.

Acknowledgements – Dankwoord

Eindelijk, na een lange strijd (dat mogen we wel zeggen) presenteer ik jullie (met toch wel enige trots) mijn doctoraat! Bijna vijf jaar heeft het gekost! Al leek er meermaals geen einde aan te komen, door de hulp van bepaalde personen is het toch gelukt. Ik mag me dan ook gelukkig prijzen dat ik jullie in mijn leven heb. Nu is het dan ook even tijd om de rollen eens om te draaien en jullie in de bloemetjes te zetten!

Als eerste moet ik toch de man bedanken die de start van dit alles mogelijk gemaakt heeft. **Jef**, bedankt om me op te nemen in jouw onderzoeksgroep. Startend als een masterstudent had je (blijkbaar genoeg) vertrouwen in mij om mij ook de kans te geven een doctoraat te starten en vervolgens af te ronden. Ook bedankt voor de tijd die je steeds nam om mijn teksten na te lezen. Uit de bijhorende correcties/opmerkingen heb ik enorm veel geleerd en ik denk dat ik dan ook wel mag zeggen dat mede dankzij jou dit boekje tot een goed einde is gekomen! Secondly, I would like to thank all the other members of my Examination Committee for all the effort and time they put into reading my manuscript and for giving their constructive advice. Your insights have elevated this work to a more comprehensive manuscript. I cannot thank you enough: **Prof. Dr. Robby Stoks**, **Prof. Dr. Roger Huybrechts**, **Prof. Dr. Liesbet Temmerman**, **Dr. José Luis Maestro, Dr. Elisabeth Marchal**, **Dr. Heleen Verlinden** and **Dr. Pieter Van Wielendaele**. Furthermore, I also gratefully acknowledge the 'Fonds voor Wetenschappelijk Onderzoek- Vlaanderen' (FWO) and the Research Foundation of KU Leuven for their financial support. I am also grateful to **Prof. Jean-Paul Delbecque** for his kind gifts of antiserum and tracer. **Prof. Dr. Johan Billen** en **An Vandoren**, jullie hulp in verband met de histologische coupes waardeer ik enorm, waarvoor een dikke dankjewel!

Colleagues of the HSTV lab, a big thanks to you all! Not only for your help and advice in the lab, but also for the nice talks whenever I needed a break. I really enjoyed all the lunches in the parc, the lab weekends, the after-work activities, etc.! Thank you all. Een doctoraat tot een goed einde brengen gaat jammer genoeg niet vanzelf. **Elke**, jij hebt hierdoor vaak op een stressy bureau gezeten, maar weet dat we dat niet expres deden (of ik toch niet). Bedankt om me telkens weer te kalmeren door samen in het park te gaan eten, een ommetje te gaan wandelen of gewoon door me je posters/tekeningen te laten ophangen in het bureau (dat taakje zal ik nooit vergeten, I loved it!). Ook een grote dank u voor mijn andere bureaugenootjes; **Elisabeth**, **Heleen**, **Darron**, **Lina M**., **Lina V**., **Jan**, **Elise**, **Emilie, Nathan** en **Areta**. Jullie zorgden er telkens maar weer voor dat er iets lekkers te snoepen was en dat er pompoenen/bloemen/plantjes uitgedeeld werden. Hierdoor werden de (soms lange) dagen op het bureau des te aangenamer. **Lina M**., jou moet ik nog in het bijzonder bedanken. Wij zijn samen gestart in ons thesisjaar en al vrij snel ben je 'gepromoveerd' tot één van mijn beste vriendinnen! Bedankt om naar mijn vele zaag momentjes te luisteren en altijd voor mij klaar te staan. **Stijn**, jij bent een kerel van goud! Bedankt om me telkens weer te helpen! **Paulien** en **Elise**, de trip met jullie naar Argentinië zal ik nooit vergeten. De eerste keer op een vlieger en dan direct tegoei! Bedankt om me wat meer van de wereld te tonen. Jullie zijn echt geweldig! **Paulien**, jou wil ik toch ook nog even extra in de bloemetjes zetten! Jij bent een vrouw uit de duizenden. Niet alleen in het labo kon ik altijd op je hulp rekenen (en op de

vele babbel momentjes), maar ook daarbuiten. Bedankt voor altijd een luisterend oor te zijn en me te steunen op de momenten dat het minder ging.

Elisabeth, jou moet ik het meest van iedereen bedanken. Jij bent een schat van een mens en ik ben dan ook blij dat ik je heb mogen leren kennen, zowel op professioneel als op persoonlijk vlak. Jij hebt er onder andere voor gezorgd dat mijn passie voor insecten enorm gegroeid is en al zeker voor onze mooie sprinkhanen. Dat was jammer genoeg geen liefde op het eerste gezicht. Ik zal dan ook nooit mijn eerste keren in de sprinkhanenkweek vergeten, amai zeg! Verder ben ik je ook nog steeds dankbaar dat je me, met jouw enorme passie voor onderzoek, overtuigd hebt om in het labo te blijven. Bedankt dat je me steeds bent blijven motiveren en dat je keer op keer tijd vrijmaakte om me te helpen waar nodig (zelfs wanneer je niet meer bij ons werkte, waarvoor chapeau!). Ik heb tijdens deze reis niet alleen super veel bijgeleerd over het leven van sprinkhanen, maar ook vrienden voor het leven gemaakt! Bedankt voor alles!

Dulce and **Cynthia**, thank you for all your help and advice, for correcting my manuscripts and just for being there when I needed you girls. Verder zou ik ook graag **Evelien** willen bedanken voor alle hulp in de sprinkhanen kweek. Zonder uw hulp zouden de sprinkhaantjes lang niet zo gelukkig zijn, dat weet ik zeker! Ook aan **Johny**, **Els, Marion** en **Marleen**, een dikke merci voor alle administratieve ondersteuning. Jullie bijdrage mag zeker niet onderschat worden!

Verder zou ik nog graag mijn auto-genootjes: **Jolien**, **Jilly**, **Leen** en **An** bedanken voor de (oneindig) vele tripjes naar de training en terug. Twee jaar lang doctoreren combineren met handballen op een hoog niveau was een uitdaging, maar jullie zorgden er keer op keer weer voor dat die lange autoritten (naar het verre Limburg) een hele tikkel aangenamer werden waarvoor dank!

Mama en **papa**, jullie zijn (jazeker) de belangrijkste personen uit mijn leven. Bedankt om mij de kans te geven om verder te studeren. Deze keuze heeft me dan ook gebracht tot waar ik nu sta, het in ontvangst nemen van mijn doctoraatstitel. Jullie zijn me altijd blijven steunen en hebben me in mijn down momentjes altijd weer weten op te beuren, dankjewel. Ook mijn twee kleine broertjes (allé klein, ze zijn 1,94 en 2,03 m groot) mag ik zeker niet vergeten. Bedankt voor de vele peptalks (die kon ik regelmatig gebruiken), maar ook gewoon bedankt voor de vele leuke momenten samen, jullie weten hoeveel familie voor mij betekent!

Als laatste wil ik ook nog **Tom** bedanken! Ik heb je leren kennen toen ik op het punt stond een doctoraatsbeurs aan te vragen. Je hebt me (waarschijnlijk zonder te weten wat het allemaal juist inhield) gesteund in deze keuze. Je bent zelfs van het verre Limburg meeverhuisd naar Leuven, zodat ik al mijn energie in mijn doctoraat kon steken. Ik weet dat je daar opofferingen voor gemaakt hebt en daar ben ik je dan ook echt enorm dankbaar voor! Nu staat ons huisje daar in het verre Limburg te stralen en ik kan niet wachten om te zien wat de toekomst met ons drieën nog allemaal in petto heeft!

Summary

This thesis focusses on the study of the physiological role and mode-of-action of hormonal and small RNA pathways in the control of post-embryonic development and reproduction in locusts, which are globally considered as the most devastating migratory pest insects.

Juvenile hormones (JH) are key endocrine regulators produced by the *corpora allata* (CA) of insects. Together with ecdysteroids, as well as nutritional cues, JH coordinates different aspects of insect post-embryonic development and reproduction. The JH signalling pathway was only recently described with the characterization of a genuine JH receptor, Methoprene-tolerant (Met), a transcription factor belonging to the basic-helix-loop-helix (bHLH)/Per-Arnt-Sim (PAS) family. Binding of JH stimulates Met to form a complex with other bHLH-PAS proteins, which in turn induces the expression of JH response genes, such as *krüppel-homolog 1* (*Kr-h1*), the main effector of the anti-metamorphic action of JH. The ecdysteroid early response gene, *E93*, is a key determinant promoting adult morphogenesis. The ancestral regulatory mechanism by which JH inhibits metamorphosis is defined as the MEKRE93 pathway.

The function of Met appears to be required in a wide variety of processes regulated by JH. However, its functional interactions with other hormonal signalling pathways seem highly dependent on the feeding habits and on the developmental and reproductive strategies employed by the insect species investigated. In this thesis, we report on the effects of RNA interference (RNAi) mediated *SgMet* knockdown during the first gonadotrophic cycle in female desert locusts (*Schistocerca gregaria*). We show that the JH receptor Met is essential for ovarian maturation, vitellogenesis and associated ecdysteroid biosynthesis in adult female *S. gregaria*. Interestingly, knockdown of *SgMet* also resulted in a significant decrease of *insulin-related peptide* (*SgIRP*) and increase of *neuroparsin* (*SgNP*) *3* and *4* transcript levels in the fat body, illustrating the existence of an intricate regulatory interplay between different hormonal factors. In addition, *SgMet* knockdown in females resulted in delayed display of copulation behaviour with virgin males, when compared with *dsGFP* injected control animals. Moreover, we observed an incapacity of adult *dsSgMet* injected female locusts to oviposit during the time of the experimental setup.

Kr-h1 is a zinc-finger transcription factor maintaining the *status quo* in immature insect stages and promoting reproduction in adult insects through transduction of the JH signal. Knockdown studies have shown that precocious silencing of *Kr-h1* in the immature stages results in premature development of adult features. However, the molecular characteristics and reproductive potential of these premature adult insect stages are still poorly understood. In this thesis, we report on an adult-like or 'adultoid' phenotype of the migratory locust, *Locusta migratoria*, obtained after a premature metamorphosis induced by silencing of *Kr-h1* in the penultimate nymph. The freshly moulted adultoid showed precocious development of adult features,

coinciding with increased *LmE93* transcript levels. Furthermore, accelerated ovarian maturation and vitellogenesis were observed in female adultoids, coinciding with elevated expression of *LmCYP15A1* in corpora allata (CA) and *LmKr-h1* and *vitellogenin* genes (*LmVg*) in fat body, whereas *LmE93* and *Methoprene-tolerant* (*LmMet*) transcript levels decreased in fat body. Expression of several *Halloween* genes in the ovaries was elevated as well. In addition, the processes of copulation and oviposition were severely disturbed in these females.

Where *Kr-h1* is maintaining the *status quo* in immature insect stages, the ecdysteroid-inducible early gene *E93* appears to be a key factor promoting metamorphosis and adult morphogenesis. In this thesis, we report on the developmental and molecular consequences of an RNAi-mediated knockdown of *SgE93* in the desert locust, *Schistocerca gregaria*. We describe a supernumerary nymphal phenotype which still displayed juvenile morphological features, such as a nymphal colour scheme and body shape, while they reached the physical body size of the adult locusts, or even surpassed it after the next supernumerary moult. Interestingly, when compared to control locusts, the total duration of the fifth, and normally final, nymphal (N5) stage was shorter than normal. This appeared to correspond with temporal and quantitative changes in the haemolymph ecdysteroid levels, as well as with altered expression of the rate-limiting *Halloween* gene, *Spook* (*SgSpo*). In addition, also the levels of the *Ecdysone receptor* (*SgEcR*) and *Retinoid-X-Receptor* (*SgRXR*) transcripts were altered, suggesting that the silencing of *Sg*E93 had affected both ecdysteroid synthesis and signalling. A very potent upregulation of the *SgKr-h1* transcript levels was also observed upon knockdown of *Sg*E93. Moreover, the process of moulting was disturbed in these supernumerary nymphs. While attempting ecdysis to the next stage, 50 % of the N6 and all N7 supernumerary nymphs eventually died.

Recently, the importance of microRNAs (miRNAs) in regulating key insect processes was established as well. Especially the study of extracellular miRNAs (ex-miRNAs) is a new, still underexplored, but very intriguing research area. In the present study, we demonstrated the presence of ex-miRNAs in the cell-free conditioned media of two *Drosophila* cell lines. More specifically, by means of quantitative real-time PCR (qRT-PCR), we analysed the presence of twelve miRNAs in extracellular vesicles (EVs) and in extracellular Argonaute-1 containing immunoprecipitates (EAgo-1), obtained from the cell-free conditioned media of S2 and Cl.8 cell cultures. Next-generation RNA-sequencing data confirmed these qRT-PCR results and provided evidence for selective miRNA secretion in EVs. To our knowledge, this is the first time that miRNAs have been identified in the extracellular medium of cultured cells derived from insects. Furthermore, we have also demonstrated the presence of extracellular miRNAs in haemolymph of fifth nymphal *L. migratoria*. More specifically, we analyzed small RNA sequencing reads of of fifth nymphal *L. migratoria* haemolymph characterized by low (early fifth nymphal) *versus* high (late fifth nymphal) ecdysteroid levels. Differential expression analysis revealed that the relative abundances of 43 miRNAs significantly differed between the tested conditions. To

our knowledge, this is the first report on the differential extracellular miRNA occurrence throughout the moulting cycle of an insect.

Although the transcriptional regulation of ecdysteroid and MEKRE93 pathway components has been extensively studied, little is known about their regulation at the post-transcriptional level. In this study, we have reported the importance of specific miRNAs in the metamorphic transition into adult *L. migratoria*. Systemic RNAi mediated silencing of *Lm*Dicer-1, an enzyme that is required for miRNA biogenesis, during the fifth nymph stage disrupted the nymphal-to-adult moult. Moreover, mimicking *Lmi*-miR-13b-3p (agomiR) in late nymphal *L. migratoria* caused a prolonged duration of the fifth nymphal stage, whereas the majority (60 %) of the *Lmi*-bantam-3p agomiR- and 20 % of *Lmi*-miR-306-5p agomiR-injected fifth nymphal locusts showed severe moulting defects and eventually died. Altogether, these findings support a role for miRNAs as important players in the metamorphic transition in *L. migratoria*.

L. migratoria and *S. gregaria* are well-known, swarm-forming pest insects that can destroy crops and harvests in different continents of the world, including some of the world's poorest countries. Even today, locusts are threatening food supply and livelihoods of millions of people. As such, components of pathways regulating crucial insect processes, as investigated in this thesis, are very promising candidate targets for future development of novel, more selective locust control strategies.

Samenvatting

Deze thesis richt zich op de studie van de fysiologische rol en het werkingsmechanisme van hormonale en kleine RNA signaalwegen bij de controle van de post-embryonale ontwikkeling en reproductie bij sprinkhanen, 's werelds meest verwoestende migrerende plaaginsect.

Juveniele hormonen (JH) zijn belangrijke endocriene regulatoren die geproduceerd worden in de *corpora allata* (CA) van insecten. Samen met ecdysteroïden en nutritionele signalen coördineert JH verschillende aspecten van de post-embryonale ontwikkeling en reproductie bij insecten. De JH signaalweg werd pas onlangs beschreven met de identificatie van een authentieke JH-receptor, Methopreen-tolerant (Met), een transcriptiefactor behorende tot de basic-helix-loop-helix (bHLH)/Per-Arnt-Sim (PAS) familie. Het binden van JH stimuleert Met tot het vormen van een complex met andere bHLH-PAS-proteïnen, dat op zijn beurt de expressie induceert van JH-responsieve genen, zoals *Krüppel-homoloog 1* (*Kr-h1*), de belangrijkste effector van het anti-metamorfose effect van JH. Het vroege ecdysteroïd-responsieve gen *E93*, is een belangrijke determinant in het bevorderen van de metamorfose tot een adult insect. Het reguleringsmechanisme waarmee JH de metamorfose remt, wordt gedefinieerd als de 'MEKRE93 pathway'.

De functie van Met blijkt vereist te zijn in een ruime verscheidenheid aan door JH gereguleerde processen. De functionele interacties met andere hormonale signaalwegen lijken echter sterk afhankelijk te zijn van de voedingsgewoonten en van de ontwikkelings- en reproductieve strategieën die worden gebruikt door de onderzochte insectensoorten. De effecten van RNA-interferentie (RNAi) gemedieerde *SgMet* neerregulatie tijdens de eerste gonadotrofe cyclus bij vrouwelijke woestijnsprinkhanen (*Schistocerca gregaria*) worden in deze thesis beschreven. We tonen aan dat de JH-receptor Met essentieel is voor de rijping van de eierstokken, vitellogenese en daarmee samenhangende ecdysteroïd biosynthese bij adulte vrouwelijke *S. gregaria*. Een interessante vaststelling is dat in het vetlichaam de neerregulatie van *SgMet* ook resulteerde in een significante afname van de niveaus voor het *insuline-verwante peptide* (*SgIRP*) transcript, evenals een toename van de *neuroparsine* (*SgNP*) *3* en *4* transcripten. Deze resultaten wijzen op het bestaan van een ingewikkeld samenspel van verschillende hormonale factoren. Bovendien vertoonden *SgMet* neer-gereguleerde vrouwtjes, in vergelijking met *dsGFP*-geïnjecteerde controledieren, ook een uitstel van hun copulatiegedrag met maagdelijke mannetjes. Verder slaagde geen enkel *dsSgMet*-geïnjecteerd adulte vrouwtje erin om eitjes af te leggen gedurende het experiment.

Kr-h1 is een zinkvinger transcriptiefactor die het *status quo* in immature insectenstadia handhaaft en de reproductie bij adulte insecten bevordert door transductie van het JH-signaal. Studies hebben al aangetoond dat het vroegtijdig neerwaarts reguleren van Kr-h1 in immature stadia resulteert in de vroegtijdige ontwikkeling van adulte kenmerken. De moleculaire kenmerken en het voortplantingspotentieel van deze

premature adulte insecten zijn echter nog steeds niet volledig begrepen. In deze context, hebben we een adult-achtig of 'adultoïd' fenotype van de treksprinkhaan, *Locusta migratoria*, bestudeerd dat verkregen werd na het induceren van een vroegtijdige metamorfose door het neerwaarts reguleren van *Kr-h1* in het voorlaatste larvale stadium. Pas vervelde adultoïden vertoonden vroegtijdige ontwikkeling van adulte kenmerken, samenhangend met verhoogde *LmE93* transcriptniveaus. Verder werden een versnelde rijping van de eierstokken en vitellogenese waargenomen bij vrouwelijke adultoïden, samengaand met een verhoogde expressie van *LmCYP15A1* in de CA en van *LmKr-h1* en *vitellogenine* genen (*LmVg*) in het vetlichaam, terwijl *LmE93* and *LmMet* transcriptniveaus afnamen in het vetlichaam. Een verhoogde expressie van de *Halloween* genen werd ook waargenomen in de ovaria. Bovendien waren de copulatie- en ovulatieprocessen bij deze adultoïden vrouwtjes ernstig verstoord.

Waar Kr-h1 het *status quo* in immature insectenstadia handhaaft, is het vroege ecdysteroïd-responsieve gen, *E93*, een sleutelfactor die de metamorfose tot adult bevordert. In deze thesis hebben we de ontwikkelings- en moleculaire gevolgen van een RNAi-gemedieerde knockdown van *SgE93* bij de woestijnsprinkhaan *S. gregaria* bestudeerd. Dit leidde tot een extra nymfaal fenotype dat nog steeds juveniele morfologische kenmerken, zoals een nymfaal kleurenpatroon en lichaamsbouw, vertoonde terwijl de fysieke lichaamsgrootte van een volwassen sprinkhaan bereikt, of na een volgende vervelling zelfs overtroffen werd. Bovendien vertoefden deze nymfen gedurende een kortere tijd in het vijfde, normaal gesproken laatste, nymfale (N5) stadium in vergelijking met controle sprinkhanen. Dit ging gepaard met temporele en kwantitatieve veranderingen van de ecdysteroïdniveaus in de hemolymfe, alsook met veranderende expressie van het snelheidbepalende *Halloween* gen, *Spook* (*SgSpo*). Bovendien werden ook de transcriptniveaus van de *Ecdyson Receptor* (*SgEcR*) en *Retinoïd-X-Receptor* (*SgRXR*) genen gewijzigd, hetgeen suggereert dat het neerwaarts reguleren van *SgE93* zowel de synthese als de signalering van ecdysteroïden beïnvloedde. Een sterke opwaartse regulatie van de *SgKr-h1* transcriptniveaus werd tevens waargenomen na de knockdown van *SgE93*. Bovendien werd bij deze extra nymfale stadia het vervellingsproces verstoord. Bij hun pogingen tot vervelling naar het volgende stadium stierven 50 % van de N6 en alle N7 nymfen.

Onlangs werd ook het belang van microRNAs (miRNAs) bij het reguleren van belangrijke insectenprocessen vastgesteld. Vooral de studie van extracellulaire miRNAs (ex-miRNAs) is een nieuw, nog weinig onderzocht, maar zeer intrigerend onderzoeksdomein. In deze thesis demonstreren we de aanwezigheid van ex-miRNAs in de cel-vrije geconditioneerde media van twee *Drosophila*-cellijnen. We analyseerden, door middel van kwantitatieve real-time PCR (qRT-PCR), de aanwezigheid van twaalf miRNAs in extracellulaire vesikels (EVs) en in extracellulaire Argonaute-1 bevattende immunoprecipitaten (EAgo-1), verkregen uit de cel-vrije geconditioneerde media van S2 en Cl.8 celculturen. Next-generation small RNA sequencing data bevestigden deze qRT-PCR-resultaten en leverden aanwijzingen op voor het bestaan van een selectieve miRNA secretie in EVs. Voor zover we weten is dit de eerste keer dat miRNAs worden geïdentificeerd in het extracellulaire

medium van gekweekte cellen afgeleid van insecten. Verder hebben we tevens de aanwezigheid van ex-miRNAs aangetoond in de hemolymfe van *L. migratoria* in het vijfde nymfale stadium. We analyseerden small RNA sequencing data van hemolymfe gekenmerkt door lage (jonge vijfde nymfale sprinkhanen) *versus* hoge (oude vijfde nymfale sprinkhanen) ecdysteroïd niveaus. Differentiële expressie-analyse toonde aan dat de abundantie van 43 miRNAs significant verschilde tussen de geteste condities. Voor zover bekend is dit de eerste studie die rapporteert over de differentiële aanwezigheid van ex-miRNA gedurende de vervellingscyclus van een insect.

Hoewel de transcriptionele regulatie van ecdysteroïd- en MEKRE93 pathway componenten uitgebreid is bestudeerd, is er weinig bekend over de regulatie op post-transcriptioneel niveau. In deze thesis hebben we het belang van bepaalde miRNAs in de transitie van nymf tot adult bij de treksprinkhaan *L. migratoria* bestudeerd. Het neerwaarts reguleren van *LmDicer-1*, via systemische RNAi, tijdens het vijfde nymfale stadium resulteerde in een verstoorde vervelling naar adult. Bovendien veroorzaakte het toedienen van een agonistische mimic voor *Lmi*-miR-13b-3p (agomiR) laat in het vijfde nymfale stadium van *L. migratoria* een verlengde duur van dit stadium, terwijl de meerderheid (60 %) van de *Lmi*-bantam-3p agomiR- en 20 % van de *Lmi*-miR-306-5p agomiR-geïnjecteerde vijfde nymfale sprinkhanen defecten in hun vervelling vertoonden en uiteindelijk stierven. Deze bevindingen wijzen op het belang van miRNAs in de transitie van nymf tot adult bij de treksprinkhaan, *L. migratoria*.

L. migratoria en *S. gregaria* zijn welbekende, zwermvormende plaaginsecten die in staat zijn om gewassen en oogsten te vernielen in verschillende continenten, waaronder enkele van de armste landen van de wereld. Ook op de dag van vandaag vormen sprinkhanen nog steeds een enorme bedreiging voor de voedselvoorziening en het levensonderhoud van miljoenen mensen. Componenten van signaalwegen die belangrijke insecten processen reguleren, zoals onderzocht in deze thesis, zijn beloftevolle potentiële targets voor de toekomstige ontwikkeling van nieuwe en meer selectieve sprinkhanenbestrijdingsstrategieën.

List of abbreviations

2,22,25dE	2,22,25-trideoxyecdysone
2,22dE	2,22-dideoxyecdysone
20E	20-hydroxyecdysone
7dC	7-dehydrocholesterol
Act	β-actin
AG	Accessory gland
Ago	Argonaute
Ago-miRNAs	Ago-associated miRNAs
AST	Allatostatin
AT	Allatotropin
BCA	Bicinchonic acid
bHLH	Basic-helix-loop-helix
Blimp-1	B lymphocyte-induced maturation protein 1
Br	Brain
Br-C	Broad complex
BSA	Bovine serum albumin
CA	Corpora allata
CC	Corpora cardiaca
CCAP	Crustacean cardioactive peptide
cDNA	Complementary DNA
Cl.8	Clone 8 cell line
CPM	Counts per million
Ct	Treshold cycle
CtBP-im	C-terminal-binding protein interaction motif
CYP15A1	MF epoxidase
D	Day
Dib	Disembodied
Dme	*Drosophila melanogaster*
DNA	Deoxyribonucleic acid
ds	Double-stranded
dsRNA	Double-stranded RNA
E	Ecdysone
E74	Ecdysone induced 74
E75	Ecdysone induced 75
E93	Ecdysone-induced protein 93
EAgo-1	Extracellular Ago-1 containing immunoprecipitates
EcR	Ecdysone receptor
EF1α	Elongation factor 1α
EH	Eclosion hormone
EIA	Enzyme ImmunoAssay

EVs	Extracellular vesicles
ex-miRNAs	Extracellular miRNAs
FA	Farnesoic acid
FAO	Food and Agricultural Organisation
Fb	Fat body
FBS	Fetal Bovine Serum
FPP	Farnesyl pyrophosphate
FTZ-F1	Fushi tarazu transcription factor 1
GFP	Green fluorescent peptide
HR3	Hormone receptor 3
HR39	Hormone receptor 39
HTH	Helix-turn-helix
IGFBP	Insulin-like growth factor binding protein
IP	Immunoprecipitation
IRP	Insulin-related peptide
JH	Juvenile hormone
JHAMT	Juvenile hormone acid methyl transferase
Kr-h1	Krüppel-homolog 1
LDS	Lithium dodecyl sulfate
Lm	*Locusta migratoria*
Lmi	*Locusta migratoria*
Met	Methoprene-tolerant
MF	Methyl farnesoate
miRNAs	MicroRNAs
miR	MicroRNA
mRNA	Messenger RNA
N	Nymph
NCBI	National center for biotechnology information
NP	Neuroparsin
NPP	Neuroparsin precursor
NR	Nuclear receptor
nt	Nucleotides
Obs2A	Obstructor protein 2A
p_{adj}	Raw p-value adjustment
PAS	Per-Arnt-Sim
PCR	Polymerase chain reaction
PG	Prothoracic gland
Phm	Phantom
PIF	Patency inducing factor
pre-miRNA	precursor miRNA
PVDF	Polyvinylidene difluoride
qRT-PCR	Quantitative real-time PCR

RISC	RNA induced silencing complex
RNA	Ribonucleic acid
RNAi	RNA interference
RNA-seq	RNA sequencing
RT	Room temperature
RXR	Retinoid-X-receptor
S2	Schneider 2 cell line
Sad	Shadow
S.E.M.	Standard error of means
Sg	*Schistocerca gregaria*
Shd	Shade
SOG	Suboesophageal ganglion
SRC	Steroid receptor coactivator
Tai	Taiman
TBS	Tris-buffered saline
TGF-β	Transforming Growth Factor-β
USP	Ultraspiracle
Vg	Vitellogenin
VKR	Venus kinase receptor

Table of contents

Acknowledgements – Dankwoord ..... **V**
Summary ..... **VII**
Samenvatting ..... **XI**
List of abbreviations ..... **XV**
Table of contents ..... **XIX**
Chapter 1: General introduction **1**
1.1 The aims of this thesis 2
1.2 The migratory locust, *Locusta migratoria* and the desert locust, *Schistocerca gregaria* 3
1.2.1 As pest insects 3
1.2.2 As model organisms 6
1.3 Insect life 7
1.3.1 Life cycle 7
1.3.2 Anatomy and morphology 8
1.3.2.1 Exoskeleton 9
1.3.2.2 Female reproductive physiology 10
1.4 The classic insect hormones 12
1.4.1 Ecdysteroids 12
1.4.2 Juvenile hormones 14
1.5 Regulation of moulting 17
1.5.1 Ecdysteroids and juvenile hormone 17
1.6 Regulation of female reproductive physiology 17
1.6.1 Ecdysteroids and juvenile hormone 17
1.6.2 (Neuro)peptides 18
1.6.2.1 Ovary maturating parsin 18
1.6.2.2 Insulin-related peptides 19
1.6.2.3 Neuroparsins 19
1.7 The RNAi pathway 20
1.7.1 PIWI-interacting RNAs 20
1.7.2 Small interfering RNAs 20
1.7.3 MicroRNAs 22
1.7.3.1 MiRNA biogenesis 22
1.7.3.2 Evolutionary conservation of miRNAs 23
1.7.3.3 MiRNAs regulating insect development 24
1.7.3.4 Extracellular presence 26
1.8 Outline of this thesis 27

Chapter 2: The presence of extracellular microRNAs in the media of cultured *Drosophila* cells 29
2.1 Introduction 30
2.2 Materials and methods 32
2.2.1 Cl.8 and S2 cell cultures 32
2.2.2 Isolation of extracellular vesicles and extracellular Argonaute-1 from conditioned media 32
2.2.3 Immunoblotting 34
2.2.4 RNA extraction and cDNA synthesis 35
2.2.5 Quantitative real-time PCR 35
2.2.6 Small RNA sequencing data and analysis 36
2.3 Results 37
2.3.1 Detection of miRNAs in extracellular vesicles and bound to extracellular Argonaute-1 37
2.3.2 MiRNA intracellular expression 38
2.3.3 Differential expression analysis of small RNA sequencing data 40
2.4 Discussion 42
2.5 Conclusion 45
Chapter 3: miRNAs regulating postembryonic development in the migratory locust, *Locusta migratoria* 47
3.1 Introduction 48
3.2 Materials and methods 50
3.2.1 Rearing of animals 50
3.2.2 Tissue and haemolymph collection 50
3.2.3 RNA extraction methods 50
3.2.3.1 Long RNA extraction and cDNA synthesis 50
3.2.3.2 Total RNA extraction including miRNA 51
3.2.4 Quantitative real-time PCR 51
3.2.5 Small RNA sequencing data and analysis 52
3.2.6 RNA interference experiments 52
3.2.7 Prediction of miRNA targets 53
3.2.8 A(nta)gomiR experiments 53
3.2.9 Observing ecdysis of *dsLmDicer-1* and a(nta)gomiR-injected locusts 55
3.2.10 Ecdysteroid measurements using an enzyme immunoassay 55
3.3 Results 57
3.3.1 Knockdown of *LmDicer-1* results in defects in moulting 57
3.3.2 Temporal profiles of ecdysteroids in haemolymph of fifth nymphal locusts 58
3.3.3 Differential expression analysis of small RNA sequencing data 58
3.3.4 Prediction of miRNAs targeting the ecdysone receptor complex or MEKRE93 pathway components 61
3.3.5 *Lmi*-bantam-3p, *Lmi*-miR-306-5p and *Lmi*-miR-13b-3p are possibly involved in moulting 61

3.3.6 Transcript levels of *LmEcR*, *LmRXR* and *LmObs2A* in *Lmi*-bantam-3p and *Lmi*-miR-13b-3p agomiR-injected locusts 63
3.4 Discussion 64
3.5 Conclusion 67
Chapter 4: RNAi-mediated knockdown of transcription factor E93 in nymphs of *S. gregaria* inhibits adult morphogenesis and results in supernumerary juvenile stages 69
4.1 Introduction 70
4.2 Materials and methods 71
4.2.1 Rearing of animals 71
4.2.2 Tissue collection 71
4.2.3 RNA extraction and cDNA synthesis 72
4.2.4 Multispecies E93 gene identification and phylogenetic analysis 72
4.2.5 Quantitative real-time PCR 75
4.2.6 RNA interference experiments 76
4.2.7 Ecdysteroid measurement 77
4.2.8 Observing ecdysis 77
4.3 Results 77
4.3.1 Identification and phylogenetic analysis of *SgE93* 77
4.3.2 Knockdown of *SgE93* resulted in supernumerary nymphal stages 81
4.3.3 *SgE93* silencing altered the duration of the moulting cycle and affected the success of moulting to later nymphal stages 81
4.3.4 Transcript levels of MEKRE93 and JH biosynthesis pathway components in *dsSgE93*- and *dsGFP*-injected locusts 83
4.3.5 Transcript levels of different *Halloween* genes and components of the ecdysone receptor complex in *dsSgE93*- and *dsGFP*-injected locusts 84
4.3.6 Temporal profiles of ecdysteroids in haemolymph of *dsSgE93*- and *dsGFP*-injected locusts 86
4.4 Discussion 89
4.4.1 *Sg*E93 is the desert locust E93 ortholog 89
4.4.2 *SgE93* knockdown has inhibited metamorphosis and adult morphogenesis 89
4.4.3 *SgE93* knockdown has influenced the ecdysteroid pathway 91
4.5 Conclusions 93
Chapter 5: Precocious downregulation of Krüppel-homolog 1 in *L. migratoria* gives rise to an adultoid phenotype with accelerated ovarian development but disturbed mating and oviposition 95
5.1 Introduction 96
5.2 Materials and methods 98
5.2.1 Rearing of animals 98
5.2.2 Tissue collection 98
5.2.3 RNA extraction and cDNA synthesis 98
5.2.4 Quantitative real-time PCR 99

5.2.5 RNA interference experiments 100
5.2.6 Observing ecdysis 102
5.2.7 Measurement of oocyte length 102
5.2.8 Microscopy and histological analysis 102
5.2.9 Observation of mating, egg deposition and hatching 103
5.3 Results 104
5.3.1 Temporal transcript profiles of MEKRE93 and JH biosynthesis pathway components 104
5.3.2 Knockdown of *LmKr-h1* results in precocious development of external adult features 105
5.3.3 Transcript levels of MEKRE93 and JH biosynthesis pathway components in dsRNA-injected fourth nymphal and freshly molted fifth nymphal, adultoid and adult female locusts 107
5.3.4 The adultoid phenotype shows an accelerated ovarian maturation 108
5.3.5 Transcript levels of MEKRE93 and JH biosynthesis pathway components in adultoid females 112
5.3.6 Transcript levels of Halloween genes and ecdysone receptor complex in adultoids and adults 115
5.3.7 Adultoid females have severe defects in mating and egg laying 119
5.4 Discussion 122
5.4.1 *DsLmKr-h1* injections in fourth nymphal stage induced the developmental transition to adultoids 122
5.4.2 Comparison between adultoid and adult female locusts during their first gonadotropic cycle 124
5.4.2.1 An accelerated ovarian maturation 124
5.4.2.2 Associated changes in gene expression profiles in fat body and CA 124
5.4.2.3 Accelerated Kr-h1 and Halloween gene expression in the ovary 125
5.4.2.4 Severe defects in mating and egg laying 126
5.5 Conclusions 127
Chapter 6: Juvenile hormone receptor Met is essential for ovarian maturation in *S. gregaria* 129
6.1 Introduction 130
6.2 Materials and methods 132
6.2.1 Rearing of animals 132
6.2.2 Tissue collection 132
6.2.3 RNA extraction and cDNA synthesis 132
6.2.4 Quantitative real-time PCR 132
6.2.5 RNA interference experiments 133
6.2.6 Measurement of oocyte length 134
6.2.7 Microscopy and histological analysis 135
6.2.8 Ecdysteroid measurements using an enzyme immunoassay 135
6.3 Results and discussion 136
6.3.1 Description of the relative transcript levels of the genes of interest 136

6.3.2 Knockdown of the JH receptor *Met* affects expression of the downstream signalling component *Kr-h1* and of JH biosynthetic enzymes 137
6.3.3 *SgMet* is crucial for initiating ovarian maturation, vitellogenesis and reproductive behavior . 139
6.3.4 *SgMet* is also crucial for ovarian ecdysteroid biosynthesis 142
6.3.5 Knockdown of JH receptor Met alters expression of *insulin-related peptide* and *neuroparsin precursor* genes in an opposite way 145
6.4 Conclusion 147
Chapter 7: General conclusions, discussion and future perspectives 149
7.1 The presence of extracellular miRNAs 150
7.2 Regulation of moulting and metamorphosis 151
7.3 Regulation of female reproductive physiology 153
7.4 MEKRE93 pathway components as molecular targets of novel insect control agents 154
7.5 General discussion and future perspectives 154
7.5.1 MiRNAs regulating postembryonic development 154
7.5.1.1 Optimisation of purification methods for ex-miRNA containing fractions 154
7.5.1.2 Ex-miRNA containing fractions regulating the transition from juvenile to adult 155
7.5.1.3 The use of miRNA a(nta)gomiRs in elucidating metamorphosis 157
7.5.2 Regulation of moulting and female reproductive success 157
7.5.2.1 Identification of JH signalling cascade components 157
7.5.2.2 Functional interactions with other signalling pathways 159
7.5.2.3 Elucidating the supernumerary nymphal phenotype in more detail 160
7.5.2.4 Unravelling the story behind the adultoid reproductive physiology 161
7.5.3 Quantification of JH titers 162
7.5.4 dsRNA and miRNAs as novel insect control agents 163
7.5.5 The limitations of RNAi 164
References 165
Publications and awards 187
Articles in internationally peer-reviewed scientific journals 187
Article on the preprint server for biology 187
Reports of communications at international scientific conferences, symposia and meetings 188
Awards 188
Appendices 189
Supplementary Figure 1 Chapter 2 189
Supplementary Figure 2 Chapter 2 190
Supplementary Table Chapter 2 191
Supplementary Table Chapter 3 206

Chapter 1: General introduction

1.1 The aims of this thesis

The migratory locust, *Locusta migratoria*, and the desert locust, *Schistocerca gregaria*, are voracious, phytophagous pest species. These locusts can live as solitarious insects, but under certain environmental conditions, they will aggregate and eventually form huge migrating swarms that devastate field crops and harvests in a very large terrestrial surface area that includes many of the world's poorest countries. Their voraciousness, migrating behaviour and high reproductive rate make them a very difficult pest to be efficiently controlled by human interventions (Pener and Simpson, 2009; Symmons and Cressman, 2001). Unfortunately, the control of such swarms still mainly implies the use of insecticides with only limited selectivity, which also results in a negative impact on the environment and non-target organisms (Zaim and Guillet, 2002). Therefore, there is an urgent need for more specific pest management strategies. Vital insect processes, such as metamorphosis and reproduction, are regulated by multiple hormonal pathways, which utilize molecular components that may prove to be excellent candidate targets for development of a next generation of more selective and eco-friendly insecticides.

The classic insect hormones, juvenile hormones (JH) and ecdysteroids, are key players in many physiological processes in insects. During juvenile stages, ecdysteroids trigger the moulting process, while JH will determine the nature of the moult (Riddiford, 2012). The ancestral regulatory mechanism by which JH inhibits metamorphosis is defined as the MEKRE93 pathway (Belles, 2019). These lipophilic hormones, together with nutritional cues, as well as signalling mechanisms directed by regulatory peptides, also control the reproductive physiology of insects. The objectives of this thesis were to investigate the possible roles of i) JH signalling pathway components in regulating key processes in locust postembryonic development, in particular metamorphosis and reproduction, as well as ii) their functional interactions with different pathways. As such, a better fundamental knowledge of the JH signalling pathway in the pest species *L. migratoria* and *S. gregaria* may contribute to the future development of novel, more target-specific insecticides.

The role of microRNAs (miRNAs) in regulating key processes in an insect's life was recently established as well. Thousands of new miRNAs have been discovered in a wide range of metazoan species, with key roles in presumably every biological/physiological process (Berezikov, 2011; Caygill and Johnston, 2008; Chawla and Sokol, 2011; Gomez-Orte and Belles, 2009; Jayachandran et al., 2013). However, little is known about the post-transcriptional regulation of MEKRE93 pathway components in insects, thereby regulating postembryonic development. A third objective was to investigate the possible role of miRNAs in regulating locust postembryonic development. Besides their characterisation at an intracellular level, miRNA molecules have also been observed in extracellular biological fluids of several organisms, including plants and animals (Etheridge et al., 2013; Makarova et al., 2015). This recent scientific progress raised the question whether extracellular miRNAs (ex-miRNAs) would also be present in insects and, if this would be the case, whether

these would also reside in similar extracellular fractions as recently demonstrated in mammals. Furthermore, another interesting question would be whether these ex-miRNAs are differentially distributed when comparing different conditions, since this could suggest potential roles of ex-miRNAs in intercellular communication in insects. These objectives were subsequently investigated during this PhD study.

In the first chapter, a short introduction on the research organisms will be given, in addition to an overview of recent literature on the role of ecdysteroids, JH and MEKRE93 pathway components in the regulation of insect postembryonic development and female reproductive physiology. Moreover, an overview of recent literature on miRNAs regulating insect postembryonic development, as well as on the presence of ex-miRNAs in insects is included.

1.2 The migratory locust, *Locusta migratoria* and the desert locust, *Schistocerca gregaria*

1.2.1 As pest insects

Insects are the most speciose group of animals, but at the same time perhaps also the most feared one. Because of their immense success, multiple insect species are well-known for their negative effect on our economy. They are called pest species for a variety of reasons, but the most economically damaging of all are phytophagous insects, such as locusts. The migratory locust, *L. migratoria,* and the desert locust, *S. gregaria*, are two famous examples of voracious agricultural pests, and moreover the research organisms in this thesis. They can threaten the livelihood of approximately one tenth of the world's population by destroying agricultural production (Pener and Simpson, 2009; Symmons and Cressman, 2001).

Being one of the ten plagues of Egypt (Exodus 10), locust swarms have been categorised as one of the most devastating natural disasters since ancient times. Throughout the 19th and 20th century, there have been nine major plagues of *S. gregaria*, each lasting from several months to several years or more. After the last major plague, from 1986 until 1989, several outbreaks still occurred (Symmons and Cressman, 2001). A recent one (2003-2004) led to an upsurge from the Sahel in western Africa to southern Europe, Cyprus and the Middle East (Pener and Simpson, 2009). In 2013, Madagascar suffered from a *L. migratoria* outbreak, having dramatic effects on agricultural production and the availability of pasture resources for livestock (Food and Agriculture Organization of the United Nations, 2013). Nevertheless, the ability of locust-affected countries to detect and respond to locust outbreaks has improved a lot. The recent technical advances make it possible to detect early locust swarming events, which results in an immediate reaction and consequently the prevention of outbreaks (Food and Agriculture Organization of the United Nations, 2015). However, recently, another important factor is causing problems, namely global warming. Changes in plant growth due to higher carbon dioxide levels, together with heat waves and tropical cyclones with intense rains, lead to more prolific and unpredictable locust swarming (FAO Locust Watch; Roussi, 2020). Moreover, poor monitoring caused by conflict and a breakdown of governance makes it harder to prevent and respond to future outbreaks. As a

result, a new locust plague has recently emerged, threatening food supply and livelihoods of at least 20 million people (Figure 1.1). In 2020, hundreds of billions of desert locusts are swarming through large parts of East Africa, the Arabian Peninsula, the Middle East and the Indian subcontinent. In the horn of Africa, this outbreak is considered the worst infestation in a quarter of a century. Cyclones in 2018 together with warm weather and unusually heavy rains at the end of 2019 set up perfect breeding conditions for these locusts (Roussi, 2020). Large swarms were first detected at the start of 2019 in the southern Arabian Peninsula and spread rapidly to other countries, including Yemen, Saudi Arabia, Iran, Pakistan and India, followed by Ethiopia, Eritrea, Djibouti, the Ogaden, Sudan, Kenya, Uganda and Tanzania. Since March 2020, widespread hatching caused a new generation of swarms to form in Ethiopia and Kenia (FAO Locust Watch). Several other locust species are swarming as well on different continents. The South American locust, *Schistocerca cancellata*, is swarming and threatening the agricultural production in several countries of Latin America (Food and Agriculture Organization of the United Nations, 2020a). In Sardinia, the recently occurring swarms of the Moroccan locust, *Dociostaurus maroccanus*, have been described as the worst agricultural threat since the end of World War II. Millions of locusts have blanketed over 6.000 acres of farmland, destroying crops and overrunning homes (Carlone and Sestito, 2020; Stephen, 2019). Moreover, outbreaks of the African migratory locust (*Locusta migratoria migratorioides*) and the red locust (*Nomadacris septemfasciata*) are currently also threatening the food security and livelihoods of millions of people in different countries of southern Africa, including Botswana, Namibia, Zambia and Zimbabwe (Food and Agriculture Organization of the United Nations, 2020b). Spraying chemicals, such as the widely used insecticide chlorpyrifos, is not an ideal option since it is harmful to humans and the environment, making alternative control measures that can target pest species without damaging the environment more than needed (Roussi, 2020). The recent outbreaks once more stress the importance of controlling these extremely harmful agricultural pests. Especially in the 21st century, as climate change and biodiversity decline are increasingly manifesting themselves on a global scale, both prevention and control measures, involving coordination at a transnational level, will be mandatory to efficiently tackle the locust problem, making the need for greener and more target-specific insecticides more urgent than ever.

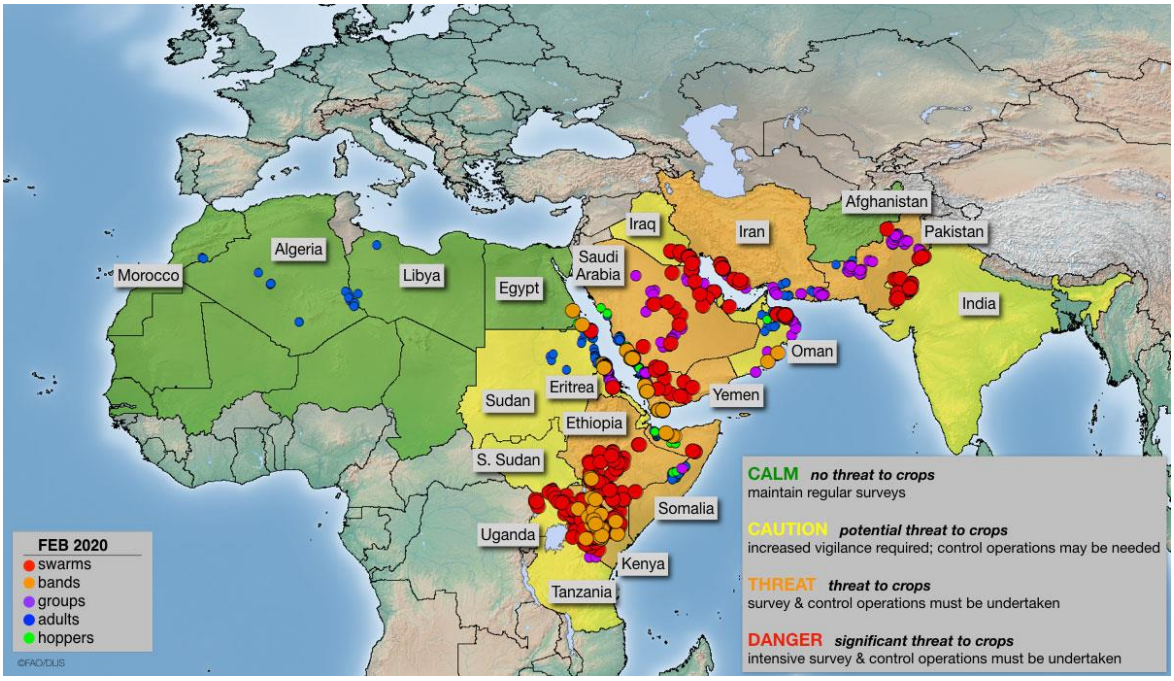

Figure 1.1: **Risk map of *S. gregaria* infestations**. A risk map summarizing the situation in February 2020 with Ethiopia, Somalia, Kenya, Yemen, Saudi Arabia and Iran suffering from multiple swarms and bands causing a real threat to crops (FAO Locust Watch).

Locusts usually live a solitary lifestyle, appearing in low densities in semi-arid to arid areas. They are shy insects that tend to avoid contact with others except for mating. Their low population densities and behaviour make them relatively harmless as they do not cause severe crop damage. Under particular environmental conditions, such as unusual heavy rainfall resulting in an increase in food availability, the population can build up rapidly. When followed by dry conditions causing food shortages, the animals start crowding (Symmons and Cressman, 2001; Uvarov, 1921). The resulting contact between one another initiates a cascade of changes, which causes the solitarious locusts to become gregarious. The central nervous system plays an important role in this transformation. Besides behavioural changes, the locusts also display physiological and morphological differences. The morphological differences are usually described as differences in the length of various body parts. Solitarious locusts tend to have longer hind femurs, but also the colour pattern of both phases differs remarkably. Where solitarious nymphs are characterized by a green to brown colour scheme, gregarious nymphs are recognizable by their yellow colour with black patterning. Sexually mature solitarious adults on the other hand, tend to be brownish whereas the gregarious adults are brownish (females) or very bright yellow (males). Moreover, the phases also differ in their reproductive physiology. Solitarious locusts will become sexually mature more slowly, but show a higher fecundity by laying more eggs during their lifespan (Symmons and Cressman, 2001). This phenomenon is an extreme form of density-dependent phase polyphenism, *i.e*. two distinctly different phenotypes encoded by the same genome (Uvarov, 1921). The transition from the solitarious to the gregarious state may cause the formation of enormous marching (nymphs) or flying (adults) insect armies, eating everything on their path. A swarm can contain up to tens of millions of locusts per square kilometre and because of a variety of reasons, *e.g*.

their ability to migrate over huge distances, their capacity to eat their own bodyweight in food per day, the unpredictability of swarm formation and the remoteness of their habitat, they are a difficult pest to control efficiently (Symmons and Cressman, 2001). Unfortunately, the most common way of controlling swarm formation includes the use of non-specific insecticides, *e.g*. carbamates and organophosphates, with a negative impact on the environment (Zaim and Guillet, 2002). In an attempt to control pest species in a more specific way, biological control agents were introduced with Green Muscle™ as the most common example. Green Muscle™ is a mycopesticide, a locust-specific biological insecticide based on the fungus *Metarhizium anisopliae* var. *acridum*. It can be used in ecologically sensitive systems, where conventional pesticides are not allowed, but this biological control agent is also characterised by a slow mode of action making it more a preventive control system (Van der Valk et al., 2006). Obviously, a next generation of more eco-friendly insecticides is needed to efficiently control pest species. Vital insect processes, such as metamorphosis and reproduction, form one of the most attractive targets making the juvenile hormone (JH) and ecdysteroid signalling pathways excellent targets in the development of more selective and eco-friendly insecticides.

1.2.2 As model organisms

Locusts belong to the family of the Acrididae, the short-horned grasshoppers. However, they differ from grasshoppers by their capacity to respond to high population densities, eventually resulting in dense hopper bands or swarming adults, capable of migrating over large distances (Symmons and Cressman, 2001). This transition from the solitarious to the gregarious stage is a remarkable phenomenon that is interesting to investigate, especially since these locust swarms are capable of ruining crops and harvests in some of the world's poorest countries (Pener and Simpson, 2009; Symmons and Cressman, 2001). But also a variety of other reasons makes these locusts interesting model organisms. Because of their relatively large size, they are ideal for physiological research in insects, especially for the study of endocrinological and neurobiological processes. Moreover, in comparison with holometabolous insects, which include intensively investigated model species, the current knowledge of these processes is much more limited in hemimetabolous insects, such as locusts.

L. migratoria and *S. gregaria* belong to the same family (Acrididae), but they are classified in different subfamilies (Oedipodinae and Cyrtacanthacridinae, respectively). Based on the transcriptome and genome data, as well as the more advanced knowledge on microRNA (miRNA), available at the start of this PhD research, the migratory locust, *L. migratoria*, was selected as the preferred organism for studying the miRNA pathway. On the other hand, the desert locust, *S. gregaria,* is considered the most dangerous locust pest species of the world and our research group in Leuven has a lot of background and expertise in studying hormonally regulated processes in this species, including moulting and reproduction. Moreover, towards the end of this PhD study, a first draft assembly of the *S. gregaria* genome also became available (Verlinden et al., 2020).

1.3 Insect life

Insects are a very speciose group of animals, considering that as many as three quarters of all animal species described on earth are insects (Stork, 2018). Probably one of the most important characteristics for the insects' success is the presence of an exoskeleton. It provides a barrier against desiccation, protects the insect from mechanical injury and gives the insect its shape. Nevertheless, living within an exoskeleton can also be challenging. In order to become a reproductive adult, insects have to pass several developmental stages. To enable growth, insects are regularly replacing their rigid exoskeleton by a new, larger one, in a process called moulting with ecdysis as the final stage of moulting, *i.e*. the shedding of the old cuticle (Ewer, 2005) as discussed in §1.3.2.1. Hemimetabolous insects, such as locusts and cockroaches, are characterized by an incomplete metamorphosis. The hatchlings appear as small, immature versions of the adult. After a series of moults, these nymphs, also designated as hoppers, pass to the reproductive adult stage. Holometabolous insects on the other hand undergo a complete metamorphosis. Upon several successive moults, the larvae enter a non-feeding pupal stage, during which a complete make-over to winged, reproductive adults occurs. Flies, butterflies, bees and beetles are well-known examples of holometabolous insects (Verlinden et al., 2014).

1.3.1 Life cycle

Hemimetabolous insects, such as the locusts *L. migratoria* and *S. gregaria*, are characterized by three life stages, *i.e*. egg (embryo), nymph (hopper) and adult (Figure 1.2). Eggs hatch into first nymphs, which undergo four successive moults until the fifth and last nymphal stage. A final moult eventually results in fully reproductive adults. Each juvenile stage lasts about seven days depending on the environmental conditions whereas the final stage takes on average two days longer. Freshly moulted adults will become reproductively active within two weeks and can live up to several months. During this period, adult female locusts are capable of producing large numbers of eggs, deposited in egg pods in bare sandy soils. The rate of egg development is dependent on the environmental conditions, ranging from 10 to 65 days after which a next generation of locusts can start their journey (Symmons and Cressman, 2001).

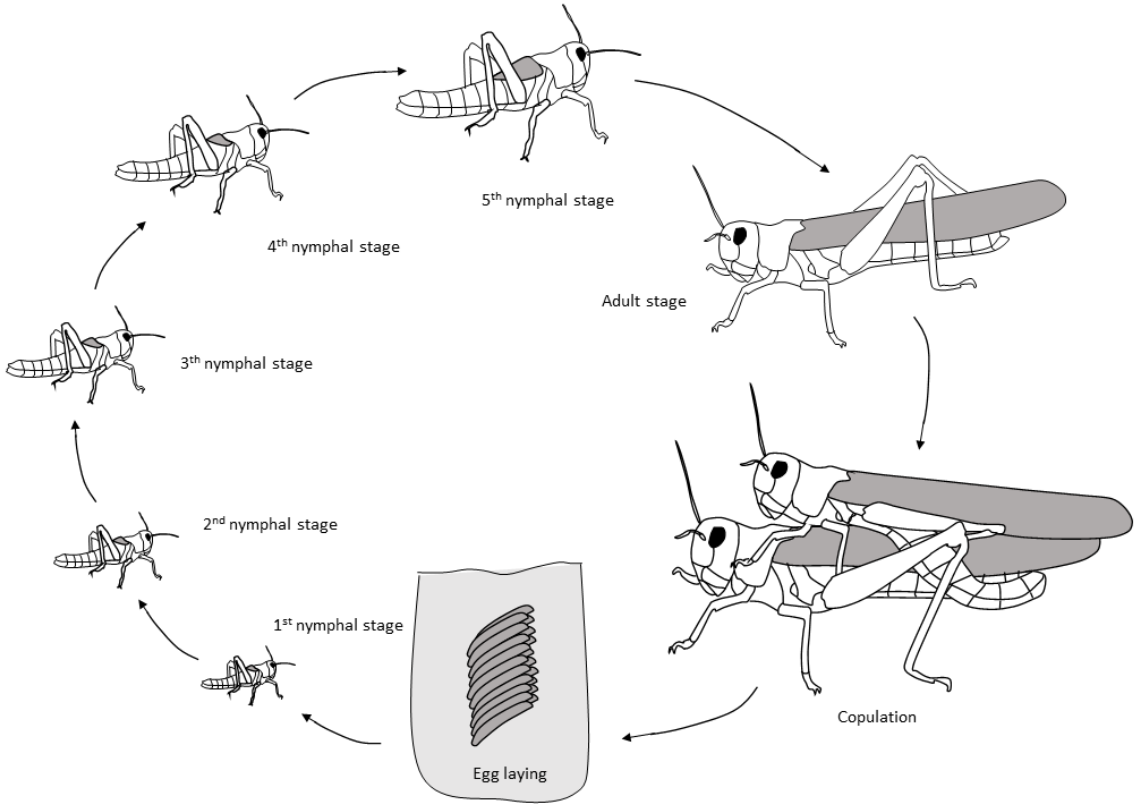

Figure 1.2: **Life cycle of locusts**. The life cycle of locusts is characterized by three life stages. After hatching, the hatchlings pass through five nymphal stages before reaching the adult, reproductive stage. Upon copulation, female locusts deposit their eggs in bare sandy soils whereafter the eggs will hatch again.

1.3.2 Anatomy and morphology

Although insects may differ morphologically, they display a similar adult body plan consisting of three main tagmata, *i.e*. the head, followed by the thorax and the abdomen (Figure 1.3). The head consists of appendages modified for feeding and sensory purposes, whereas the thorax bears the legs and wings (Chapman, 2012).

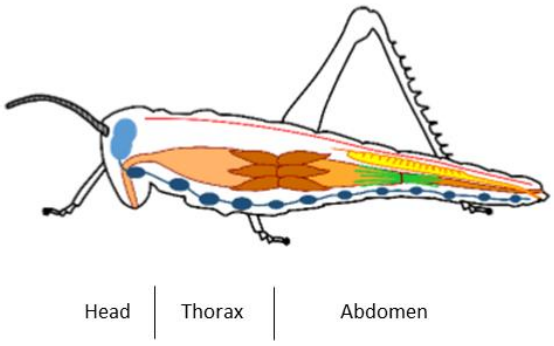

Figure 1.3: **Insect morphology and anatomy**. Schematic overview of the adult body plan and major anatomical features in insects. Light blue: brain, dark blue: ventral nerve cord, brown/orange: gut, green: Malpighian tubules, yellow: reproductive system, red: dorsal vessel (adapted from Lenaerts, 2017; PhD dissertation).

Also anatomically, insects show some common features (Figure 1.3). The major metabolic tissue, the fat body, can be found throughout the entire body. Besides playing a metabolic role, the fat body is also involved in nutrient storage and in female reproductive physiology (§1.3.2.2). Next, the trachea are located throughout the entire body as well. They transport gasses such as oxygen through a network of specialised tubes. The gut runs from the mouth to the anus and can be divided in three parts, *i.e*. the foregut, the midgut and the hindgut. The transitions between these three regions are marked by tubule-shaped structures. The gastric caeca occur between the foregut and midgut, but the presence of a digestive flow between both classifies the gastric caeca as part of the midgut. The Malpighian tubules can be found on the transition of the midgut to the hindgut and serve as excretory organs. Through their excretory function, the Malpighian tubules are categorised as part of the hindgut. The dorsal vessel runs along the dorsal midline of the insect and pumps the haemolymph from the abdomen towards the head. The head contains a part of the central nervous system, *i.e*. the brain and several ganglia whereas in the thorax and the abdomen, a series of connected ganglia forms the nerve cord, situated ventrally from the gut. The central nervous system controls and coordinates most physiological processes in insects via neuronal or neurohormonal signals. Neurohormones are produced in the neurosecretory cells of the brain whereafter they are subsequently transferred to neurohemal release sites, such as the corpora cardiaca (CC), for storage and secretion. The CC are also connected to the corpora allata (CA), a pair of specialised, small glands synthesising juvenile hormone (JH) (§1.4.2). The prothoracic glands (PG), synthesising ecdysteroids in juveniles, are located in the prothorax of insects, the first segment of the thorax (§1.4.1). The reproductive system can be found in the abdomen and will be discussed in more detail in §1.3.2.2 (Chapman, 2012).

1.3.2.1 Exoskeleton

The exoskeleton is a multi-layered structure and can be subdivided in a cuticle and epidermis, the latter being responsible for the production of the cuticle. The cuticle can be subdivided in three layers, *i.e*. endo-, exo- and epicuticle and is the outermost part of insects covering the outside of the body as well as ectodermal invaginations such as the foregut, hindgut and tracheal system. A downside of the exoskeleton, protecting the insect against desiccation and mechanical injury, is the near inextensibility of the cuticle. In order to grow, the cuticle must be shed and replaced. Moulting or ecdysis involves a sequence of events starting with the separation of the old cuticle from the underlying epidermal cells, a process called apolysis. Next, moulting fluid is produced and a new epicuticle is deposited. Subsequently, the digestion of the old endocuticle starts with the activation of enzymes found in the moulting fluid. At the same time, a new exo- and endocuticle is synthesized. At last, the shedding of the old cuticle takes place whereafter the new cuticle expands (Chapman, 2012).

1.3.2.2 Female reproductive physiology

Insect ovarioles can be classified into two major types that differ in the way that nutrients, RNAs and other products are supplied to the oocyte, *i.e*. meroistic or panoistic ovarioles. In meroistic ovaries, the germline cells give rise to both oocytes and nurse cells with nurse cells transferring their products to the developing oocyte with which they have a cytoplasmic connection (Figure 1.4A2 and 3).

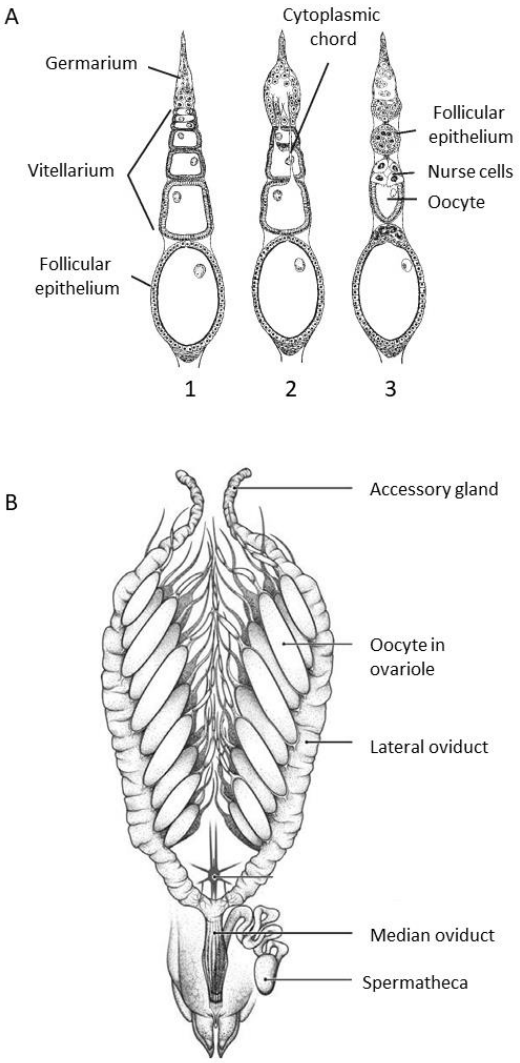

Figure 1.4: **Schematic representation of the female reproductive system**. (A) The three main types of insect ovarioles with 1. the panoistic ovariole, where the follicular epithelium nourishes the oocyte, 2. the telotrophic meroistic ovariole, where the nurse cells remain in the germarium and are connected to the descending oocyte via a cytoplasmic chord and 3. the polytrophic meroistic ovariole with the nurse cells contained within the follicle (adapted from Klowden, 2008). (B) The locust's female reproductive system with ovarioles containing oocytes at different developmental stages. All ovarioles are synchronized in their maturation as the terminal or basal oocytes undergo vitellogenesis simultaneously. The mature eggs pass into one of the two muscular later oviducts, carrying the accessory glands anteriorly, which merge in a posterior median oviduct. The end of the median oviduct contains the spermatheca (adapted from Lange, 2009).

In the panoistic type, every germline cell develops into an oocyte which is surrounded by a single layer of follicle cells (Figure 1.4A1). Furthermore, meroistic ovaries can be subdivided in telotrophic and polytrophic ovaries. In telotrophic meroistic ovaries, which are found in Hemiptera and basal Holometabola, such as Coleoptera, the nurse cells remain in the apex of the ovariole, the germarium, and are connected to the oocytes by nutritive chords (Figure 1.4A2). In polytrophic meroistic ovarioles, which occur in more distal Holometabola, such as Lepidoptera and Diptera, the nurse cells are anteriorly localized within the follicle, while remaining connected with the more posterior oocyte. This makes that nurse cells and oocytes alternate along the ovariole (Figure 1.4A3). The more ancestral panoistic type of ovarioles can be found in more primitive insect orders, such as the Dictyoptera and Orthoptera, which include locusts (Belles and Piulachs, 2015; Chapman, 2012; Klowden, 2008).

Adult female locusts have well-timed, hormonally controlled reproductive cycles. Only when the fully developed eggs are laid, a new cycle will start. Their reproductive system consists of two paired ovaries, each composed of several tubules, the ovarioles (Figure 1.4B). An ovariole contains oocytes at different developmental stages, still, all ovarioles are synchronized in their maturation, since the terminal or basal oocytes undergo vitellogenesis simultaneously (Lange and da Silva, 2007; Peel and Akam, 2007). The mature eggs pass into one of the two muscular lateral oviducts, which are anteriorly associated with the accessory glands and posteriorly merge into the median oviduct. Subsequently, the process of oviposition is initiated. The terminal segments of the female locusts' abdomen are long and telescopic, forming a type of ovipositor, playing a crucial role in oviposition. During digging, the ventral valves of the ovipositor lever the abdomen downwards while the upper valves push soil away. When a suitable hole has been constructed, egg deposition can begin (Chapman, 2012). During oviposition, the accessory glands are responsible for the production of a foamy substance, a requirement for both the attachment to the substratum and the production of a covering that protects the eggs from environmental conditions. At the end of egg deposition, the egg pod is capped with accessory gland secretions, which harden, still enabling the offspring to respire and hatch efficiently (Lange and da Silva, 2007; Szopa, 1980; Uvarov, 1977). The end of the median oviduct is connected with the spermathecal duct, releasing stored sperm right before oviposition, ensuring fertilisation of all eggs (Lange and da Silva, 2007).

The first gonadotropic cycle of female locusts can be divided in different stages, for which the rate of development is strongly determined by environmental factors. First, an early growth period during which the oocytes reach a length of 0.8 - 0.9 mm is observed followed by the previtellogenic stage, where oocytes grow until they reach about 1.8 mm. The vitellogenic stage is characterized by a process called patency, the shrinkage of the follicular epithelial cells, allowing passage of lipids and vitellogenin from the haemolymph into the developing oocytes. This allows the oocytes to grow until they reach a length of 7.5 mm followed by the formation of an egg shell during the choriogenic stage, ovulation and oviposition. All mature eggs are

deposited at once in one egg pod whereafter the next batch of oocytes enters the vitellogenic stage (Peel and Akam, 2007; Tobe and Pratt, 1975).

Resorption of oocytes, *i.e.* the destruction of oocytes in the ovarioles and the subsequent resorption of their content by the insect, may occur when an oocyte is at any developmental stage. However, it is most commonly observed when oocytes are in the vitellogenic stage of oocyte maturation. During resorption, the yolk spheres break down and protein, lipids and vitellogenins (or vitellins) are released from the oocyte and returned to the haemolymph. The follicle cells become folded on each other as the oocyte shrinks and finally collapse to form a resorption body which is coloured orange in Orthoptera. Resorption is a widespread phenomenon and mostly occurs under adverse conditions. However, in several insects, some degree of resorption is seen under apparently optimal conditions. *L. migratoria* females are known to resorb about 25 % of their oocytes, although an access to unlimited amounts of high-quality food was secured. Furthermore, the inability to produce or lay fertile eggs can also lead to resorption. When *S. gregaria* females are unable to copulate, a high rate of oocyte resorption was observed. Introducing mature males, producing a maturation pheromone, reduces the amount of resorption, even without mating taking place. At last, the absence of JH, which is known to play a role in the control of yolk accumulation in the oocytes, as discussed in §1.6.1, is also associated with resorption (Chapman, 2012).

1.4 The classic insect hormones

JH together with ecdysteroids are crucial endocrine regulators coordinating insect postembryonic development and reproduction. Their biosynthesis, mode of action and role in the regulation of the different insect processes will be discussed in more detail below.

1.4.1 Ecdysteroids

The moulting hormone ecdysone was first isolated in 1954 by Butenandt and Karlson (Butenandt and Karlson, 1954; Karlson, 1996). In juvenile insects, ecdysone is mainly produced by the PG, an endocrine organ expressing genes encoding ecdysone biosynthetic enzymes. Once released into the haemolymph, ecdysone is converted to the active form 20-hydroxyecdysone (20E) in peripheral tissues, such as the Malpighian tubules. This hormone binds to a nuclear receptor, initiating various processes associated with moulting and metamorphosis (Yamanaka et al., 2013). Besides the function in post-embryonic development, ecdysone is also important in the insects' reproductive physiology with the reproductive tissues as the main site of ecdysteroidogenesis.

Cholesterol and/or plant sterols are the universal precursors of steroid hormones. In contrast to vertebrate species, insects are not capable of synthesizing steroids from simple precursor molecules. Instead, they need

to ingest sterols via their diet, whereafter plant sterols (campesterol and sitosterol) are dealkylated to cholesterol (Gilbert et al., 2002; Gilbert and Warren, 2005). Next, a series of reactions results in the conversion of cholesterol to ecdysone and finally to the more active moulting hormone, 20E (Figure 1.5). The initial step in 20E biosynthesis is the conversion of cholesterol to 7-dehydrocholesterol (7dC). Next, 7dC is oxidized to diketol by a series of hypothetical, unidentified reactions, called the 'Black Box' with *a.o*. *Spook* (*Spo*, *Cyp307a1*) (Warren et al., 2009). Then, diketol is converted to ketodiol (2,22,25-trideoxyecdysone; 2,22,25dE) by a reduction at C3, followed by a series of hydroxylation reactions, catalysed by enzymes encoded by the *Halloween* genes (Niwa and Niwa, 2014). These genes belong to the family of the cytochrome P450 enzymes, known to catalyse hydroxylation reactions. Many intensive studies have identified and characterized the components responsible for those hydroxylation reactions. *Phantom* (*Phm*, *Cyp306a1*) encodes a 25-hydroxylase catalysing the reaction from ketodiol to ketotriol (2,22-dideoxyecdysone, 2,22dE) followed by *Disembodied* (*Dib*, *Cyp302a1*), encoding a 22-hydroxylase, mediating the conversion of ketotriol to 2-deoxyecdysone (Chávez et al., 2000; Niwa et al., 2004; Warren et al., 2004, 2002). In a next step, a 2-hydroxylase is encoded by *Shadow* (*Sad*, *Cyp315a1*) converting 2-deoxyecdysone to ecdysone (E) (Warren et al., 2002). The final hydroxylation of E to the active hormone, 20E occurs through the action of a 20-hydroxylase encoded by *Shade* (*Shd*, *Cyp314a1*) (Petryk et al., 2003).

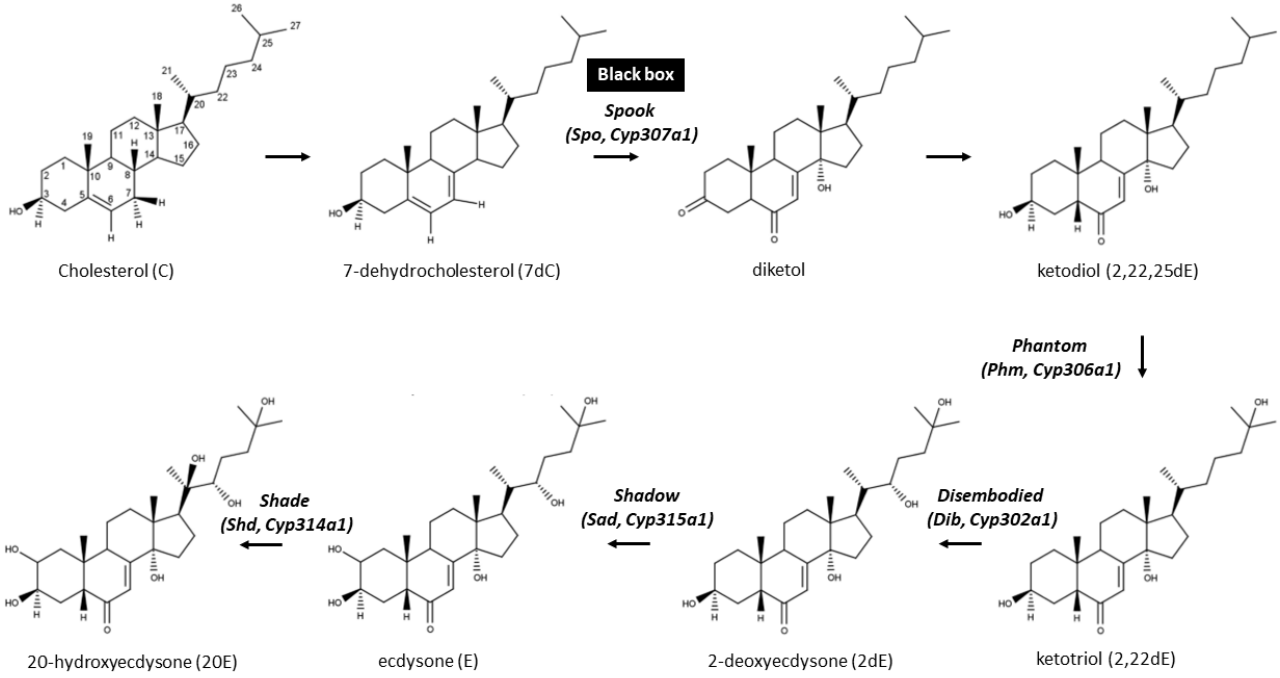

Figure 1.5: **Biosynthetic pathway of 20E in the fly *D. melanogaster***. The ecdysteroid biosynthesis pathway including the different cytochrome P450 enzymes involved in the conversion of cholesterol into the active 20E.

Subsequently, 20E binds to a nuclear receptor complex that consists of two dimerization partners, *i.e*. the Ecdysone Receptor (EcR) and Ultraspiracle (USP). Retinoid-X-receptor (RXR) is the hemimetabolan orthologue of USP. The resulting 20E/EcR/RXR complex binds to an ecdysone response element thereby

initiating transcription of the early, early-late and late response genes respectively, which in turn activate certain developmental processes such as the biosynthesis of a new cuticle (Hill et al., 2013). *Ecdysone-induced protein 74* and *75* (*E74* and *E75*), *Broad-Complex* (*BrC*) and *B lymphocyte-induced maturation protein 1* (*Blimp-1*) are classified as early genes (Agawa et al., 2007; Karim and Thummel, 1992). With a slight delay, the transcription of the early-late genes, such as *hormone receptor 39* and *3* (*HR39* and *HR3*), is initiated as well (Huet et al., 1995). These early and early-late genes are responsible for the transcription of the late genes, *e.g*. *fushi tarazu transcription factor 1* (*FTZ-F1*) (Parvy et al., 2005).

1.4.2 Juvenile hormones

A humoral factor preventing metamorphosis, the transition from the last larval to adult stage, was first discovered in the kissing bug, *Rhodnius prolixus,* in 1934 (Wigglesworth, 1934). Two years later, this humoral factor was unravelled by Wigglesworth as a juvenile hormone secreted by the CA (Wigglesworth, 1936). It still lasted several decades before the importance of this hormone in the reproductive physiology of insects was established as well (Wyatt and Davey, 1996). The site of JH biosynthesis, the CA, remains the same in juvenile and adult insect stages.

JH is a sesquiterpenoid, produced and secreted by a pair of specialized endocrine glands, the CA (Wigglesworth, 1936). As in most insects, the major circulating JH in the haemolymph of *L. migratoria* and *S. gregaria* is JHIII (Tawfik et al., 2000). Exceptions to this rule are the Lepidoptera (JH0, JHI, JHII) and Diptera (JHIII bisepoxide) (Goodman and Granger, 2005). Juvenile hormone biosynthesis starts with the mevalonate pathway, *i.e*. the conversion of acetyl-CoA to farnesyl pyrophosphate (FPP; Figure 1.6). Next, FPP is hydrolysed to farnesol which in turn is oxidized to farnesal and farnesoic acid, respectively. Farnesoic acid is finally converted to the active JH by means of an epoxidation and methyl transfer. The order in which these two final steps occur seems to be insect order dependent. In Orthoptera and Dictyoptera, FA is first methylated to methyl farnesoate (MF) followed by a C10,C11 epoxidation to the functional JH. In lepidopteran species, the epoxidation precedes the methylation (Defelipe et al., 2011). The two genes involved in these two last steps are *juvenile hormone acid methyl transferase* (*JHAMT*) and *MF epoxidase* or *cytochrome P450 enzyme 15A1* (*CYP15A1*), with JHAMT acting as the rate-limiting enzyme in JH biosynthesis (Huang et al., 2015; Marchal et al., 2011b; Mayoral et al., 2009; Shinoda and Itoyama, 2003).

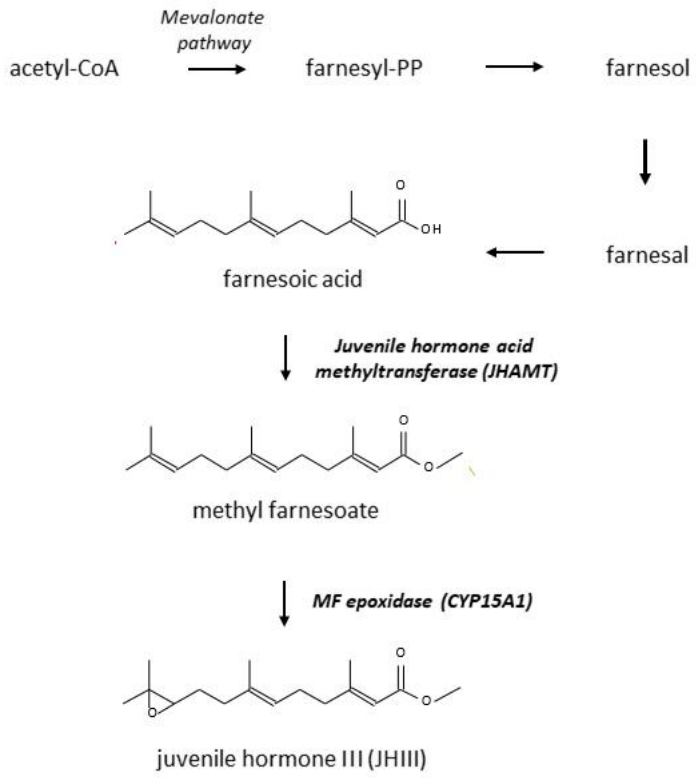

Figure 1.6: **Biosynthetic pathway of JH in Orthoptera and Dictyoptera**. The JH biosynthesis pathway with *JHAMT* converting farnesoic acid to methyl farnesoate via a methyl transfer followed by an epoxidation by *CYP15A1* resulting in the active JHIII.

JH biosynthesis must be strictly regulated to efficiently respond to the insects' developmental needs. The production and/or release of JH is mediated by at least two different classes of neuropeptides, the allatotropines (ATs) and allatostatins (ASTs), which stimulate or inhibit the CA, respectively (Weaver and Audsley, 2009). But, presumably, several more as yet unknown factors can also influence JH production and secretion.

The first AT was isolated from the nervous system of the tobacco hornworm, *Manduca sexta*. It was found to stimulate JH biosynthesis and its subsequent release from the CA *in vitro* (Kataoka et al., 1989). The downregulation or suppression of AT in *T. castaneum* and dipterans resulted in a disrupted adult development and fecundity or the stimulation of reproductive diapause respectively (Abdel-Latief and Hoffmann, 2014; Kang et al., 2014). However, recent research revealed that the action of AT may not be unidirectional with AT having a stimulatory effect on JH synthesis and release by suppression of the inhibition by short neuropeptide F (Yamanaka et al., 2008). Besides the stimulatory effect of ATs on JH biosynthesis by the CA in several insect species, ATs were found to prevent JH biosynthesis in adult female *B. mori* (Kaneko and Hiruma, 2015).

The widely pleiotropic ASTs are present in many insect orders, although, their role in inhibiting JH production is only observed in some insect groups. These allatostatic peptides originate from neurosecretory cells of the brain and are axonally transported to the CA. So far, three types of ASTs have been isolated in insects, named A, B and C-type ASTs also known as FGLa/ASTs, MIP/ASTs and PISCF/ASTs, respectively (Coast and Schooley, 2011). Type-A ASTs were first isolated from the Pacific beetle cockroach, *D. punctata,* where they rapidly and reversibly inhibit JH biosynthesis by the CA *in vitro* (Pratt et al., 1989; Woodhead et al., 1989). Currently, the role of type-A ASTs as inhibitors of JH production has been observed in only a few insect species such as crickets, termites and cockroaches (Elliott et al., 2009; Neuhäuser et al., 1994; Woodhead et al., 1989). Using recent molecular tools available in *D. melanogaster*, it was determined that type-A ASTs regulate growth and metamorphosis by controlling the secretion of insulin-like peptides and prothoracicotropic hormone (Deveci et al., 2019). Type-B ASTs were first isolated as myoinhibitory peptides (MIP) from the brain-CC-CA-suboesophageal ganglion complexes of the migratory locust, *L. migratoria* (Schoofs et al., 1991). Only later, an allatostatic activity was identified in *G. bimaculatus* and the role of type-B ASTs as negative regulators of JH biosynthesis appears to be confined to crickets (Lorenz et al., 1995). The type-C ASTs were first characterized in *Manduca sexta* (Kramer et al., 1991) and were shown to have allatostatic properties (Yiping Li et al., 2006). However, both allatostatic and allatotropic properties have also been observed in several insects. In mosquitoes and moths, type-C ASTs are potent inhibitors of JH biosynthesis (Audsley et al., 1999; Griebler et al., 2008; Jansons et al., 1996; Kaneko and Hiruma, 2014; Kramer et al., 1991; Yiping Li et al., 2006), whereas in *D. melanogaster*, a stimulatory effect of type-C ASTs on JH biosynthesis was observed (Wang et al., 2012). Moreover, both inhibitory and stimulatory effects of type-C ASTs on JH biosynthesis can be observed, depending on the age of the insects, suggesting a complex role of allatoactive neuropeptides in the regulation of JH biosynthesis (Abdel-latief and Hoffmann, 2010; Stay et al., 2002). For a more in depth review on the role of ATs and ASTs on JH biosynthesis, the reader is referred to Verlinden et al. (2015) and Bendena et al. (2020). Except for their role in regulating JH biosynthesis, the allatoregulatory peptides were suggested to also be involved in other reproductive physiology-related processes. Since (some) ASTs and their receptors are localized in the reproductive system of females, these peptides may also directly act on the reproductive system (Audsley et al., 2013; Lange, 2009a, 2009b; Lange et al., 2012; Schoofs et al., 1996). Moreover, ATs were shown to influence motility of some muscular structures of the reproductive system (Nouzova et al., 2012; Vuerinckx et al., 2011).

The JH signalling pathway was only recently described with the characterization of a genuine JH receptor, Methoprene-tolerant (Met). Met is a transcription factor belonging to the basic-helix-loop-helix (bHLH)/Per-Arnt-Sim (PAS) family (Charles et al., 2011; Wilson and Fabian, 1986). Binding of JH stimulates Met to become accessible to other bHLH-PAS proteins, such as Taiman (Tai), also known as steroid receptor co-activator (SRC) (Godlewski et al., 2006). The resulting JH-Met-Tai complex induces the expression of JH response genes, such as *Krüppel-homolog 1* (*Kr-h1*), mediating the anti-metamorphic effect of JH in several insect species

(Gujar and Palli, 2016a; Jindra et al., 2013; Konopova et al., 2011; K. L. Li et al., 2018; Lozano and Belles, 2011; Smykal et al., 2014a). Kr-h1, in turn, influences the expression of the early ecdysteroid response gene, *E93*, a key determinant promoting adult metamorphosis. In several holometabolan insects, an ecdysone response element (EcRE) was identified in the E93 sequence confirming the induction of E93 by ecdysone (Baehrecke and Thummel, 1995; Kayukawa et al., 2017; X. Liu et al., 2015; Ureña et al., 2014). The situation in hemimetabolan insects, including locusts, still has to be elucidated.

1.5 Regulation of moulting

1.5.1 Ecdysteroids and juvenile hormone

The transition from juvenile insect stages to fully reproductive adults is highly dependent on JH and ecdysteroids. Where the concentration of JH will determine the nature of the moult, periodic pulses of ecdysteroids trigger each moulting process (Riddiford, 2012). This ancestral regulatory mechanism by which JH inhibits metamorphosis is now defined as the MEKRE93 pathway. High JH titers (via binding to Met) induce expression of Kr-h1, which in turn represses the expression of *E93* resulting in a nymphal-to-nymphal transition. During the final nymphal stage, JH titers drop causing arrested Kr-h1 expression, which results in a strong induction of E93 through ecdysone signalling, triggering adult development (Belles, 2019). Moreover, it is confirmed that JH sensitivity during the immature life stages is restricted to several critical periods. This makes that the nature of the moult is not only defined by the presence or absence of JH, but is defined by the presence or absence of JH during these critical periods (Kikukawa and Tobe, 1986).

In order to successfully fulfil their role in moulting and metamorphosis, it is crucial that the biosynthesis of both hormones is strictly regulated, with the presence of certain cross-talks between these two classic insect hormones playing an important factor.

1.6 Regulation of female reproductive physiology

1.6.1 Ecdysteroids and juvenile hormone

Next to their role in juvenile insects, both ecdysteroids and JH are endocrine regulators of reproduction as well. The role of JH as a master regulating gonadotropin in insect female reproduction is established in phylogenetically basal species, such as orthopterans (the insect order to which locusts belong), while ecdysteroids seem to have taken over this leading role in some lepidopteran and most dipteran species (Huybrechts and De Loof, 1977; Raikhel et al., 2005; Roy et al., 2018). Several studies in multiple insect species confirmed the involvement of JH in lipid accumulation in the primary oocyte, vitellogenin synthesis in the fat body, regulation of mating and sex pheromone production (Bilen et al., 2013; Gujar and Palli, 2016b; Lin et al., 2015; Liu et al., 2016; Ma et al., 2018; Marchal et al., 2014; Naghdi et al., 2016; Parthasarathy et al., 2010; Saiki et al., 2015; Sheng et al., 2011; Smykal et al., 2014a; Tang et al., 2019; J. L. Wang et al., 2017; X. Wang

et al., 2017; Zou et al., 2013). Primarily, JH is known to act as the primary regulator of ovarian development by regulating the synthesis of vitellogenins (Vgs) in the fat body, the proteins forming most of the yolk found in the eggs (Wyatt and Davey, 1996). Moreover, via binding of JH to membrane receptor sites in the ovarian follicular epithelium, the shrinkage of cells is initiated in a process called patency (Davey et al., 1993; Jing et al., 2018; Sevala, V.L. & Davey, 1989; Sevala et al., 1995). Patency ensures that Vgs, which are mainly produced in the fat body and are released in the haemolymph, can be taken up by the developing oocytes. Furthermore, it is recently confirmed that JH is also responsible for boosting an oviduct derived Patency Inducing Factor which is involved in the initiation of patency in the terminal follicle via the pedicel (Seidelmann et al., 2016).

Besides JH, ecdysteroids play an important role in female reproduction as well. In adult females, they are produced in the ovarian follicular cell layer and appear to have multiple functions. They were reported to induce meiotic re-initiation in the oocyte (Lanot et al., 1987) and are incorporated as conjugates into the growing oocytes where they act as a source of ecdysteroids during embryogenesis (Isaac and Rees, 1984) as observed in *L. migratoria* and *S. gregaria*, respectively. Besides, in both locust species, these conjugates bind to vitellins, thereby preventing their leakage into the haemolymph (Isaac and Rees, 1984; Lagueux et al., 1981; Tawfik et al., 1999). Moreover, they also appear to play a role in reproductive diapause (Tawfik et al., 2002) and choriogenesis (Hult et al., 2015; Lenaerts et al., 2019a) as has been described in *L. migratoria* and in *D. punctata* and *S. gregaria*, respectively. Furthermore, in most dipteran and some hymenopteran and lepidopteran species, vitellogenesis is regulated by ecdysteroids. In these insects, ecdysteroids seem to have taken over the role of JH as a master regulating gonadotropin in insect female reproduction (Raikhel et al., 2005; Roy et al., 2018).

1.6.2 (Neuro)peptides

The insulin signalling pathway (ISP), sensing nutrient status, plays an important role in female reproduction as well, determining the trade-off between reproduction and survival in insects, positively controlling vitellogenesis and oocyte growth (Lenaerts et al., 2019c; Mirth et al., 2019). The role of JH and/or ecdysteroids in mediating the action of ISP remains unclear. Presumably, an intricate cross-talk exists between insulin-related peptide (IRP), JH and ecdysteroids, with the insect's nutritional status as a key determinant. Moreover, also other (neuro)peptides are demonstrated to be involved in the regulation of locust reproductive physiology.

1.6.2.1 Ovary maturating parsin

The ovary maturating parsin (OMP) from *L. migratoria* was the first gonadotropic neurohormone identified in insects. This neurohormone was isolated from the pars intercerebralis, based on its gonadotropic effects

(Girardie et al., 1991). Stimulated oocyte growth and vitellogenesis as well as precocious appearance of haemolymph ecdysteroids were witnessed upon daily injecting OMP in adult female locusts (Girardie et al., 1991; Girardie and Girardie, 1996). Several years later, some OMP-isoforms were purified from *S. gregaria* (Girardie et al., 1998). In 2012, two highly similar *S. gregaria* OMP-diuretic hormone precursor cDNAs were cloned by Van Wielendaele and coworkers, both encoding an OMP-isoform as well as a member of the corticotropin releasing factor-like diuretic hormone peptide family. When injecting dsRNA against the OMP and diuretic hormone containing precursor in adult female desert locusts, *i.e.* knocking down both OMP and diuretic hormone, resulted in a stimulation of oocyte growth as well as precocious ecdysteroid production. Likely, the reduced corticotropin releasing factor/diuretic hormone signalling resulting from this knockdown had overruled the effect of an OMP depletion (Van Wielendaele et al., 2013, 2012).

1.6.2.2 Insulin-related peptides

The first discovered insect insulin-like molecule was bombyxin, derived from the silk moth, *Bombyx mori* (Nagasawa et al., 1984b, 1984a, 1980). Subsequently, another insect insulin-like peptide was identified in Orthoptera. More specifically, IRPs were discovered in the pars intercerebralis-CC neurohaemal complex of locusts (Hetru et al., 1991; Hietter et al., 1990; Laguex et al., 1990). Later, they were also identified in other insect species and the importance of the insulin/IRP signalling pathway in a variety of physiological processes, including reproduction, was demonstrated (as reviewed by Claeys et al. (2002)). In *S. gregaria*, an increase in *SgIRP* transcript levels can be observed during specific reproductive events such as vitellogenesis and the intensive growth of the oocytes (Badisco et al., 2008). Moreover, lower *SgVg* transcript levels and smaller oocytes were observed upon knocking down *SgIRP*. In dipterans, the yellow fever mosquito, *A. aegypti*, the fruit fly, *D. melanogaster*, the German cockroach, *B. germanica,* and the red flour beetle, *T. castaneum*, insulin-like peptides (ILPs) are involved in multiple reproductive processes, from stimulating egg production, inducing vitellogenin production in the fat body and yolk uptake by the developing eggs to stimulating ecdysteroid production in the ovaries and regulating JH biosynthesis (Abrisqueta et al., 2014; Brown et al., 2008; Gulia-Nuss et al., 2011; LaFever and Drummond-Barbosa, 2005; Roy et al., 2007; Tatar et al., 2001; Tu et al., 2005, 2002; Wen et al., 2010). Moreover, it was shown in *T. castaneum* that JH is able to regulate ILP synthesis as well, which in turn regulates Vg synthesis (Sheng et al., 2011).

1.6.2.3 Neuroparsins

Neuroparsins (NPs) were discovered as anti-gonadotropic factors in female reproductive physiology of locusts, showing activities opposite to these of JH (Badisco et al., 2007; Girardie et al., 1998, 1989). The first NP was isolated from the CC of the migratory locust, *L. migratoria*, and displayed inhibitory effects on oocyte growth (Girardie et al., 1989). Later on, the amino acid sequence of the *S. gregaria* NP was determined by Girardie et al. (1998). More recently, four *S. gregaria* neuroparsin precursors (*Sg*NPPs) were identified from

brain (*Sg*NPP1 and 2) and fat body (*Sg*NPP3 and 4) tissues (Badisco et al., 2007). They belong to a conserved family of arthropod peptides and share sequence similarity with the binding region of vertebrate insulin-like growth factor binding proteins (IGFBP). Moreover, in *S. gregaria*, NP4 is capable of interacting with IRP *in vitro* (Badisco et al., 2008). A consistent cross-talk between *Sg*NP and *Sg*IRP signalling is suggested *in vivo* as well and seems to be situated downstream of JH (Gijbels et al., 2019).

1.7 The RNAi pathway

The mechanism of RNA interference (RNAi) was elucidated in the nematode *C. elegans*. With only several dsRNA molecules delivered into a cell, a complete inhibition of gene expression was obtained (Fire et al., 1998). This discovery establishes the study of regulatory RNAs. Small RNA molecules (*ca*. 18-31 nucleotides long) bind to complementary regions situated in longer RNAs in order to post-transcriptionally silence gene expression through cleavage or blockage of these longer RNAs (Siomi and Siomi, 2009). They can be classified based on their origin, biogenesis, structure and role in three main cell-autonomous pathways: i) PIWI-interacting RNAs (piRNAs), ii) small interfering RNAs (siRNAs) and iii) miRNAs. Throughout this thesis, a short introduction is given on piRNAs whereas the siRNA and miRNA pathways are discussed in more detail.

1.7.1 PIWI-interacting RNAs

PIWI-interacting (pi)RNAs are a novel type of non-coding small RNAs, which are highly enriched in the germline. They are longer than siRNAs and miRNAs (*ca*. 24-31 nucleotides long) and are processed from a single-stranded precursor via a Dicer-independent mechanism. In *Drosophila*, two classic biogenesis pathways have been discovered, *i.e.* the primary processing pathway and the secondary processing pathway, also known as the ping-pong cycle. Furthermore, they bind to Piwi, Aub and Ago3, another class of Ago proteins in the PIWI subfamily. PiRNAs mainly regulate the activity of transposable elements at the transcriptional and post-transcriptional level. For a more in depth view on the piRNA pathway, the reader is referred to Kolliopoulou et al. (2019) and Li et al. (2019).

1.7.2 Small interfering RNAs

The siRNA pathway defends the organism against invading viruses. When viruses replicate, double-stranded RNA (dsRNA) molecules are emitted into the cytoplasm, which are subsequently recognized by the insect cell, thereby activating the siRNA pathway (Figure 1.7). In a first step, Dicer-2 processes the dsRNA molecules into siRNAs of *ca*. 18-24 nucleotides long which are further cleaved by an Ago-2 protein containing RNA induced silencing complex (RISC). Dicer-2 is classified as an RNase type III enzyme as the siRNAs show characteristics of a RNase type III mediated cleavage, *i.e*. generating cleavage products with a 5’ phosphate group, a 3’ hydroxyl group and a 2-nucleotide overhang at the 3’ end (Bernstein et al., 2001; Kim et al., 2009). In a following step, the siRNA passenger strand is degraded by the RISC, whereas the siRNA guide strand,

which is complementary to the target gene, can fulfil its function. The mechanism of strand selection and the possible role of Dicer-2 in this process remains unclear, but the thermodynamic stability of both strands seems to be essential. The strand whose 5'-end is situated at the less thermodynamically stable end of the helix is preferentially loaded as the guide strand (Czech et al., 2009; Khvorova et al., 2003; Schwarz et al., 2003).

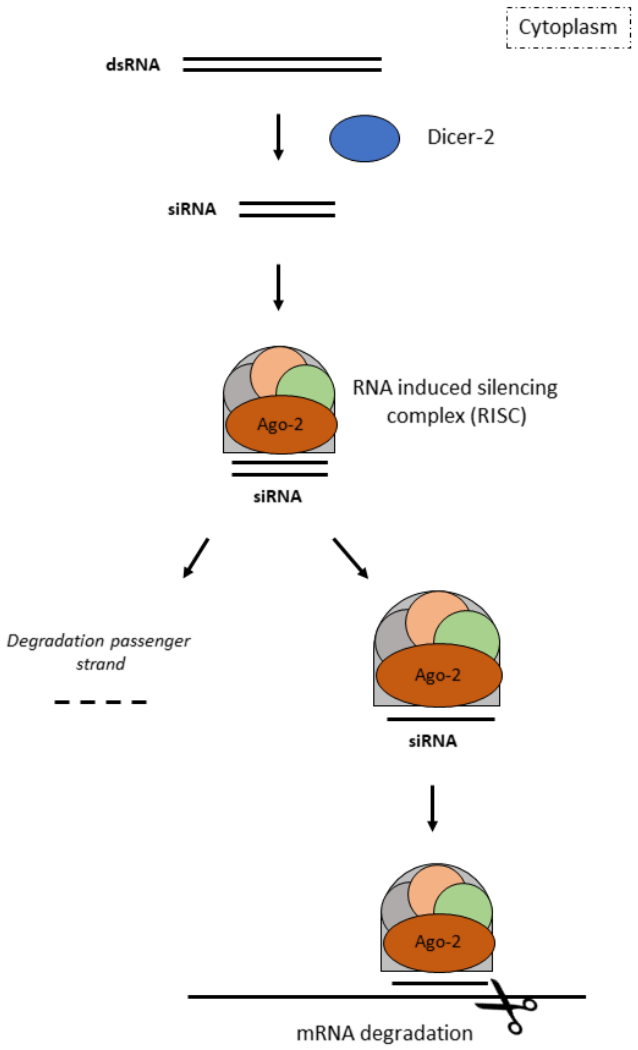

Figure 1.7: **Schematic representation of the siRNA pathway**. The siRNA pathway is triggered by dsRNA molecules, which are recognized in the cytoplasm and processed into siRNAs by Dicer-2. Further cleavage is exerted by RISC containing an Ago-2 protein, encompassing the siRNA guide strand and degrading the siRNA passenger strand. The resulting siRNA/RISC complex further directs degradation of cognate mRNAs.

Remarkably, researchers succeeded in triggering this RNA silencing mechanism in several insect species by artificial administration of gene-specific long dsRNA, either via injection in the body cavity or simply via feeding. This dsRNA treatment, called RNAi, can result in functional knockdown effects since the siRNA pathway is being misled to target an endogenous transcript instead of a viral one. Moreover, in some insect species, administration of dsRNA can result in an RNAi response throughout the entire body, also known as systemic RNAi. Furthermore, because of the specificity of RNAi, it holds great potential in the species-specific

control of pest insects and to combat viral infections in disease-vectoring and beneficial insects as well. These interesting observations make RNAi one of the most widely used reverse genetics research tools in insects (as reviewed by Vogel et al. (2019).

1.7.3 MicroRNAs

MiRNAs are small (*ca*. 21 nucleotides long), non-coding RNA molecules, first reported in *C. elegans* to regulate timing of development (Lee et al., 1993). Shortly thereafter, numerous miRNAs have been found in worms as well as in flies, plants and vertebrates. These discoveries established miRNAs as a new class of small non-coding regulatory RNAs (Bartel, 2004; Lagos-Quintana et al., 2001; Lee and Ambros, 2001) and ever since, thousands of new miRNAs have been discovered playing key roles in presumably all physiological processes. Also in insects, miRNAs are being intensively studied. On miRBase (Release 22.1), already 4795 mature miRNAs are recorded in 31 insect species (Griffiths-Jones, 2018). However, almost half of the recorded miRNAs are from *Drosophila* species, suggesting that the study of miRNAs in other insect species is still less established.

1.7.3.1 MiRNA biogenesis

MiRNAs belong to the non-coding small RNAs, playing a significant role in the post-transcriptional regulation of gene expression (Figure 1.8). In insects, miRNA biogenesis is initiated in the nucleus where RNA polymerase II mediates the transcription of miRNA loci (Rodriguez et al., 2004). Next, these transcripts fold into a hair-loop structure, the primary miRNA (pri-miRNA). This pri-miRNA is processed by a Drosha/Pasha microprocessor complex in order to form a precursor miRNA (pre-miRNA) (Denli et al., 2004; Gregory et al., 2004), which is subsequently transported out of the nucleus into the cytoplasm by RanGTP/Exp-5. Usually, the pre-miRNA contains a 2-nucleotide overhang at the 3’ end, which is crucial for the nuclear transport (Lund, 2004). In the cytoplasm, the ribonuclease III Dicer-1 (Knight and Bass, 2001) processes the pre-miRNA into a miRNA duplex which is loaded into an RNA induced silencing complex (RISC). In here, strand selection occurs where after the miRNA guide strand targets mRNA via complementary base pairing (Miyoshi et al., 2009). The passenger strand is degraded (Okamura et al., 2004). The mechanism of strand selection depends on the thermodynamic stability of each end of these duplexes. In *D. melanogaster,* the selected strand was thermodynamically unstable, due to bulges in the region of nucleotide seven to 11, and was characterized by a 5’ terminal uracil (Okamura et al., 2009). The expression levels of cognate mRNAs are regulated either by translational blockage or by cleavage via an Argonaute (Ago), the catalytic component located in the RISC (Miyoshi et al., 2009). The level of sequence complementarity between the miRNA and the target sequence determines the type of regulation with the seed region, a contiguous string of at least six nucleotides starting from position two of the miRNA’s 5’ end, playing an essential role (Ellwanger et al., 2011).

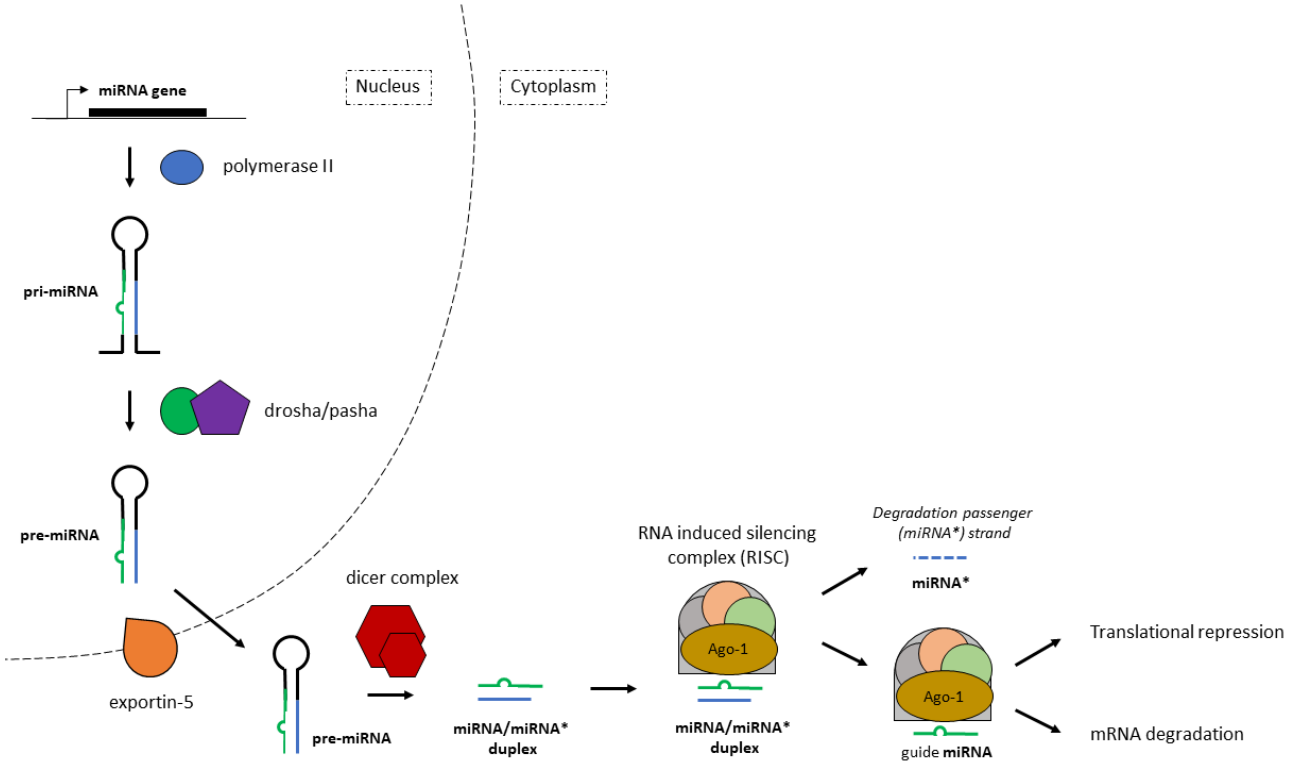

Figure 1.8: **Schematic representation of the miRNA pathway**. The miRNA pathway is initiated by the transcription of miRNA loci. The resulting primary miRNAs (pri-miRNAs) are processed by Drosha/Pasha to precursor miRNAs (pre-miRNAs) which are subsequently exported out of the nucleus by Exportin-5. Dicer-1 completes the processing and delivers the mature miRNA/miRNA* duplex to the Ago-1 containing RISC. The passenger strand is degraded whereas the guide miRNA directs translational repression or degradation of the cognate mRNA.

1.7.3.2 Evolutionary conservation of miRNAs

Previously, miRNA evolution has been linked to developmental innovations. Ylla et al. (2016) showed that the variation of insect miRNAs is an artefact mainly resulting from poor sampling and inaccurate miRNA annotation. They demonstrated that insects share a conserved miRNA toolkit of 65 families exhibiting low variation. For example, the acquisition of only three and the loss of only one miRNA family was witnessed during the evolutionary shift towards a complete metamorphosis. On the other hand, Belles (2017) assumed that the innovation of the pupal stage and the dramatically derived morphology exhibited by holometabolan larvae would require the concourse of new miRNA families. The study of these new miRNAs will reveal new and specific functions in holometabolous metamorphosis.

MiRNAs can be grouped into families according to sequence similarity, especially in the seed region. A relevant example of such a miRNA family is the let-7 family. In most insects investigated to date, let-7, miR-125 and miR-100 are encoded by the same primary transcript. This miRNA cluster was repeatedly associated with the regulation of insect metamorphosis, as reported in several model species from cockroaches to flies (Roush and Slack, 2008). Interestingly, these miRNAs are among the evolutionary oldest miRNAs, as they are even conserved in mammals, including humans (Fromm et al., 2015). By contrast, miR-2 [belonging to the

miR-2 family (miR-2, miR-13a and miR-13b)] controls the JH signalling pathway through Kr-h1 in the cockroach species *B. germanica*, ensuring a correct nymphal-to-adult moult. However, the holometabolan species studied to date do not possess a miR-2 target site in their *Kr-h1* mRNA, which implies that the above mechanism was lost in holometabolans. For a more in depth view on the evolutionary conservation of insect miRNAs, the reader is referred to Ylla et al. (2016) and Belles (2017).

1.7.3.3 MiRNAs regulating insect development

AgomiRs and antagomiRs, *i.e.* chemically modified miRNA mimics and inhibitors, respectively, are widely used for *in vivo* functional studies of miRNAs. AgomiRs and antagomiRs can be introduced either via injection into the body cavity or via feeding, depending on the insect used. A 3' terminal cholesterol modification ensures proper uptake of the agomiR/antagomiR, whereas thiol- and OMe-modifications guarantee stability when introduced in the insects' harsh extracellular environment (X. Wang et al., 2013).

Nowadays, it is well accepted that miRNAs play a crucial role in almost all biological processes. By studying insect development, it already becomes evident that elucidating the roles of miRNAs can be quite complicated. Previous studies have reported the involvement of insect miRNAs in insecticide resistance (Li et al., 2015) and insect-pathogen interactions (Asgari, 2013; Belles, 2017; Hussain and Asgari, 2014, 2010; P. Wu et al., 2016; Zhang et al., 2009). Moreover, studies have shown that miRNAs have a modified expression in different developmental stages as well as in different tissues of insects (Aravin et al., 2003; Behura and Whitfield, 2010; Cristino et al., 2011; Yu et al., 2008). The study by Zhang et al. (2015) nicely illustrates these findings as they found three miRNAs, *i.e*. miR-10-1a, miR-4924 and miR-9, to be differentially expressed during larval stages of *Spodoptera exigua*. Oral feeding experiments using synthetic miRNA mimics resulted in suppressed growth of *S. exigua* and mortality. Rubio et al. (2012) found three miRNAs to be important in the metamorphic stage (N6) of *B. germanica*, *i.e*. let-7-5p, miR-100-5p and miR-125-5p, whereas miR-252-3p appeared to be important in the pre-metamorphic stage (N5). Depletion of miR-252-3p levels in the penultimate (N5) nymphal stage caused retarded growth and developmental delays within the nymphal stage. Furthermore, insect miRNAs are also known to play an important role in the regulation of embryonic development (Freitas et al., 2017; Ninova et al., 2016), reproduction (Epstein et al., 2017; Lucas et al., 2015; Zhang et al., 2016) and tissue development (Bejarano et al., 2010; Karres et al., 2007; Li et al., 2014; Li and Carthew, 2005; Yan Li et al., 2006; Ling et al., 2017; Lucas et al., 2015; Sokol and Ambros, 2005; B. Zhao et al., 2017).

When focussing on moulting and metamorphosis, the best-known layer of regulation is the endocrine, which is based on the effects of JH and ecdysteroids, but recently, another layer of regulation is discovered based on miRNAs. It is already shown that several miRNAs target genes in the ecdysone and JH cascade, thereby regulating these processes (Belles, 2017; Gomez-Orte and Belles, 2009; Ling et al., 2014; Sokol et al., 2008;

Wu et al., 2017). Silencing the expression of *Dicer-1* in the penultimate nymphal stage of the hemimetabolan cockroach, *B. germanica*, resulted in a depletion of miRNA contents in the last nymphal stage. This, in turn, inhibited metamorphosis after the next moult as the resulting insects showed nymphoid features and were able to moult again (Gomez-Orte and Belles, 2009). Five years later, Lozano et al. (2015) showed that the miRNAs involved are those of an miR-2 family with the transcription factor Kr-h1 as target. A similar phenomenon was observed when silencing *Dicer-1* in *L. migratoria*, with reduced miRNA contents disrupting both nymphal-to-nymphal and nymphal-to-adult moults (Y. L. Wang et al., 2013). However, a role of the miR-2 family miRNAs in targeting Kr-h1 was not demonstrated. Application of let-7 and miR-278 mimics (agomiRs), on the other hand, significantly reduced the level of Kr-h1 transcripts resulting in partially precocious metamorphosis in *L. migratoria* nymphs as well as markedly decreased yolk protein precursors, arrested ovarian development and blocked oocyte maturation in adults (Song et al., 2018). Jayachandran et al. (2013) demonstrated by oral feeding of miRNA inhibitors and mimics that miR-2002b plays a role in fecundity and metamorphosis in *Helicoverpa armigera*. Likewise, Chen et al. (2013) demonstrated the importance of miR-8-5p and miR-2a-3p in regulating the chitin biosynthesis pathway in response to 20E signalling in *N. lugens*. He et al. (2017) found seven miRNAs involved in ecdysteroid biosynthesis in *Chilo suppressalis*. Overexpression of miR-9b, novel-260, bantam, novel-154, novel-80, novel-89 and novel-257 reduced the titer of 20E, induced mortality and retarded development. Subsequent treatment with 20E rescued these phenotypes. Although a different number of miRNAs have been studied in relation to insect metamorphosis, the miR-100/let-7/miR-125 cluster is repeatedly associated with the regulation of this process (as reviewed by Belles, 2017). Interestingly, a miRNA regulating phase transition in the migratory locust, *L. migratoria*, has been reported as well. Genes involved in dopamine synthesis have been shown to regulate the transition between the gregarious and solitary phases. Yang et al. (2014) reported the involvement of miR-133 in dopamine production and subsequently the behavioural transition by negatively regulating two critical genes (*henna* and *pale*) in the dopamine pathway. For a more in depth view on the different examples, the reader is referred to Li et al. (2019) and Belles (2017).

Recently, the study by Yogindran and Rajam (2020) demonstrated the use of an artificial miRNA mediated gene silencing approach to generate insect resistant tomato plants. Continuous feeding on tomato leaves expressing the miRNA-319a targeting the ecdysone receptor gene of the target pest, *Helicoverpa armigera*, affected the overall growth and survival of this lepidopteran species. Moreover, the expression of downstream genes involved in the ecdysone signalling pathway was affected. These results established the crucial role of EcR in insect development and the effectiveness of the artificial miRNA technology for efficient control of *H. armigera*.

1.7.3.4 Extracellular presence

Regulatory RNA pathways are traditionally described at an intracellular level. Nevertheless, miRNAs have been observed extracellularly as well, in the biological fluids of some plants and animals (Etheridge et al., 2013; Makarova et al., 2015). These extracellular miRNAs (ex-miRNAs) were mainly studied in mammalian systems due to their potential as biomarkers for *a.o*. several types of cancer, viral infections, cardiovascular diseases and brain and liver damage (Acuña et al., 2020; Javidi et al., 2014; Kawano et al., 2013; Sayed et al., 2014; Turchinovich et al., 2011). Given the high RNase activity found in the extracellular environment, questions regarding the stability of these miRNAs remain to be answered. Recent studies reveal that circulating ex-miRNAs appear to be extremely stable (Chen et al., 2008; Turchinovich et al., 2016, 2011) and are protected against plasma RNase activity (Mitchell et al., 2008). The hypothesis that ex-miRNAs are protected by encapsulation in extracellular vesicles (EVs) was recently confirmed, since many miRNAs were found to co-purify with exosomes and microvesicles (Turchinovich et al., 2015; Valadi et al., 2007). Moreover, miRNAs have been observed in EVs from human blood to basically all other extracellular fluids such as cerebrospinal fluid, saliva, breast milk, urine and semen (Amanda et al., 2010; Chen et al., 2008; Delić et al., 2016; El-Khoury et al., 2016; McDonald et al., 2013; Vojtech et al., 2014; Zhang et al., 2013; Zhao et al., 2019; Zhou et al., 2011). Besides being EV-encapsulated, ex-miRNAs were also found in complexes with proteins of the Ago family. In fact, 95 to 99 % of ex-miRNAs found in mammalian plasma, serum and cell culture media are rather bound to the remarkably stable Ago proteins (Arroyo et al., 2011; Turchinovich et al., 2015).

Despite the progress made in elucidating the role of ex-miRNAs in mammalian extracellular fluids, little is known about this in other organisms. So far, only a few studies reported on the presence of ex-miRNAs in insects. In the honey bee, *Apis mellifera*, it has been demonstrated that caste determination can be regulated by ex-miRNAs found in worker and royal jellies. When supplementing an artificial diet fed to queen larvae with miRNAs which were more abundant in worker jelly, the phenotype of the adult queen was affected towards a worker phenotype (Guo et al., 2013). In *Drosophila*, ex-miRNAs were discovered which were RNase resistant, reflecting the situation in humans. They were suggested to reside in fractions which confer their protection (Dhahbi et al., 2016). Moreover, Dhahbi et al. (2016) also demonstrated that ex-miRNAs reflect the physiological status, as they accumulate in an age-dependent manner. In 2018, our lab demonstrated the presence of ex-miRNAs in the cell-free culture media of two *Drosophila* cell lines, more specifically in EVs and in extracellular Ago-1 containing immunoprecipitates (EAgo-1). This study is the first report in insects confirming the association of ex-miRNAs with the same fractions as found in mammals (Van den Brande et al., 2018). The study also showed that the miRNA profiles identified in cells and in their EVs are distinct, suggesting selective secretion of ex-miRNAs. Two years later, our lab also demonstrated the presence of ex-miRNAs, amongst a wide variety of other small non-coding RNAs, in EVs of *Tribolium castaneum* TcA cells (Mingels et al., 2020). Furthermore, a recent study showed that larvae of the parasitoid wasp, *Cotesia vestalis*, growing in their host, secrete miRNAs that silence the host's ecdysone receptor to arrest its growth

(Wang et al., 2018). The mechanism(s) by which certain miRNAs are selected and potentially modified to be encapsulated remains to be elucidated. However, for human cell cultures, several hypotheses have been proposed. The heterogenous nuclear ribonucleoprotein A2B1, which recognizes and binds specific sequence motifs, is found to be over-represented in ex-miRNAs, directing them to be loaded into EVs (Villarroya-Beltri et al., 2013). Furthermore, post-transcriptional modification could be essential as well, since 3'-uridylated miRNAs were found to be enriched in EVs. In contrast, 3'-adenylated miRNAs resided more intracellularly (Koppers-Lalic et al., 2014).

1.8 Outline of this thesis

To investigate the presence of ex-miRNAs in insects and, if this would be the case, to further examine whether these ex-miRNAs would also reside in similar extracellular fractions as recently demonstrated in mammals, the cultured media of two *Drosophila* cell lines were studied in Chapter two. Moreover, to identify ex-miRNAs that potentially might play a role in intercellular communication in insects, haemolymph samples of early *versus* late fifth nymphal *L. migratoria* were examined in more detail in Chapter three. To resolve the lack of knowledge about the post-transcriptional regulation of MEKRE93 pathway components in insects, thereby regulating postembryonic development, miRNA agomiRs and antagomiRs, respectively mimicking and inhibiting the effects of miRNAs, were administered to *L. migratoria* nymphs to evaluate subsequent effects on moulting (Chapter three).

In order to achieve a better knowledge of the JH signalling pathway in the pest species *L. migratoria* and *S. gregaria*, we decided to investigate in more detail the role of MEKRE93 pathway components in regulating postembryonic development in juvenile locusts and promoting reproduction in adults. Using RNAi, the function of the JH receptor, Met, the downstream transcription factor, Kr-h1, and the ecdysteroid-inducible early gene, *E93*, as well as the functional interactions with other signalling pathways were thoroughly examined in Chapters four, five and six.

The main conclusions, general discussion and future perspectives will be presented in Chapter seven.

Chapter 2: The presence of extracellular microRNAs in the media of cultured *Drosophila* cells

This chapter was based on:

Van den Brande, S*., Gijbels, M*., Wynant, N., Santos, D., Mingels, L., Gansemans, Y., Van Nieuwerburgh, F. and Vanden Broeck, J. (2018). The presence of extracellular microRNAs in the media of cultured *Drosophila* cells. Sci. Rep. 8, 17312. (*equally contributing first authors)

2.1 Introduction

Non-coding small RNAs play a significant role in regulating gene expression in various organisms. One main class of these are the microRNAs (miRNAs) which were first reported in *Caenorhabditis elegans* to regulate timing of development (Lee et al., 1993). Since then, thousands of new miRNAs have been discovered in a wide range of metazoan species, with key roles in presumably every biological/physiological process (Berezikov, 2011; Caygill and Johnston, 2008; Chawla and Sokol, 2011; Gomez-Orte and Belles, 2009; Jayachandran et al., 2013). Until now, a substantial number of insect miRNAs has been recorded in miRBase (Release 21.0): more than 3000 miRNAs are already identified in 26 insect species (Griffiths-Jones et al., 2006).

MiRNAs are small, *ca*. 21 nucleotides (nt) long, non-coding RNA molecules playing a crucial role in the post-transcriptional regulation of gene expression. The miRNA biogenesis pathway in insects starts in the nucleus and consists of several steps. In brief, RNA polymerase II mediates the transcription of miRNA loci (Rodriguez et al., 2004). The resulting transcripts fold into a hair-loop structure, called the primary miRNA, which is processed in the nucleus by the Drosha/Pasha microprocessor complex to form a precursor miRNA (pre-miRNA) of approximately 70 nt (Denli et al., 2004; Gregory et al., 2004). Subsequently, this pre-miRNA is transported into the cytoplasm by RanGTP/Exp-5 (Lund, 2004), where the ribonuclease III Dicer-1 (Knight and Bass, 2001) processes it into a miRNA duplex. This duplex is loaded into an RNA induced silencing complex (RISC) where strand selection occurs (Miyoshi et al., 2009). The miRNA guide strand targets messenger RNA (mRNA) via complementary base pairing, whereas the passenger strand is degraded (Okamura et al., 2004). The resulting miRNA-RISC regulates the expression levels of cognate mRNAs either by translational blockage or by cleavage via its catalytic component, an Argonaute (Ago) protein (Miyoshi et al., 2009). This regulation is highly dependent on the level of sequence complementarity between the miRNA and the target sequence, especially in the seed region, a contiguous string of at least six nt starting from position two of the miRNA's 5' end (Ellwanger et al., 2011). In insects, miRNAs associate with Ago-1 to mediate gene regulation (Miyoshi et al., 2009) while siRNAs interact with Ago-2 for antiviral immunity (Vodovar and Saleh, 2012). Mammals, however, obtained an adaptive immune response through evolution and do not seem to strongly rely on siRNA-mediated antiviral immunity; hence, mammalian Ago-2 mainly associates with miRNAs (Wynant et al., 2017).

Even though regulatory RNA pathways are traditionally described at an intracellular level, miRNA molecules have also been observed in the biological fluids of some plants and animals (Creemers et al., 2012; Etheridge et al., 2013). In recent years, these extracellular miRNAs (ex-miRNAs) were extensively studied in mammalian systems due to their potential as biomarkers for several life threatening conditions (Javidi et al., 2014). In this context, many studies report on the presence of specific circulating miRNA repertoires in several types of

cancer, cardiovascular diseases, viral infections, as well as in brain and liver injury (Javidi et al., 2014; Kawano et al., 2013; Sayed et al., 2014; Turchinovich et al., 2011).

Given that extracellular fluids contain high levels of RNase activity, the stability of ex-miRNAs in blood plasma was investigated. Incubation of synthetic miRNAs in human plasma resulted in their rapid degradation, while endogenous plasma miRNAs remained stable, suggesting that they are protected against plasma RNase activity (Mitchell et al., 2008). Moreover, circulating ex-miRNAs appeared to be extremely stable as they can survive multiple freeze-thaw cycles, extreme variations in pH, boiling and extended storage (Chen et al., 2008; Turchinovich et al., 2016, 2011). Although the mechanism for this remarkable stability was initially unclear, it has been observed that many miRNAs co-purify with exosomes and microvesicles exported by cultured mammalian cells. This raised the hypothesis that ex-miRNAs are protected by encapsulation in extracellular vesicles (EVs) (Turchinovich et al., 2015; Valadi et al., 2007). Likewise, miRNAs have been observed in EVs from human blood and basically all other extracellular fluids, such as semen, urine, cerebrospinal fluid, saliva and breast milk (Amanda et al., 2010; Chen et al., 2008; Delić et al., 2016; El-Khoury et al., 2016; McDonald et al., 2013; Vojtech et al., 2014; Zhang et al., 2013; Zhou et al., 2011).

Nevertheless, the assumption that only EV-encapsulated miRNAs are present in biological fluids was challenged by the observation that 95-99% of ex-miRNAs are EV-free but rather bound to proteins of the Ago family in mammalian plasma, serum and cell culture media (Arroyo et al., 2011; Turchinovich et al., 2015). In addition, the fact that mature miRNAs are associated with the (remarkably stable) Ago proteins to mediate RNAi intracellularly can explain the persistence of Ago-associated miRNAs in harsh extracellular environments (Turchinovich et al., 2015).

In this context, progress has been made regarding the role of ex-miRNAs in mammalian fluids. Multiple studies describe the absence of numerous miRNAs in human plasma and conditioned media, although the miRNAs are present intracellularly, suggesting controlled secretion (Shurtleff et al., 2016; Turchinovich et al., 2011). Moreover, the functional transfer of exosomal mRNA and miRNA to recipient mammalian cells has also been demonstrated (Lotvall and Valadi, 2007; Valadi et al., 2007). Taken together, these observations point towards the possible role of ex-miRNAs in intercellular communication.

Interestingly, in the honey bee, *Apis mellifera*, it has been demonstrated that ex-miRNAs in worker and royal jellies can regulate caste determination (Guo et al., 2013). However, in insects, no other studies reporting on the presence of ex-miRNAs have been published. In particular, the presence of miRNAs in cell-free culture media of insect cells has not been assessed as yet. Therefore, we investigated the presence of ex-miRNAs in EVs and extracellular Ago-1 containing immunoprecipitates (EAgo-1) in the conditioned cell-free media of two cultured *Drosophila* cell lines. Here, we show that ex-miRNAs are indeed present in EVs and EAgo-1

derived from the extracellular media of cultured Cl.8 and S2 cells. Moreover, observations based on the comparison of cellular miRNA expression levels and their respective abundances in EVs point towards the selective miRNA sorting and secretion.

2.2 Materials and methods

2.2.1 Cl.8 and S2 cell cultures

To investigate the presence of ex-miRNAs, the well-known *Drosophila* S2 and Cl.8 cell lines were cultured. These cell lines were selected based on their distinct origin and different sensitivity for exogenous dsRNA. Haemocyte-like S2 cells were originally derived from late stage embryos and perform exogenous dsRNA uptake to effectuate a systemic RNAi response (Saleh et al., 2006; Schneider, 1972). Cl.8 cells were originally obtained from wing imaginal discs and are characterized for their inability to take-up exogenous dsRNA, but rather require transfection to elicit a potent silencing response (Lum et al., 2003; Peel and Milner, 1990). Based on both distinct features, a differential analysis of the ex-miRNAs of both cell lines was performed to study commonalities and cell-type dependent discrepancies.

The Clone 8 (Cl.8) cell line was maintained in Shields and Sang M3 Insect medium (Sigma-Aldrich), supplemented with 2 % heat-inactivated Fetal Bovine Serum (FBS) (Sigma-Aldrich), 2,5 % fly extract, 5 µg/ml human insulin (Sigma-Aldrich), 0.25 µg/ml Amphotericin B (Gibco, Life Technologies), 100 U/ml penicillin and 100 µg/ml streptomycin (Gibco, Life Technologies). The Schneider 2 (S2) cell line was also maintained in Shields and Sang M3 Insect medium supplemented with 1 g/l yeast extract (Sigma-Aldrich) and 2.5 g/l bactopeptone (BD Biosciences), 10 % heat-inactivated FBS, 0.25 µg/ml Amphotericin B, 100 U/ml penicillin and 100 µg/ml streptomycin. The cells were subcultured weekly and maintained at 25 °C.

To study the presence of miRNAs in EVs or bound to EAgo-1, optimized cell culture media lacking vesicles and Ago proteins were required. EV-depleted FBS and fly extract were obtained by ultracentrifugation (110,000 g, 4 h, 4 °C). In addition, the fly extract was depleted of Ago proteins by using a 30 kDa MWCO Centriprep™ Centrifugal Filter Units (Millipore®).

2.2.2 Isolation of extracellular vesicles and extracellular Argonaute-1 from conditioned media

Conditioned media were obtained by seeding Cl.8 and S2 cells (1.5 x 106 cells/ml) in T-150 cell culture flasks using the optimized cell culture media. After reaching 80 % confluency, the cells were collected by centrifugation (1000 g, 10 min, 4 °C) and stored in 100 µl PBS at -80 °C until further use. Supernatants (*e.g.* the conditioned media) were depleted from apoptotic bodies by centrifugation at 5000 g for 10 min at 4 °C and subsequently further concentrated using 30 kDa MWCO Centriprep™ Centrifugal Filter Units (Millipore®) as Ago-1 and EVs are considered to have a size of 95 kDa and 450-700 kDa, respectively. Finally, each sample was divided in half for further processing, namely for EV and EAgo-1 isolation.

EVs were purified using part one of the exoRNeasy serum/plasma kit (Qiagen) according to the manufacturer's protocol. The exoRNeasy serum/plasma kit uses a membrane-based affinity binding step to isolate exosomes and other EVs from serum and plasma. In brief, each sample was mixed with an equal volume of XBP buffer and applied to the exoEasy spin column. After centrifugation, the bound EVs were washed with XWP washing buffer.

EAgo-1 was isolated by means of immunoprecipitation (IP). Briefly, 75 µl of Dynabeads M-280 Sheep Anti-Mouse IgG slurry (Thermo Fisher Scientific) were washed with washing buffer (PBS supplemented with 0.1 % BSA and 2 mM EDTA) according to the manufacturer's protocol and incubated with 1 µg of mouse monoclonal anti-Ago-1 antibody (gift from Prof. Haruhiko Siomi, Keio University School of Medicine, Japan) for 2 h at 4 °C. The pre-incubated beads and antibody were added to the sample and incubated overnight at 4 °C. Beads were washed three times with washing buffer and eluted in 250 µl of QIAzol Lysis Reagent (Qiagen) for RNA isolation or in 50 µl NuPAGE LDS Sample Buffer (4x) (Invitrogen™) for immunoblotting.

Both the purified EV and EAgo-1 fraction were subjected to immunoblot analysis to verify proper isolation (Fig. 2.1). In addition, a mock IP experiment (Fig. 2.2) was included as a negative control for EAgo-1 isolation.

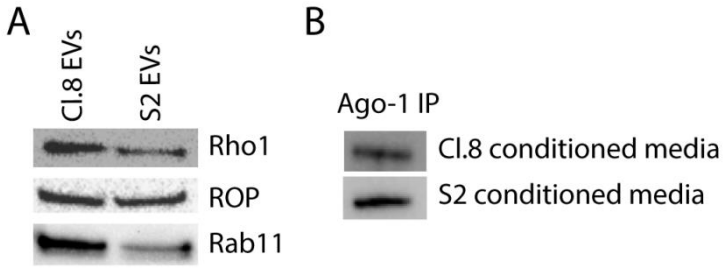

Figure 2.1: Immunoblot analysis on EVs and EAgo-1 immunoprecipitates. (A) EVs of both cell lines were subjected to immunoblot analysis for three common EV markers, which were clearly detected in the EV fractions purified from the extracellular media of both cell lines. (B) EAgo-1 IP was performed on the conditioned S2 and Cl.8 media as described in Methods section, but eluted in lithium dodecyl sulfate (LDS) instead of Qiazol. After elution, S2 and Cl.8 IP products were subjected to immunoblot analysis for EAgo-1, which was clearly detected in both IP products. Full-length blots are presented in Appendices (Supplementary Figure 1 Chapter 2).

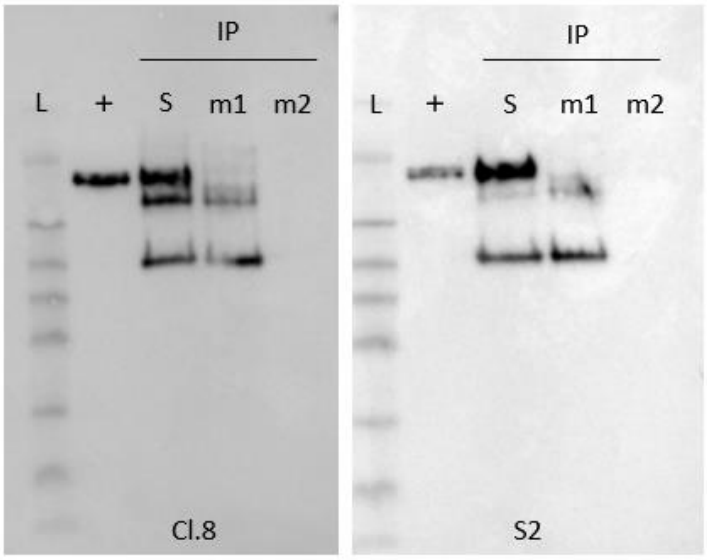

Figure 2.2: Mock IP controls. Two mock IPs were performed as negative controls to verify specific isolation of EAgo1. In mock 1 (m1), fresh cell culture medium was added to the beads instead of the conditioned medium (S). In the second mock (m2), no primary antibody was used during the IP protocol. EAgo-1 IP (S) and mock IPs (m1 & m2) were performed as described in Methods section, but eluted in lithium dodecyl sulfate (LDS) instead of Qiazol. After elution, the IP products were subjected to immunoblot analysis for Ago-1, which was clearly detected in the positive control and in the EAgo-1 IP (S) products, but not in the mock IPs eluates. In m1 eluate, only co-eluted antibody bands are seen; in m2 eluate, no bands are seen. Abbreviations: L: Seeblue Prestained 2 Protein Standard (Thermo Fisher); + : positive control sample (*i.e.* a protein extract of respectively Cl.8 and S2 cells); IP: Immunoprecipitation; S: sample (conditioned medium); m1: mock 1 control; m2: mock 2 control.

2.2.3 Immunoblotting

Protein concentrations of isolated Cl.8 and S2 EVs were determined by the bicinchoninic acid (BCA) assay. Equal protein amounts were analysed by SDS-PAGE using a NuPAGE 4-12 % Bis-Tris gradient gel (Thermo Fisher Scientific) and subsequently electroblotted to polyvinylidene difluoride (PVDF) membranes (Thermo Fisher Scientific). The PVDF membrane was blocked in 5 % low-fat dry milk powder in Tris-buffered saline (TBS) for 2 h at room temperature (RT) and subsequently incubated with primary antibodies overnight at 4 °C. The PVDF membrane was subsequently washed in TBS and then incubated with horseradish peroxidase (HRP)-conjugated goat anti-Mouse secondary antibody (Dako, Glostrup, Denmark) for 45 min at RT. Finally, the membrane was washed in Tris buffer and proteins were visualized using the SuperSignalTM West Dura Extended Duration Substrate (Thermo Fisher Scientific) and imaged on the Chemidoc MP Imaging System (Bio-Rad). The primary antibodies used were Rho1 (DSHB Hybridoma Product p1D9 (anti-rho1), Parkhurst, S.), ROP (DSHB Hybridoma Product Rop 4F8, Rubin, G.M.) and Rab 11 (cat.no 610656, BD Biosciences), three common EV-marker proteins.

EAgo-1 immunoprecipitates were eluted in 50 µl NuPAGE LDS Sample Buffer (4x) (Invitrogen™) at 70 °C for 10 min. Afterwards, S2 and Cl.8 IP products were analysed by immunoblotting according to the above-

mentioned protocol. The primary antibody used was anti-Ago-1 (gift from Prof. Haruhiko Siomi, Keio University School of Medicine, Japan), the secondary antibody HRP-conjugated goat anti-mouse (Dako, Glostrup, Denmark).

2.2.4 RNA extraction and cDNA synthesis

RNA encapsulated in EVs was collected using the second part of the exoRNeasy serum/plasma kit, RNA from immunoprecipitated EAgo-1 was extracted with the miRNeasy Serum/Plasma Kit (Qiagen) and a separate miRNA-enriched fraction could be purified from the cellular fraction with the miRNeasy Mini kit and RNeasy MinElute Cleanup kit (Qiagen), all according to the manufacturer's protocol. In brief, QIAzol Lysis Reagent was added to the samples to facilitate lysis. Upon addition of chloroform, the lysate was separated into an aqueous and organic phase by centrifugation, with RNA partitioning to the upper aqueous phase, which was subsequently purified on a silica-column. Quality and concentration of the resulting RNA samples were measured on a Nanodrop spectrophotometer (NanoPhotometer N60, Implen) and analysed using the Agilent Bioanalyzer Small RNA chip (Agilent Technologies, Inc.). Equal amounts of RNA (20 ng for EAgo-1 immunoprecipited RNA and 100 ng for EV encapsulated RNA) were used for cDNA synthesis using the qScript™ microRNA cDNA Synthesis Kit (Quanta Bio) following the manufacturer's protocol. This protocol includes polyadenylation of the miRNAs in a poly(A) polymerase reaction followed by cDNA synthesis using an oligo-dT adapter primer (Supplementary Figure 2 Chapter 2). This adapter primer allows amplification of cDNAs in quantitative real-time PCR (qRT-PCR) reactions due to a unique sequence at its 5' end. The obtained cDNA was then diluted ten-fold with Milli-Q water (Millipore).

2.2.5 Quantitative real-time PCR

QRT-PCR is a specific and sensitive method to measure the relative quantity of a target RNA. The target sequence will be amplified during the PCR reaction using gene-specific primers and a PCR mastermix containing a fluorescent reporter dye (SYBR® Green, Applied Biosystems). The PCR amplification can be followed in 'real time' as the incorporation of the dye into the dsDNA will result in an increase in the intensity of the fluorescence.

Using a specific forward and a universal poly(T) adaptor reverse primer (Table 2.1; Supplementary Figure 2 Chapter 2), amplification of cDNA samples was performed. Forward primers were designed to cover at least 80% of the miRNA sequence and random nt were added on the 5' end to raise the melt temperature to 60 °C. Primer pairs were validated by designing relative standard curves for gene transcripts with serial (5x) dilutions of appropriate cDNA samples. The correlation coefficient and efficiency of the qRT-PCR reaction were measured (R^2 = 0.995 – 1; Eff% = 90% - 110%). All qRT-PCR reactions were performed in duplicate in 96-well plates on a StepOne Plus System (ABI Prism, Applied Biosystems) according to the Fast SYBR Green PCR Master Mix protocol. Each reaction contained 5 µl of PerfeCTa SYBR Green FastMix, ROX (Quanta Bio), 0.5 µl

of each forward and reverse primer (10 µM), 1.5 µl of Milli-Q water and 2.5 µl of cDNA. A no template control reaction was always included. The following thermal cycling profile was used: 95 °C for 10 min, followed by 40 cycles of 95 °C, 15 s and 60 °C, 1 min. Then, a melt curve analysis was performed to confirm the specificity of the qRT-PCR reactions. In addition, the amplification products of three miRNAs were analysed using horizontal agarose gel electrophoresis (1.2 % agarose gel containing GelRedTM, Biotium) and visualized using UV. A single band of the expected size for each transcript was observed, which was further cloned and sequenced (TOPO® TA Cloning Kit for sequencing, Invitrogen) to confirm amplicon specificity. MiR-276a, bantam and miR-100 were chosen since they respectively represent miRNAs with high, intermediate and low abundances.

Table 2.1: Oligonucleotide sequences of primers used for qRT-PCR. The forward (F-) primer is a *D. melanogaster* miRNA specific primer, the reverse primer a universal one with sequence 5'- GCATAGACCTGAATGGCGGTA -3'. Accession numbers are included (miRBase Release 21.0).

MiRNAs	F-primer	Accession number
miR-1-3p	5'- CGCGGCTGGAATGTAAAGAAGTATGG -3'	MIMAT0000105
miR-2-3p	5'- CGCCTAGTATCACAGCCAGCTT -3'	MIMAT0000106, MIMAT0000107, MIMAT0000411
miR-14-3p	5'- AGGGCGGTCAGTCTTTTTCTCTC -3'	MIMAT0000120
miR-34-5p	5'- AGTGGCAGTGTGGTTAGCTGG -3'	MIMAT0000350
miR-100-5p	5'- GGCGAACCCGTAAATCCGAACTTG -3'	MIMAT0000357
miR-125-5p	5'- CGTCGCTTCCCTGAGACCCTAAC -3'	MIMAT0000397
miR-190-5p	5'- GCGGGGCAGATATGTTTGATATTCTTGG -3'	MIMAT0005467
miR-210-3p	5'- GTGCGTGTGACAGCGGCTAT -3'	MIMAT0000355
miR-252-5p	5'- GCCTAAGTACTAGTGCCGCAGG -3'	MIMAT0005516
miR-276a-3p	5'- GCGTAGGAACTTCATACCGTGCT -3'	MIMAT0000337
bantam-3p	5'- CGGGCAGTGAGATCATTTTGAAAGC -3'	MIMAT0020823
let-7-5p	5'- GCGGCTGAGGTAGTAGGTTGT -3'	MIMAT0000396

2.2.6 Small RNA sequencing data and analysis

Briefly, small RNA libraries of S2 cells and derived EVs were prepared using the TailorMix microRNA Sample Preparation Kit V2 (SeqMatic) according to the manufacturer's protocol. These small RNA libraries were sequenced on the Illumina MiSeq® System with a single read length of 50 nt. Sequencing quality control was monitored via PhiX spike-ins (2 %). The PhiX Control v3 is derived from the well-characterized bacteriophage genome, PhiX. It is a concentrated Illumina library that has an average size of 500 bp and consists of balanced base composition at 45 % GC and 55 % AT, which makes it an ideal sequencing control for run quality monitoring. Illumina adapters/primers were removed from the raw reads with BBDuk (version 37.33; Bushnell B.). Subsequently, the processed reads were aligned to the available *D. melanogaster* mature miRNAs from miRBase (release 21.0) (Griffiths-Jones et al., 2006) using Bowtie 2 (Galaxy Version 2.3.4.1; https://doi.org/10.1186/gb-2009-10-3-r25) and mapped read counts were obtained using the Idxstats command of SAMtools (Galaxy Version 2.0.1; https://doi.org/10.1093/bioinformatics/btp352). Differential expression analysis was performed using the R (R Core Team; version 3.3.3) packages Sartools (version 1.6.1: https://doi.org/10.1371/journal.pone.0157022) and edgeR (version 3.16.5;

https://doi.org/10.1093/bioinformatics/btp616) (Appendices: Supplementary Table Chapter 2). MiRNAs were only retained if they displayed a counts-per-million (cpm) above 1 in at least 3 samples.

2.3 Results

2.3.1 Detection of miRNAs in extracellular vesicles and bound to extracellular Argonaute-1

Two extracellular fractions were purified from the cell-free conditioned media of the selected cell lines, namely the EVs and EAgo-1, and subjected to immunoblot analysis to verify proper isolation (Fig. 2.1). Afterwards, the presence of twelve specific miRNAs was analysed via qRT-PCR: miR-1-3p; miR-2-3p; miR-14-3p; miR-34-5p; miR-100-5p; miR-125-5p; miR-190-5p; miR-210-3p; miR-252-5p; miR-276a-3p; bantam-3p; and let-7-5p. These miRNAs were selected from miRBase (Griffiths-Jones et al., 2006) (Release 21.0) based on their known role in regulating several aspects of fruit fly development (Aravin et al., 2003; Thompson and Cohen, 2006; Waldron and Newbury, 2012). In addition, this pool of miRNAs contains both 5p- and 3p-miRNAs, which is of interest considering that not only 5p- miRNAs are functional as it was initially thought, but also 3p- miRNAs (*i.e*. derived from the 5' and 3' arm of the precursor, respectively) (Yang et al., 2011). The twelve miRNAs revealed to be present in the analysed extracellular fractions, *i.e*. EVs and EAgo-1, purified from the extracellular media of both cell lines (Fig. 2.3A and B). Moreover it is interesting to note that no obvious biases towards the 5p- or 3p- type of miRNAs are observed (for example, miR-14-3p and miR-34-5p are more abundant while miR-210-3p and let-7-5p are less abundant).

Noteworthy, in order to allow comparisons of each fraction between both cell lines, Cl.8 and S2 cells were both seeded at the same density and each incubated until confluence was achieved before collecting the conditioned media. In addition, for cDNA synthesis, equal quantities of RNA were used for the EV and EAgo-1 fraction of both cell lines. Although all miRNAs are present in both extracellular fractions of the two cell lines, their abundance is variable, with significant differences between the cell lines. In fact, when compared to the data obtained from S2 cell cultures, six miRNAs are significantly less abundant in EVs derived from Cl.8 cell cultures, namely miR-100, miR-125, miR-210, miR-252, miR-276a and let-7, as shown by their higher Ct values. On the contrary, miR-1 is more abundant in Cl.8 EVs than in S2 EVs, *i.e*. lower Ct value. The presence of the remaining miRNAs in EVs does not differ significantly between the cell lines (Fig. 2.3A). On the other hand, the abundance of miR-1, miR-100, miR-125, miR-210 and let-7 is higher in the Cl.8 EAgo-1 fraction, while miR-252 is more abundant in EAgo-1 from S2 cells. The levels of the remaining EAgo-1 miRNAs do not differ between both cell lines (Fig. 2.3B).

Finally, it is interesting to note that the relative abundance of miR-100, miR-125, miR-210 and let-7 in extracellular fractions of S2 versus Cl.8 is inverted, as these miRNAs are more abundant in S2 EVs compared to Cl.8 EVs, although less abundant in S2 EAgo-1 compared to Cl.8 EAgo-1.

2.3.2 MiRNA intracellular expression

Since the abundance of several miRNAs revealed to be significantly different between the Cl.8 and S2 extracellular fractions, the question whether these differences would correlate with differences in their intracellular expression remains to be answered. Therefore, the intracellular expression levels of these miRNAs were also measured (Fig. 2.3C). Interestingly, with the exception of miR-252 and miR-276a, all measured miRNAs exhibit a higher expression (*i.e*. lower Ct values) in Cl.8 cells. This is in accordance with the higher abundance of these miRNAs in Cl.8 derived EAgo-1 compared to S2 EAgo-1 (Fig. 2.3B). In this context, it is noteworthy that an inverted trend is observed in the EV fractions, since these miRNAs, except for miR-1, are more abundant in S2 EVs than in Cl.8 EVs (Fig. 2.3A).

On the other hand, lower expression of miR-252 in S2 versus Cl.8 cells is in line with its lower abundance in both S2 EVs and EAgo-1 (Fig. 2.3). In addition, although the intracellular expression levels of miR-276a do not differ between Cl.8 and S2 cells (Fig. 2.3C), this miRNA is remarkably more abundant in S2 EVs than in Cl.8 EVs (Fig. 2.3A). In conclusion, Table 2.2 offers a summary of the significant differences.

Moreover, although the abundance of these miRNAs is not significantly different between the Cl.8 and S2 extracellular fractions, the intracellular expression levels of miR-2, miR-14 and miR-34 are higher in Cl.8 cells compared to S2 cells, while bantam is more expressed in S2 cells than in Cl.8 cells (Fig. 2.3C).

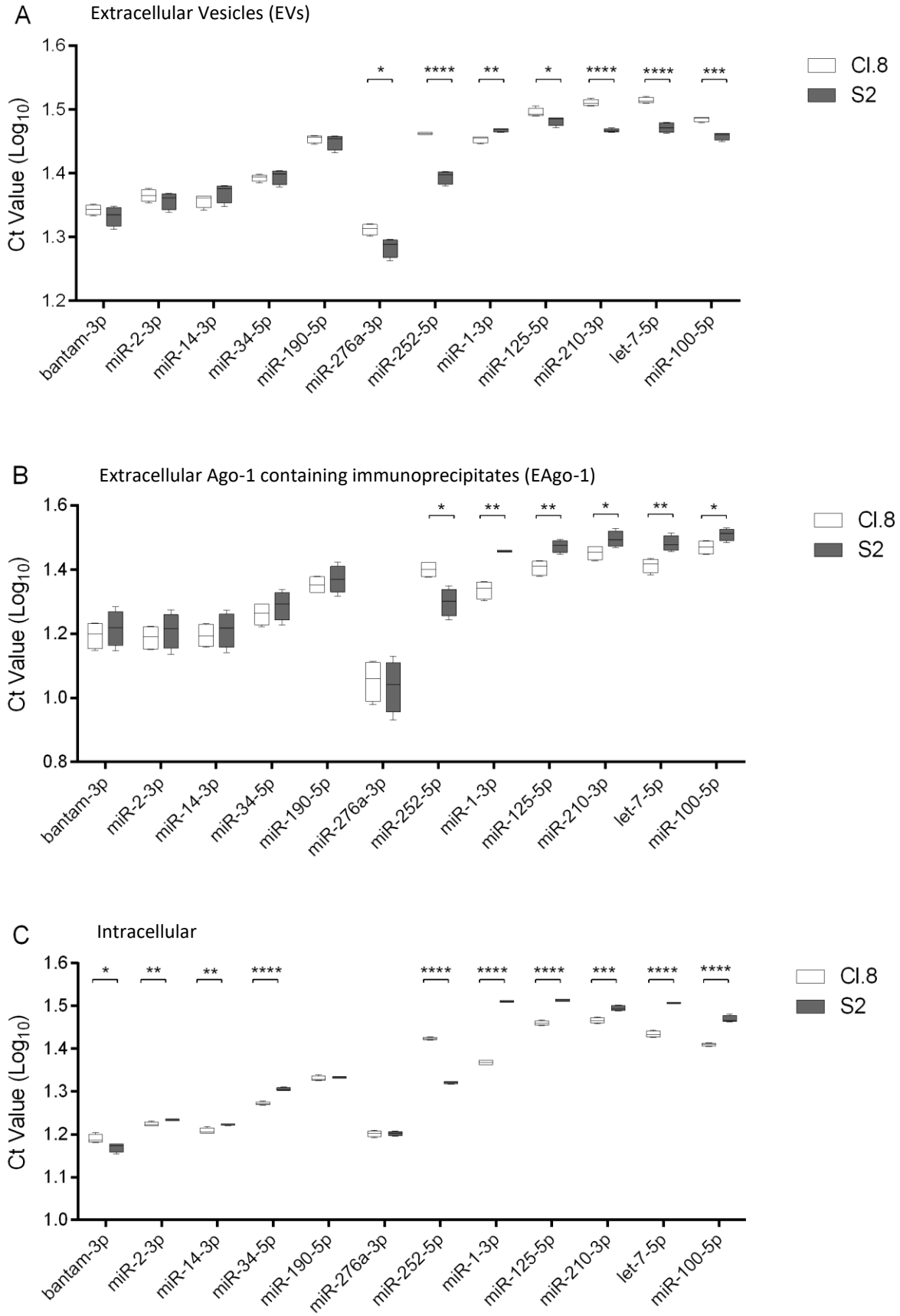
A
Extracellular Vesicles (EVs)
Ct Value (Log10)
1.6
1.5
1.4
1.3
1.2
*
****
**
*
****
****
***
Cl.8
S2
bantam-3p
miR-2-3p
miR-14-3p
miR-34-5p
miR-190-5p
miR-276a-3p
miR-252-5p
miR-1-3p
miR-125-5p
miR-210-3p
let-7-5p
miR-100-5p
B
Extracellular Ago-1 containing immunoprecipitates (EAgo-1)
Ct Value (Log10)
1.6
1.4
1.2
1.0
0.8
*
**
**
*
**
*
Cl.8
S2
bantam-3p
miR-2-3p
miR-14-3p
miR-34-5p
miR-190-5p
miR-276a-3p
miR-252-5p
miR-1-3p
miR-125-5p
miR-210-3p
let-7-5p
miR-100-5p
C
Intracellular
Ct Value (Log10)
1.6
1.5
1.4
1.3
1.2
1.1
1.0
*
**
**
****
****
****
****
***
****
****
Cl.8
S2
bantam-3p
miR-2-3p
miR-14-3p
miR-34-5p
miR-190-5p
miR-276a-3p
miR-252-5p
miR-1-3p
miR-125-5p
miR-210-3p
let-7-5p
miR-100-5p

Figure 2.3: qRT-PCR data for microRNAs detected in extra- and intracellular fractions of Cl.8 and S2 cell lines. (A) Extracellular vesicles (EVs) and (B) extracellular Ago-1 containing immunoprecipitates (EAgo-1) were isolated from the cell-free conditioned media of Cl.8 and S2 cell cultures and different miRNAs were detected using qRT-PCR. (C) The intracellular expression levels of the selected miRNAs were measured as well. The data (log10 Ct values) are shown as box plots (min to max with the rectangle spanning the first to the third quartile including median) of four biological replicates, run in duplicate. Statistical analyses were performed with GraphPad Prism 6 (Graphpad Software Inc.). Significant differences ($p < 0.05$, $p < 0.01$, $p < 0.001$ and $p < 0.0001$) between the data obtained for specific miRNAs in the extracellular media of the two cell lines were found, after a log transformation, via a t-test (with or without two-sided Welch's correction) and are indicated by (an) asterisk(s) (*, **, *** and **** respectively).

Table 2.2: Significantly differential abundance of *D. melanogaster* miRNAs when comparing the Cl.8 and S2 cell lines. Significant differences (p) (* = p < 0.05; ** = p = < 0.01; *** = p < 0.001; **** = p < 0.0001). Abbreviations: EVs: extracellular vesicles; EAgo-1: extracellular Argonaute-1 containing immunoprecipitates; Intra: intracellular; ns: not significant.

	Higher abundance in					
	EVs		**EAgo-1**		**Intra**	
bantam-3p	ns		ns		S2	(*)
miR-2-3p	ns		ns		Cl.8	(**)
miR-14-3p	ns		ns		Cl.8	(**)
miR-34-5p	ns		ns		Cl.8	(****)
miR-276a-3p	S2	(*)	ns		ns	
miR-252-5p	S2	(****)	S2	(*)	S2	(****)
miR-1-3p	Cl.8	(**)	Cl.8	(**)	Cl.8	(****)
miR-125-5p	S2	(*)	Cl.8	(**)	Cl.8	(****)
miR-210-3p	S2	(****)	Cl.8	(*)	Cl.8	(***)
let-7-5p	S2	(****)	Cl.8	(**)	Cl.8	(****)
miR-100-5p	S2	(***)	Cl.8	(*)	Cl.8	(****)

2.3.3 Differential expression analysis of small RNA sequencing data

In a complementary approach, small RNA sequencing (RNA-seq) reads of S2 cells and derived EVs were analysed and compared with corresponding qRT-PCR results. Abundant miRNAs in S2 EVs and S2 cells (Fig. 2.3A and C), *i.e*. bantam, miR-14, miR-34 and miR-276a, also display a higher number of read counts in the RNA-seq data (Table 2.3). In addition, less abundant miRNAs in S2 cells and S2 EVs (miR-100, miR-125, miR-210 and let-7) are characterized by high Ct values (Fig. 2.3A and C) and very low read count numbers (Table 2.3). Taken together, these observations are in line with the qRT-PCR results. Here, it is important to note that small RNA-seq can discriminate miR-2-3p in three different subtypes (miR-2a-3p, miR-2b-3p and miR-2c-3p) which only differ 1 or 2 nucleotides (outside the seed region). Nevertheless, it is interesting that a certain subtype is more present (miR-2b-3p) than others. This might indicate that a certain miR-2-3p subtype might be more secreted or retained in the cell compared to other subtypes.

At last, based on the differential expression analysis, the abundances of 31 miRNAs significantly differed between S2 EVs and S2 cells (Fig. 2.4). Seven out of 31 miRNAs were significantly more abundant in S2 cells compared to S2 EVs, while the remaining 24 miRNAs were more abundant in S2 EVs (Table 2.4).

Table 2.3: Small RNA sequencing data are in agreement with qRT-PCR results (Fig. 2.3). Small RNA sequencing data of S2 cells and derived EVs, on three biological replicates, were analysed using edgeR. Normalised counts per sample of the twelve miRNAs studied with qRT-PCR and their corresponding adjusted p-values ($\alpha < 0.05$). Abundant miRNAs (low Ct values in qRT-PCR) display high read counts, while less abundant miRNAs (high Ct values in qRT-PCR) are characterized by (very) low read counts. NA values indicate miRNAs which have no reads in at least four out of six samples. Log2FoldChange values reflect the differential expression between S2 cells and EVs. Positive and negative values indicate upregulated and downregulated miRNA abundances in EVs, respectively. Abbreviations: EV: extracellular vesicle; p_{adj}: raw p-value adjustment.

miRNA	S2 Cell			S2 EV			Log2FoldChange	p_{adj} value
dme-bantam-3p	9909	832	752	524	534	309	-3.07	0.042
dme-miR-2a-3p	8	18	11	6	11	17	-0.07	0.968
dme-miR-2b-3p	111	237	230	124	388	244	0.39	0.800
dme-miR-2c-3p	0	2	1	0	8	3	1.80	0.310
dme-miR-14-3p	1889	2519	1525	92	287	404	-2.92	0.024
dme-miR-34-5p	610	728	481	255	468	228	-0.94	0.434
dme-miR-190-5p	61	10	10	17	4	4	-1.70	0.275
dme-miR-276a-3p	513	1165	942	392	1946	1375	0.50	0.736
dme-miR-252-5p	0	9	10	2	10	7	0.02	0.987
dme-miR-1-3p	1	1	2	8	0	4	1.50	0.377
dme-miR-125-5p	NA	NA	NA	NA	NA	NA	NA	NA
dme-miR-210-3p	NA	NA	NA	NA	NA	NA	NA	NA
dme-let-7-5p	4	0	1	6	27	13	3.10	0.052
dme-miR-100-5p	0	0	1	0	6	6	3.24	0.077

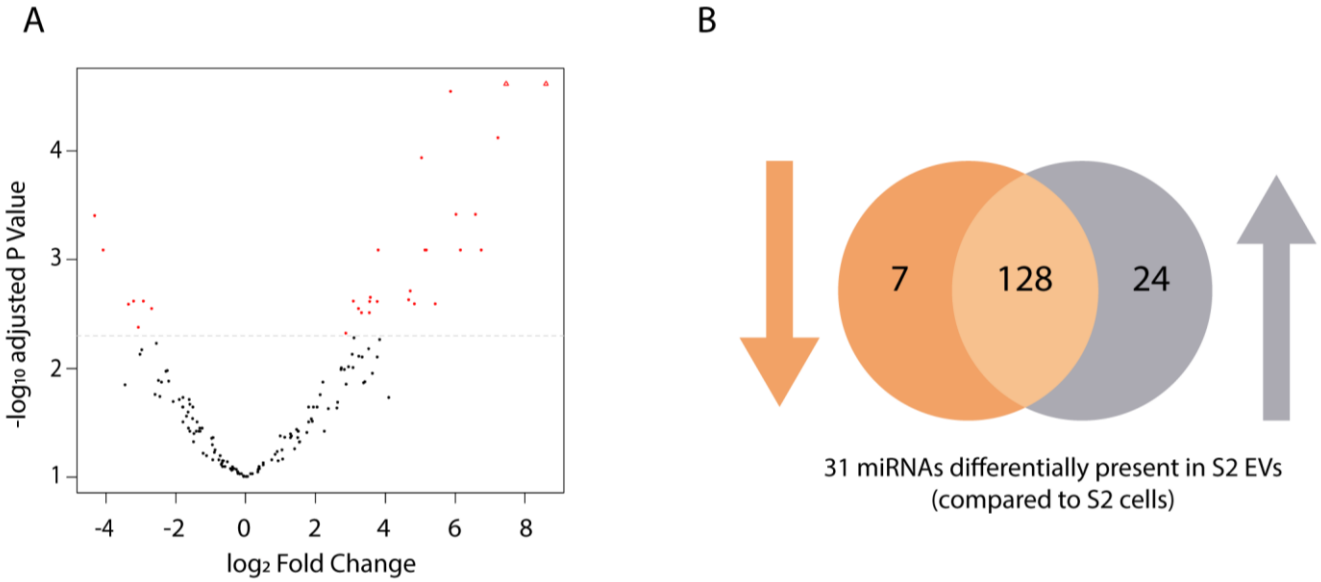

Figure 2.4: Differentially expressed miRNAs as measured in small RNA-seq data of S2 cells and derived EVs. Differential expression analysis was performed using edgeR on three biological replicates of both groups. MiRNAs were retained with a CPM above 1 in at least 3 samples. (A) Volcano plot indicating 31 significantly different miRNAs in S2 cells and EVs (red dots) and (B) the corresponding Venn diagram presenting the amount of miRNAs with increased (24) or decreased (7) abundance in S2 EVs compared to S2 cells. Abbreviations: EV: extracellular vesicle.

Table 2.4: Differentially expressed miRNAs. Normalised counts per sample of miRNAs with an increased (grey, **A**) and decreased (orange, **B**) abundance in S2 EVs. Log2FoldChange values reflect the differential expression between S2 cells and EVs. Positive and negative values indicate upregulated and downregulated miRNA abundances in EVs, respectively. MiRNAs were ranked in both tables (top to bottom) based on their adjusted p-values ($\alpha < 0.05$). Abbreviations: EV: extracellular vesicle; p_{adj}: raw p-value adjustment.

A)

miRNA	S2 Cell			S2 EV			Log2FoldChange	p_{adj} value
dme-miR-9381-5p	7	16	2	319	1730	2406	7.46	0.000004
dme-miR-9378-3p	0	0	0	3	45	96	8.60	0.000192
dme-miR-9377-3p	1	7	1	67	171	262	5.87	0.000283
dme-miR-303-3p	1	0	0	2	65	119	7.22	0.000757
dme-miR-4958-5p	1	6	1	32	84	156	5.04	0.001156
dme-miR-2c-5p	0	0	0	24	1	11	6.58	0.003838
dme-miR-9369-5p	0	0	0	2	9	13	6.02	0.003838
dme-miR-4949-3p	1	0	0	86	1	2	6.15	0.008146
dme-miR-4962-3p	0	0	0	5	2	6	5.13	0.008146
dme-miR-4963-3p	1	3	1	36	26	24	3.80	0.008146
dme-miR-4970-5p	0	0	0	6	2	5	5.18	0.008146
dme-miR-9379-5p	0	0	0	38	1	2	6.75	0.008146
dme-miR-133-3p	0	0	0	3	2	4	4.72	0.019416
dme-miR-979-5p	2	2	0	11	14	32	3.57	0.022128
dme-miR-316-3p	1	0	0	27	2	3	4.67	0.023358
dme-miR-313-5p	4	7	2	36	26	52	3.08	0.024110
dme-miR-9380-3p	1	0	0	6	3	8	3.77	0.024288
dme-miR-990-3p	1	4	1	8	18	58	3.55	0.024288
dme-miR-9370-3p	1	0	0	56	1	3	4.83	0.025413
dme-miR-989-3p	2	1	0	163	2	0	5.43	0.025413
dme-miR-279-5p	2	20	3	38	78	121	3.23	0.028122
dme-miR-1016-3p	1	0	0	3	4	5	3.32	0.030763
dme-miR-960-5p	1	1	0	2	11	22	3.54	0.030763
dme-miR-289-5p	4	6	2	16	13	56	2.87	0.047273

B)

miRNA	S2 Cell			S2 EV			Log2FoldChange	p_{adj} value
dme-miR-2a-2-5p	243	54	76	3	11	3	-4.32	0.004
dme-miR-34-3p	10	72	53	3	3	2	-4.07	0.008
dme-bantam-5p	2734	673	482	260	103	58	-3.21	0.024
dme-miR-14-3p	1889	2519	1525	92	287	404	-2.92	0.024
dme-miR-980-5p	10	99	83	3	11	3	-3.35	0.026
dme-miR-8-3p	2784	1054	861	244	267	216	-2.69	0.028
dme-bantam-3p	9909	832	752	524	534	309	-3.07	0.042

2.4 Discussion

In this work, we have investigated the presence of ex-miRNAs in insect cell cultures. We have addressed this question by studying two *Drosophila* cell lines, namely Cl.8 and S2, which have different origins and properties. Our study shows the presence of miRNAs in the cell-free conditioned media of both cell lines. More specifically, we demonstrate that ex-miRNAs are present in two fractions, namely EVs and EAgo-1 (Fig. 2.2A and B). This suggests that ex-miRNAs are protected from degradation by either encapsulation in EVs or association with the stable Ago-1 protein. Likewise, studies in blood and plasma identified stable circulatory RNAs, suggesting their presence in an RNase-resistant form (Mitchell et al., 2008; Tsui et al., 2002). In

accordance with our data, several studies in mammals have indicated the presence of miRNAs in EVs derived from human blood, cultured cells and virtually all other extracellular fluids, such as breast milk, semen, cerebrospinal fluid, urine and saliva (Amanda et al., 2010; Chen et al., 2008; Delić et al., 2016; El-Khoury et al., 2016; McDonald et al., 2013; Vojtech et al., 2014; Zhang et al., 2013; Zhou et al., 2011). Although in mammals EV-associated miRNA was originally thought to be the main extracellular form, two independent studies showed that most of the miRNAs in plasma, serum and conditioned media were EV-free but associated with proteins of the Ago family (Arroyo et al., 2011; Turchinovich et al., 2011). More specifically, human Ago-2 was clearly detected in plasma and associated with myriad miRNAs. A plausible explanation for stable Ago-associated miRNAs (Ago-miRNAs) in the harsh extracellular environment is that mature miRNAs naturally associate with them within the cell (Miyoshi et al., 2009) as part of the RISC and that Ago-miRNA complexes are highly nuclease/protease resistant, as they can remain stable in cell lysates for up to two months (Turchinovich et al., 2011; Vodovar and Saleh, 2012). Our results clearly indicate that the presence of miRNAs in extracellular vesicles and Ago-containing ribonucleoprotein complexes (Fig. 2.3 and B) is a more widespread phenomenon that is not restricted to mammalian systems.

Each miRNA of the analysed group, which includes 5p- and 3p- miRNAs, was detected in both the EV and EAgo-1 fraction of both cell lines (Fig. 2.3). Likewise, it has been shown in mammals that certain miRNAs are present in both fractions, although others appear to be exclusively present in only one of them. For example, miR-100 and miR-210 (two miRNAs we clearly detect in both fractions) exclusively associate with extracellular Ago-2 in human plasma (Arroyo et al., 2011). Here, it is important to note that only a very small set of miRNAs was tested in comparison to the referred studies. Thus, also in insects, it cannot be excluded that certain miRNAs exclusively associate with either EVs or EAgo-1.

In addition, small RNA-seq data of S2 cells and S2 EVs were included as a second approach to verify our qRT-PCR data. Small RNA-seq reads were aligned to all available mature *D. melanogaster* miRNAs on miRBase(Griffiths-Jones et al., 2006) enabling the comparison of intracellular and extracellular reads of 469 miRNAs. The read counts of the twelve miRNAs under study are in line with our qRT-PCR data, since abundant miRNAs (low Ct values in qRT-PCR; Fig. 2.3) display higher read count numbers (Table 2.3) while less abundant miRNAs (high Ct values; Fig. 2.3) are characterized by low read count numbers (Table 2.3). Moreover, based on differential expression analysis, 31 miRNAs were identified with significantly different abundances between S2 cells and S2-derived EVs (Fig. 2.4). While seven out of 31 miRNAs were significantly more abundant in S2 cells compared to S2 EVs, the opposite is witnessed for the remaining 24 miRNAs (Table 2.4). Taken together, these observations point towards the controlled miRNA secretion in EVs, as certain miRNAs are retained more in the cells while others are relatively more abundant in EVs. In accordance with our data, multiple studies in mammals demonstrate controlled and selective miRNA secretion, as numerous miRNAs

could not be detected in human plasma and conditioned media, although they are present intracellularly (Shurtleff et al., 2016; Turchinovich et al., 2011).

Since the levels of certain miRNAs are significantly different between each extracellular fraction of both cell lines (Fig. 2.3A and B), we hypothesized that this might result from differences in their intracellular expression levels (Fig. 2.3C). Remarkably, although a higher intracellular expression seems to correlate with a higher abundance in the EAgo-1 fraction, an inverted trend is observed for the EV fraction (Table 2.2). In addition, even though the intracellular expression of miR-276a does not differ between S2 and Cl.8 cells, this miRNA is significantly more abundant in S2 EVs compared to EVs derived from Cl.8 culture medium. Taken together, these observations indicate that S2 derived EVs contain more copies of several miRNAs although their intracellular expression is lower compared to Cl.8 cells. In other words, our results support the occurrence of selective miRNA secretion and sorting in EVs. Interestingly, antiviral siRNAs have recently been demonstrated to be present in haemocyte-derived EVs in adult flies in order to potentiate a systemic antiviral response (Tassetto et al., 2017). Likewise, EVs derived from haemocyte-like S2 cells might also be selectively loaded and able to mediate intercellular communication.

In recent years, studies of ex-miRNAs in mammalian systems accumulated, since these ex-miRNAs are secreted by cancer cells and might therefore be promising non-invasive biomarkers of tumorigenesis (Rabinowits et al., 2009; Taylor and Gercel-Taylor, 2008; Turchinovich et al., 2015). Nevertheless, whether ex-miRNAs might mediate intercellular communication remains debatable. For example, although protein complexes can be secreted, multiple studies suggest that extracellular Ago-miRNA complexes are by-products released during cell death and are able to circulate for a long time due to the stability of Ago proteins (Makarova et al., 2016; Turchinovich et al., 2016, 2015, 2011). Likewise, it has been demonstrated *in vitro* that the miRNA content in culture media of mammalian cells coincides with cell death rate and *in vivo* studies indicate that damage of certain organs causes an increase of tissue-specific miRNAs in circulation (Akat et al., 2014; Corsten et al., 2010; Laterza et al., 2009; Makarova et al., 2016; Turchinovich et al., 2011). Nevertheless, even though they would be released during cell death, the exact potential of the extracellular Ago-miRNA complexes remains unidentified. Our data show that insect EAgo-1 associated miRNAs are present in the (cell-free) conditioned media of *Drosophila* cell lines, but whether they are a result of non-selective release during cell death or selective secretion remains unknown. On the contrary, in mammalian biofluids, the situation is clearer for miRNAs encapsulated in EVs. EV sorting and secretion is controlled by the cell and specific EV-surface proteins enable targeted delivery (Makarova et al., 2015). In this context, several studies demonstrated the functional transfer of exosomal RNA to recipient cells (Lotvall and Valadi, 2007; Valadi et al., 2007). Nevertheless, the question was also raised whether EVs contain miRNAs in physiologically relevant concentrations (Makarova et al., 2015; Turchinovich et al., 2016). Thus, the hypothesis of ex-miRNAs in EVs or bound to EAgo-1 mediating intercellular communication remains to be further studied.

2.5 Conclusion

To conclude, we have shown the presence of ex-miRNAs in extracellular conditioned media of insect cells. To our knowledge, this is the first time ex-miRNAs are identified in different fractions (namely EVs and EAgo-1) of extracellular media of cultured *Drosophila* cells. Comparison of miRNA abundancies between both cell lines indicate selective miRNA sorting and/or secretion. Our findings open new avenues to study the potential role of ex-miRNAs in intercellular communication in insects, a so far underexplored, but conceptually very intriguing, research question.

Chapter 3: miRNAs regulating postembryonic development in the migratory locust, *Locusta migratoria*

3.1 Introduction

The genome of all Metazoa and some eukaryotes largely exists of non-coding DNA. One main class of these non-coding RNAs are the microRNAs (miRNAs). These small, endogenous, non-coding RNA molecules of *ca*. 21 nucleotides long, regulate gene expression post-transcriptionally (Ambros, 2004).

MiRNAs, for which the miRNA biogenesis pathway is described in Chapter 1, are crucial in almost all biological processes. Studies have reported the involvement of insect miRNAs in insecticide resistance (Li et al., 2015) and insect-pathogen interactions (Asgari, 2013; Belles, 2017; Hussain and Asgari, 2014, 2010; P. Wu et al., 2016; Zhang et al., 2009). Moreover, insect miRNAs are known to play an important role in the regulation of embryonic development (Freitas et al., 2017; Ninova et al., 2016), reproduction (Epstein et al., 2017; Jayachandran et al., 2013; Lucas et al., 2015; Song et al., 2018; Zhang et al., 2016) and tissue development (Bejarano et al., 2010; Karres et al., 2007; Li et al., 2014; Li and Carthew, 2005; Yan Li et al., 2006; Ling et al., 2017; Lucas et al., 2015; Sokol and Ambros, 2005; Suh et al., 2015; B. Zhao et al., 2017). Furthermore, several studies report on a modified miRNA expression in different developmental stages as well as in different tissues of insects (Aravin et al., 2003; Behura and Whitfield, 2010; Cristino et al., 2011; Yu et al., 2008). The study of Zhang et al. (2015) for example found three miRNAs, *i.e*. miR-10-1a, miR-4924 and miR-9, to be differentially expressed during larval stages of *Spodoptera exigua*. Oral feeding experiments using synthetic miRNA mimics resulted in suppressed growth and mortality.

MiRNAs have also been shown to target genes involved in the ecdysone and juvenile hormone (JH) signalling cascades, thereby regulating hormonally controlled processes (Belles, 2017; Gomez-Orte and Belles, 2009; Ling et al., 2014; Sokol et al., 2008; Wu et al., 2017). The transition from immature insect stages to fully reproductive adults is dependent on these two hormones. Whereas periodic pulses of ecdysteroids trigger the moulting process in juvenile insects, the absence or presence of JH will determine the nature of the moult (Riddiford, 2012). Both hormones act through a cascade of transcription factors that transduce the hormonal signal. The molecular action of JH is mediated by its receptor, Methoprene-tolerant (Met), belonging to the basic helix–loop–helix (bHLH)/Per-Arnt-Sim (PAS) family (Charles et al., 2011; Wilson and Fabian, 1986). The binding of JH stimulates Met to form a complex with other bHLH-PAS proteins such as Taiman (Tai), a steroid receptor co-activator. The resulting JH-Met-Tai complex induces the expression of JH response genes such as *Krüppel-homolog 1* (*Kr-h1*), the main effector of the anti-metamorphic action of JH (Godlewski et al., 2006; Song et al., 2014). Ecdysteroids induce their effects by binding to a heterodimeric complex of two nuclear receptors, the ecdysone receptor (EcR) and the retinoid-X-receptor/ultraspiracle (RXR/USP), as reviewed by Hill et al. (2013). Silencing the expression of *Dicer-1*, a key enzyme involved in miRNA biosynthesis (Krol et al., 2010), in late larval *Locusta migratoria* and *Blattella germanica* resulted in a depletion of miRNA contents in the last nymphal stage. This, in turn, inhibited metamorphosis as the resulting cockroaches showed

nymphoid features and were able to moult again (Gomez-Orte and Belles, 2009). The resulting Dicer-1 depleted *L. migratoria* were characterized by disrupted nymphal-to-nymphal and nymphal-to-adult moults (Y. L. Wang et al., 2013). Lozano et al. (2015) showed that, for *B. germanica*, the miRNAs involved are those of an miR-2 family with the transcription factor Kr-h1 as target. Recently, Song et al. (2018) revealed the regulatory role of let-7 and miR-278 on Kr-h1 expression in *L. migratoria*. Application of let-7 and miR-278 mimics (agomiRs) significantly reduced the level of Kr-h1 transcripts resulting in partially precocious metamorphosis. Rubio et al. (2012) found three miRNAs to be important in the metamorphic stage (N6) of *B. germanica*, *i.e*. let-7-5p, miR-100-5p and miR-125-5p, whereas miR-252-3p appeared to be important in the pre-metamorphic stage (N5). Depletion of miR-252-3p levels in the penultimate (N5) nymphal stage caused retarded growth and developmental delays within the nymphal stage. Also in other insect species, miRNAs are shown to play a significant role in post-embryonic development. In the holometabolan insect, *Helicoverpa armigera*, miR-2002b plays a role in metamorphosis as demonstrated by Jayachandran et al. (2013) via oral administration of miRNA inhibitors and mimics. Likewise, Chen et al. (2013) demonstrated the importance of miR-8-5p and miR-2a-3p in regulating the chitin biosynthesis pathway in response to 20E signalling in the hemimetabolan *Nilaparvata lugens*. He et al. (2017) found seven miRNAs involved in ecdysteroid biosynthesis in *Chilo suppressalis*. Overexpression of miR-9b, novel-260, Bantam, novel-154, novel-80, novel-89 and novel-257 reduced the titer of 20E, induced mortality and retarded development. All the observed effects could be rescued with 20E treatment.

Besides the role of miRNAs at an intracellular level, miRNA molecules have also been observed in the biological fluids of some plants and animals (Etheridge et al., 2013; Makarova et al., 2015). Despite the progress made in elucidating the role of ex-miRNAs in mammalian extracellular fluids, only a few studies reported on the presence of ex-miRNAs in insects (Dhahbi et al., 2016; Guo et al., 2013; Mingels et al., 2020; Van den Brande et al., 2018; Wang et al., 2018). For a more in-depth view on this topic, the reader is referred to Chapter 1 and 2.

Our study shows that miRNAs play a significant role in metamorphosis in the migratory locust, *L. migratoria*, as an RNA-mediated silencing of *LmDicer-1* during the fifth nymphal stage results in moulting defects. Furthermore, our study describes the presence of ex-miRNAs in the haemolymph of *L. migratoria*. Moreover, differentially expressed ex-miRNAs were observed when comparing low *versus* high haemolymph ecdysteroid levels and were shown to interfere with metamorphosis when injected into late nymphal locusts.

3.2 Materials and methods

3.2.1 Rearing of animals

The migratory locusts (*L. migratoria*) were reared under crowded conditions in a room with controlled temperature (32 ± 1 °C) and day/night cycle (photoperiod of 13 h) at an ambient relative humidity between 40 % and 60 %. The locusts were fed freshly sprouted wheat leaves and dry oat flakes ad libitum. Pots containing a slightly moistened sand/turf mixture were placed in the breeding cages allowing mated females to deposit their eggs after which these pots were set apart once a week in clean cages where eggs were allowed to hatch into first nymphal locusts.

3.2.2 Tissue and haemolymph collection

Tissues of interest (fat body and hind leg) were dissected under a binocular microscope in *L. migratoria* Ringer solution (1 L: 9.82 g NaCl; 0.32 g CaCl2; 0.48 g KCl; 0.73 g MgCl2; 0.25 g NaHCO3; 0.19 g NaH2PO4; pH 6.5), collected in MagNA Lyser Green Beads containing tubes (Roche) and snap-frozen in liquid nitrogen to prevent RNA degradation. The fat body, as the main metabolic tissue, was collected from control animals as a source for *dsLmDicer-1* synthesis. For analyzing possible effects on expression of MEKRE93 pathway and ecdysteroid receptor components, hind legs of agomiR-injected locusts were collected, since these can be dissected without sacrificing the animal.

In a follow-up experiment, 20 µl of locust haemolymph was daily collected in capillary tubes from days two (D2) until eight (D8) after the moult to the fifth nymphal stage (N5) by carefully piercing each insect's cuticle behind the hind leg. The collected haemolymph samples were pooled [three pools of three (N5 D2, D6 and D7) or four animals (N5 D3, D4, D5 and D8) each] and depleted from apoptotic bodies by centrifugation at 5000 g for 10 min at 4 °C. Subsequently, samples were placed in liquid nitrogen to prevent RNA degradation. From the same individuals, 5 µl of haemolymph was collected for ecdysteroid measurements.

3.2.3 RNA extraction methods

3.2.3.1 Long RNA extraction and cDNA synthesis

Samples were homogenized using a MagNA Lyser instrument (30 sec, 5000 rpm; Roche). Total RNA was extracted using the RNeasy Lipid Tissue Kit (Qiagen) following the manufacturer's protocol. This protocol uses a phenol/guanidine-based lysis of the samples followed by purification of the total RNA on a silica-column as described in §2.2.4. An on-column DNase digestion (RNase-free DNase set, Qiagen) was performed to prevent genomic DNA contamination. The quality and concentration of the resulting RNA sample were determined using a Nanodrop spectrophotometer (NanoDrop ND-1000, Thermo Fisher Scientific Inc.). 1000 ng of RNA was reverse-transcribed using a mix of random hexamers and oligo(dT) primers according to the

manufacturer's protocol (PrimeScript™ RT Reagent Kit, TaKaRa, Invitrogen Life Technologies). The obtained cDNA was diluted ten-fold with Milli-Q water (Millipore).

3.2.3.2 Total RNA extraction including miRNA

Haemolymph samples were homogenized by vortexing. Total RNA, including miRNA, was extracted using the miRNeasy Serum/Plasma kit (Qiagen) following the manufacturer's protocol and as described in §2.2.4. The miRNeasy Serum/Plasma kit (Qiagen) is designed for purification of cell-free total RNA, which constitutes primarily miRNA and other small RNA molecules, from small volumes of serum and plasma. Quality and concentration of the resulting RNA samples were determined on a Nanodrop spectrophotometer (NanoPhotometer N60, Implen) and a more detailed analysis was performed using the Agilent Bioanalyzer Small RNA chip (Agilent Technologies, Inc.).

3.2.4 Quantitative real-time PCR

QRT-PCR is a specific and sensitive method to measure the relative quantity of a target mRNA as described in §2.2.5. QRT-PCR primers for the different target genes (Table 3.1) were designed using Primer Express software (Applied Biosystems). These primer pairs were validated by designing relative standard curves for gene transcripts with serial (5x) dilutions of appropriate cDNA samples. The correlation coefficient and efficiency of the qRT-PCR reaction were measured (R^2 = 0.995–1; Eff% = 90%–110%) for each primer pair. All qRT-PCR reactions were performed in duplicate in 96-well plates on a StepOne Plus System (ABI Prism, Applied Biosystems) according to the Fast SYBR Green PCR Master Mix protocol. Each reaction contained 5.0 µL of fast SYBR Green, 0.5 µL of each Forward and Reverse primer (10 µM), 1.5 µL of Milli-Q water and 2.5 µL of cDNA. A "no template control" reaction was always included. The following thermal cycling profile was used: 95 °C for 10 min, followed by 40 cycles of 95 °C for 15 s and 60 °C for 60 s. Then, a melt curve analysis was performed to confirm the specificity of the qRT-PCR reactions. Additionally, the amplification products were analyzed using horizontal agarose gel electrophoresis (1.2% agarose gel containing GelRed™, Biotium) and visualized under UV light. Only a single band of the expected size for each transcript was observed, which was further cloned and sequenced (TOPO® TA Cloning Kit for sequencing, Invitrogen) to confirm target specificity.

Optimal housekeeping genes were selected using geNorm software (Vandesompele et al., 2002). In the designed experiment rp49 and GAPDH appeared to be most stable in the studied hind leg samples. Relative expression levels were determined according to the comparative Ct method (ΔΔCt) (Vandesompele et al., 2002). Statistically significant differences between the bantam and miR-13b agomiR and negative control-injected locusts were found via a t-test on the log transformed data (with or without two-sided Welch's correction) using GraphPad Prism 6 (GraphPad Software Inc.).

Table 3.1: Oligonucleotide sequences of primers used for qRT-PCR.

Reference/ target genes	Forward primer	Reverse primer
LmRP49	5'- CGCTACAAGAAGCTTAAGAGATCATG -3'	5'- CTTAAACCTACGGCGAACTCTGTT -3'
LmGAPDH	5'- CTGATGACAACAGTGCATGCT -3'	5'- GTCCATCACGCCACAACTTTC -3'
LmEcR	5'- AGCGCCCATCTCTTGTTGAA -3'	5'- CGCCTGTTGTCCACATATGC -3'
LmRXR	5'- AATGCCTTGCTATGGGAATG -3'	5'- TCCTTTGTTCGCTGCCTTTC -3'
LmObs 2A	5'- GTGCAGTGCGACCTGTACTA -3'	5'- AGCTCCTCGGGATTGTTGTT -3'

Abbreviations: *Lm = Locusta migratoria*; *RP49 = Ribosomal protein 49; GAPDH = Glyceraldehyde 3-phosphate dehydrogenase; EcR = Ecdysone Receptor; RXR = Retinoïd X Receptor; Obs 2A = Obstructor protein 2A.*

3.2.5 Small RNA sequencing data and analysis

A small RNA library of fifth nymphal haemolymph samples (N5 D2 and N5 D3; N5 D6 and N5 D7) was prepared using the TailorMix microRNA Sample Preparation Kit V2 (SeqMatic) according to the manufacturer's protocol. Subsequently, the small RNA library was sequenced on the Illumina MiSeq® System with a single read length of 50 nt and sequencing quality control was monitored via PhiX spike-ins (2%). Next, illumina adapters/primers were removed from the raw reads with BBDuk (version 37.33; Bushnell B.) and the processed reads were aligned to the available *L. migratoria* mature miRNAs, as well as to sequences from *D. melanogaster* and other insects, from miRBase (release 21.0) and to the small RNA transcriptome of *L. migratoria* by (Wei et al., 2009) using Bowtie 2 (Galaxy Version 2.3.4.1; https://doi.org/10.1186/gb-2009-10-3-r25). Mapped read counts were obtained using the Idxstats command of SAMtools (Galaxy Version 2.0.1; 10.1093/bioinformatics/btp352). Differential expression analysis was performed using the R (R Core Team; version 3.3.3) packages Sartools (version 1.6.1: 10.1371/journal.pone.0157022) and edgeR (version 3.16.5; 10.1093/bioinformatics/btp616) (Appendices: Supplementary Table Chapter 6). MiRNAs were only retained if they displayed a counts-per-million (cpm) above 1 in at least 3 samples. Using the search for similarity with miRBase miRNA sequences (miRBase release 21.0), several differentially expressed novel miRNAs were identified.

3.2.6 RNA interference experiments

Double-stranded (ds)RNA constructs for *LmDicer-1* and *GFP* (control) were prepared using Ambion's MEGAScript RNAi kit following the manufacturer's protocol. A user-provided DNA template with a T7 promoter sequence at the 5' ends of each strand was used in a high yield *in vitro* transcription reaction. Forward and reverse primers flanked by the T7 promoter sequence (given in Table 3.2) were used in a PCR reaction with REDTaq DNA Polymerase (Sigma) to amplify the targets of interest. The resulting amplicons were analysed using horizontal agarose gel electrophoresis (1.2 % agarose gel containing GelRedTM, Biotium) and visualised under UV light. Only a single band of the expected size was observed, which was further cloned and sequenced (TOPO® TA Cloning Kit for sequencing, Invitrogen) to confirm target specificity. The resulting constructs were used as templates in high-yield *in vitro* transcription reactions using T7 RNA polymerase.

Remaining ssRNA and DNA were further removed in a nuclease digestion step. The produced dsRNA was checked by horizontal agarose gel electrophoresis (1.2 % agarose gel containing GelRedTM, Biotium) and using a Nanodrop spectrophotometer (NanoDrop ND-1000, Thermo Fisher Scientific Inc.) for determining integrity, quality and concentration.

Newly moulted fifth nymphal (N5) locusts, synchronised on the day of ecdysis (D0), were injected with 6 µl dsRNA against *LmDicer-1* (*dsLmDicer-1*) (300 ng dsRNA/locust, diluted in *L. migratoria* Ringer). A second injection was given on day three of the fifth nymphal stage (N5 D3) to ensure an efficient knockdown of *LmDicer-1* during this nymphal stage. As a control condition, another group of locusts was injected with dsRNA against *GFP* (*dsGFP*) following the same injection scheme.

Table 3.2: Oligonucleotide sequences of primers used for dsRNA synthesis. Oligonucleotide sequences indicated in 'bold' represent the T7 promoter sequences used for the preparation of dsRNA constructs.

dsRNA constructs	Forward primer	Reverse primer
dsLmDicer -1	5'- **TAATACGACTCACTATAGGG** ATTATGCGGTGGGTGTATT -3'	5'- **TAATACGACTCACTATAGGG** GCAAGAGAAAATGCCTTTCG-3'
dsGFP	5'-**TAATACGACTCACTATAGGGAGA** AAGGTGATGCTACATACGGAA -3'	5'-**TAATACGACTCACTATAGGGAGA** ATCCCAGCAGCAGTTACAAAC-3'

Abbreviations: *Lm = Locusta migratoria; GFP = Green fluorescent protein.*

3.2.7 Prediction of miRNA targets

The identified differentially expressed miRNAs (using miRBase miRNA sequences), as well as several miRNAs selected from literature, were subsequently used for target prediction. Sequences from the Transcriptome Shotgun Assembly (TSA) of *L. migratoria*, as found on NCBI (AVCP01.12, GBDZ01.1, GBFE01.1, GCGJ0.1 and GETS01.1), were used to predict the miRNA targets. miRanda (V3.3a) (Enright et al., 2003), RNAhybrid (V2.2) (Krüger and Rehmsmeier, 2006) and MicroTar (Thadani and Tammi, 2006) were selected as the prediction tools. A miRanda score greater than 150 and an RNAhybrid mfe-value smaller than -40.0 kcal/mol were used to select targets. At the core of the MicroTar algorithm lies the estimation of miRNA-mRNA duplex energy.

3.2.8 A(nta)gomiR experiments

Three (*Lmi*-bantam-3p, *Lmi*-miR-13b-3p and *Lmi*-miR-12-5p) of the 43 significantly different miRNAs were investigated further by *in vivo* injection experiments to analyse their possible effects on moulting and metamorphosis in *L. migratoria*. Three other miRNAs (*Lmi*-miR-306-5p, *Lmi*-miR-1-3p and *Lmi*-miR-14-3p), selected based on their predicted ability to target components in the ecdysteroid and/or MEKRE93 pathway, were also included in the study. AgomiRs and antagomiRs, *i.e*. chemically modified miRNA mimics and inhibitors, respectively, are widely used for *in vivo* functional studies of miRNAs. Injection of an agomiR

elevates the total abundance of this miRNA without overexpressing the endogenous miRNA. In contrast, injection of an antagomiR inhibits the function of the endogenous miRNA (GenePharma).

AgomiRs for *Lmi*-miR-306-5p, *Lmi*-miR-13b-3p, *Lmi*-Bantam-3p, *Lmi*-miR-12-5p, *Lmi*-miR-14-3p and *Lmi*-miR-1-3p and antagomiRs for *Lmi*-miR-306-5p, *Lmi*-miR-13b-3p and *Lmi*-Bantam-3p were synthesized by GenePharma (Table 3.3). Newly moulted fifth nymphal (N5) locusts, synchronised on the day of ecdysis (D0), were injected with 0.1 nmol agomiR or antagomiR for *Lmi*-miR-306-5p or *Lmi*-Bantam-3p. A second injection was given on day three of the fifth nymphal stage (N5 D3) to ensure a continuous overload or an efficient knockdown of *Lmi*-miR-306-5p and *Lmi*-Bantam-3p, respectively during this nymphal stage. During a second experiment, 4-day-old fourth nymphal locusts (N4 D4) were injected with 0.1 nmol agomiR or antagomiR for *Lmi*-miR-13b-3p. A second and third injection was given in newly moulted fifth nymphal (N5) locusts, synchronised on the day of ecdysis (D0), and on day three of the fifth nymphal stage (N5 D3) to ensure a continuous overload or an efficient knockdown of *Lmi*-miR-13b-3p, respectively during this nymphal stage. In a third experiment, newly moulted fourth nymphal (N4) locusts, synchronised on the day of ecdysis (D0), were injected with 0.1 nmol agomiR for *Lmi*-miR-1-3p, *Lmi*-miR-12-5p or *Lmi*-miR-14-3p. A second injection was given on day three of the fourth nymphal stage (N4 D3) to ensure a continuous overload of *Lmi*-miR-1-3p, *Lmi*-miR-12-5p or *Lmi*-miR-14-3p during this nymphal stage. As a control condition, another group of locusts was injected with agomiR or antagomiR negative control sequence following the same injection schemes. The negative control sequence is a random sequence miRNA agomiR or antagomir molecule that has been extensively tested and validated to not produce any effects on known miRNA function. Hind legs were collected on day five of the fifth nymphal stage for *Lmi*-Bantam-3p and *Lmi*-miR-13b-3p agomiR-injected locusts.

Table 3.3: Oligonucleotide sequences used for a(nta)gomiRs synthesis. The agomiR sense strand is equal to the concerning miRNA, while the agomiR antisense strand constitutes the reverse complement, minus 2 nucleotides at the 5' end and plus UU at the 3' end. Antagomirs are synthesised as the reverse complement of the concerning miRNAs.

miRNA	AgomiR	AntagomiR
Lmi-miR-306-5p	Sense 5'- UCAGGUACUGAGUGACUCUGA -3'	5'- UCAGAGUCACUCAGUACCUGA -3'
	Antisense 5'- AGAGUCACUCAGUACCUGAUU -3'	
Lmi-miR-13b-3p	Sense 5'- UAUCACAGCCAUUUUUGACGAGUU -3'	5'- AACUCGUCAAAAAUGGCUGUGAUA -3'
	Antisense 5'- CUCGUCAAAAAUGGCUGUGAUAUU -3'	
Lmi-Bantam-3p	Sense 5'- UGAGAUCAUUGUGAAAGCUGAUU -3'	5'- AAUCAGCUUUCACAAUGAUCUCA -3'
	Antisense 5'- UCAGCUUUCACAAUGAUCUCAUU -3'	
Lmi-miR-1-3p	Sense 5'- UGGAAUGUAAAGAAGUAUGGAG -3'	
	Antisense 5'- CCAUACUUCUUUACAUUCCAUU -3'	
Lmi-miR-12-5p	Sense 5'- UGAGUAUUACAUCAGGUACUGAC -3'	
	Antisense 5'- CAGUACCUGAUGUAAUACUCAUU -3'	
Lmi-miR-14-3p	Sense 5'- UCAGUCUUUUUCUCUCUCCUAU -3'	
	Antisense 5'- AGGAGAGAGAAAAAGACUGAUU -3'	
Negative control	Sense 5'- UUCUCCGAACGUGUCACGUTT -3'	5'-CAGUACUUUUGUGUAGUACAA -3'
	Antisense 5'- ACGUGACACGUUCGGAGAATT -3'	

Abbreviations: *Lmi* = *Locusta migratoria*; miR = miRNA.

3.2.9 Observing ecdysis of *dsLmDicer-1* and a(nta)gomiR-injected locusts

The ecdysis of *dsLmDicer-1* and *dsGFP*-injected, as well as of the different agomiR and antagomir-injected locusts was closely observed. Starting from fifth nymphal locusts (N5), synchronised on the day of ecdysis (D0), the duration of the fifth nymphal stage was monitored in detail. Data were analyzed with a log-rank (Mantel-Cox) test using GraphPad Prism 6 (GraphPad Software Inc.).

3.2.10 Ecdysteroid measurements using an enzyme immunoassay

Ecdysteroid titers in *L. migratoria* haemolymph were measured using an EIA, modified from Porcheron et al. (1989) and discussed by Pascual et al. (1995) and Lafont et al. (2012). This protocol uses a peroxidase conjugate of 20E as tracer together with rabbit L2 polyclonal antibodies against ecdysteroids. This L2 antiserum has a strong affinity for E, 3-deoxyecdysone and 2-deoxyecdysone and a 6- to 8-fold lower affinity for 20E. Both serum and tracer were very kindly supplied by Prof. J.P. Delbecque (Université de Bordeaux, France).

Haemolymph samples were collected from *L. migratoria* fifth nymphal locusts by piercing the insect's cuticle behind its hind leg. Using a capillary tube, 5 µl of haemolymph was collected from each animal. The collected 5 µl haemolymph samples were pooled [three pools of three (N5 D2, D6 and D7) or four animals (N5 D3, D4, D5 and D8) each] and immediately transferred to 95 µl of 100 % ethanol and stored at -20 °C until further processing, as previously described by Marchal et al. (2011a). The haemolymph samples were extracted as follows: the samples were vortexed and centrifuged for 10 min at maximum speed, after which the supernatant was transferred to a fresh Eppendorf tube. The remaining pellet was extracted two more times

and the combined extracts were then dried in a SpeedVac concentrator and redissolved in EIA sample buffer (80 mM K2HPO4, 20 mM KH2PO4, 0.4 M NaCl, 1.25 mM EDTA, 0.1% BSA, 0.01% thimerosal, pH 7.4). A dilution series of known concentrations of 20E, ranging from 10^{-12} to 10^{-8} M, was used as a standard (Sigma-Aldrich Co., St-Louis, MO). Previously coated MaxiSorp 96-well plates (Nunc, Roskilde, Denmark), with secondary (goat anti-rabbit IgG, Jackson Immuno Research, West Grove, PA) antibodies, were washed with a poly-sorbate based wash buffer and loaded with i) 50 µl tracer, ii) 50 µl sample or standard and iii) 50 µl polyclonal antibodies. 0 % (tracer and buffer) and 100 % (tracer, buffer and antibody) reactions were included. Following a 3-hour incubation, the plates were washed and a colouration substrate mixture (containing 0.42 mM 3,3',5,5'-tetramethylbenzidine in dimethylsulfoxide, 165.8 mM sodium acetate, 0.85 mM urea hydrogen peroxide and 1.6 mM citric acid, pH 6) was added. Absorbance values were measured in a UV spectrophotometer-microplate reader (Mithras LB 940, Berthold technologies GmbH & Co. KG, Germany) at 370 nm and 37°C every five minutes for one hour.

The resulting absorbance values were compared to the calibration curve obtained with 20E as a standard. A t-test (with or without two-sided Welch's correction) was performed using GraphPad Prism 6 (GraphPad Software Inc.) to test for statistically significant differences between the different timepoints.

3.3 Results

3.3.1 Knockdown of *LmDicer-1* results in defects in moulting

Injections of *dsLmDicer-1* during the fifth nymphal stage (on D0 ad D3) affected development of *L. migratoria* (Fig. 3.1). Although the knockdown (*dsLmDicer-1*) animals remained in the fifth nymphal stage for a similar time period as the control (*dsGFP*) locusts, 40 % of the experimental locusts did not successfully moult into the adult stage, while 90 % of the *dsGFP* injected (control) locusts successfully completed this nymphal-to-adult moult (Fig. 3.1B and C). When attempting ecdysis to the adult stage, six out of ten *dsLmDicer-1* injected (experimental) animals appeared to be unable to shed their old cuticle and eventually died (Fig. 3.1D).

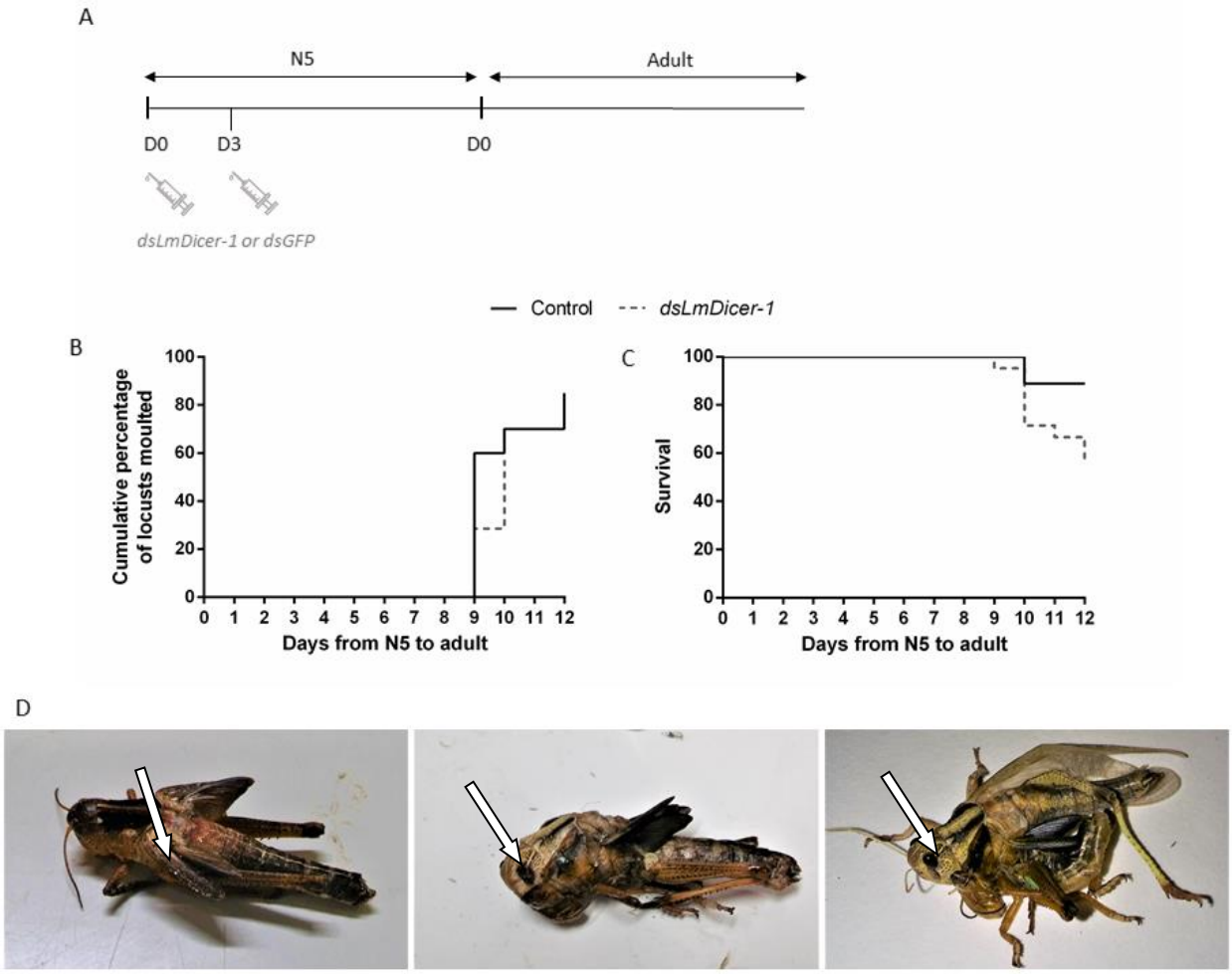

Figure 3.1: The timing of ecdysis of *dsLmDicer-1* injected locusts and the observed defects in moulting. (A) Time scheme showing the different time points of *dsLmDicer-1* (knockdown condition) or *dsGFP* (control condition) injections. (B) The cumulative percentage of 9 *dsGFP* (control) and 21 *dsLmDicer-1* (*LmDicer-1* knockdown) injected locusts that moulted from the fifth nymphal (N5) to the adult stage. (C) A survival plot representing the percentages of locusts still alive after successfully moulting to the adult stage. With a log-rank (Mantel-Cox) test, no significant differences were found between the conditions. (D) Observed difficulties during moulting of the *dsLmDicer-1* injected locusts to adults, with arrows indicating the region of interest. Some experimental locusts died during the process of ecdysis, whereas others remained in the fifth nymphal stage, were weakened and eventually died.

3.3.2 Temporal profiles of ecdysteroids in haemolymph of fifth nymphal locusts

Ecdysteroid levels were measured in haemolymph samples that were collected every day starting on day two of the fifth nymphal (N5 D2) stage until day 8 (N5 D8) (Fig. 3.2). A peak of ecdysteroids was witnessed several days before moulting.

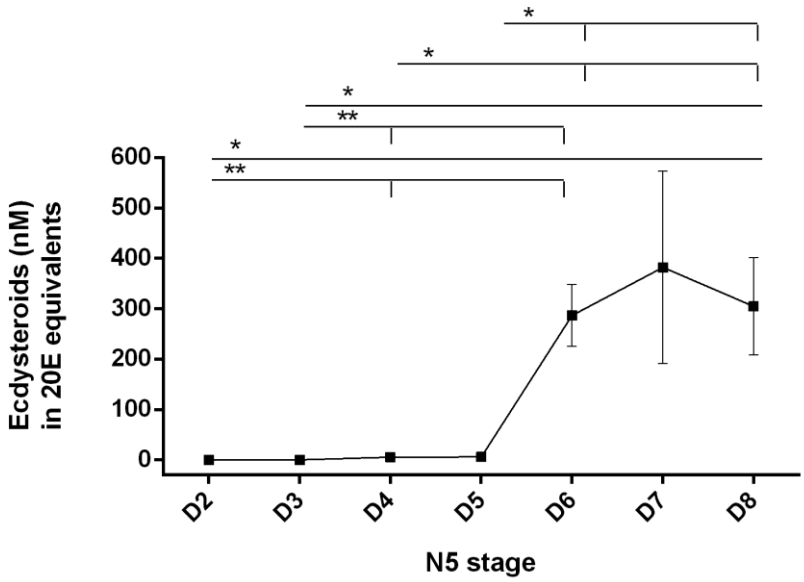

Figure 3.2: Ecdysteroid levels in haemolymph of fifth nymphal locusts. Ecdysteroid levels (20E equivalents in nM) were measured in locust haemolymph samples that were collected daily from day two (N5 D2) until day eight (N5 D8) in the fifth nymphal stage. The data represent mean ± S.E.M. of three independent pools of three (N5 D2, D6 and D7) or four (N5 D3, D4, D5 and D8) animals each. Statistically significant differences between the measurements were found via a t-test (with or without two-sided Welch's correction) and are indicated by (an) asterisk(s) (* $p < 0.05$; ** $p < 0.01$).

3.3.3 Differential expression analysis of small RNA sequencing data

Small RNA sequencing (RNA-seq) reads of fifth nymphal *L. migratoria* haemolymph characterized by low (N5 D2 and N5 D3) *versus* high (N5 D6 and N5 D7) ecdysteroid levels were analyzed. Abundant miRNAs display a high number of read counts. Based on the differential expression analysis, the abundances of 43 miRNAs significantly differed between the tested conditions (Table 3.4 and 3.5). 26 out of 43 miRNAs were significantly more abundant in low compared to high haemolymph ecdysteroid levels, while the remaining 17 miRNAs were more abundant in high haemolymph ecdysteroid levels. 12 out of 43 miRNAs were characterized either as a known *L. migratoria* miRNA (miRBase) or a miRNA found based on similarity with miRBase miRNA sequences. The remaining 31 miRNAs represent novel miRNA sequences yet to be clarified (Table 3.4). Table 3.5 shows the sequences of the differentially expressed miRNAs. In addition, the pool of identified differentially expressed miRNAs contains both 5p- and 3p- miRNAs. This is of interest considering that not only 5p- miRNAs are functional, as initially thought, but also 3p- miRNAs (*i.e*. derived from the 5' and 3' arm of the precursor, respectively) (Rubio et al., 2012; Yang et al., 2011).

Table 3.4: Small RNA sequencing data. Small RNA sequencing data of high (N5 D6 and D7) compared to low ecdysteroid levels (N5 D2 and D3), on three and four biological replicates, respectively, were analysed using edgeR. Normalised counts per sample of the differential expressed miRNAs and their corresponding adjusted p-values ($\alpha < 0.05$). Abundant miRNAs display high read counts, while less abundant miRNAs are characterized by low read counts. Log2FoldChange values reflect the differential expression between high and low ecdysteroid levels. Positive and negative values indicate upregulated (miRNAs above dotted line) and downregulated (miRNAs below dotted line) miRNA abundances in low ecdysteroid levels, respectively. MiRNAs were ranked (top to bottom) based on their adjusted p-values ($\alpha < 0.05$). MiRNAs indicated in bold represent known *L. migratoria* miRNAs (miRBase) or miRNAs found based on similarity with miRBase miRNA sequences. The remaining miRNAs represent novel miRNA sequences.

miRNA	**High ecdysteroid level**			**Low ecdysteroid level**				**Log2Fold - Change**	**Padj value**
	N5 D7	N5 D6		N5 D3		N5 D2			
Lmi-novel-miR-47	40	15	31	120	195	131	146	2,292	1,93E-09
Lmi-novel-miR-17/18/19	37	20	16	83	103	100	97	1,864	2,86E-07
***Lmi*-bantam-3p** (*Lmi*-miR-novel-80/81/82)	87	54	36	197	213	164	194	1.627	9.27E-07
Lmi-novel-miR-29	0	0	0	7	14	7	13	6,387	6,70E-06
***Lmi*-miR-8-3p**	1792	1940	1504	3348	3075	3365	3203	0.896	3.64E-05
***Lmi*-miR-306-5p** (*Lmi*-miR-novel-27/115)	20	22	10	80	59	51	52	1.727	3.64E-05
***Lmi*-miR-279-3p** (*Lmi*-miR-novel-125-128)	48	32	29	90	101	100	97	1.341	2.37E-06
Lmi-novel-miR-87	5	12	5	49	42	25	27	2,3	6,03E-05
ID50	23	27	13	82	65	55	51	1,541	0,000139
IM18	18	12	16	38	46	38	53	1,481	0,000540
***Lmi*-miR-9a-5p**	264	219	161	480	349	430	394	0.925	7.74E-05
Lmi-novel-miR-23	5	7	5	20	18	18	18	1,669	0,002458
***Lmi*-miR-13b-3p** (*Lmi*-miR-novel-58)	15	5	8	19	38	32	28	1.502	0.0005
ID1142	1	0	0	15	2	8	6	3,419	0,005971
IM59	32	7	3	86	28	73	43	1,816	0,006296
Lmi-novel-miR-119/118	18	22	16	43	40	33	46	1,13	0,009873
Lmi-novel-miR-121	195	197	154	293	274	279	291	0,635	0,012620
***Lmi*-miR-12-5p** (*Lmi*-miR-novel-24)	5	7	5	19	16	17	13	1.469	0.0128
Lmi-novel-miR-120	14	7	16	27	27	30	26	1,127	0,013569
Lmi-novel-miR-45	2	2	0	3	8	12	7	2,132	0,016563
ID1281	0	2	3	6	4	8	8	2,357	0,019450
***Lmi*-miR-315-5p** (ID1582)	0	0	0	2	0	6	3	4.48	0.0227
Lmi-novel-miR-129	1	2	5	12	12	8	5	1,908	0,022719
***Lmi*-miR-190-5p** (Lmi-miR-novel-37)	57	32	34	60	129	64	89	1.007	0.0242
Lmi-novel-miR-54/55/56/57	1	2	3	7	7	8	5	1,92	0,02974
Lmi-novel-miR-77	17	30	5	27	38	38	31	0,974	0,049578
***Lmi*-miR-275-3p** (*Lmi*-miR-novel-28)	473	524	640	262	289	281	315	-0.921	4.60E-05
Lmi-novel-miR-16	0	12	23	1	0	1	1	-3,945	0,000414
ID1794	4	2	8	0	0	0	1	-3,897	0,000526
***Lmi*-miR-8-5p**	88	103	120	43	46	49	58	-1.049	0.0006
ID604	48	74	78	20	27	30	30	-1,238	0,000651
ID1454	15	10	5	3	2	4	3	-1,754	0,003746
ID607	42	74	83	18	30	29	35	-1,166	0,004984
Lmi-novel-miR-32	5	2	3	0	1	0	0	-3,028	0,006296
Lmi-novel-miR-1/2	10	17	18	7	7	5	4	-1,328	0,019689
Lmi-novel-miR-63/64	8	15	34	3	6	6	9	-1,471	0,020665
Lmi-novel-miR-46	23	86	44	15	20	29	18	-1,27	0,020947
ID877	1	7	5	1	0	0	1	-2,355	0,035641
Lmi -novel-miR-67/68/69/70	30	42	49	12	21	24	23	-0,931	0,035641
Lmi -novel-miR-113	29	62	75	24	28	30	28	-0,929	0,036781
ID1684	2	0	8	0	1	1	0	-2,561	0,037335
***Lmi*-miR-281-5p**	11	0	10	2	1	5	3	-1.492	0.0420
Lmi-novel-miR-86	7	22	10	2	5	7	4	-1,271	0,043240

Abbreviations: D = day; *Lmi* = *Locusta migratoria*; miR = miRNA; N = nymphal stage; p_{adj} = raw p-value adjustment.

Table 3.5: Sequences of differentially expressed miRNAs. MiRNA sequences above and below the dotted line represent miRNAs upregulated and downregulated in haemolymph of locusts with low ecdysteroid levels, when compared to locusts with high ecdysteroid levels, respectively. MiRNAs indicated in bold represent known *L. migratoria* miRNAs (miRBase) or miRNAs found based on similarity with miRBase miRNA sequences. The remaining miRNAs represent novel miRNA sequences.

miRNA	Sequence (5' – 3')
Lmi-novel-miR-47	UAGCUGCCUAGAGAAGGGCAUC
Lmi-novel-miR-17/18/19	AAAUAUCAGUUGGUAAUUCUGG
***Lmi*-bantam-3p** (*Lmi*-miR-novel-80/81/82)	UGAGAUCAUUGUGAAAGCUGAUU
Lmi-novel-miR-29	UAAGCUCGUCUUUCUGAGCAGU
***Lmi*-miR-8-3p**	UAAUACUGUCAGGUAACGAUGUC
***Lmi*-miR-305-5p** (*Lmi*-miR-novel-27/115)	AUUGUACUUCAUCAGGUGCUC
***Lmi*-miR-279-3p** (*Lmi*-miR-novel-125-128)	UGACUAGAUCCAUACUCGUCU
Lmi-novel-miR-87	UGACUAGAGUGACACUCGUC
ID50	ATTGTACTTCATCAGGTGCTCTGG
IM18	TCAGGTACTGAGTGACTCTGAG
***Lmi*-miR-9a-5p**	UCUUUGGUUAUCUAGCUGUAUGA
Lmi-novel-miR-23	UGAGUAUUACAUCAGGUACUGAC
***Lmi*-miR-13b-3p** (*Lmi*-miR-novel-58)	UAUCACAGCCAUUUUUGACGAGUU
ID1142	ACTATTCTGTTAGTGACACTGAT
IM59	TCTTTGGTTATCTAGCTGTATGA
Lmi-novel-miR-119/118	UCAGGUACUGAGUGACUCUGAGA
Lmi-novel-miR-121	UCUUUGGUGAUCUAGCUGUAUGA
***Lmi*-miR-12-5p** (*Lmi*-miR-novel-24)	UGAGUAUUACAUCAGGUACUGACG
Lmi-novel-miR-120	CUUUGGUGAUGUAGCUGUAUGA
Lmi-novel-miR-45	GGUCGGGAGUUCGAUCCUCC
ID1281	TCGCTATTATCTGTGACGATAT
***Lmi*-miR-315-5p** (ID1582)	TTTTGATTGTTGCTCAGAAAGC
Lmi-novel-miR-129	GGGGAAAGGAGGAGGAGG
***Lmi*-miR-190-5p** (*Lmi*-miR-novel-37)	AGAUAUGUUUGAUAUUCUUGGUUG
Lmi-novel-miR-54/55/56/57	UAUCACAGCCACUUUGAUGAGC
Lmi-novel-miR-77	AUGAGCAAUGUUAUUCAAAUGG
***Lmi*-miR-275-3p** (*Lmi*-miR-novel-28)	UCAGGUACCUGAAGUAGCGCGC
Lmi-novel-miR-16	GGCCACUACGGUCGGGGG
ID1794	GTGTCCTGTCAGCGTCGATCTTCG
***Lmi*-miR-8-5p**	CAUCUUACCGGGCAGCAUUAGA
ID604	TAGGTAACAGAACCCCGAGTGT
ID1454	AAGATCTAGTAGAGACGGCTGC
ID607	TAGGTAACAGAACCCCGAGTGT
Lmi-novel-miR-32	UGGUAACUGGCAGAACUUUUUC
Lmi-novel-miR-1/2	UCUUCGUCGCGGUUUGCUGCCA
Lmi-novel-miR-63/64	CUAGGUAACAGAACCCCGAGUAU
Lmi-novel-miR-46	CGGCUCAUCUCUGGGCACCUUGU
ID877	ATCCCCTGGTGAAACTTTCCGC
Lmi-novel-miR-67/68/69/70	UAGGUAACAGAACCCCGAGUGU
Lmi-novel-miR-113	CAACAUAGCGGCGAACACGGGU
ID1684	ATGGTGTCAGGAATATGAGTCG
***Lmi*-miR-281-5p**	AAGAGAGCUAUCCGUCGACAGU
Lmi-novel-miR-86	GACGGGUGCACUCUGGGUCACG

Abbreviations: *Lmi* = *Locusta migratoria*; miR = miRNA.

3.3.4 Prediction of miRNAs targeting the ecdysone receptor complex or MEKRE93 pathway components

Next, we identified miRNAs potentially involved in the expression regulation of the ecdysone receptor complex and/or MEKRE93 pathway components in *L. migratoria*. Besides the significantly expressed miRNAs of the small RNA sequencing, a few additional miRNAs were included because of i) their presence in the investigated *L. migratoria* haemolymph samples (although not differentially regulated between the conditions tested) and ii) their potential relevance in the context of moulting and metamorphosis (Rubio et al., 2012; Varghese and Cohen, 2007). *Lmi*-bantam-3p was predicted to bind *LmRXR* whereas *Lmi*-miR-306-5p was predicted to bind *LmEcR*. Regarding the MEKRE93 pathway components, *Lmi*-miR-1-3p, *Lmi*-miR-12-5p and *Lmi*-miR-14-3p were predicted to bind *LmKr-h1* and *Lmi*-miR-13b-3p was predicted to bind *LmE93*. Moreover, an additional target of interest for *Lmi*-miR-13b-3p was predicted, *i.e*. the mRNA encoding Obstructor protein 2A (*LmObs2A*).

3.3.5 *Lmi*-bantam-3p, *Lmi*-miR-306-5p and *Lmi*-miR-13b-3p are possibly involved in moulting

Injections of *Lmi*-miR-13b-3p agomiR during the fourth and fifth nymphal stage of *L. migratoria* significantly affected the duration of the fifth nymphal stage. While in negative control animals the N5 stage lasted for 6-8 days, *Lmi*-miR-13b-3p agomiR-injected locusts remained in the fifth nymphal stage for a longer period, i.e. 8-10 days (Fig. 3.3B). However, no significant differences on survival were observed (Fig. 3.3C). Injections of *Lmi*-miR-13b-3p antagomiR during the fifth nymphal stage (on D2 ad D4) did not result in differences on duration or survival of the fifth nymphal stage when compared to negative control animals (Fig. 3.3H and I).

Injections of *Lmi*-bantam-3p and *Lmi*-miR-306-5p during the fifth nymphal stage affected development of *L. migratoria* (Fig. 3.3D – I). Although the *Lmi*-bantam-3p and *Lmi*-miR-306-5p agomiR-injected (on D0 and D3) animals remained in the fifth nymphal stage for a similar time period as the negative control locusts, 60 % of the *Lmi*-bantam-3p agomiR-injected locusts did not successfully moult into the adult stage, while 100 % of the negative control locusts successfully completed this nymphal-to-adult moult (Fig. 3.3E and F). While attempting ecdysis to the adult stage, six out of ten *Lmi*-bantam-3p agomiR-injected animals appeared to be unable to shed their old cuticle and eventually died in a similar manner as observed for the *dsLmDicer-1*-injected locusts (Fig. 3.1D). *Lmi*-miR13b-3p and *Lmi*-miR-306-5p antagomiR-injected locusts remained in the fifth nymphal stage for a longer time than the negative control locusts, although all locusts successfully moulted to the adult stage (Fig. 3.3H and I).

Injections of *Lmi*-miR-1-3p, *Lmi*-miR-12-3p and *Lmi*-miR-14-5p agomiR during the fourth nymphal (on D0 and D3) stage did not affect development of *L. migratoria*.

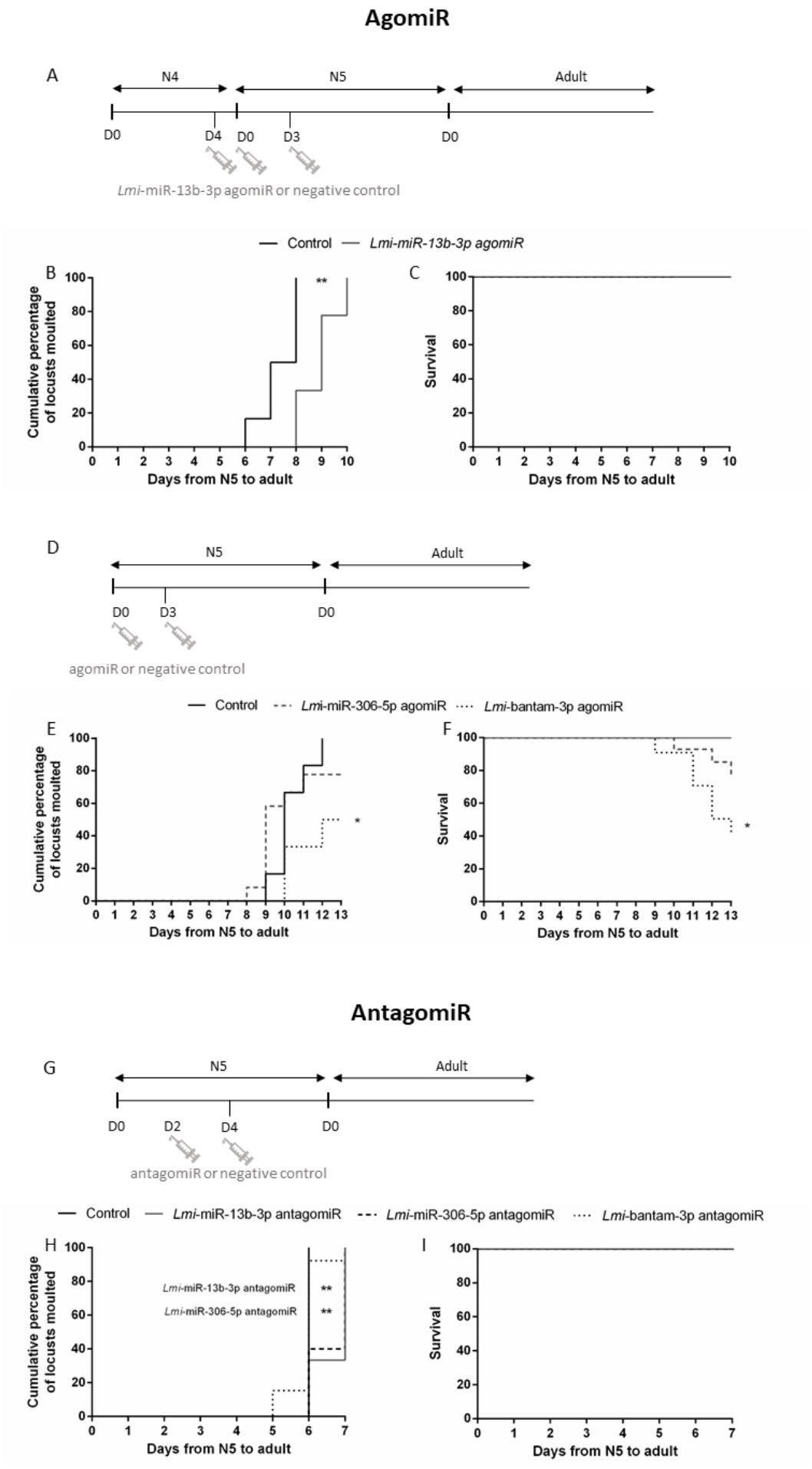
AgomiR
A
N4
N5
Adult
D0
D4
D0
D3
D0
Lmi-miR-13b-3p agomiR or negative control
Control
Lmi-miR-13b-3p agomiR
B
Cumulative percentage of locusts moulted
Days from N5 to adult
**
C
Survival
Days from N5 to adult
D
N5
Adult
D0
D3
D0
agomiR or negative control
Control
Lmi-miR-306-5p agomiR
Lmi-bantam-3p agomiR
E
Cumulative percentage of locusts moulted
Days from N5 to adult
*
F
Survival
Days from N5 to adult
*
AntagomiR
G
N5
Adult
D0
D2
D4
D0
antagomiR or negative control
Control
Lmi-miR-13b-3p antagomiR
Lmi-miR-306-5p antagomiR
Lmi-bantam-3p antagomiR
H
Cumulative percentage of locusts moulted
Lmi-miR-13b-3p antagomiR
Lmi-miR-306-5p antagomiR
**
**
Days from N5 to adult
I
Survival
Days from N5 to adult

Figure 3.3: The timing of ecdysis of *Lmi*-miR-13b-3p, *Lmi*-miR-306-5p and *Lmi*-bantam-3p agomiR or antagomiR injected locusts and the observed defects in moulting. Time schemes showing the different time points of (A) *Lmi*-miR-13b-3p, (D) *Lmi*-miR-306-5p and *Lmi*-bantam-3p agomiR and (G) *Lmi*-miR-13b-3p, *Lmi*-miR-306-5p and *Lmi*-bantam-3p antagomiR (experimental condition) or negative control (control condition) injections. The cumulative percentage of (B) 6 control and 9 *Lmi*-miR-13b-3p agomiR, (E) 6 control and 11 *Lmi*-miR-306-5p and 10 *Lmi*-bantam-3p agomiR and (H) 10 control and 15 *Lmi*-miR-13b-3p, 15 *Lmi*-miR-306-5p and 13 *Lmi*-bantam-3p antagomiR injected locusts that moulted from the fifth nymphal (N5) to the adult stage. (C + E + I) Survival plots representing the percentages of locusts still alive after successfully moulting to the adult stage. Statistically significant differences (p) between the conditions were found via a log-rank (Mantel–Cox) test and are indicated by (an) asterisk(s) (* $p < 0.05$; ** $p < 0.01$).

3.3.6 Transcript levels of *LmEcR*, *LmRXR* and *LmObs2A* in *Lmi*-bantam-3p and *Lmi*-miR-13b-3p agomiR-injected locusts

Transcript levels of the ecdysone receptor complex were determined in hind legs of *Lmi*-bantam-3p agomiR-injected and negative control locusts on day five after the moult to the fifth nymphal stage (N5 D5). No significant changes were observed in the levels of *LmEcR* and *LmRXR* transcripts at this time point (Fig. 3.4A and B). Transcript levels of *LmObs2A* were determined in hind legs of *Lmi*-miR-13b-3p agomiR-injected compared to negative control locusts on day five of the fifth nymphal stage (N5 D5). No significant differences were observed (Fig. 3.4C).

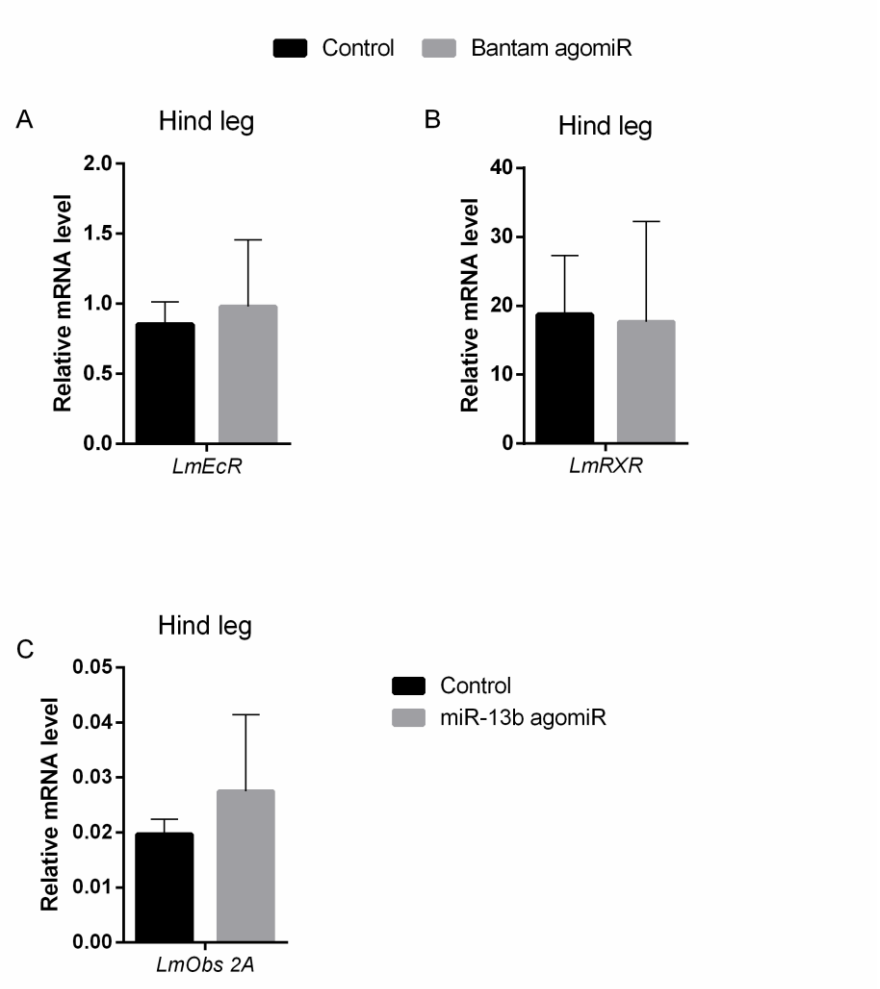

Figure 3.4: Relative *LmEcR, LmRXR* and *LmObs2A* transcript levels in agomiR-injected locusts. Relative (A) *LmEcR* and (B) *LmRXR* transcript levels were measured in hind legs of *Lmi*-bantam-3p agomiR-injected and negative control locusts on day five of the fifth nymphal stage (N5 D5). The data represent mean ± S.E.M. of five experimental and ten control animals, run in duplicate and normalized to rp49 + GAPDH transcript levels. (C) Relative *LmObs2A* transcript levels were measured in hind legs of *Lmi*-miR-13b-3p agomiR-injected and negative control locusts on day five of their fifth nymphal stage (N5 D5). The data represent mean ± S.E.M. of five experimental and five control animals, run in duplicate and normalized to rp49 + GAPDH transcript levels. No statistically significant differences between the measurements were found via a t-test on log-transformed data (with or without two-sided Welch's correction).

3.4 Discussion

In the present study, we describe the developmental effects when mimicking or inhibiting several miRNAs predicted to regulate metamorphosis in the migratory locust, *L. migratoria*. Dicer-1 is a key enzyme involved in miRNA biosynthesis (Krol et al., 2010). Using systemic RNAi to silence the expression of *LmDicer-1* during the fifth nymphal stage, we disrupted the nymphal-to-adult moult. While attempting ecdysis to the adult stage, 60 % of *dsLmDicer-1* injected (experimental) animals appeared to be unable to shed their old cuticle and eventually died (Fig. 3.1). Our results corroborated the findings of Wang et al. (2013) revealing that *LmDicer-1* is essential for miRNA regulation and development of *L. migratoria*. Similar observations were made after *Dicer-1* knockdown in the hemimetabolan *B. germanica* (Gomez-Orte and Belles, 2009). Silencing of Dicer-1 depleted miRNA contents and practically inhibited metamorphosis, only the resulting animals showed nymphoid features and were able to moult again. A further study on *B. germanica* revealed that *Dicer-1* depletion increased *Kr-h1* mRNA levels, a JH-dependent transcription factor targeted by the miR-2 family. This observation suggests that miRNAs directly regulate insect metamorphosis by controlling the JH signalling pathway (Lozano et al., 2015). These experiments showed that miRNAs play a significant role in hemimetabolan metamorphosis. Interestingly, reduced levels of Dicer-1 in the holometabolan *Tribolium castaneum* resulted in a mild morphological phenotype with only occasional wing expansion defects (Tomoyasu et al., 2008). This may suggest that there are important differences concerning the role of miRNAs in holometabolan and hemimetabolan metamorphosis. However, Wu et al. (2017) demonstrated that *Dicer-1* RNAi led to critical miRNA-induced metamorphosis defects in *T. castaneum*, including abnormal pupae and adults which eventually all died. Altogether, these studies point to miRNAs as important players in the metamorphic transition in a variety of insect species.

To further unravel the regulatory role of miRNAs in the process of metamorphosis, a differential expression analysis of small RNAs of *L. migratoria* haemolymph samples was performed. Ecdysteroids are known to initiate the moulting process in insects (as reviewed by Yamanaka et al., 2013). The EIA-based quantification of ecdysteroids in this study showed that ecdysteroid levels peak in haemolymph of fifth nymphal locusts on days six to eight, *i.e*. two-three days before the final moult to the adult stage (Fig. 3.2). Small RNA sequencing of haemolymph miRNAs before (N5 D2 and N5 D3, low ecdysteroid) and around the peak (N5 D6 and N5 D7,

high ecdysteroid) of 20E in fifth nymphal *L. migratoria* revealed a total of 43 miRNAs that significantly differed between the two conditions (Fig. 3.2 and Table 3.1). To our knowledge, we are the first reporting on the differential miRNA expression throughout the final nymphal stage of *L. migratoria*. A high throughput sequencing study in the German cockroach, *B. germanica*, allowed the identification of three and 37 miRNAs to be more expressed around the peak of 20E in N5 compared to N6 (Rubio et al., 2012), but no studies report on the differential miRNA expression between low *versus* high ecdysteroid levels within the final nymphal stage. Moreover, we demonstrated the extracellular presence of miRNAs in *L. migratoria*. Only a few studies reported on the presence of ex-miRNAs in insects (Dhahbi et al., 2016; Guo et al., 2013; Van den Brande et al., 2018; Wang et al., 2018).

To analyse the possible effects of several miRNAs on moulting and metamorphosis in *L. migratoria*, *in vivo* injection experiments were performed. Interestingly, the total duration of the fifth nymphal stage of *Lmi*-miR-13b-3p agomiR-injected locusts was on average two days longer than that of a normal fifth nymphal stage (Fig. 3.3B), although no effects on survival were witnessed (Fig. 3.3C). Using *in silico* prediction tools, *Lmi*-miR-13b-3p was predicted to bind *Lm*Obs2A. *Obs* genes play fundamental roles in maintaining the structural integrity of the cuticle (Behr and Hoch, 2005; Wang et al., 2015). X. Zhao et al. (2017) already demonstrated high expression levels of Obs2A at day seven of the fifth nymphal stage of *L. migratoria*, pointing towards a possible role in metamorphosis, more specifically during the formation of the cuticle. Wang et al. (2015) confirmed this role by showing that injecting dsRNA against *Obs2A* in fifth nymphal *L. migratoria* resulted in a delayed timing of moulting, without visible abnormal phenotypes. Similar observations were made in the current study with *Lmi*-miR-13b-3p agomiR-injected locusts. Nevertheless, no clear differences in transcript levels of *LmObs2A* were observed in our *Lmi*-miR-13b-3p agomiR-injected locusts (Fig. 3.4C). Perhaps, *LmObs2A* is not targeted by *Lmi*-miR-13b-3p. *In silico* tools are used to predict potential miRNA targets, but they do not guarantee effective binding *in vivo*. Or perhaps, the agomiR does not easily diffuse to the hindlegs after injection in the haemocoel. Next, miRNAs regulate expression levels of cognate mRNAs either by translational blockage or by cleavage (Miyoshi et al., 2009). When translational blockage of *LmObs2A* mRNAs is the preferred mode of action for *Lmi*-miR-13b-3p, differences on *LmObs2A* transcript levels will be neglectable. In addition to qRT-PCR, future Western Blot analysis, using antibodies against proteins encoded by the target mRNAs, would probably enable a more comprehensive interpretation of these data. At last, it is difficult to point towards a specific mRNA as target, since miRNAs are known to regulate multiple targets at once and one mRNA can be regulated by multiple miRNAs (Peter, 2010). Besides *LmObs2A*, *Lmi*-miR-13b-3p was predicted to bind *LmE93* as well. Lozano et al. (2015) reported that the miRNAs of the miR-2 family (miR-2, miR-13a and miR-13b) rapidly clear *Kr-h1* transcripts in the last nymphal stage of *B. germanica*, a process crucial for proper metamorphosis. However, no metamorphic abnormalities were detected in *Lmi*-miR-13b-3p agomiR-injected locusts. A possible regulating role of *Lmi*-miR-13b-3p in the MEKRE93 pathway of locusts therefore remains to be elucidated. Including an *in vitro* functional analysis

to verify proper binding of *Lmi*-miR-13b-3p to *LmE93* as well as optimising the experimental setup would probably enable a more comprehensive interpretation of these data.

The transition from immature insect stages to fully reproductive adults is dependent on ecdysteroids and JH (Riddiford, 2012). Ecdysteroids induce their effects by binding to EcR/RXR, as reviewed by Hill et al. (2013). *Lmi*-bantam-3p and *Lmi*-miR-306-5p were predicted to bind *LmRXR* and *LmEcR* mRNA, respectively. Locusts were injected with *Lmi*-bantam-3p or *Lmi*-miR-306-5p agomiR on the day of their moult to the fifth nymphal stage and a second injection was given three days later (Fig. 3.3D). Interestingly, the majority (60 %) of the *Lmi*-bantam-3p agomiR-injected locusts did not successfully develop into adults (Fig. 3E and F). *Lmi*-miR-306-5p agomiR-injected locusts showed similar moulting defects as 20 % of the experimental locusts were not able to successfully complete this final transition (Fig. 3.3E and F). Lenaerts et al. (2016) demonstrated the crucial role the ecdysone receptor complex in metamorphosis of *Schistocerca gregaria*. Injecting fifth nymphal *S. gregaria* with dsRNA against RXR and EcR resulted in nymphs that were not able to moult into the adult stage. Some experimental locusts died during the process of ecdysis, whereas others remained in the fifth nymphal stage, were weakened and eventually died. A similar situation was observed in *Lmi*-bantam-3p and *Lmi*-miR-306-5p agomiR-injected locusts. Several studies in other insects confirmed the significant role of the ecdysone receptor complex in moulting and metamorphosis (Cruz et al., 2006; Davis et al., 2005; Hult et al., 2015; Martín et al., 2006; Wang et al., 2002). Moreover, Mello et al. (2014) demonstrated that an RNAi-mediated knockdown of *EcR* in the honeybee, *Apis mellifera*, affects the expression of miR-306-5p, suggesting a close association of miR-306-5p with EcR action and consequently pupal-adult metamorphosis. He et al. (2017) found bantam to be involved in ecdysteroid biosynthesis in *C. suppressalis* as overexpression of bantam reduced the titer of 20E, induced mortality and retarded development. However, no clear differences in transcript levels of *LmRXR* and *LmEcR* were observed in *Lmi*-bantam-3p agomiR-injected locusts (Fig. 3.4A and B). Whether this outcome can be explained by *Lmi*-bantam-3p not targeting *LmRXR in vivo* or by the incapacity of qRT-PCR measurements to measure on protein level, as miRNAs can regulate cognate mRNAs by translational blockage as well, is still to be elucidated.

AntagomiRs were used as well to further unravel the possible function of selected miRNAs in the metamorphosis process of *L. migratoria*. Interestingly, the total duration of the fifth nymphal stage was on average one day longer in *Lmi*-miR13b-3p and *Lmi*-miR-306-5p antagomir-injected locusts than that of a normal fifth nymphal stage (Fig. 3.3H), although no effects on survival were witnessed (Fig. 3.3I). The observed effects elicited by the antagomiRs were relatively mild, which may refer to the fact that these substances only indirectly interfere with miRNA activity through a competitive inhibition mechanism, which implies that high concentrations of an antagomir might be needed to effectively neutralize the corresponding endogenous miRNA. This may explain why only a relatively subtle disruption of the processes, in which the

miRNA is playing a regulatory role, was achieved, but additional research will be needed to further elucidate these pathways.

Besides ecdysteroids regulating post-embryonic development in insects, the MEKRE93 pathway components play a significant role as well (Belles, 2019; Riddiford, 2012), with Kr-h1 as the main effector of the anti-metamorphic effect of JH (Godlewski et al., 2006; Song et al., 2014). In Chapter 5, we already demonstrated that precocious downregulation of Kr-h1 in the migratory locust gives rise to an adultoid phenotype. Similar observations were made in other insects (Gujar and Palli, 2016a; K. L. Li et al., 2018; Lozano and Belles, 2011; Minakuchi et al., 2009). Although the transcriptional regulation of Kr-h1 has been extensively studied, little is known about its regulation at the post-transcriptional level. *Lmi*-miR-1-3p, *Lmi*-miR-12-3p and *Lmi*-miR-14-5p were predicted to bind *LmKr-h1*, however, injecting locusts with *Lmi*-miR-1-3p, *Lmi*-miR-12-3p or *Lmi*-miR-14-5p agomiRs during the fourth nymphal (on D0 and D3) stage did not affect their development. Nevertheless, miRNAs binding Kr-h1 thereby downregulating its expression are described in literature. Song et al. (2018) reported that application of let-7 and miR-278 agomiRs in *L. migratoria* resulted in partially precocious metamorphosis. Lozano et al. (2015) demonstrated that the miR-2 family scavenges *Kr-h1* transcripts when the transition from nymphal to adult *B. germanica* should be taking place. Other studies report on a possible role of miR-1-3p, miR-12-5p, miR-14-3p in ecdysone signalling. Ecdysteroid signalling was shown to be linked to the expression levels of miR-14 during insect development (as reviewed by Kucherenko and Shcherbata, 2013). Mello et al. (2014) demonstrated that the RNAi-mediated knockdown of *EcR* in *A. mellifera*, perturbs the expression of 70 miRNAs, *a.o*. miR-1-3p, miR-12-5p and miR-14-3p. These data lead to infer that these miRNAs are, at least, closely associated with EcR action and consequently connected to pupal-adult metamorphosis. These miRNAs have previously been reported as putatively involved in the regulation of *D. melanogaster* immune genes as well stressing the broad regulatory capacity of miRNAs. Nevertheless, our study has clearly shown that experimental manipulation by mimicking certain miRNAs resulted in a severe disruption of post-embryonic development in the migratory locust, a very harmful swarming pest species.

3.5 Conclusion

In conclusion, our findings show that the knockdown of *LmDicer-1* during the fifth nymphal stage resulted in severe moulting defects establishing the regulatory role of miRNAs during metamorphosis (Figure 3.5). Moreover, our study described the presence of ex-miRNAs in the haemolymph of fifth nymphal *L. migratoria*. Furthermore, differential ex-miRNAs were observed when comparing haemolymph samples of early *versus* late fifth nymphal locusts and were shown to interfere with metamorphosis when injected into fifth nymphal locusts.

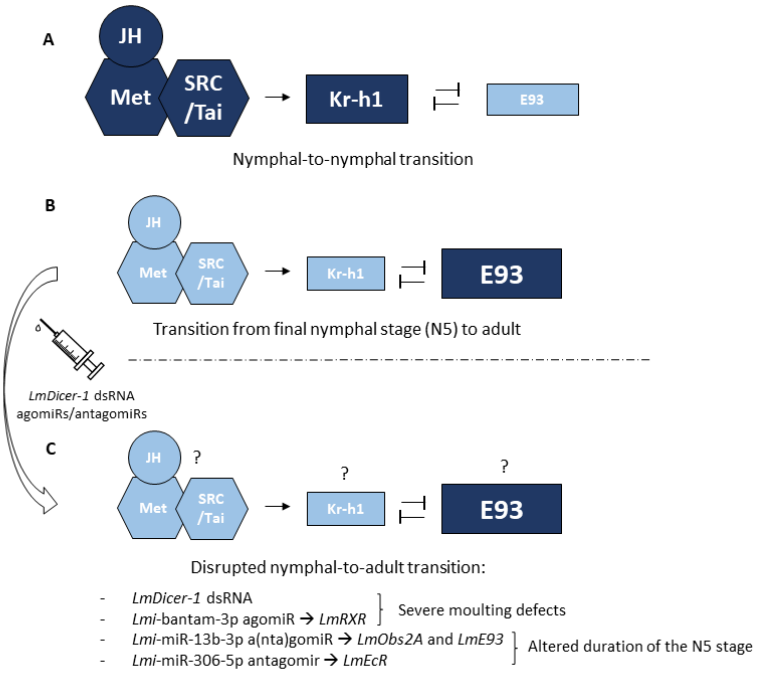

Figure 3.5: The MEKRE93 pathway in hemimetabolan metamorphosis. (A) During a nymphal-to-nymphal transition, JH (through Met/Tai) induces the expression of Kr-h1, a transcription factor which in turn, represses the expression of the adult specifier gene, *E93*. (B) A decline of JH production during the final nymphal stage (N5) interrupts the expression of Kr-h1 allowing a strong induction of E93 by ecdysone signalling, triggering the transition to adult (Belles and Santos, 2014). (C) Injection of dsRNA targeting *LmDicer-1* or injection of certain agomiRs/antagomiRs in final nymphal *L. migratoria* results in a disrupted nymphal-to-adult transition. Injection of *LmDicer-1* dsRNA and *Lmi*-bantam-3p agomiR predicted to target *LmRXR* results in severe moulting defects. Injection of *Lmi*-miR-13b-3p a(nta)gomiR and *Lmi*-miR-306-5p antagomiR, predicted to bind *LmObs2A* and *LmE93* and *LmEcR*, respectively, results in an altered duration of the fifth nymphal (N5) stage. The exact mode-of-action and molecular consequences of these treatments are yet to be further clarified (as indicated by question marks).

Chapter 4: RNAi-mediated knockdown of transcription factor E93 in nymphs of *S. gregaria* inhibits adult morphogenesis and results in supernumerary juvenile stages

This chapter was based on:

Gijbels, M., Marchal, E., Verdonckt, T.W., Bruynickx, E. and Vanden Broeck, J. (2020). RNAi-mediated knockdown of transcription factor E93 in nymphs of the desert locust (*Schistocerca gregaria*) inhibits adult morphogenesis and results in supernumerary juvenile stages. Int. J. Mol. Sci. 21, 7518.

4.1 Introduction

Juvenile hormones (JH) together with ecdysteroids play critical roles in insect postembryonic development. Where the moulting process in juvenile insects is triggered by periodic pulses of ecdysteroids, the absence or presence of JH determines the nature of the moult (Riddiford, 2012). The ecdysteroid signal is mediated by binding to a heterodimeric complex of two nuclear receptors (*i.e*. the ecdysone receptor (EcR) and the retinoid-X-receptor/ultraspiracle (RXR/USP)), as reviewed by Hill et al. (2013). JH is a sesquiterpenoid hormone synthesized in the *corpora allata* (CA) of insects. The molecular signalling pathway induced by JH has only recently been discovered with the characterization of a JH receptor, methoprene-tolerant (Met), which is a transcription factor belonging to the basic-helix-loop-helix (bHLH)/Per-Arnt-Sim (PAS) family (Charles et al., 2011; Wilson and Fabian, 1986). Binding of JH to Met stimulates the formation of a complex with other bHLH-PAS proteins, such as the steroid receptor co-activator Taiman (Tai) (Charles et al., 2011). The resulting JH-Met-Tai complex induces the expression of JH response genes, including the gene coding for Krüppel-homolog 1 (Kr-h1), a Zn-finger containing transcription factor (Godlewski et al., 2006; Song et al., 2014). RNA interference (RNAi) studies have demonstrated the importance of the JH receptor Met, as well as the downstream-acting transcription factor Kr-h1, in mediating the anti-metamorphic effects of JH in the red flour beetle, *Tribolium castaneum*, the German cockroach, *Blattella germanica*, the kissing bug, *Rhodnius prolixus*, the two-spotted cricket, *Gryllus bimaculatus*, the brown planthopper, *Nilaparvata lugens*, the common bed bug, *Cimex lectularius*, the migratory locust, *Locusta migratoria* and the fire bug, *Pyrrhocoris apterus* (Chafino et al., 2019; Gijbels et al., 2020; Gujar and Palli, 2016a; Ishimaru et al., 2019; Konopova et al., 2011; Konopova and Jindra, 2007; K. L. Li et al., 2018; Lozano and Belles, 2014, 2011; Minakuchi et al., 2009; Smykal et al., 2014a).

Our current study focuses on the role of the ecdysteroid-induced early response gene, E93, a helix-turn-helix transcription factor. This gene was first reported to be involved in the regulation of programmed cell death in *Drosophila melanogaster* prepupae (Baehrecke and Thummel, 1995; Lee et al., 2000). The concept that E93 is crucial for adult morphogenesis was proposed several years later (Mou et al., 2012). Whereas Kr-h1 mediates the *status quo* action of JH, E93 acts as a key determinant that promotes adult morphogenesis. RNAi-mediated knockdown of *E93* in larvae of the holometabolan insect *T. castaneum* has induced reiteration of larval development or resulted in the formation of supernumerary second pupae, depending on the time of dsRNA injection (Chafino et al., 2019; Ureña et al., 2014). In nymphs of the hemimetabolan insect species *B. germanica*, *G. bimaculatus*, *C. lectularius* and *N. lugens,* knockdown of E93 prevented the nymphal-to-adult transition, giving rise to supernumerary nymphal stages (Gujar and Palli, 2016a; Ishimaru et al., 2019; K. L. Li et al., 2018; Ureña et al., 2014). The gene regulatory mechanism by which JH inhibits metamorphosis involves the transcription factors Met, Kr-h1 and E93 and is defined as the MEKRE93 axis (Belles and Santos, 2014). During juvenile-to-juvenile transitions, high JH titres induce (via Met) expression

of Kr-h1, which in turn represses the expression of *E93*. In the final juvenile stage, *Kr-h1* expression is interrupted by the drop in JH titre, resulting in a strong induction of E93 through ecdysone signalling, which triggers metamorphosis and adult development (as reviewed by Belles, 2019). An inhibitory effect of Kr-h1 on *E93* expression and *vice versa* has been established in several insect species (Chafino et al., 2019; Ureña et al., 2016, 2014).

In the present study, we investigate the role of the adult specifier gene *E93* in the postembryonic development of the desert locust, *Schistocerca gregaria*, in its gregarious phase. We describe a supernumerary nymphal phenotype, the result of a redefined development caused by the RNAi-mediated silencing of *E93* starting in the penultimate nymphal stage. Supernumerary nymphs are characterised by a nymphal colour scheme while growing to the physical size of an adult locust, as well as the presence of wings, although these are not functional. Moreover, these supernumerary nymphs remain in the fifth nymphal stage for a shorter time when compared to control fifth nymphal locusts. In this context, we analyze and compare the expression of genes contributing to the MEKRE93 axis and to hormone biosynthetic pathways, as well as the temporal ecdysteroid profiles in the haemolymph of both control and *dsSgE93*-injected nymphal locusts.

4.2 Materials and methods

4.2.1 Rearing of animals

The desert locusts (*S. gregaria*) were reared under crowded conditions at a controlled temperature of 32 ± 1 °C, a constant day/night cycle (13 h photophase; 11 h scotophase) and an ambient relative humidity between 40 % and 60 %. The animals were fed fresh cabbage leaves supplemented with dry oat flakes *ad libitum.* Pots containing a slightly moistened mixture of turf and sand were placed in the breeding cages allowing mated females to deposit their eggs. Once a week, these pots were set apart in clean cages to allow eggs to hatch into first nymphal locusts.

4.2.2 Tissue collection

The tissues of interest were dissected under a binocular microscope and rinsed in *S. gregaria* Ringer solution (1 L: 8.766 g NaCl; 0.188 g $CaCl_2$; 0.746 g KCl; 0.407 g $MgCl_2$; 0.336 g $NaHCO_3$; 30.807 g sucrose; 1.892 g trehalose; pH 7.2) whereafter they were snap-frozen by pooling them in MagNA Lyser Green Beads Tubes (Roche) which were placed in liquid nitrogen to prevent RNA degradation. For every tissue that was analysed, samples were collected in five different pools of three dissected animals each and were stored at -80 °C until further processing. For analyzing possible effects on expression of MEKRE93 pathway components and enzymes involved in hormone biosynthesis, the head was collected, since this contains both the CA and prothoracic glands (Joly et al., 1956) that synthesize JH and ecdysteroids, respectively. The fat body, as the

main metabolic tissue, was collected to investigate possible effects on expression of MEKRE93 pathway and ecdysteroid receptor components.

4.2.3 RNA extraction and cDNA synthesis

Samples of head and fat body, which were obtained from fifth nymphal (N5) desert locusts on day four (D4) after the N4-to-N5 moult, were homogenized in MagNA Lyser Green Beads Tubes (Roche) using a MagNA Lyser instrument (30 s, 5000 rpm; Roche). Subsequently, total RNA was extracted from these homogenates using the RNeasy Lipid Tissue Kit (Qiagen) following the manufacturer's protocol as described in §2.2.4. To prevent genomic DNA contamination, an on-column DNase digestion (RNase-free DNase set, Qiagen) was performed. The quality and concentration of the resulting RNA samples were measured using a Nanodrop spectrophotometer (Nanodrop ND-1000, Thermo Fisher Scientific, Inc.). From each RNA sample, cDNA was synthesized by reverse transcription. Of each sample equal quantities of RNA (500 ng) were reverse-transcribed using a mix of random hexamers and oligo(dT) primers according to the manufacturer's protocol (PrimeScriptTM RT Reagent Kit, TaKaRa, Invitrogen Life Technologies). The obtained cDNA was then diluted 10-fold with Milli-Q water (Millipore, Darmstadt, Germany).

4.2.4 Multispecies E93 gene identification and phylogenetic analysis

The previously published sequence of *SgE93* (LC215000.1, Fig. 4.1, Sugahara et al., 2017) was verified by using it as a query for a BLASTn (version 2.5.0+, Expectation value 0.001, Altschul et al., 1990) search towards the most recently curated *Schistocerca gregaria* transcriptome and genome data (Verlinden et al., 2020). Less similar sequences were identified using a tBLASTn (version 2.5.0+, Expectation value 0.001) search using the protein sequence BBA65756.1 as the query and the most recent *Schistocerca gregaria* transcriptome data as the subject. Published and predicted E93 orthologs from different species were collected from NCBI (Table 4.1). As the published *Bombyx mori* E93 protein with accession number AIL29268.1 was significantly shorter than the orthologous sequences, a tBLASTn search was performed using the same parameters as previously described, using the AIL29268.1 sequence as the query and the NCBI Transcriptome Shotgun Assembly database limited by taxonomy for *Bombyx mori* as the subject. Significant matches were analyzed, the open reading frames identified, and the best candidate was added to the ortholog collection. These E93 sequences were then aligned using MUSCLE (Gap penalties: Gap Open -2.9, Gap Extend 0, Hydrophobicity Multiplier 1.2, 20 iterations, Edgar, 2004) and directly used for a maximum likelihood analysis with IQ-tree (version 1.6.12, VT+F+R5 model, 1000 SH-aLRT replicates and 10.000 ultrafast bootstrap replicates, Hoang et al., 2018 and Nguyen et al., 2015). Arachnida sequences were used as the outgroup.

ATGGCGGAGTGCTCCTATGCTCGCTGTGTTCAGGAGCGCCGAGCAATCAAAAAAGAGCTGCAAAGATGGACGAAGAATATGGTTT
TCGTAGTAGGTTTGGAACGGGTAGCGGAGGAGTTAATGGGCAGAAGGAAATGGAAACATTATCAGGAGTCAGTTTTGAGAAGTA
GACCGCAAGCAGACATAGAACCCAGCAGCAGTGATTGGCAAGTTGAAGACAAATGCTGCTTTTGCGACGGTGGGATGTTCCTGAG
ACCAGCAACAAGTCCACAGTCAGACAGCTGCAGTAGTTCCAACAGCCACAGCAGTTTTCACGAAACTCAGTCGACAGTAGCAGCA
GACAGTTCCCCTCCCAGGCTGGCGATGACAACACTCGAACCGGTCACGTCGCTGGCCGCGTCACTGGCAGCTGTCCCGACCTACAG
CCCGGGACCCGCACAGGGGCACTCCGCAATGGCAACCACCCCTCCAGCAGGCCTCTCTCTCTACCCCACAGTAGCACGCCATCGGA
CACCTGCGGGACTCTTCCCTCCGTGGTACCTGTCACCGACGGCACCTGCTCCGAATGTTCGATCGGAAGGAAAGACTGAACCGGA
AACTCCACCCGTCGTCGTATCCCTCCCTGCATCTACACCGCTGTCGGTGCCGTCAGCTGCGGCGAGTGAGCAGCCTTTGGACTTGA
GTGCCAAAGCCAAGGAAGAAGCATCTGCACCCAGCACCTCACCCGTGCCTCAGCCTTTGGGATTGGCAACTTTGAGTTTGGACAGC
AAGCAGATATTCAAGGCGAAACCAAGAATGAGTGCAGTGGCAGGTCGAAGGACATACACAGAAGAAGAGCTTCAAGCTGCTCTG
AGAGATATCCAGAGTGGAAAATTAGGAACTCGGCGTGCAGCTGTTATTTATGGTATACCACGCTCCACACTTCGGAACAAAGTGTA
CAAGTTGGCTATGGAGCGTGAACGTGACGCACACTTAGTGGTTCCTACAGTAGAGGAAAGAGACCTGTCTGGCGCTGAGGATGA
GAAGGAAGTTGAACGTGCTTTAAGTCGTCCTCTTCTTTCTGTTGACGATCTTCTGCGATTATCTGTGCTAGATGGGGATGCTCTTAG
AGTTCTTCTGGAGGAAGTTTCTGCAGGACACAATCGTGAAGCAAGTGAGTCAGCATCTTCCCCAGTGTTTCCACAATCTAGTGAAC
TTTGGCATGGTCTAGAACAGAGTGCATTGGGACCTTACATCTCCCAGCTTCTGATAGCTGGAAGTGCTCAAGATCCTTGCCATGCT
GAAAGCGGAGGTACACTCCCAAAATTTACTTCCCCTCTTCTCCCCGAACTTGTCCGTCGCATGATGGCAGAGGAGCAGCAACAGCA
GATAAAGAAGCTAGGTAGTGCCAATAATTTGGAAGCAAATACAAATATAACATTGAATGGTGCTTCAGGTGATGAGATACAGAAG
TTAGGTGATAGCGACAACAGTGCTGGGCCACCGAGAGTTCCATCTGCATCATCTCAAACAGACCCTGTGAAAGCTACAACAAAAG
TTGGGGAAGCAGATGAATCATCTGACACAGATGCAACAGCTTCCACTTCTAGAGTTGCCACACCACCAAATGTGATACTGAGAATT
CCGTCCTTTAAACCAACTACGAAAAATGGTGTGGCTACTCCAGGAAGTGGAAGTTTGCCTTCTAGTGAAATTCCATTCCAGACTGTT
GGAGTTCCTGCATTTCCTGGCCAGGAATCTAGTCATGTATTGAACAGCAGCAGTAACAATAGTAATGAGTCTTGTTCACCACCAGC
ATCTAACCTTGTAGGAAAAGGGATTGGGGTCAGTTTACGTGATGTTATAGCCAAAAGCATTAGTCAGAAGTTTCAACCAACTGATC
TTCCAATGTCACAGAAGCTCTTATTATCAGCAGATGAACAACCCCCATTTAAGAGAGGTCGTTTTACTCCTCCATTAAATACAAATAT
CACATCGTGCACTATAAAACACAATAACAATAACAACACTAATGTTGATGATAAAAACAAGACATCCTCTGCAGGTGGAAAAACTT
CATCAAATTCTACTGGCAAAGGAACCCGGCCAAAACGTGGAAAATACCGTAATTATGATCGTGATAGTTTGGTAGAAGCTGTTAG
AGCAGTGCAGAGGGGTGAAATGAGTGTCCATCGGGCAGGATCATATTATGGTGTTCCACATTCAACATTAGAATACAAGGTGAAA
GAGAGACATTTGATGAGACCTCGGAAGAGGGAGCCCAAGCAACAACAGTCTGATGAAGTTAAAAGGAAAGATGAATCTGGGACT
TCAATTCCAAGGAGTACAGCAACAACCTCATCAGCACTGGCAAATGATAAACTTAAAACTTTGCCTAAACCTCCCAAGACTGCCTTT
AATTCACCTGCTCCATTACCTGGTGCACCAAATGGTCTGAAAATACCACCCTTGTTTGATCCCAGTTTATCTCTTGCCGCATATGCTA
ATGTTACAACAGCCTTTCCATTTTGGCCTGGTCCATTTCATGCCTTACCAGTTCCAGATTTTACCACTCCTACTGGTAGCTTTCCTCCA
AATCCTGAACATTTCTTTGCACCACAAATGATACACAGGCTACAAGATGAAACTAGGACTGCACCACGAACGAGCCCCTCTTCAGT
AGTTCCTCCTCTTGGGAAGACTGCACGAGAGATGGCAGCATCTTTGTATGATGGAACAGGAGCTAATGGTAATTTTCTTGATGGAA
TAATTCGTTCAAGTCTTGAGATGGGTTTGCCATCATCCTCACCCAAAGAAGGCAGTACAGGTGTGGGAAATAGCGGAAAAATGTCT
AACAAAGCACTCATTGACCAGCTTTGTCGTAACAGTTGTGTCACTCCTCTGCCCAAAGCTCCGACACCTTTTAGTATGAAAGATTGC
AGTACTAGTGTAAATAGCTCAGATGAAGAACCTGTAAAGCAAGAAAGTGTCATCCCGGAACAGCCCTTAGAATCTGCTTCTCCTGC
AGAGCCTGTAGTTTGTCTATCAAATTCATCCAGTGGCCTGCCAGAACATGACTGTAGAATAGATAGTGAACATGTTACTTCAGTTCC
AGATGAAAAACATAGCAAGGACAGTGTTTTGCCACTGTCAGGGGTGCACTGTGTGTCATCAACTGAAGATAGTTCTGAATTATTTA
CTAAAGATTCAAGTGAATTCCATAAAGAACATGTTCATAATCCAACTGAAGAAAGTGCCTGTGATAGTAAAACTGTAAAAATACTT
GGTGATATTGAAGCTGCCAAAGACTTACTCCCTAAAGAAGAAGGCAACGAGGATTCAGAACAAACTGAGGATACCAAATCAATGA
CGGTCAACTCATAG

Figure 4.1: *SgE93* nucleotide sequence with primer sets indicated. Complete coding sequence of *S. gregaria E93* mRNA as found on NCBI (accession number LC215000.1) (Sugahara et al., 2017) with localisation of the different primers that were selected for production of the dsRNA construct or for performing qRT-PCR assays. Sequence regions highlighted in yellow indicate the position of the primer set that was used for generating the *dsSgE93* construct. Sequence regions highlighted in purple indicate the primer set used for qRT-PCR.

Table 4.1: Species and accession numbers of sequences used for constructing the phylogenetic tree shown in Fig. 4.4.

Species:	Accession number:
Acromyrmex echinatior	EGI58724.1
Acyrthosiphon pisum	XP 008189864.1
Aedes aegypti	EAT44017.1
Aethina tumida	XP 019872192.1
Agrilus planipennis	XP 018321151.1
Amyelois transitella	XP 013188059.1
Apis mellifera	BAB64310.1
Araneus ventricosus	GBL83064.1
Bemisia tabaci	XP 018900968.1
Blattella germanica	CCM97102.1
Bombus impatiens	XP 003490553.1
Bombyx mori	AIL29268.1
Bombyx mori isoform 2	ICPK01035599.1 derived
Centruroides sculpturatus	XP 023227973.1
Cimex lectularius	XP 014260111.1
Coptotermes formosanus	GFG28607.1
Cryptotermes secundus	XP 023704791.1
Culex quinquefasciatus	XP 001863525.1
Cyphomyrmex costatus	KYN00623.1
Dendroctonus ponderosae	XP 019771885.1
Dinothrombium tinctorium	RWS15376.1
Drosophila melanogaster	NP 652002.2
Drosophila simulans	EDX13858.1
Eufriesea mexicana	XP 017758118.1
Gryllus bimaculatus (partial)	BBJ70113.1
Ixodes scapularis	EEC08637.1
Laodelphax striatellus	RZF34802.1
Leptinotarsa decemlineata	AQN67828.1
Myzus persicae	XP 022167663.1
Nesidiocoris tenuis	CAA9993019.1
Nicrophorus vespilloides	XP 017770390.1
Nilaparvata lugens	APO13600.1
Operophtera brumata	KOB75508.1
Papilio machaon	KPJ20458.1
Parasteatoda tepidariorum	XP_015926289.1
Planococcus kraunhiae	BBD13408.1
Schistocerca gregaria	BBA65756.1
Stegodyphus dumicola	XP 035205796.1
Trachymyrmex zeteki	KYQ50221.1
Tribolium castaneum	KYB25179.1
Trichonephila clavipes	PRD31503.1
Xenos vesparum	AYD60146.1
Zootermopsis nevadensis	KDR22086.1

4.2.5 Quantitative real-time PCR

QRT-PCR primers for the different target genes are given in Figure 4.1 and Table 4.2. These primers were designed using the Primer Express software (Applied Biosystems) and primer pairs were validated by analysing relative standard curves for gene transcripts with serial dilutions (5x) of appropriate cDNA samples. The correlation coefficient (R^2 = 0.995 – 1) and efficiency (Eff% = 90 % - 110 %) of the qRT-PCR reaction were determined for each primer pair. All qRT-PCR reactions were performed in duplicate in 96-well plates on a StepOne System (ABI Prism, Applied Biosystems) following the Fast SYBR Green PCR Master Mix protocol as described in §2.2.5. Each reaction contained 5.0 µl of Fast SYBR Green Master Mix (Applied Biosystems), 0.5 µl of each Forward and Reverse primer (10 µM), 1.5 µl of Milli-Q water and 2.5 µl of cDNA. Following thermal cycling profile was applied: 95 °C for 10 min, followed by 40 cycles of 95 °C for 15 s and 60 °C for 60 s, whereafter a melt curve analysis was performed to verify the specificity of the qRT-PCR reactions. A no-template control reaction was always included to confirm absence of contamination and RT-minus reactions were performed to check for possible genomic DNA contamination. Moreover, the amplification products were analysed using horizontal agarose gel electrophoresis (1.2 % agarose gel containing GelRed™, Biotium) and visualized under UV light. For each transcript, a single band of the expected size was observed, which was further cloned and sequenced (TOPO® TA Cloning Kit for sequencing, Invitrogen) to confirm target specificity.

Table 4.2: Oligonucleotide sequences of primers used for qRT-PCR.

Reference/ target genes	Forward primer	Reverse primer
SgAct	5'- AATTACCATTGGTAACGAGCGATT -3'	5'- TGCTTCCATACCCAGGAATGA -3'
SgEF1α	5'- GATGCTCCAGGCCACAGAGA -3'	5'- TGCACAGTCGGCCTGTGAT -3'
SgE93	5'- CGCAAGCAGACATAGAACCC -3'	5'- TGGTCTCAGGAACATCCCAC -3'
SgMet	5'- GGTGCCTGAAGAGGAAGAAA -3'	5'- ATGGAGGTGATGAAGGAGAAAG -3'
SgKr-h1	5'- CTCCAAGACGTTCATCCAGAG -3'	5'- TGCTTGGAGCAGGTGAAG -3'
SgCYP15A1	5'- AAAGCAACTTCATCATTCACAGATG -3'	5'- CAGAGCCAGCCATGAACAAA -3'
SgJHAMT	5'- CGGAGCAAAGGCAAGCA -3'	5'- CCACTTCACCGCCTGGTTT -3'
SgSpo	5'- CAACATCTTCACCAGCTACATGTG -3'	5'- GGGTCGTCGTAGTCGAAGGA -3'
SgPhm	5'- CGCAGAGCCCGGACAAC -3'	5'- CGAACATGTCGGCCATGA -3'
SgSad	5'- ATCGTGGCCGAGATTACGAA -3'	5'- AGCACCATCTCCGGATCCT -3'
SgDib	5'- CCCAGGCTGCTATCGAGACT -3'	5'- CGACGACCAGGCCTATGTAGTT -3
SgEcR	5'- AAGGTTGATAATGCGGAATATGC -3'	5'- GTGATGGGCGCTCTGAAAAT -3'
SgRXR	5' -AATGCCTCGCTATGGGAATG -3'	5'- TCCTTTGTTCGCTGCCTTTC -3'

Abbreviations: *Sg = Schistocerca gregaria*; *Act = β-actin*; *EF1α = Elongation factor 1α*; *Met = Methoprene-tolerant*; *Kr-h1 = Krüppel-homolog 1*; *CYP15A1 = Cytochrome P450 enzyme 15A1 (methyl farnesoate epoxidase)*; *JHAMT = Juvenile hormone acid methyltransferase*; *Spo = Spook*; *Phm = Phantom*; *Sad = Shadow*; *Dib = Disembodied*; *EcR = Ecdysone receptor; RXR = Retinoid X receptor.*

Optimal housekeeping genes were selected from a pool of candidate housekeeping genes (Van Hiel et al., 2009) using the geNorm software (Vandesompele et al., 2002). In the designed experiment *EF1α* and *β-actin* appeared to be most stable in the studied head and fat body samples. Relative expression levels were

determined according to the comparative Ct method (ΔΔCt) (Vandesompele et al., 2002). Statistically significant differences between locusts in the knockdown and control conditions were found via a t-test on the log transformed data (with or without two-sided Welch's correction) using GraphPad Prism 6 (GraphPad Software Inc., San Diego, CA, USA).

4.2.6 RNA interference experiments

Double-stranded (ds)RNA constructs for *SgE93* (*dsSgE93*) (knockdown condition) and *GFP* (*dsGFP*) (control condition) were produced by means of Ambion's MEGAScript RNAi kit according to the manufacturer's protocol (Fig. 4.1). This procedure is based on a high-yield *in vitro* transcription reaction from a user-provided DNA template with 5' T7 promoter sequences. Forward and reverse primers flanked by the T7 promoter sequence (given in Table 4.3) were used in a PCR reaction with REDTaq DNA polymerase (Sigma) to amplify a fragment of the target gene. The resulting amplicons were analysed using horizontal agarose gel electrophoresis (1.2 % agarose gel containing GelRed™, Biotium) and visualised under UV light. Only a single band was observed, which was subsequently cloned and sequenced (TOPO® TA Cloning Kit for sequencing, Invitrogen) to confirm target specificity. Subsequently, the verified constructs were used in a high-yield *in vitro* transcription reaction using T7 RNA polymerase. Remaining ssRNA and DNA were removed in a nuclease digestion step. The quality and concentration of the produced dsRNA were determined by means of spectrophotometry (Nanodrop ND-1000, Thermo Fisher Scientific, Inc.). To confirm dsRNA integrity, a small amount of the reaction product was checked on a 1.2 % agarose gel.

Table 4.3: Oligonucleotide sequences of primers used for dsRNA synthesis. Nucleotides indicated in 'bold' represent the T7 promoter sequences used for preparing the dsRNA constructs.

RNAi constructs	F-primer	R-primer
dsSgE93	5'- **TAATACGACTCACTATAGGGAGA** GCCCAAGCAACAACAGTCTG -3'	5'- **TAATACGACTCACTATAGGGAGA** GGCAAGCCCATCTCAAGACT -3'
dsGFP	5'-**TAATACGACTCACTATAGGGAGA** AAGGTGATGCTACATACGGAA -3'	5'-**TAATACGACTCACTATAGGGAGA** ATCCCAGCAGCAGTTACAAAC-3'

Abbreviations: *Sg = Schistocerca gregaria*; *GFP = Green fluorescent protein.*

Freshly moulted fourth nymphal locusts, synchronized on the day of ecdysis (D0), were each injected with 4 µl *dsSgE93* (500 ng diluted in *S. gregaria* Ringer). Boost injections were given every next moult, *i.e.* in freshly moulted fifth, sixth and seventh nymphal locusts, to ensure a lasting knockdown of *SgE93* mRNA levels. A second group of locusts was injected with *dsGFP* (control) following the same injection scheme until the final moult to adult. Tissue samples of control and knockdown conditions were obtained from fifth nymphal locusts on day four (D4) after the N4-to-N5 nymphal moult. Haemolymph samples were collected every day, starting on day one (D1) after the N4-to-N5 nymphal moult (Fig. 4.3A and B).

4.2.7 Ecdysteroid measurement

Using a capillary tube, 5 µl of haemolymph was collected from each animal by piercing the insect's cuticle behind its hind leg. Subsequently, the collected haemolymph samples were immediately transferred to 95 µl of 100 % ethanol and stored at -20 °C until further processing, as previously described in §3.2.10. Ecdysteroid titers were measured using an EIA, modified from Porcheron et al. (1989) and discussed by Pascual et al. (1995) and Lafont et al. (2012). This protocol uses a peroxidase conjugate of 20E as tracer together with rabbit L2 polyclonal antibodies against ecdysteroids. This L2 antiserum has a strong affinity for E, 3-deoxyecdysone and 2-deoxyecdysone and a 6- to 8-fold lower affinity for 20E. Both serum and tracer were very kindly supplied by Prof. J.P. Delbecque (Université de Bordeaux, France).

4.2.8 Observing ecdysis

The ecdysis of *dsSgE93*- (knockdown) and *dsGFP*- (control) injected locusts was monitored. Starting from freshly moulted fifth nymphal locusts, the duration and phenotype of each developmental stage were closely observed. Statistically significant differences between *dsSgE93*- and *dsGFP*-injected locusts were found via a log-rank (Mantel-Cox) test using GraphPad Prism 6 (GraphPad Software Inc.).

4.3 Results

4.3.1 Identification and phylogenetic analysis of *SgE93*

The nucleotide and amino acid sequences of *S. gregaria E93* (*SgE93*) were found on NCBI (accession numbers LC215000.1 and BBA65756.1, respectively, Sugahara et al., 2017) (Fig. 4.1 and 4.2). An identical *SgE93* sequence was also found in the recently published first draft assembly of the *S. gregaria* transcriptome and genome (Verlinden et al., 2020, transcript SCHGR_00000941 from locus 1287777-1299780 of the seq2 contig). The comparison with other E93 sequences revealed that *SgE93* possesses two helix-turn-helix (HTH) DNA binding motifs of the pipsqueak family, named RHF1 and RHF2, one nuclear receptor interaction motif (NR-box, also named as LXXLL motif) and the co-repressor C-terminal-binding protein interaction motif (CtBP-im, also named as PLDLSAK motif) (Fig. 4.2 and 4.3). Our *in silico* analysis revealed *B. mori* transcripts (as sequenced by read ICPK01035599.1 and ICPK01035595.1) that encode isoforms with high similarity to the predicted *Bm*E93 protein sequences available on NCBI. The isoform identified from read ICPK01035599.1 was added to the list of orthologs used in the phylogenetic analysis (Table 4.1). A maximum-likelihood phylogenetic analysis of E93 sequences for selected species showed that the *SgE93* is most closely related to the (partial) orthologous sequence of *G. bimaculatus*, another orthopteran species, followed by a larger group of Blattodea orthologs (Fig. 4.4).

MAECSYARCVQERRAIKKELQRWTKNMVFVVGLERVAEELMGRRKWKHYQESVLRSRPQADIEPSSSDWQVEDKCCFCDGGMFLRP
ATSPQSDSCSSSNSHSSFHETQSTVAADSSPPRLAMTTLEPVTSLAASLAAVPTYSPGPAQGHSAMATTPPAGLSLYPTVARHRTPAGLF
PPWYLSPTAPAPNVRSEGKTEPETPPVVVSLPASTPLSVPSAAASEQPLDLSAKAKEEASAPSTSPVPQPLGLATLSLDSKQIFKAKPRMSA
VAGRRTY**TEEELQAALRDIQSGKLGTRRAAVIYGIPRSTLRNKVYKLAMERER**DAHLVVPTVEERDLSGAEDEKEVERALSRPLLSVDDL
LRLSVLDGDALRVLLEEVSAGHNREASESASSPVFPQSSELWHGLEQSALGPYISQLLIAGSAQDPCHAESGGTLPKFTSPLLPELVRRMM
AEEQQQQIKKLGSANNLEANTNITLNGASGDEIQKLGDSDNSAGPPRVPSASSQTDPVKATTKVGEADESSDTDATASTSRVATPPNVIL
RIPSFKPTTKNGVATPGSGSLPSSEIPFQTVGVPAFPGQESSHVLNSSSNNSNESCSPPASNLVGKGIGVSLRDVIAKSISQKFQPTDLPMS
QKLLLSADEQPPFKRGRFTPPLNTNITSCTIKHNNNNNNTNVDDKNKTSSAGGKTSSNSTG**KGTRPKRGKYRNYDRDSLVEAVRAVQRG**
EMSVHRAGSYYGVPHSTLEYKVKERHLMRPRKREPKQQQSDEVKRKDESGTSIPRSTATTSSALANDKLKTLPKPPKTAFNSPAPLPGA
PNGLKIPPLFDPSLSLAAYANVTTAFPFWPGPFHALPVPDFTTPTGSFPPNPEHFFAPQMIHRLQDETRTAPRTSPSSVVPPLGKTAREM
AASLYDGTGANGNFLDGIIRSSLEMGLPSSSPKEGSTGVGNSGKMSNKALIDQLCRNSCVTPLPKAPTPFSMKDCSTSVNSSDEEPVKQE
SVIPEQPLESASPAEPVVCLSNSSSGLPEHDCRIDSEHVTSVPDEKHSKDSVLPLSGVHCVSSTEDSSELFTKDSSEFHKEHVHNPTEESACD
SKTVKILGDIEAAKDLLPKEEGNEDSEQTEDTKSMTVNS

Figure 4.2: *Sg*E93 amino acid sequence with protein domains indicated. The amino acid sequence of *S. gregaria* E93 as found on NCBI (accession number BBA65756.1) with localisation of the different protein domains. The amino acid sequence regions highlighted in yellow and green indicate the CtBP-interaction motif and NR-box, respectively. The amino acid sequences indicated in bold represent the two HTH-DNA binding motifs, RHF1 (bold and underlined) and RHF2 (bold).

```
SgE93   MAECSYARCVQERRAIKKELQRWTKNMVFVVGLERVAEELMGRRKWKHYQESVLRSR----------------------
BgE93   ----------------------------------------MGRRRWKQYQDSVLRSP----------------------
DmE93   ----------------------MHISSYEISLERVAEECMGRRQWKHYQDKLTCSHLNIEEQQPIAIAGSEDEPSQYNH
Bm2E93  ------------------MYWYPRDRKRNRGLERVAEELMGRRKWKLYQDALIPKR-NEQDDSDDSMPSTDPPPALKIK
BmE93   ----------------------------------------MGRRKWKLYQDALIPKR-NEQDDSDDSMPSTDPPPALKIK
LdE93   ----------------------------------------MGRRKWKLYQESMSRSYLQPLNNNIKRSNPPEEDLDEYHH

SgE93   ------------------------------------------------------PQADIEPSSSDWQVEDKCCFC-DGGMF
BgE93   ------------------------------------------------------LRVDVEPRIQDWEPQEKCCMC-DGKPF
DmE93   SSKEISQSNPNHCKTENHRLEQQHNGSQLLEEEDSENNQTSHDSSRTPTPGATSTPSPPPEPIDWRPSAKCNFCVNGRLL
Bm2E93  TIEE----------INAPEDERPRVESDGNGQESKTSRPETILESLIKRPATQPKVEVLEEPADWKPPDKCYFCVDGEP-
BmE93   TIEE----------INAPEDERPRVESDGNGQESKTSRPETILESLIKRPATQPKVEVLEEPADWKPPDKCYFCVDGEP-
LdE93   HHKDYKQN------LHPHQADSEGNEPKTGGKEEEARGEGGGGDRAIEGHQKENEKDVD-RLKDWTPQDKCYFCVDGKLD

SgE93   LRPAT----SPQSDSCSSSNSHSSF-----------------HETQSTVAADSSPPRLAMTTLEP--------VTSLAAS
BgE93   FDSAT----SPAASDSGSTGTSSSL-----------------RETPPHEAAP------AMTTLQS--------VTSMAAS
DmE93   TVNAQGKLVAESAATATSSSTSNSHI----------------HQHDSDSNSSASLPHHISSSSSSNNNSSGNRARHIAAA
Bm2E93  --RATAEAAQPVGATSPASESDSSSV----------------SGTNSPAAAPPLLQHLLQLQAQN--------PQTIAQF
BmE93   --RATAEAAQPVGATSPASESDSSSV----------------SGTNSPAAAPPLLQHLLQLQAQN--------PQTIAQF
LdE93   SEHTTHGVLSPRPPDSDTSDSHSDSEVPASLTPTSRGLLNNNHHHHRHNVQHPVTPSSAMTTIEN--------V-----S

SgE93   LAAVPTYSPGPAQGHSAMATTP--PAGLSLYPTVARHRTPAGLFPP-WYLSPTAP----APNVRSEGKTEPETPPVVVSL
BgE93   IAAVAALSSSSGTGTTTNPLLPSQPSAMPFYP-------PPPHFPP-WYLSPPHSHLPGRPVLADAKQDPSATPPAVVHL
DmE93   SARATPAAATPANSLELYKLLTQRAAKMTSMDSMAAQLAQFSLLAD-FNLINSLASQQQQQQQQQQIASAVTPTTSEVSAA
Bm2E93  QQMIAALT-ALGTGLV----------------------PPPLTQA-WMMQRFAQQRHQADRLSESDKAAAPSSP-----
BmE93   QQMIAALT-ALGTGLV----------------------PPPLTQA-WMMQRFAQQRHQADRLSESDKAAAPSSP-----
LdE93   MAALAAAALSGGASPVGTPAAP----HLPFYN-------PASVLTHNWYLANVVRFQNAAANDAAVDKAS----------

SgE93   PASTPLSVPSAAASEQPLDLSAKAKEEAS-APSTSPVPQPLGLATLSLDSKQI----FKAKPRMSAVAGRRTYTEEELQA
BgE93   PASS-------SASEQPLDLSAKTAA----VEIPSPAPPDPSLKVPSIDNKHI----FKAKPRMSTVAGRRTYTEEELQA
DmE93   AISPALKDTPSPSVDAPLDLSSK-------PSPNSSISGDVKSVRACAT--------------PTPSGRRAYSEEDLSR
Bm2E93  -----------SPVEQPLDLSAKSTSSTSGTPPPDPKFLDSRLRRTALDGA-------------SNSTGRRTYTEDELQS
BmE93   -----------SPVEQPLDLSAKSTSSTSGTPPPDPKFLDSRLRRTALDGA-------------SNSTGRRTYTEDELQS
LdE93   -----------GAGEQPLDLSKGGSNNNP-PATDRKVPLAINVRLPTLDTKHIFNSDFRAKPRMSAVAGRRTYTEDELQA

SgE93   ALRDIQSGKLGTRRAAVIYGIPRSTLRNKVYKLAMERERDAHLVVPTV----------EERDLSGAEDEKEVERALSRPL
BgE93   ALRDIQSGKLGTRRAAVIYGIPRSTLRNKVYKLALEKERDSHLVAPAVPKVEEE----DEKELSGAEEEREVEKALRKPL
DmE93   ALQDVVANKLDARKSASQHHEQRSILDNRLFKMKHHDQEQDHDG-------------DELEDSNDDAEAEVDSNASTPV
Bm2E93  ALRDIQSGRLGTRRAAVLYGIPRSTLRNKVNKF-----------------------------------------------
BmE93   ALRDIQSGRLGTRRAAVLYGIPRSTLRNKVNKF-----------------------------------------------
LdE93   ALRDIQSGKLGTRRAAVIYGIPRSTLRNKVYKLALERERESHINSSAPLKLEEEEAMDDDKELSGAEEEKEVEKALQAPL

SgE93   LSVD----DLLRLSVLDGDALRVLLEEVSAGHNREASESASSPVFPQSSELWHGLEQSALGPYI-SQLLIA--GSAQDPC
BgE93   LSME----DLVRFSVFKDAN----------------------YPDA---WGGLEHSALGPYV-AELLAAQKNPASTPG
```

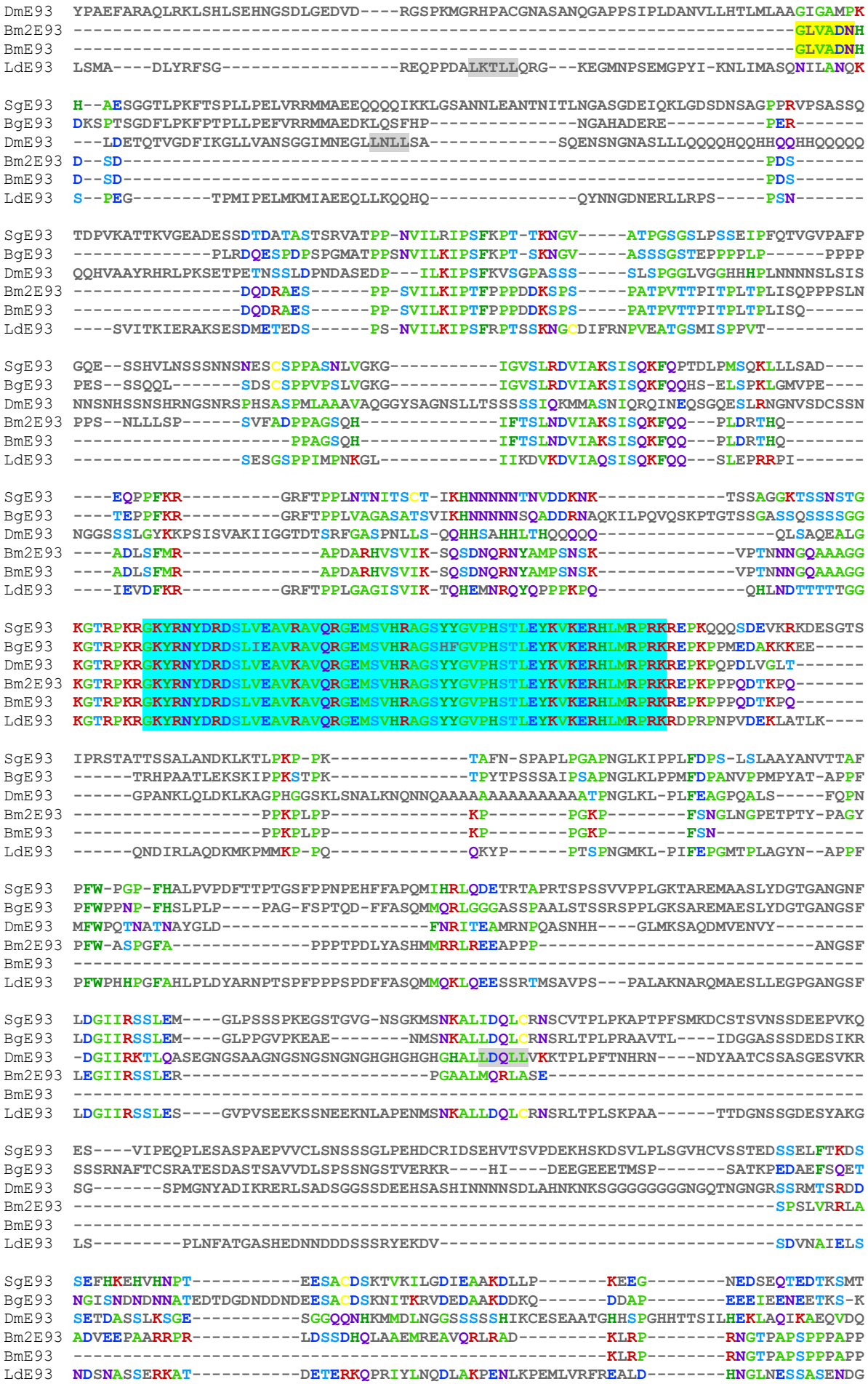
DmE93 YPAEFARAQLRKLSHLSEHNGSDLGEDVD----RGSPKMGRHPACGNASANQGAPPSIPLDANVLLHTLMLAAGIGAMPK
Bm2E93 ----------GLVADNH
BmE93 ----------GLVADNH
LdE93 LSMA----DLYRFSG----------REQPPDALKTLLQRG---KEGMNPSEMGPYI-KNLIMASQNILANQK
SgE93 H--AESGGTLPKFTSPLLPELVRRMMAEEQQQQIKKLGSANNLEANTNITLNGASGDEIQKLGDSDNSAGPPRVPSASSQ
BgE93 DKSPTSGDFLPKFPTPLLPEFVRRMMAEDKLQSFHP----------NGAHADERE----------PER-------
DmE93 ---LDETQTVGDFIKGLLVANSGGIMNEGLLNLLSA----------SQENSNGNASLLLQQQQHQQHHQQHHQQQQQ
Bm2E93 D--SD----------PDS-------
BmE93 D--SD----------PDS-------
LdE93 S--PEG--------TPMIPELMKMIAEEQLLKQQHQ----------QYNNGDNERLLRPS-----PSN-------
SgE93 TDPVKATTKVGEADESSDTDATASTSRVATPP-NVILRIPSFKPT-TKNGV-----ATPGSGSLPSSEIPFQTVGVPAFP
BgE93 ----------PLRDQESPDPSPGMATPPSNVILKIPSFKPT-SKNGV-----ASSSGSTEPPPPLP------PPPP
DmE93 QQHVAAYRHRLPKSETPETNSSLDPNDASEDP---ILKIPSFKVSGPASSS-----SLSPGGLVGGHHHPLNNNNSLSIS
Bm2E93 ----------DQDRAES------PP-SVILKIPTFPPPDDKSPS-----PATPVTTPITPLTPLISQPPPSLN
BmE93 ----------DQDRAES------PP-SVILKIPTFPPPDDKSPS-----PATPVTTPITPLTPLISQ------
LdE93 ----SVITKIERAKSESDMETEDS------PS-NVILKIPSFRPTSSKNGCDIFRNPVEATGSMISPPVT----------
SgE93 GQE--SSHVLNSSSNNSNESCSPPASNLVGKG----------IGVSLRDVIAKSISQKFQPTDLPMSQKLLLSAD----
BgE93 PES--SSQQL-------SDSCSPPVPSLVGKG----------IGVSLRDVIAKSISQKFQQHS-ELSPKLGMVPE----
DmE93 NNSNHSSNSHRNGSNRSPHSASPMLAAAVAQGGYSAGNSLLTSSSSSIQKMMASNIQRQINEQSGQESLRNGNVSDCSSN
Bm2E93 PPS--NLLLSP------SVFADPPAGSQH----------IFTSLNDVIAKSISQKFQQ---PLDRTHQ--------
BmE93 ----------PPAGSQH----------IFTSLNDVIAKSISQKFQQ---PLDRTHQ--------
LdE93 ----------SESGSPPIMPNKGL----------IIKDVKDVIAQSISQKFQQ---SLEPRRPI-------
SgE93 ----EQPPFKR----------GRFTPPLNTNITSCT-IKHNNNNNTNVDDKNK----------TSSAGGKTSSNSTG
BgE93 ----TEPPFKR----------GRFTPPLVAGASATSVIKHNNNNNSQADDRNAQKILPQVQSKPTGTSSGASSQSSSSGG
DmE93 NGGSSSLGYKKPSISVAKIIGGTDTSRFGASPNLLS-QQHHSAHHLTHQQQQQ----------QLSAQEALG
Bm2E93 ----ADLSFMR----------APDARHVSVIK-SQSDNQRNYAMPSNSK----------VPTNNNGQAAAGG
BmE93 ----ADLSFMR----------APDARHVSVIK-SQSDNQRNYAMPSNSK----------VPTNNNGQAAAGG
LdE93 ----IEVDFKR----------GRFTPPLGAGISVIK-TQHEMNRQYQPPPKPQ----------QHLNDTTTTTGG
SgE93 KGTRPKRGKYRNYDRDSLVEAVRAVQRGEMSVHRAGSYYGVPHSTLEYKVKERHLMRPRKREPKQQQSDEVKRKDESGTS
BgE93 KGTRPKRGKYRNYDRDSLIEAVRAVQRGEMSVHRAGSHFGVPHSTLEYKVKERHLMRPRKREPKPPMEDAKKKEE-----
DmE93 KGTRPKRGKYRNYDRDSLVEAVKAVQRGEMSVHRAGSYYGVPHSTLEYKVKERHLMRPRKREPKPQPDLVGLT-------
Bm2E93 KGTRPKRGKYRNYDRDSLVEAVKAVQRGEMSVHRAGSYYGVPHSTLEYKVKERHLMRPRKREPKPPPQDTKPQ-------
BmE93 KGTRPKRGKYRNYDRDSLVEAVKAVQRGEMSVHRAGSYYGVPHSTLEYKVKERHLMRPRKREPKPPPQDTKPQ-------
LdE93 KGTRPKRGKYRNYDRDSLVEAVRAVQRGEMSVHRAGSYYGVPHSTLEYKVKERHLMRPRKRDPRPNPVDEKLATLK----
SgE93 IPRSTATTSSALANDKLKTLPKP-PK----------TAFN-SPAPLPGAPNGLKIPPLFDPS-LSLAAYANVTTAF
BgE93 ------TRHPAATLEKSKIPPKSTPK----------TPYTPSSSAIPSAPNGLKLPPMFDPANVPPMPYAT-APPF
DmE93 ------GPANKLQLDKLKAGPHGGSKLSNALKNQNNQAAAAAAAAAAAAAAATPNGLKL-PLFEAGPQALS-----FQPN
Bm2E93 ----------PPKPLPP----------KP--------PGKP--------FSNGLNGPETPTY-PAGY
BmE93 ----------PPKPLPP----------KP--------PGKP--------FSN----------
LdE93 ------QNDIRLAQDKMKPMMKP-PQ----------QKYP------PTSPNGMKL-PIFEPGMTPLAGYN--APPF
SgE93 PFW-PGP-FHALPVPDFTTPTGSFPPNPEHFFAPQMIHRLQDETRTAPRTSPSSVVPPLGKTAREMAASLYDGTGANGNF
BgE93 PFWPPNP-FHSLPLP----PAG-FSPTQD-FFASQMMQRLGGGASSPAALSTSSRSPPLGKSAREMAESLYDGTGANGSF
DmE93 MFWPQTNATNAYGLD----------FNRITEAMRNPQASNHH----GLMKSAQDMVENVY---------
Bm2E93 PFW-ASPGFA----------PPPTPDLYASHMMRRLREEAPPP----------ANGSF
BmE93 ----------
LdE93 PFWPHHPGFAHLPLDYARNPTSPFPPPSPDFFASQMMQKLQEESSRTMSAVPS---PALAKNARQMAESLLEGPGANGSF
SgE93 LDGIIRSSLEM----GLPSSSPKEGSTGVG-NSGKMSNKALIDQLCRNSCVTPLPKAPTPFSMKDCSTSVNSSDEEPVKQ
BgE93 LDGIIRSSLEM----GLPPGVPKEAE--------NMSNKALLDQLCRNSRLTPLPRAAVTL----IDGGASSSDEDSIKR
DmE93 -DGIIRKTLQASEGNGSAAGNGSNGSNGNGHGHGHGHALLDQLLVKKTPLPFTNHRN----NDYAATCSSASGESVKR
Bm2E93 LEGIIRSSLER----------PGAALMQRLASE----------
BmE93 ----------
LdE93 LDGIIRSSLES----GVPVSEEKSSNEEKNLAPENMSNKALLDQLCRNSRLTPLSKPAA------TTDGNSSGDESYAKG
SgE93 ES----VIPEQPLESASPAEPVVCLSNSSSGLPEHDCRIDSEHVTSVPDEKHSKDSVLPLSGVHCVSSTEDSSELFTKDS
BgE93 SSSRNAFTCSRATESDASTSAVVDLSPSSNGSTVERKR----HI----DEEGEEETMSP-------SATKPEDAEFSQET
DmE93 SG-------SPMGNYADIKRERLSADSGGSSDEEHSASHINNNNSDLAHNKNKSGGGGGGGGNGQTNGNGRSSRMTSRDD
Bm2E93 ----------SPSLVRRLA
BmE93 ----------
LdE93 LS---------PLNFATGASHEDNNDDDSSSRYEKDV----------SDVNAIELS
SgE93 SEFHKEHVHNPT----------EESACDSKTVKILGDIEAAKDLLP-------KEEG--------NEDSEQTEDTKSMT
BgE93 NGISNDNDNNATEDTDGDNDDNDEESACDSKNITKRVDEDAAKDDKQ-------DDAP--------EEEIEENEETKS-K
DmE93 SETDASSLKSGE----------SGGQQNHKMMDLNGGSSSSSHIKCESEAATGHHSPGHHTTSILHEKLAQIKAEQVDQ
Bm2E93 ADVEEPAARRPR----------LDSSDHQLAAEMREAVQRLRAD---------KLRP--------RNGTPAPSPPPAPP
BmE93 ----------KLRP--------RNGTPAPSPPPAPP
LdE93 NDSNASSERKAT----------DETERKQPRIYLNQDLAKPENLKPEMLVRFREALD--------HNGLNESSASENDG

```
SgE93   VNS-
BgE93   INS-
DmE93   ADQL
Bm2E93  DRA-
BmE93   DRA-
LdE93   PQD
```

Figure 4.3: Multiple sequence alignment of *Sg*E93 with other E93 proteins. The multiple sequence alignment of *Sg*E93 (BBA65756.1) with E93 proteins from the German cockroach, *Blattella germanica* (*Bg*E93, CCM97102.1), the fruit fly, *Drosophila melanogaster* (*Dm*E93, NP_652002.2), the silkworm, *Bombyx mori* (*Bm*E93 and *Bm*2E93 sequences were obtained from AIL29268.1 and the ORF of ICPK01035599.1, respectively) and the Colorado potato beetle, *Leptinotarsa decemlineata* (*Ld*E93, AQN67828.1). The sequences were aligned with MUSCLE and colored by 70% consensus using MView.Several domain structures for E93 are shown: the two HTH-DNA binding motifs, RHF1 (highlighted in yellow) and RHF2 (highlighted in blue), the CtBP-interaction motif (CtBP-im, highlighted in pink) and the NR-boxes (highlighted in grey).

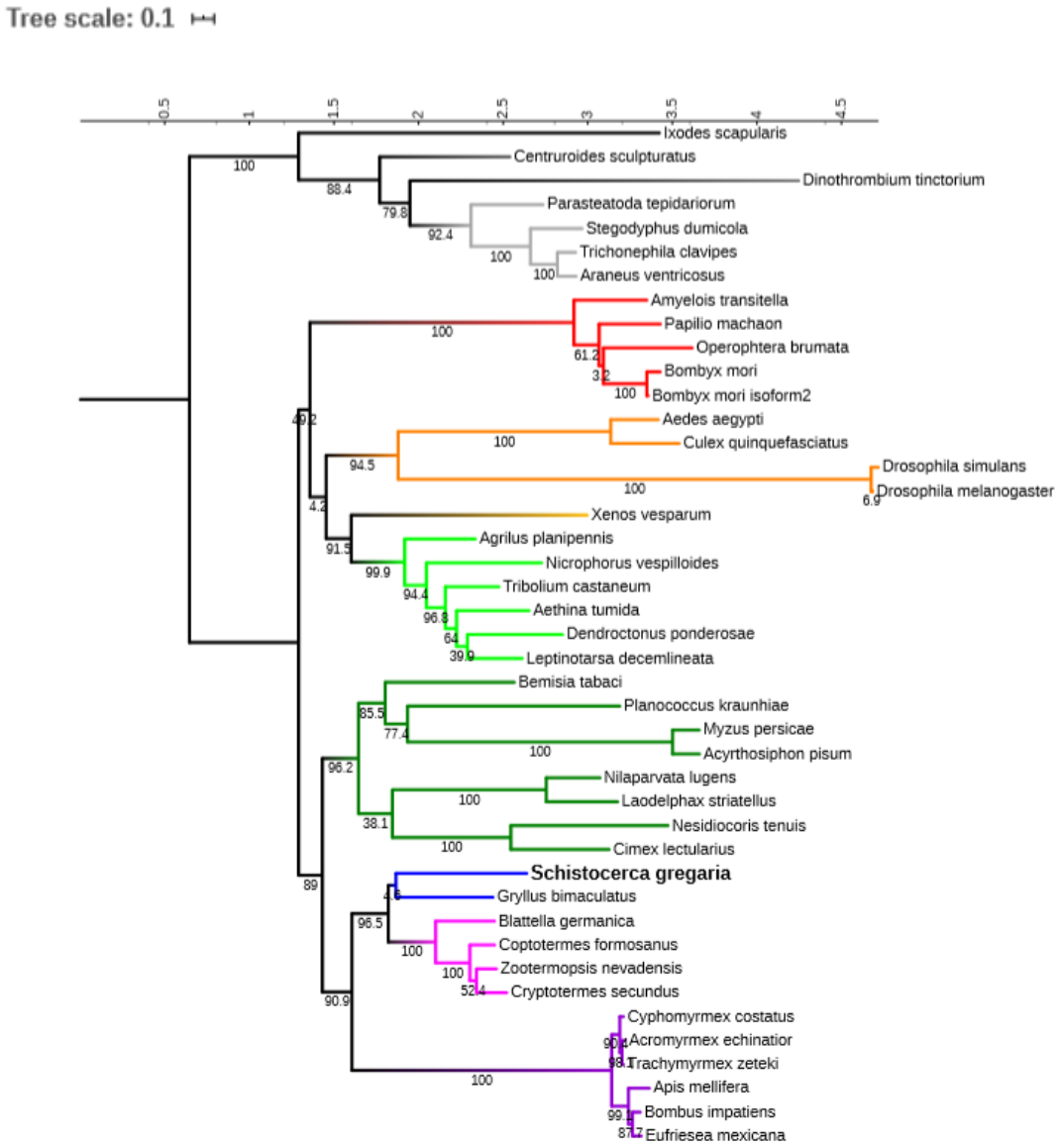

Figure 4.4: phylogenetic analysis of E93 orthologs from insect and arachnid species. E93 sequences listed in Supplementary Table S1 were aligned with MUSCLE and used for a maximum likelihood analysis using IQ-tree. The resulting tree was rooted using the Arachnida class branch as the outgroup. The branches are colour coded according to the insect order. Scale values indicate evolutionary distance. Tree rendered with iTol. Bootstrap values are included in the tree.

4.3.2 Knockdown of *SgE93* resulted in supernumerary nymphal stages

Injections of *dsSgE93* (knockdown condition) or *dsGFP* (control) started on day 0 in the fourth nymphal stage (N4 D0) and were repeated on the day of moulting to the following stage(s) (Fig. 4.5A and B). When compared to the *dsGFP*-injected control condition, *Sg*E93 knockdown significantly affected development of *S. gregaria* (Fig. 4.5C – E and 4.6). All of the experimental (*dsSgE93*) locusts moulted into a supernumerary nymph, *i.e*. a sixth nymphal stage (N6), while all control (*dsGFP*) locusts successfully completed their final moult to the adult stage (Fig. 4.5C – E and Fig. 4.6B). The supernumerary nymphs displayed the typical colour pattern of a juvenile locust, whereas they had a physical body size similar to (in case of N6), or even larger than (in case of N7) that of an adult locust. Moreover, non-functional wings were visible, which were larger than the wing primordia of normal N5 nymphs, but had a smaller, deformed and less pigmented appearance when compared to these of adult locusts (Fig. 4.5C – E). Figure 4.5D and E shows pictures of the different developmental stages of *S. gregaria*, including the supernumerary sixth (N6) and seventh (N7) nymphal stages that were obtained after *Sg*E93 knockdown during this study. Although the supernumerary stages clearly display the typical nymphal characteristics, a very notable difference can be observed in body size and wings, when compared to normal fifth nymphal (N5) locusts (*dsGFP* control).

4.3.3 *SgE93* silencing altered the duration of the moulting cycle and affected the success of moulting to later nymphal stages

dsSgE93-injected locusts remained in the fourth nymphal stage (N4) for a significantly shorter time period when compared to the control (*dsGFP*-injected) locusts, with a median duration of five and six days, respectively (Fig. 4.6A). The knockdown (*dsSgE93-injected*) animals also remained in the fifth nymphal stage for a significantly shorter time period than the control (*dsGFP*-injected) locusts (Fig. 4.6B). For the locusts of the *Sg*E93 knockdown condition, which moulted to the supernumerary nymphal N6 stage, the median duration of the N5 stage was only five days, resembling the normal duration of the N4 stage, while for those moulting (and metamorphosing) to the adult stage (*dsGFP*) this was nine days (Fig. 4.6A and B). Moreover, the supernumerary N6 nymphal insects further developed to generate a supernumerary N7 stage (Fig. 4.6C and D). However, six out of twelve locusts did not successfully complete their moult to this seventh nymphal stage (N7). After initiating ecdysis, the respective locusts appeared to be unable to shed their old cuticle and eventually died (Fig. 4.6D). None of the supernumerary N7 nymphal locusts survived the moulting process to the next nymphal stage (N8). The supernumerary nymphs that died during ecdysis to N7 or N8 all displayed a juvenile coloration pattern and had short, deformed wings. Moreover, adult genitalia were not observed.

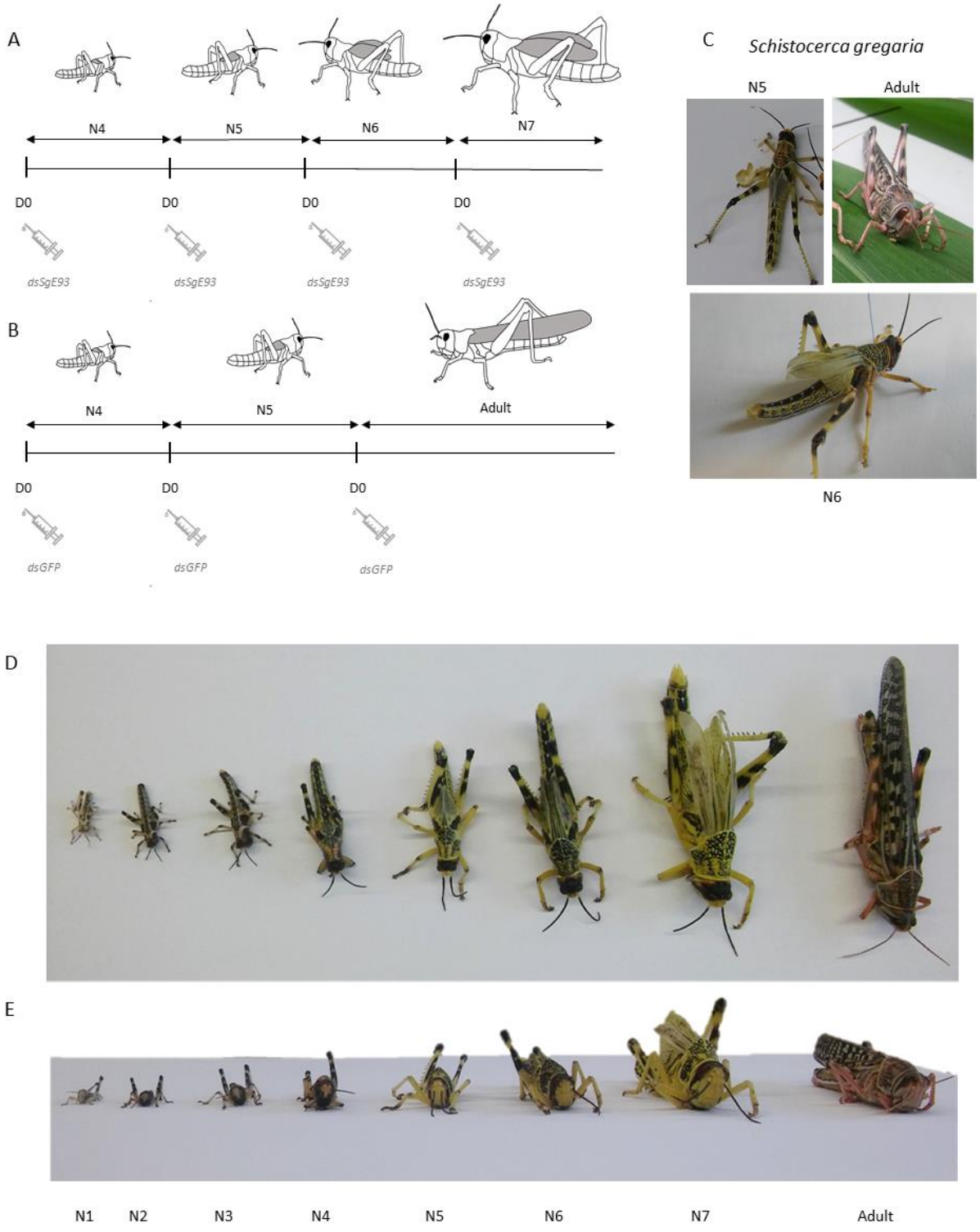

Figure 4.5: Time scheme of *dsSgE93* injections and phenotype of *dsSgE93*-injected desert locusts. (A and B) Time scheme showing the different time points of *dsSgE93* (knockdown condition) or *dsGFP* (control condition) injections together with the duration of each developmental stage. Haemolymph samples were collected daily starting on day one in the fifth nymphal stage (N5 D1). (C) Observed phenotypes of control (dsGFP-injected) N5 (top left) and adult (top right) locusts, as well as a *dsSgE93*-injected (N6; bottom) supernumerary nymphal locust obtained after moulting from N5. (D and E) Representation of postembryonic developmental stages, from hatchling (N1) to adult, including the observed supernumerary nymphal stages (N6 and N7) obtained in this study upon silencing *SgE93*. The normal stages of the desert locust are represented as N1, N2, N3, N4, N5 and Adult. Pictures were taken in (D) top view and (E) front view.

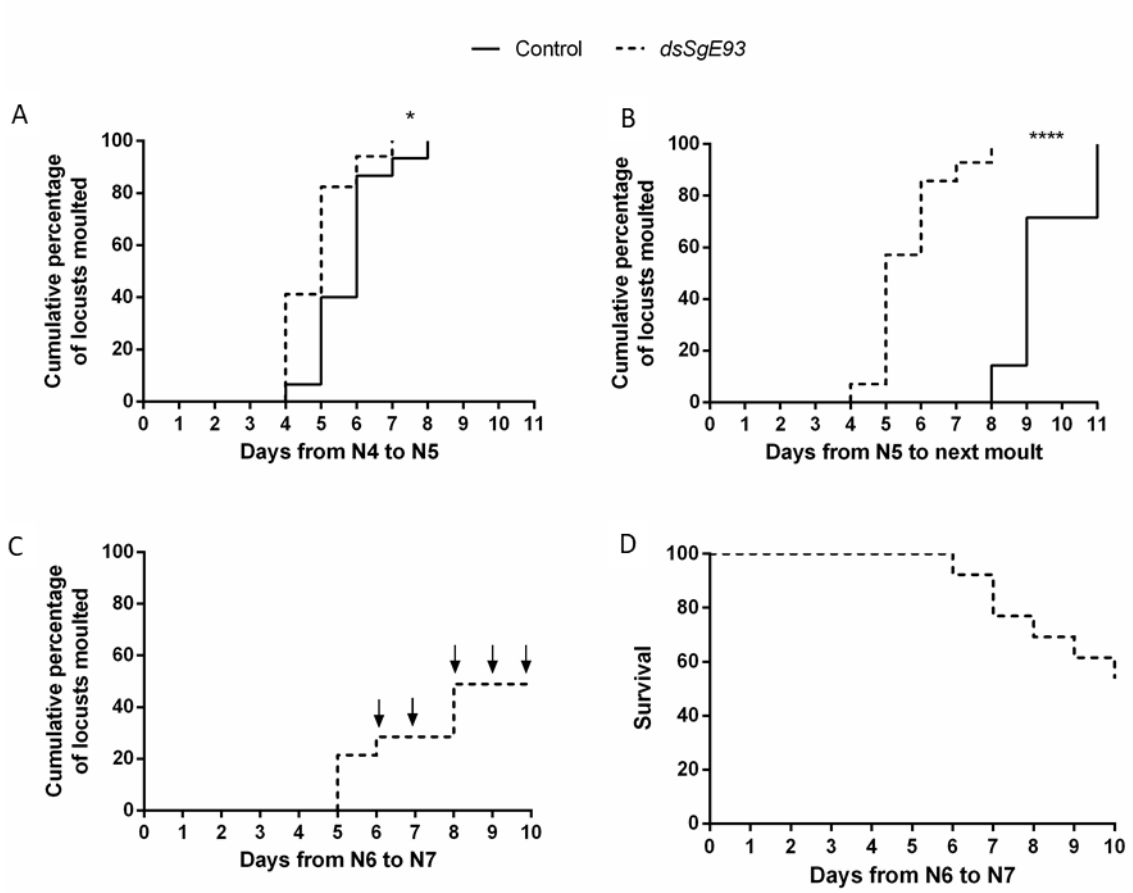

Figure 4.6: Timing of ecdysis of *dsSgE93*-injected locusts. The timing of ecdysis of *dsGFP*- (control) and *dsSgE93*- (*SgE93* knockdown) injected locusts was observed starting from freshly molted fourth-nymphal locusts. (A) The cumulative percentage of 15 *dsGFP*- (control) and 17 *dsSgE93*- (*SgE93* knockdown) injected locusts that molted from the fourth nymphal (N4) stage to the fifth nymphal (N5) stage. (B) The cumulative percentage of six *dsGFP*- (control) and 14 *dsSgE93*- (*SgE93* knockdown) injected locusts that molted from the fifth nymphal (N5) stage to the adult or to a sixth nymphal (N6) stage. Statistically significant differences (*p*) between the two conditions were found via a log-rank (Mantel–Cox) test and are indicated by asterisks (* $p < 0.05$; **** $p < 0.0001$). (C) The cumulative percentage of 12 *dsSgE93*- (*SgE93* knockdown) injected locusts that successfully molted from the sixth nymphal (N6) stage to the seventh nymphal (N7) stage. Arrows indicate the time points characterized by N6 locusts attempting ecdysis to the next stage, but that eventually died. (D) A survival plot representing the percentages of locusts still alive after successfully molting to the seventh nymphal stage (N7).

4.3.4 Transcript levels of MEKRE93 and JH biosynthesis pathway components in *dsSgE93*- and *dsGFP*-injected locusts

The levels of transcript coding for the components of the MEKRE93 pathway, as well as the enzymes catalyzing the two final steps of JH biosynthesis, were determined in head and fat body samples in fifth nymphal (N5) locusts on day four after the N4-to-N5 nymphal moult. A significant downregulation of *SgE93* mRNA levels (-54 %) was detected in the head of fifth nymphal *dsSgE93*-injected locusts, when compared with control (*dsGFP-injected*) locusts, while no significant difference was observed in the fat body at this time point (Fig. 4.7C). In comparison with control (*dsGFP*) locusts, the *SgKr-h1* mRNA levels were significantly

higher in both head and fat body of *dsSgE93*-injected locusts on day 4 of the fifth nymphal stage (N5 D4) (Fig. 4.7B). For *SgMet,* as well as the two JH biosynthetic enzymes, no significant differences were observed between *dsSgE93*-injected and control (*dsGFP*) locusts (Fig. 4.7A, D and E).

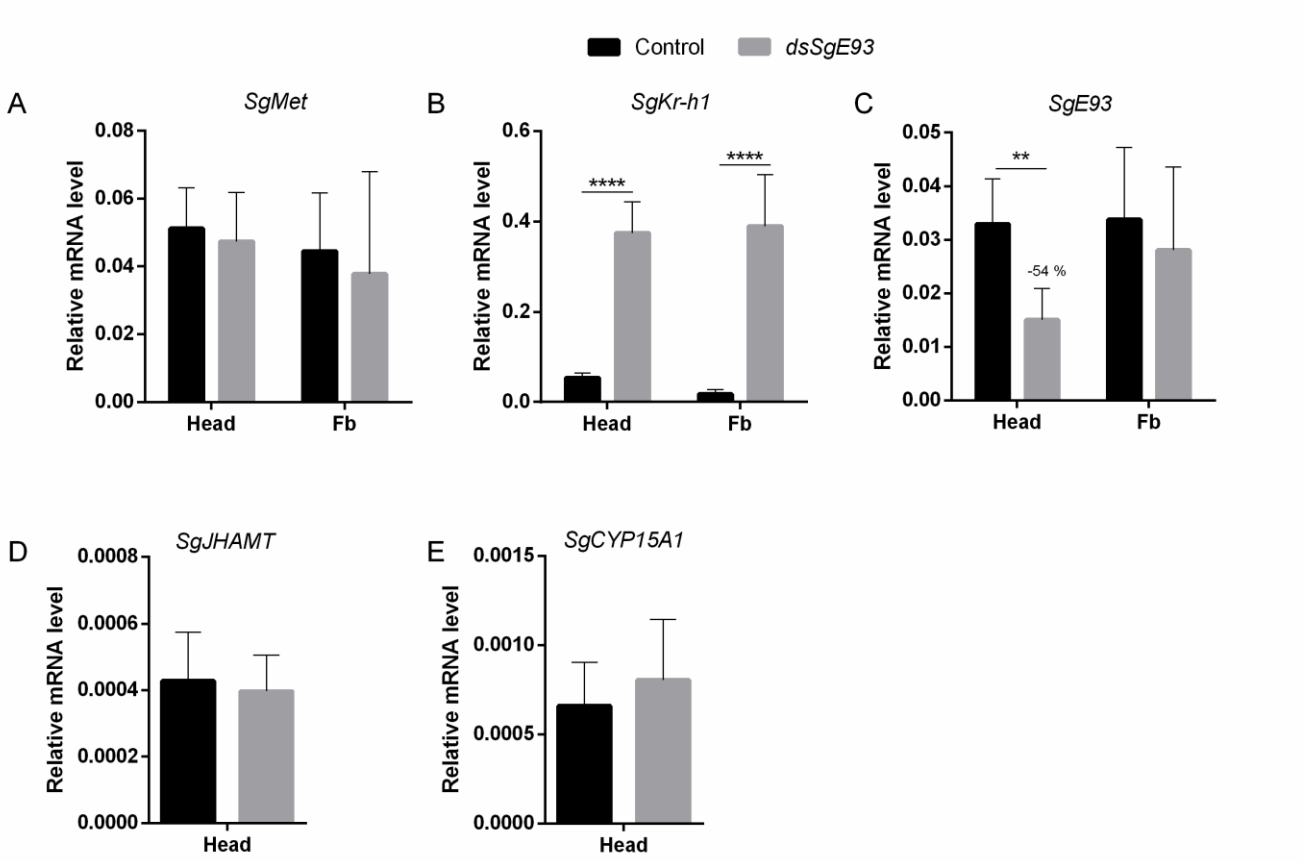

Figure 4.7: Relative transcript levels of MEKRE93 and JH biosynthesis pathway components in *dsSgE93*- and *dsGFP*-injected desert locust nymphs. Relative (A) *SgMet,* (B) *SgKr-h1* and (C) *SgE93* transcript levels were measured in the fat body and the head of *dsSgE93*- (*Sg*E93 knockdown) and *dsGFP*- (control) injected fifth nymphal (N5) locusts on day four after the N4-to-N5 moult. (D and E) Relative *SgJHAMT* and *SgCYP15A1* transcript levels were measured in the head as well. The data represent mean ± S.E.M. of five independent pools of three animals each, run in duplicate and normalized to *EF1α* and *β-actin* relative transcript levels. Statistically significant differences between the measurements were found via a t-test on log-transformed data (with or without two-sided Welch's correction) and are indicated by asterisks (** $p < 0.01$; **** $p < 0.0001$).

4.3.5 Transcript levels of different *Halloween* genes and components of the ecdysone receptor complex in *dsSgE93*- and *dsGFP*-injected locusts

The expression profiles of different *Halloween* genes, *Spook* (*SgSpo*), *Phantom* (*SgPhm*), *Disembodied* (*SgDib*) and *Shadow* (*SgSad*), which encode Cytochrome P450 enzymes involved in ecdysteroid biosynthesis (Marchal et al., 2012, 2011a), were compared between *dsSgE93*- and *dsGFP*- (control) injected fifth nymphal (N5) locusts on day four after the N4-to-N5 moult (Fig. 4.8). Relative *SgSpo* mRNA levels of *dsSgE93*-injected locusts were significantly higher in the head, whereas for the other *Halloween* genes no significant

differences were observed (Fig. 4.8A - D). In addition, we have also analysed the transcript levels of *SgEcR* and *SgRXR*, the genes that code for the components of the ecdysone receptor complex in both *Sg*E93 knockdown and *dsGFP* control animals. When compared to control (*dsGFP*) fifth nymphal locusts, a significant upregulation of *SgRXR* transcript levels was observed in the head of *dsSgE93*-injected nymphs (Fig. 4.8F), while in fat body of these animals, expression of both *SgRXR* and *SgEcR* was significantly upregulated (Fig. 4.8E and F).

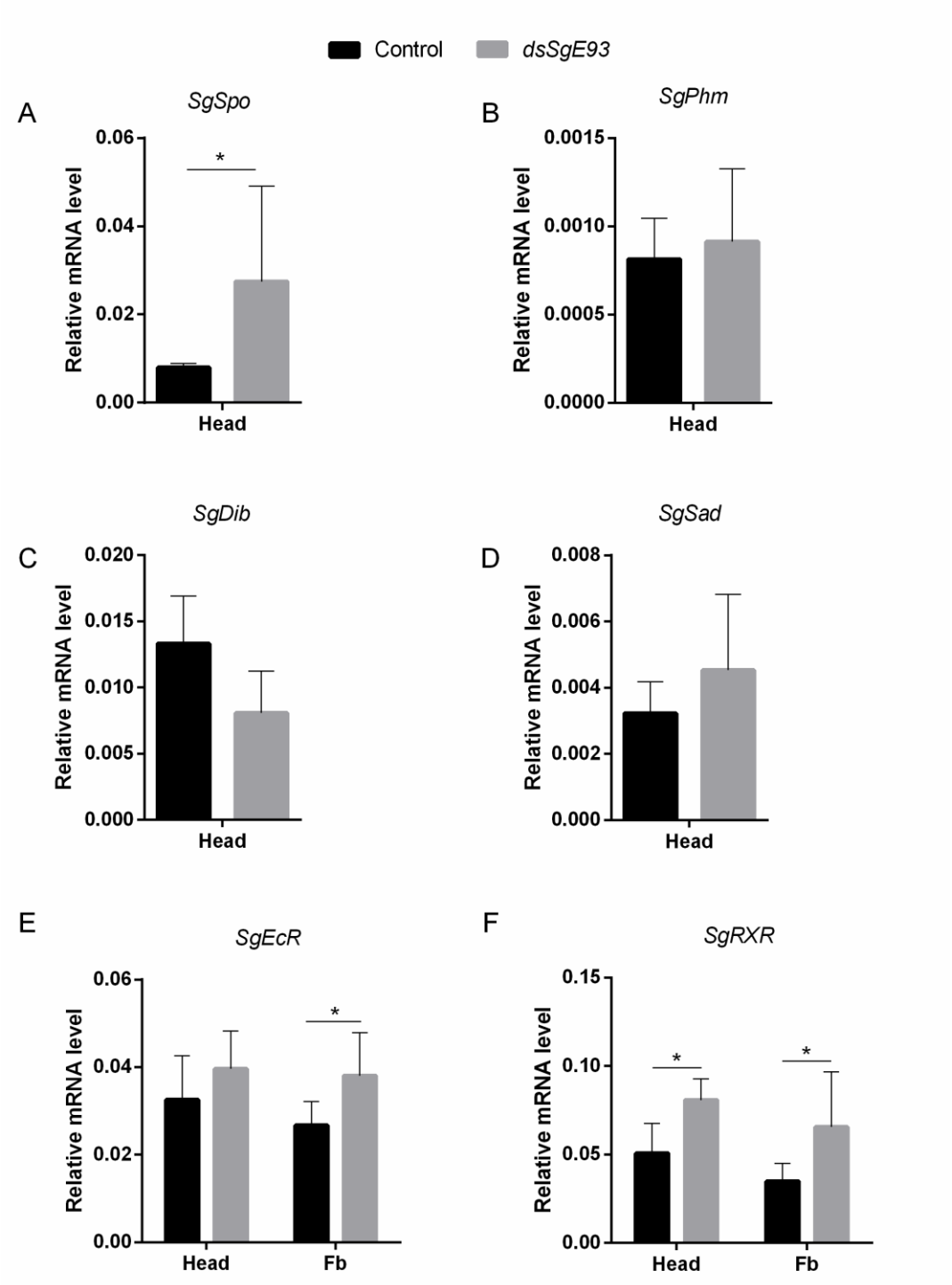

Figure 4.8: Relative transcript levels of different *Halloween* genes as well as *LmEcR and LmRXR* in *dsSgE93*- and *dsGFP*-injected desert locust nymphs. Relative (A) *SgSpo,* (B) *SgPhm*, (C) *SgDib* and (D) *SgSad* transcript levels were measured in the head of *dsSgE93*- (*Sg*E93 knockdown) and *dsGFP*- (control) injected fifth nymphal (N5) locusts on day four after

the N4-to-N5 moult. (E and F) Relative *SgEcR* and *SgRXR* transcript levels were measured in the head and the fat body. The data represent mean ± S.E.M. of five independent pools of three animals each, run in duplicate and normalized to *EF1α* and *β-actin* relative transcript levels. Statistically significant differences between the measurements were found via a t-test on log-transformed data (with or without two-sided Welch's correction) and are indicated by an asterisk (* $p < 0.05$).

4.3.6 Temporal profiles of ecdysteroids in haemolymph of *dsSgE93*- and *dsGFP*-injected locusts

Ecdysteroid levels were measured in haemolymph samples that were collected every day starting on day one of the fifth nymphal (N5 D1) stage (Fig. 4.9). When comparing control (*dsGFP*) and *dsSgE93*-injected locusts, a peak of ecdysteroids was witnessed a few days before moulting. However, a temporal shift of this peak was noticed. Whereas the ecdysteroid titres in the *dsSgE93*-injected condition already started rising on day two in fifth nymphal (N5 D2) locusts, they only rose several days later in the control (*dsGFP*) (N5 D5) locusts (Fig. 4.9A and C). Nevertheless, the overall quantity of ecdysteroids measured in *dsSgE93*-injected fifth nymphal locusts tended to be lower when compared to the control (*dsGFP*) (N5) locusts (Fig. 4.9A and C). Although the duration of the N5 stage was far from uniform for all nymphs within the same condition, the timing of the ecdysteroid peak appeared to be much more synchronized when relating it to the time of moulting to the next stage (Fig. 4.9B and D). Also in this comparison, a temporal shift in the ecdysteroid peak was observed, which for control (dsGFP-injected) locusts was situated three days before their final moult to the adult stage and two days for the locusts of the *SgE93* knockdown condition before their moult to a supernumerary N6 stage (Fig. 4.9B and D). Ecdysteroid titres that were measured during the sixth (N6) nymphal stage before moulting to a seventh one showed a more variable profile with ecdysteroids peaking 2-3 days before moulting (Fig. 4.9E and F). Figure 4.10 shows the ecdysteroid levels as measured in the haemolymph samples derived from each individual locust, demonstrating the existing variation.

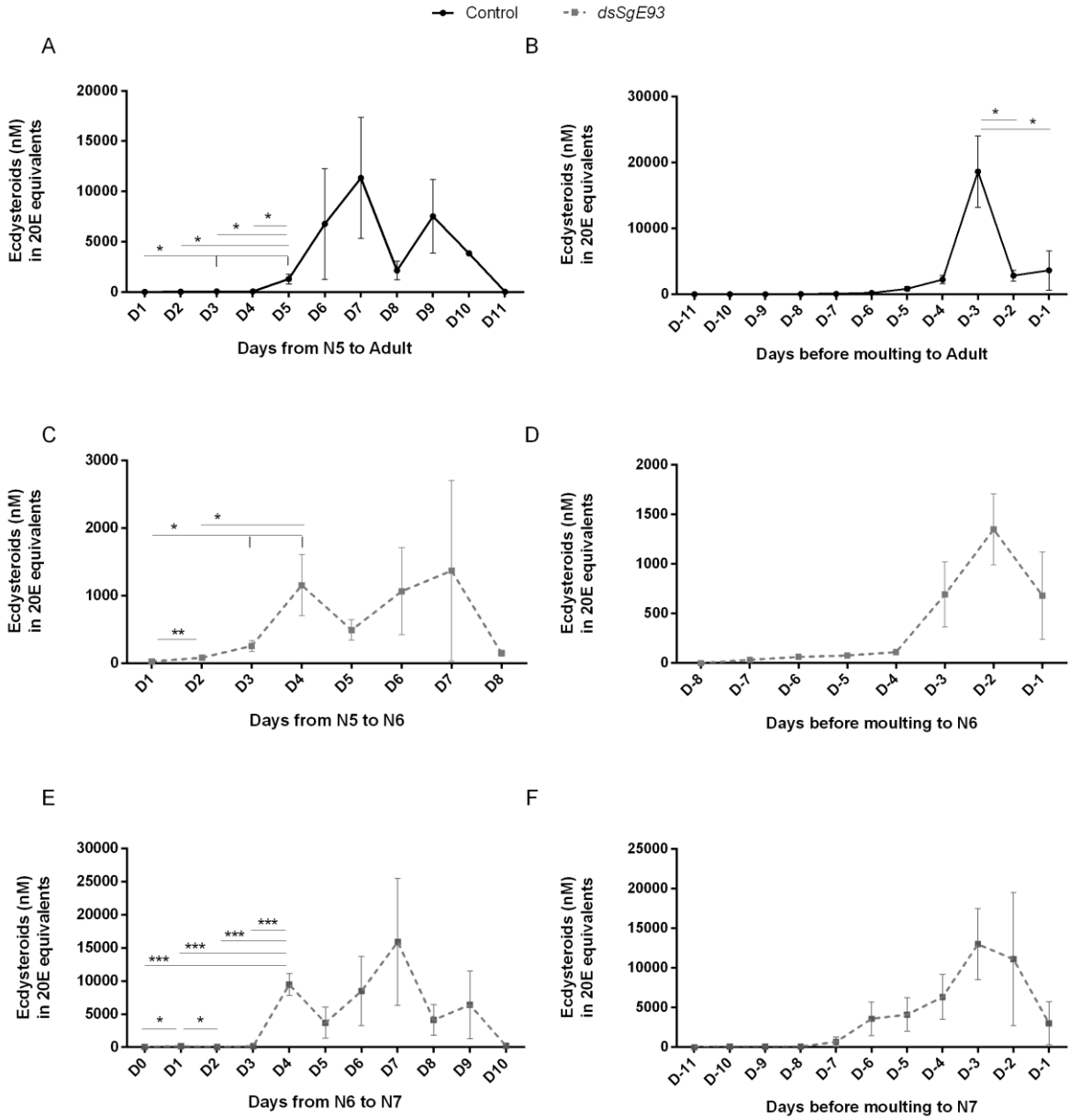

Figure 4.9: Temporal ecdysteroid profiles in haemolymph of *dsSgE93*- and *dsGFP*-injected desert locust nymphs. Ecdysteroid levels (20E equivalents in nM) were measured in haemolymph samples that were collected daily from *dsGFP*-injected (control) fifth nymphal (N5) locusts (A and B), as well as *dsSgE93-injected* (*Sg*E93 knockdown) fifth nymphal (N5) (C and D) and sixth nymphal (N6) (E and F) locusts. Data are shown in two ways: the X-axis in panels A, C and E shows the number of days after the previous (N4-to-N5) moult, while in the X-axis of panels B, D and F the number of days before moulting to the next stage is indicated. Each data point in the figure represents mean ± S.E.M of 5 control (*dsGFP*) or 6 experimental (*dsSgE93*) locusts. Statistically significant differences between the measurements (starting on D0/1 or D-1 until the following ecdysteroid peak) were found via a t-test (with or without two-sided Welch's correction) and are indicated by (an) asterisk(s) (* $p < 0.05$; ** $p < 0.01$; *** $p < 0.001$).

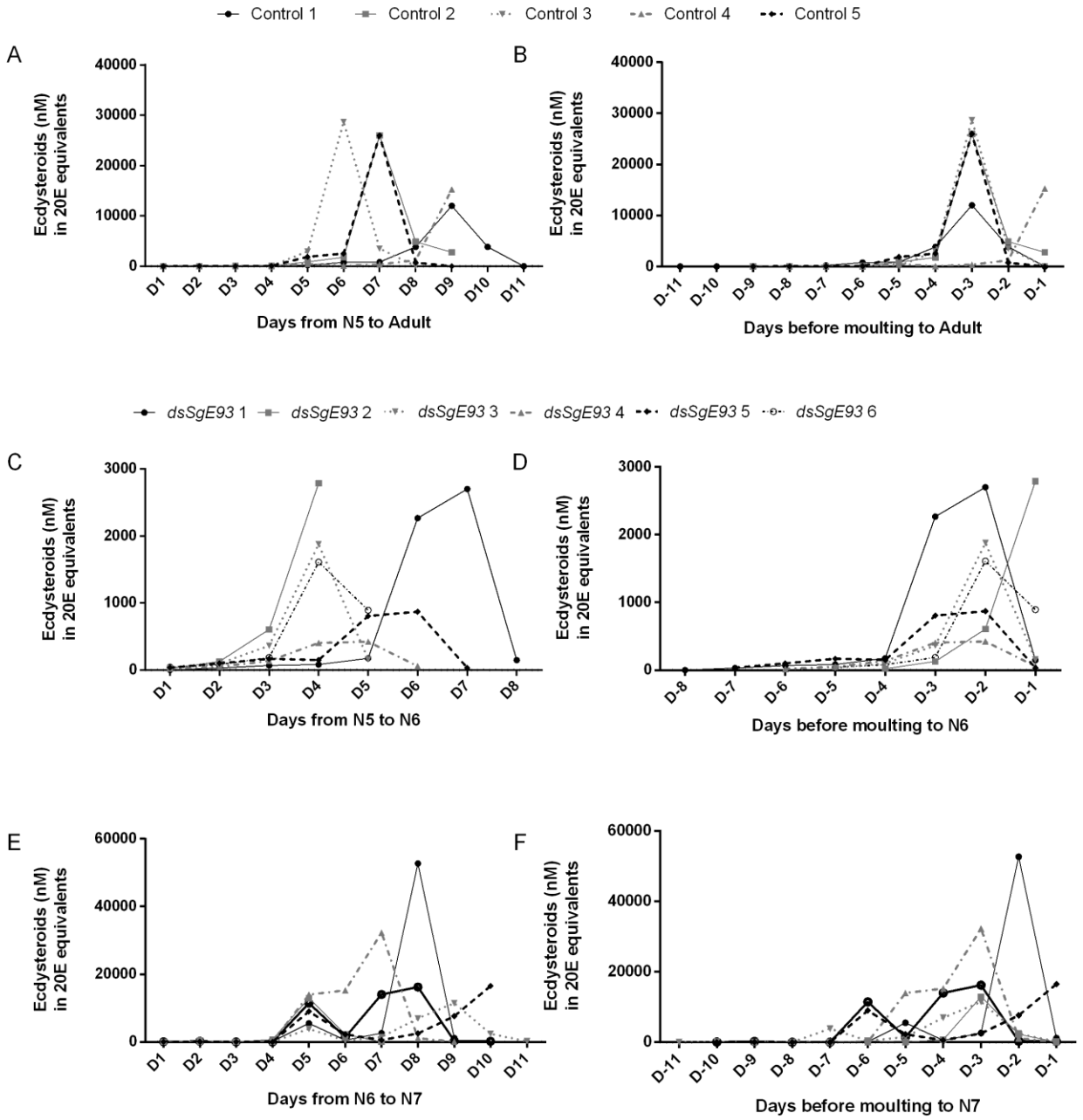

Figure 4.10: Temporal ecdysteroid profiles in haemolymph of control (*dsGFP*) and *SgE93* knockdown (*dsSgE93*) nymphs. Ecdysteroid levels (20E equivalents in nM) were measured in the haemolymph of *dsGFP*- (control) and *dsSgE93*- (knockdown) injected locusts in the fifth nymphal stage (A - D) and of *dsSgE93*- (knockdown) injected locusts in the sixth nymphal stage (E + F). Each data point represents a measurement and each line represents an individual locust. In total, haemolymph samples from 5 control (*dsGFP*) and 6 experimental (*dsSgE93*) locusts were analysed.

4.4 Discussion

The desert locust, *S. gregaria*, is a hemimetabolan insect species that develops through five nymphal stages before entering the final adult stage via an incomplete metamorphosis process. During the final moult, functional wings and reproductive organs are formed. In the present study, we describe the developmental and molecular effects of RNAi-mediated silencing of *SgE93,* which was induced by intrahaemocoelic injection of dsRNA at the beginning of each nymphal stage of gregarious desert locusts (*S. gregaria*) starting on the day of their moult to the fourth stage (Fig. 4.5A and B).

4.4.1 *Sg*E93 is the desert locust E93 ortholog

When comparing the cloned *Sg*E93 with other E93 sequences, a similar structural organization was observed (Fig. 4.3). In the silk moth, *B. mori,* RHF1 and RHF2 domains are critical for inducing the expression of a subset of 20E response genes, including EcR and USP. By contrast, the LXXLL and PLDLSAK motifs of E93 inhibit its transcriptional activity. *Bm*E93 can also interact with USP through the NR-box to impair the transcriptional activity of the USP/EcR heterodimer (X. Liu et al., 2015). Based on the highly conserved protein domains observed in all E93 homologs, *Sg*E93 more than likely functions through similar molecular mechanisms. Our *in silico* analyses indeed indicate that *Sg*E93 is a true ortholog of known insect E93 genes. The phylogenetic tree (Fig. 4.4) comparing several characterized and putative E93 sequences derived from various arthropod species seems to be well in line with the known evolutionary relationships between the represented species and their orders. The obtained tree also overlaps with data published by Chafino et al. (2018), albeit with a clearer grouping of the insect orders.

4.4.2 *SgE93* knockdown has inhibited metamorphosis and adult morphogenesis

Our results show that knockdown of *SgE93* interfered with the locusts' normal development by generating supernumerary nymphal stages instead of reaching the final, adult stage (Fig. 4.5C - E). The appearance of this supernumerary nymphal phenotype indicates that the experimental treatment inhibited the process of incomplete (*cf.* hemimetabolan) metamorphosis. Similar observations of supernumerary nymphal phenotypes were made after silencing E93 in several other insect species, such as *B. germanica*, *G. bimaculatus*, *C. lectularius* and *N. lugens* (Gujar and Palli, 2016a; Ishimaru et al., 2019; K. L. Li et al., 2018; Ureña et al., 2014). Interestingly, for the *dsSgE93*-injected locusts in this study the median duration of the fifth nymphal stage (from the N4-to-N5 until the N5-to-N6 moult) was on average four days shorter than for the *dsGFP*-injected controls (from the N4-to-N5 until the N5-to-Adult moult) and therefore resembled the normal duration of the N4 stage (Fig. 4.6A and B). This observation indicates that the transition process from N5 to N6 can be considered as a true nymphal-to-nymphal transition, by which the locusts remain programmed to invest energy and nutrients in body growth, instead of reallocating their metabolic

capabilities to support reproduction and flight in adults. Remarkably, for the *dsSgE93*-injected locusts also the median duration of the fourth nymphal stage was slightly shortened, on average by one day, in comparison with the *dsGFP*-injected (control) nymphs (Fig. 4.6A), although this did not affect the nature of the moult. This observation suggests that downregulation of *E93,* even in stages already characterized by low *E93* transcript levels, can still have an influence on the developmental timing. Although Ureña et al. (2014) and Li et al. (2018) also started injecting *E93* dsRNA into newly emerged penultimate nymphal *B. germanica* and *N. lugens*, respectively, they did not check for differences in the duration of this stage. Future experiments during the four initial nymphal stages would enable further investigation of the possible role of *SgE93* in developmental timing. The duration of the N6 stage cannot be compared with the *dsGFP*-injected controls, which all reached their final, adult stage. The duration appeared to be more variable, which might refer to the difficulties experienced by many supernumerary nymphs in shedding their old cuticle (Fig. 4.6C and D). Similar difficulties were also reported in E93-silenced supernumerary nymphs of the German cockroach, *B. germanica,* and the brown planthopper, *N. lugens* (K. L. Li et al., 2018; Ureña et al., 2014).

Significant differences in expression levels of the MEKRE93 pathway components *E93* and *Kr-h1* were detected during this time. Normally, the expression level of the adult specifier gene *E93* increases in the second half of the final nymphal stage, when JH levels drop and ecdysteroid levels rise, to ensure the final transition to adult (Belles, 2019). Significantly downregulated *SgE93* transcript levels were detected in the head of *dsSgE93*-injected locusts on day four in the fifth nymphal stage, which can explain the transition to a supernumerary nymph instead of an adult locust (Fig. 4.7C). In the fat body, *SgE93* levels were not significantly affected. The exact reason for this is still unclear, but absence of a significant change in E93 expression was also reported by Ureña et al. (2014), who studied supernumerary nymphs in the German cockroach, *B. germanica.* The observed effects in the fat body on the levels of several other transcripts suggest that *SgE93* has effectively been downregulated in this tissue. Considering the very dynamic nature of its regulation, it seems plausible that *Sg*E93 gene expression at the examined time point, four days post-injection (N5 D4), may have been influenced in a compensatory manner, but still remained below a threshold needed to induce adult morphogenesis. In future studies, a more complete view on the effects of *Sg*E93 knockdown in supernumerary nymphs would probably be obtained by an analysis of the changes in gene expression of MEKRE93 and ecdysteroid signaling pathway components in a wider range of tissues.

At the same time point, *i.e*. day four of the fifth nymphal stage (N5 D4), very significantly upregulated *SgKr-h1* transcript levels were detected in *dsSgE93*-injected locusts in head and fat body samples (Fig. 4.7B). Indeed, *Kr-h1* is an early JH response gene, which has been reported in several insect species to mediate the metamorphosis-inhibiting *status quo* action downstream of the JH signal and its receptor Met (Gijbels et al., 2020; Konopova et al., 2011; Lozano and Belles, 2011; Minakuchi et al., 2009, 2008b; Smykal et al., 2014b). *Kr-h1* levels normally drop in the final nymphal stage, when JH titers are low, to ensure a final transition to

the adult stage (Belles, 2019). The very significantly increased *SgKr-h1* expression in *dsSgE93*-injected desert locust nymphs may thus have inhibited metamorphosis to the adult stage and instead resulted in supernumerary juvenile stages. In the German cockroach, *B. germanica,* Ureña et al. (2014) demonstrated that the metamorphosis process is not exclusively channelled through the reduction of JH and consequent decrease of *Kr-h1*, but that the ecdysone-inducible transcription factor E93 is also playing a crucial role in controlling the developmental switch from nymph to adult. Moreover, these authors also showed the existence of an inverse relationship between *Kr-h1* and *E93* expression resulting from mutual repression effects. Our current findings therefore appear to be in agreement with the MEKRE93-based regulatory model for the control of metamorphosis (as reviewed by Belles, 2019). According to this recently proposed model, low JH titres in the final nymphal stage result in decreased signalling via Met, and this leads to reduced *Kr-h1* expression, which will further result in de-repression of the *E93* gene when a certain threshold is reached. The temporal onset of *E93* expression may be triggered by reaching a critical size and is mediated by ecdysteroid signalling (Nijhout, 1979; Ureña et al., 2014). Subsequently, full expression of E93 contributes to the repression of the *Kr-h1* gene. The competence of juvenile stages to undergo metamorphosis and become adult is neither solely dependent on a low JH titre, followed by a decrease in *Kr-h1* expression, nor on an increased ecdysteroid titre, followed by an increase in *E93* expression, but also on the crosstalk between different signalling systems, including the regulatory networking interactions between their downstream mediators (Ureña et al., 2014). In this context, it is interesting to mention the study by Santos et al. (2016), who demonstrated that the expression of *E93* at the beginning of the final nymphal stage of *B. germanica* is also co-activated by Smox-Medea, two components of the transforming growth factor-β (TGF-β) signalling pathway. In addition, the existence of an epistatic relationship between Fushi tarazu factor-1 (FTZ-F1) and E93 was recently proposed in the German cockroach, *B. germanica* (De Mendonça et al., 2002; Kamsoi and Belles, 2020; Ohno et al., 1994). These studies further emphasize the complexity of the gene regulatory network controlling adult morphogenesis.

4.4.3 *SgE93* knockdown has influenced the ecdysteroid pathway

Pulses of ecdysteroids are known to initiate the moulting process in insects (as reviewed by Yamanaka et al., 2013). The EIA-based quantification of ecdysteroids in this study showed that ecdysteroid levels peak in haemolymph of *dsGFP*-injected (control) fifth nymphal locusts approximately three days before the final moult to the adult stage (Fig.4.9B and Fig. 4.10B). In haemolymph of *dsSgE93*-injected fifth nymphal locusts, a temporal shift in the ecdysteroid profile was witnessed, which was characterized by an accelerated temporal increase (Fig. 4.9C and Fig. 4.10C), as well as a reduced time span between the ecdysteroid peak and the next moult (Fig. 4.9D and Fig. 4.10D), in comparison with the control (*dsGFP*) N5 locusts (Fig. 4.9A, B and Fig. 4.10A, B) These observations probably relate to the shorter duration of the N4 and N5 nymphal stages in the *Sg*E93 knockdown condition, when compared to the control condition (Fig. 4.6A and B). The

interindividual variation of N6 nymphs was much higher (Fig. 4.9E, F and Fig. 4.10E, F), which may refer to a wider variation in duration of this stage, as well as the fact that many of these locusts had problems to shed their cuticle (Fig. 4.6C and D).

In the current study, the significant increase of relative *SgSpo, SgEcR* and *SgRXR* transcript levels upon knockdown of *SgE93* (Fig. 4.8) might further explain the observed temporal shift in the ecdysteroid profile (Fig. 4.9A-D) and a shorter nymphal-to-nymphal (instead of a final nymphal-to-adult) moulting cycle (Fig. 4.5C-E and Fig. 4.6B). On day four in the fifth nymphal stage (N5 D4), ecdysteroid titres still remained low in haemolymph of *dsGFP*-injected (control) locusts, whereas they were significantly increased in haemolymph of *dsSgE93*-injected locusts (Fig. 4.9A and C). The elevated expression levels of the rate-limiting enzyme *SgSpo*, measured at this time point in head samples of *dsSgE93*-injected locusts, containing the ecdysteroid biosynthesizing prothoracic glands (Joly et al., 1956), correlate well with these higher ecdysteroid titres (Fig. 4.8A). The significantly increased *SgEcR* and *SgRXR* transcript levels, in turn, might be responsible for a high responsiveness of the *dsSgE93*-injected locusts to these precociously circulating ecdysteroids, which may explain the shorter duration of their fifth nymphal stage and consequently, in combination with high *Sg*Kr-h1 expression levels, the transition to a new nymphal stage instead of metamorphosing to an adult.

Although the ecdysteroid levels detected in haemolymph of *dsSgE93*-injected fifth nymphal increased faster, they did not reach the same levels as measured in control fifth nymphal locusts (Fig. 4.9A – B and Fig. 4.9A - D). This observation may be explained by the reorientation of the fifth and normally final moult into a next juvenile moult, since Morgan and Poole (1976) already reported more than forty years ago that the final (*i.e.* fifth) nymphal stage of *S. gregaria* was characterized by higher ecdysteroid levels than the penultimate (*i.e*. fourth) one. A recent study by Lenaerts et al. (2017) corroborated this finding. However, Tawfik et al. (1996) reported the reverse situation, with the fourth nymphal stage of *S. gregaria* having more ecdysteroids than the fifth. Later studies have also suggested that the absolute peak levels of circulating ecdysteroids might be less crucial in initiating moulting in *S. gregaria* than the timing of the ecdysteroid surges (Marchal et al., 2011a; Morgan and Poole, 1976; Tawfik et al., 1996). Marchal et al. (2011; 2012) studied the role of the Halloween genes *Spo*, *Phm* and *Shd* in ecdysteroidogenesis in the desert locust, *S. gregaria*. Although circulating ecdysteroid levels were found to be significantly reduced upon RNAi knockdown of the *Halloween* genes, no disruptions of the moulting process were observed. Several explanations for this remarkable observation were suggested that may also apply to the current study. First, it is possible that a sufficient treshold level of 20E, needed to complete the moulting process, was still reached. It must be kept in mind that the L2 polyclonal antibody used for the ecdysteroid measurements exhibits a strong affinity for E, but a 6 – 8 times lower affinity to 20E (Aribi et al., 1997). Another possibility is that perhaps, a portion of the ecdysteroids was hidden from detection, since conjugated forms of ecdysteroids are not detected by this antiserum. Moreover, physiological compensatory mechanisms, for instance resulting in an upregulation

and/or activation of ecdysteroid pathway components might also occur. Further studies have shown that knockdown of the ecdysteroid receptor complex can indeed severely disrupt the moulting process (Lenaerts et al., 2019a). Interestingly, in the current study the expression of both *SgEcR* and *SgRXR* was increased upon silencing of *Sg*E93, which may have compensated for reduced absolute ecdysteroid peak levels.

4.5 Conclusions

In conclusion, our findings show that the knockdown of *SgE93* in late nymphal *S. gregaria* resulted in supernumerary nymphal stages characterised by a colouration pattern that is typical for juvenile locusts, the presence of deformed, transparent, non-functional wings and a body size comparable to, or even larger than adult locusts (Figure 4.12). Moreover, *dsSgE93*-injected fifth nymphal locusts showed a very prominent increase in *SgKr-h1* relative transcript levels in head and fat body. The duration of the fifth nymphal stage was significantly shorter in *dsSgE93*-injected animals, compared to the animals in the *dsGFP*-injected control condition. In line with this, a temporal shift was observed in the ecdysteroid profile in haemolymph, as well as altered transcript levels of the *Halloween* gene *SgSpo* and ecdysteroid receptor components *SgEcR* and *SgRXR*. Moreover, some supernumerary N6 and all supernumerary N7 nymphal stages were unable to shed their old cuticle during the moulting process and eventually died.

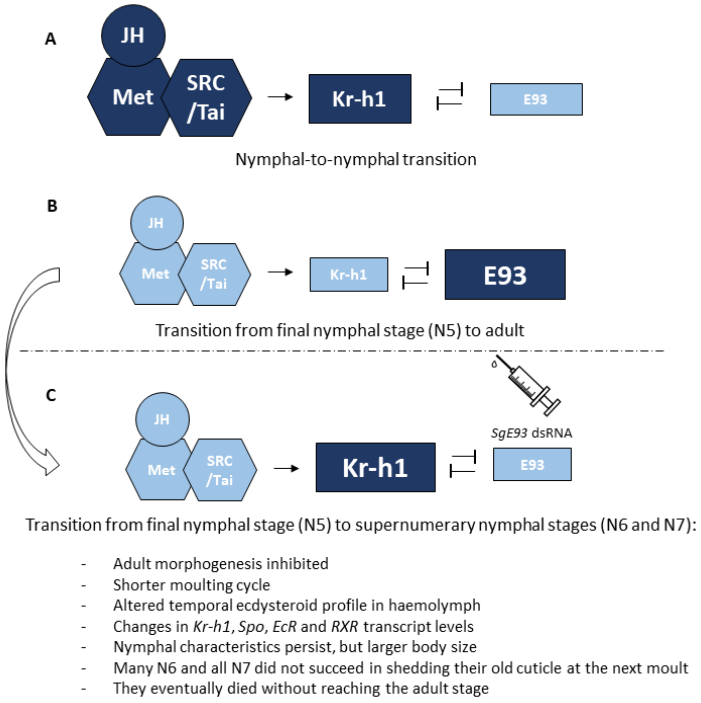

Figure 4.12: The MEKRE93 pathway in hemimetabolan metamorphosis. (A) During a nymphal-to-nymphal transition, JH (through Met/Tai) induces the expression of Kr-h1, a transcription factor which in turn, represses the expression of the adult specifier gene, *E93*. (B) A decline of JH production during the final nymphal stage (N5) interrupts the expression of Kr-h1 allowing a strong induction of E93 by ecdysone signalling, triggering the transition to adult (Belles and Santos, 2014). (C) Injection of dsRNA targeting *SgE93* in juvenile *S. gregaria* results in supernumerary nymphal stages.

Chapter 5: Precocious downregulation of Krüppel-homolog 1 in *L. migratoria* gives rise to an adultoid phenotype with accelerated ovarian development but disturbed mating and oviposition

This chapter was based on:

Gijbels, M., Schellens, S., Schellekens, T., Bruynickx, E., Marchal, E. and Vanden Broeck, J. (2020). Precocious downregulation of Krüppel-homolog 1 in the migratory locust, *Locusta migratoria*, gives rise to an adultoid phenotype with accelerated ovarian development but disturbed mating and oviposition. Int. J. Mol. Sci. 21, 6058.

5.1 Introduction

The transition from immature insect stages to fully reproductive adults is dependent on two hormones, *i.e*., Juvenile Hormone (JH) and ecdysteroids. Whereas periodic pulses of ecdysteroids trigger the molting process in juvenile insects, the absence or presence of JH will determine the nature of the molt (Riddiford, 2012). JH is a sesquiterpenoid hormone synthesized in the *corpora allata* (CA), which are part of the retrocerebral complex of insects. In addition to their role in immature insect stages, both ecdysteroids and JH are endocrine regulators of reproduction in adult insects. Ecdysteroids induce their effects by binding to a heterodimeric complex of two nuclear receptors, the ecdysone receptor (EcR) and the retinoid-X-receptor/ultraspiracle (RXR/USP), as reviewed by Hill et al. (2013). The JH signaling pathway was only recently described with the *in vitro* and *in vivo* characterization of a genuine JH receptor, Methoprene-tolerant (Met). Met is a transcription factor belonging to the basic helix–loop–helix (bHLH)/Per-Arnt-Sim (PAS) family (Charles et al., 2011; Wilson and Fabian, 1986). The binding of JH stimulates Met to form a complex with other bHLH-PAS proteins such as Taiman (Tai), a steroid receptor co-activator. The JH-Met-Tai complex then induces the expression of JH response genes such as *Krüppel-homolog 1* (*Kr-h1*), the main effector of the anti-metamorphic action of JH (Godlewski et al., 2006; Song et al., 2014). In a variety of insect species, RNA interference (RNAi) studies have demonstrated the importance of Met and its downstream transcription factor Kr-h1 in the anti-metamorphic effects of JH. Knockdown of either *Met* or *Kr-h1* in larvae of the red flour beetle, *Tribolium castaneum*, induced a precocious metamorphosis to pupae (Chafino et al., 2019; Konopova and Jindra, 2007; Minakuchi et al., 2009). Reduced *Met* or *Kr-h1* transcript levels in nymphs of the German cockroach, *Blattella germanica*, the kissing-bug, *Rhodnius prolixus*, the cricket, *Gryllus bimaculatus*, the brown planthopper, *Nilaparvata lugens*, the common bed bug, *Cimex lectularius*, and the fire bug, *Pyrrhocoris apterus*, resulted in precocious development of adult features (Gujar and Palli, 2016a; Ishimaru et al., 2019; Konopova et al., 2011; K. L. Li et al., 2018; Lozano and Belles, 2014, 2011; Smykal et al., 2014b; Villalobos-Sambucaro et al., 2015). Although the occurrence of a precocious metamorphosis resulting in adultoid insects is well known, its impact on reproductive physiology is only poorly understood. Nowadays, only the morphology of reproductive organs has been described in adultoids of a few species. In adultoids of the bed bug, *C. lectularius*, induced by RNAi-mediated knockdown of *Kr-h1,* precocious development of ovaries and oviducts was observed (Gujar and Palli, 2016a). In addition, external genitals were found in *dsKr-h1*-injected *N. lugens* and *P. apterus* (Jin et al., 2014; Konopova et al., 2011; K. L. Li et al., 2018), while an aberrant ovipositor morphology was described in adultoid crickets of the species *G. bimaculatus* (Ishimaru et al., 2019).

While Kr-h1 mediates the status quo action of JH, the ecdysteroid early response gene, E93, is a key determinant promoting adult morphogenesis in both holo- and hemimetabolan insects. In nymphs of *B. germanica*, *G. bimaculatus*, *C. lectularius* and *N. lugens*, E93 depletion prevented the nymphal-to-adult transition, giving rise to supernumerary nymphal stages (Gujar and Palli, 2016a; Ishimaru et al., 2019; K. L. Li

et al., 2018; Ureña et al., 2014). In the holometabolan insect *T. castaneum*, E93 depletion in larvae prevented the larval-to-pupal or pupal-to-adult transition, resulting in the formation of a supernumerary second pupa or inducing reiteration of larval development depending on the time of double-stranded (ds)RNA injection (Chafino et al., 2019; Ureña et al., 2014). These studies have established the inhibitory effect of Kr-h1 on E93 expression and *vice versa* (Chafino et al., 2019; Ureña et al., 2016, 2014). This ancestral regulatory mechanism by which JH inhibits metamorphosis is now defined as the MEKRE93 axis. During nymphal-to-nymphal transitions, high JH titers induce *Kr-h1* expression (via Met), which in turn represses the expression of *E93*. In the final juvenile stage, when JH titers drop, *Kr-h1* expression is interrupted, resulting in a strong induction of E93 through ecdysone signaling, which triggers adult development (as reviewed by Belles, 2019).

Moreover, in adult insects, JH transduces its signal via Met and Kr-h1. Multiple studies have confirmed the involvement of JH in vitellogenin synthesis in the fat body, lipid accumulation in the primary oocyte, regulation of mating and sex pheromone production in several insects (Bilen et al., 2013; Gujar and Palli, 2016b; Lin et al., 2015; Liu et al., 2016; Ma et al., 2018; Marchal et al., 2014; Naghdi et al., 2016; Parthasarathy et al., 2010; Saiki et al., 2015; Sheng et al., 2011; Smykal et al., 2014a; Tang et al., 2019; J. L. Wang et al., 2017; X. Wang et al., 2017; Zou et al., 2013). Moreover, an effect on the number of eggs deposited could be attributed to JH as well, since a reduced number of eggs laid was observed upon silencing *Met* or *Kr-h1* in the brown planthopper, *N. lugens* (Lin et al., 2015). Furthermore, in locusts, such as *L. migratoria*, RNAi-studies have shown the importance of *Met* and *Kr-h1* in female reproductive physiology. A knockdown of these genes caused lowered *vitellogenin* (*Vg*) expression in the fat body, reduced lipid accumulation in the oocytes and inhibition of patency in the follicular epithelium, thereby preventing oocyte growth (Song et al., 2014; Z. Wang et al., 2017). A recent study in the desert locust, *Schistocerca gregaria*, confirmed these findings, since a knockdown of *Met* in female adult locusts resulted in a failure to initiate *Vg* expression in the fat body, as well as basal oocyte growth in the ovaries. Moreover, these ds*Met*-treated locusts showed delayed mating behavior and were unable to oviposit, as described in Chapter 6. In female locusts, JH is known to stimulate Vg production by inducing *Vg* gene transcription in the fat body (Wyatt et al., 1996). Via binding of JH to membrane receptor sites in the ovarian follicular epithelium, a process called patency, the shrinkage of cells, is initiated (Davey et al., 1993; Jing et al., 2018; Sevala, V.L. & Davey, 1989; Sevala et al., 1995). As a result, Vgs, which are mainly produced by the fat body and then released into the hemolymph, can be taken up by the developing oocyte. Moreover, an oviduct derived Patency Inducing Factor was recently discovered. This factor, clearly boosted by JH, is involved in the initiation of patency in the terminal follicle via the pedicel (Seidelmann et al., 2016). Apart from JH, ecdysteroids also play an important role in the reproductive physiology of female locusts. Produced in the ovarian follicular cell layer, they appear to induce meiotic re-initiation in the oocyte (Lanot et al., 1987) and they are incorporated as conjugates into the eggs where they act as a source of ecdysteroids during embryogenesis (Isaac and Rees, 1984). Moreover, they can bind to vitellins, thereby preventing their leakage into the hemolymph (Isaac and Rees, 1984; Lagueux et al., 1981;

Tawfik et al., 1999). Furthermore, in the desert locust *S. gregaria*, the ecdysteroid receptor complex is playing a crucial role in chorion formation (Lenaerts et al., 2019a).

Our study describes a premature adult-like (adultoid) *L. migratoria* phenotype, the result of a reprogrammed development caused by the precocious RNAi-mediated silencing of *LmKr-h1* during the fourth (and normally penultimate) nymphal stage. Adultoid locusts are characterized by an adult color scheme and the presence of wings, although not fully extended, while maintaining the physical size of a fifth nymphal locust. Whereas several studies in different insect species already described the remarkable morphological consequences of such a knockdown, here we primarily focus on the reproductive properties of these adultoids and compare these with normal adult females. In this context, we analyze and compare the expression of genes contributing to the MEKRE93 axis, vitellogenesis and hormone biosynthetic pathways during the first gonadotrophic cycle of both adult and adultoid females. Moreover, effects on mating, oviposition, fecundity and fertility are monitored as well.

5.2 Materials and methods

5.2.1 Rearing of animals

The migratory locusts (*L. migratoria*) were reared under crowded conditions in cages that were situated in a room with controlled temperature (32 ± 1 °C) and day/night cycle (photophase of 13 h) at an ambient relative humidity between 40% and 60%. The animals were fed freshly sprouted wheat leaves and dry oat flakes ad libitum. Pots containing a slightly moistened mixture of sand and turf were placed in the breeding cages allowing mated females to deposit their eggs. These pots were collected once a week and transferred to clean cages where eggs were allowed to hatch into first nymphal locusts.

5.2.2 Tissue collection

The tissues of interest were dissected under a binocular microscope in *L. migratoria* Ringer solution (1 L: 9.82 g NaCl; 0.32 g $CaCl_2$; 0.48 g KCl; 0.73 g $MgCl_2$; 0.25 g $NaHCO_3$; 0.19 g NaH_2PO_4; pH 6.5) and snap-frozen by pooling them in MagNA Lyser Green Beads Tubes (Roche, Mannheim, Germany) or RNase-free Screw Cap Microcentrifuge tubes which were placed in liquid nitrogen to prevent RNA degradation. Tissues were collected in four pools of three animals each and were used in an RNA extraction protocol or stored at −80 °C until further processing.

5.2.3 RNA extraction and cDNA synthesis

Fat body and ovary samples of female migratory locusts were pooled in MagNA Lyser Green Beads Tubes (Roche) and homogenized using a MagNA Lyser instrument (30 sec, 5000 rpm; Roche). Total RNA was

extracted using the RNeasy Lipid Tissue Kit (Qiagen, Austin, Texas) according to the manufacturer's protocol as described in §2.2.4. An on-column DNase digestion (RNase-free DNase set, Qiagen) was performed to prevent genomic DNA contamination. The CA were pooled in RNase-free Screw Cap Microcentrifuge tubes. According to the manufacturer's protocol, total RNA was extracted using the RNAqueous-Micro Kit (Ambion; Life Technologies, Carlsbad, CA, USA), a specialized kit for total RNA extraction of small sized tissues. A DNase incubation step was included here as well. Subsequently, the quality and concentration of the resulting RNA samples were measured using a Nanodrop spectrophotometer (NanoPhotometer N60, Implen, München, Germany). From each RNA sample equal amounts (150 ng for fat body and ovaries and 50 ng for CA) were reverse-transcribed using a mix of random hexamers and oligo(dT) primers according to the manufacturer's protocol (PrimeScript™ RT Reagent Kit, TaKaRa, Invitrogen Life Technologies, Carlsbad, CA, USA). The obtained cDNA was then diluted ten-fold with Milli-Q water (Merck Millipore, Darmstadt, Germany).

5.2.4 Quantitative real-time PCR

QRT-PCR primers for the different target genes (Table 5.1) were designed using Primer Express software (Applied Biosystems, Foster City, CA, USA). These primer pairs were validated by designing relative standard curves for gene transcripts with serial (5x) dilutions of appropriate cDNA samples. The correlation coefficient and efficiency of the qRT-PCR reaction were measured (R^2 = 0.995 - 1; Eff% = 90%–110%) for each primer pair. All qRT-PCR reactions were performed in duplicate in 96-well plates on a StepOne Plus System (ABI Prism, Applied Biosystems, Foster City, CA, USA) according to the Fast SYBR Green PCR Master Mix protocol as described in §2.2.5. Each reaction contained 5.0 µl of fast SYBR Green, 0.5 µl of each Forward and Reverse primer (10 µM), 1.5 µL of Milli-Q water and 2.5 µl of cDNA. "No template control" reactions were included to confirm absence of contamination; RT^- reactions were performed to check for possible genomic DNA contamination. The following thermal cycling profile was used: 95 °C for 10 min, followed by 40 cycles of 95 °C for 15 s and 60 °C for 60 s. Afterwards, a melt curve analysis was performed to confirm the specificity of the qRT-PCR reactions. Additionally, the amplification products were analyzed using horizontal agarose gel electrophoresis (1.2% agarose gel containing GelRed™, Biotium, Fremont, CA, USA) and visualized under UV light. Only a single band of the expected size for each transcript was observed, further cloned and sequenced (TOPO® TA Cloning Kit for sequencing, Invitrogen, Carlsbad, CA, USA) to confirm target specificity.

Optimal housekeeping genes were selected using geNorm software (Vandesompele et al., 2002). In the designed experiment *rps13* + *CG13220*, *CG13220* + *TubA1* and *rp49* + *rps13* appeared to be most stable in the studied fat body, ovary and CA samples, respectively. Relative expression levels were determined according to the comparative Ct method (ΔΔCt) (Vandesompele et al., 2002). QRT-PCR was used to determine the temporal distributions of the transcripts of interest. Moreover, statistically significant differences between the *dsLmKr-h1* and *dsGFP* (control)-injected female locusts were found via a t-test on

the log transformed data (with or without two-sided Welch's correction) using GraphPad Prism 6 (GraphPad Software Inc., San Diego, CA, USA). The correlation coefficient (r) between the transcript profiles of adult and adultoid locusts was obtained by a Pearson correlation calculation.

Table 5.1: Oligonucleotide sequences of primers used for qRT-PCR.

Reference/ target genes	Forward primer	Reverse primer
LmCG13220	5'- CGGCTTGGGAGTAAGGATGTT -3'	5'- CAATTAACGTGGACAGGAGCAA -3'
LmTubA1	5'- GTTGGCGTTTCGATTTTTCTTC -3'	5'- TGAGATACATTCACGCATTTTGC -3'
LmRPS13	5'- CGTGAAGGGTGATATTTTGCA -3'	5'- GCTGACTGGGATATACCCTTACCAG -3'
LmRP49	5'- CGCTACAAGAAGCTTAAGAGATCATG -3'	5'- CTTAAACCTACGGCGAACTCTGTT -3'
LmKr-h1	5'- GCCCTACTCGTGCGACAT -3'	5'- AGCTTGAGCACGTGGTTGTA -3'
LmMet	5'- GGTGCCTGAAGAAGAAGAAC -3'	5'- ATGGAGGTGATGAAGGAGAGAG -3'
LmE93	5'- CGCAAGTAGAGCAAGAACCT -3'	5'- TGGTCTTAGGAACATCCCAC-3'
LmVg1	5'- CCACTCAACGTCACCGCAGT -3'	5'- ACTTGAGCCAAATGGATGAG -3'
LmVg2	5'- ACGCCGACAGTGTTGGTATT -3'	5'- TGCTTCTCCGCAAAGACGTA -3'
LmCYP15A1	5'- GTCTGGGAGAAGGTCTTGCA -3'	5'- CTGGCACACTGATGCTGAAT -3'
LmJHAMT	5'- GTTCCTCGAGGACTGCATGA -3'	5'- CGTTTCCGCTCTTGTTGTTGT -3'
LmSpo	5'- CAACATCTTCACCTCCTACATGTG -3'	5'- GGGTCGTCGTAGTCGAAGGA -3'
LmPhm	5'- GGATGACGACGGCAACCT -3'	5'- TGCCTGTCTGGAAGGGTATG -3'
LmShd	5'- GTGCTCCAGTGACCAGTGAA -3'	5'- TTCGGGCAAGACAGATAGCA -3'
LmDib	5'- GCTGCGATCGTGCTACTTTG -3'	5'- GGATAGCCTGGCAACTTCTCA -3'
LmSad	5'- TCCTCGCCCTCCATGAAGA -3'	5'- CAACCAGGTCTACGGCTACA -3'
LmEcR	5'- AGCGCCCATCTCTTGTTGAA -3'	5'- CGCCTGTTGTCCACATATGC -3'
LmRXR	5'- AATGCCTTGCTATGGGAATG -3'	5'- TCCTTTGTTCGCTGCCTTTC -3'

Abbreviations: *Lm = Locusta migratoria*; *TubA1 = Tubulin A1*; *RPS13 = Ribosomal protein S13*; *RP49 = Ribosomal protein 49*; *Kr-h1 = Krüppel-homolog 1*; *Met = Methoprene-tolerant*; *E93 = Ecdysone-induced protein 93; Vg = Vitellogenin*; *CYP15A1 = Cytochrome P450 enzyme 15A1 (methyl farnesoate epoxidase)*; *JHAMT = Juvenile hormone acid methyltransferase*; *Spo = Spook*; *Phm = Phantom*; *Shd = Shade*; *Dib = Disembodied; Sad = Shadow; EcR = Ecdysone receptor; RXR = Retinoid X receptor.*

5.2.5 RNA interference experiments

Double-stranded (ds)RNA constructs for *LmKr-h1* and *GFP* (control) were produced using Ambion's MEGAScript RNAi kit following the manufacturer's protocol (Figure 5.1). This procedure is based on a high-yield in vitro transcription reaction from a user-provided DNA template with a T7 promoter sequence at the 5' ends of each strand. Forward and reverse primers flanked by the T7 promoter sequence (given in Table 5.2) were used in a PCR reaction with REDTaq DNA polymerase (Sigma-Aldrich, Darmstadt, Germany) to amplify a fragment of the target gene. The resulting amplicons were analyzed using horizontal agarose gel electrophoresis (1.2% agarose gel containing GelRed™, Biotium, Fremont, CA, USA) and visualized under UV light. Only a single band was observed, which was subsequently cloned and sequenced (TOPO® TA Cloning Kit for sequencing, Invitrogen, Carlsbad, CA, USA) to confirm target specificity. The verified constructs were used as template in a high-yield in vitro transcription reaction with T7 RNA polymerase. Remaining ssRNA and DNA were removed in a nuclease digestion step. Quality and concentration of the produced dsRNA were determined using a Nanodrop spectrophotometer (NanoPhotometer N60, Implen, München, Germany). To

confirm dsRNA integrity, a small amount of the reaction product was checked by horizontal agarose gel electrophoresis (1.2% agarose gel containing GelRed™, Biotium, Fremont, CA, USA).

ATGGTGGGCTACTTCAACGGCGAGGGMCAGGCGCAGGGYCCCGGCCCGGCGCCMGCGCCCGCGGCCGCGGCCGGC
CCGCCKGCGCCGCAGGGCGAGGAGCTGTCGCCTAAGCGCGTCGTCTGCAGCCCCGACCTGCCCGTCTTCTCGCTGAC
GCGCGCCTTCGAGGAGGCGGGCAAGGCGGCYGAGCAGGCGGCAGCCGTCGCCGCCGCCTCCGCCACCGCCGCCGCC
GCCGCCCCCGCRCAGGGCCCGCCCGGCGCCTTCCAGTGCTCCTTCTGCCAGAAGACGTTCTCGCAGAAGAACACCTAC
CAGAACCAYGTGCGCTCGCACGGCAAGGAGGGCGACGACCCCTACCCGTGCACCATCTGCGGCAAGACGTTCGCGGT
GCCGGCGCGCCTCACGCGCCACTTCCGCACGCACACGGGCGAGAAGCCGTACCAGTGCGAGTTCTGCAAGAAGGCCT
TCTCCGTCAAGGAGAACCTGAGCGTGCACCGGCGCATCCACACCAAGGAGCGGCCGTACAAGTGCGACGTGTGCGA
GCGCGCCTTCGAGCACAGCGGCAAGCTGCACCGGCACATGCGCATCCACACGGGCGAGCGGCCGCACAAGTGCCAG
GTGTGCTCCAAGACGTTCATCCAGAGCGGCCAGCTCGTCATCCACATGCGCACGCACACGGGCGAGAAGCCGTACGT
GTGCAAGGCGTGCGGCAAGGGCTTCACCTGCTCCAAGCAGCTCAAGGTGCACACGCGCACGCACACGGGCGAGAAG
CCCTACTCGTGCGACATCTGCGGCAAGTCGTTCGGCTACAACCACGTGCTCAAGCTGCACCAGGTGGCGCACTACGGC
GAGAAGGTGTACAAGTGCACCATCTGCAGCGAGACGTTCACCTCCAAGAAGACGATGGAGGTGCACATCAAGAGCC
ACTCGGAGCAGCAGCACCCCCAGCAACAGCAGCAGCAGGCGCCGCCTCAGCAGCCGCCGGCGGGGAGCTCTGCCCA
GCAACCTTGGCACTCGCCATGGTCGCAACAGCAGCAACAGCAGCATCATCACCAGCAGCCGCAGCATCAACAACCGC
CCCAGCAGCAGCAACAGCTCGTCGTCCGAGGGCGTGGGCGGCAGCCTGACGCCGCCCGCCAGCGTCGAGGACGACG
AGCACTTCGCGCGCGCCGACACGGCCGTGCCGCTGAACGAGCCGCCCGTCTACCTGTTCCCCGGGCCTCTGGGTTCGA
TGCGCGGTCGCGCCACGCCCTACGACCTGCCCGTACCCGCGTGCCTCGCGGCGTCCAGCCCCTCGCCGCCCCTGACGC
CGCCCTCCAGCAACCCCGTGTCGCACGTGCCCGCCGCCCCCGCGTCGCCCGACCGCCGCGACGCCAGCTCGCTGCCGC
CCCGCAAGCGCTGCAAGGAGATTCTCAAGTCCATCGCGGCCGCCGCCGCCGCCGAACCCGCCATCCGCTACAGCTCCG
TCATACACTACGCGGGCGCCTCGTAAGGGCACCTCGCGAGCAGGACACTGGGACTTCTCACGAGTGA

Figure 5.1: *LmKr-h1* sequence with primer sets indicated. Complete coding sequence of *L. migratoria Krüppel-homolog 1* mRNA as found on NCBI (accession number KJ425482.1) with localisation of the different primers that were selected for production of dsRNA constructs or for performing qRT-PCR assays. Sequence regions highlighted in yellow and green indicate the position of the primer sets that were used for synthesising the *dsLmKr-h1* and *dsLmKr-h1_2* constructs, respectively. Sequence regions highlighted in purple indicate the primer set used for qRT-PCR.

83 Newly molted fourth nymphal (N4) female locusts, synchronized on the day of ecdysis (D0), were injected with 6 µl dsRNA against *LmKr-h1* (*dsLmKr-h1*) (400 ng dsRNA/locust, diluted in *L. migratoria* Ringer). A second injection was given on day three of the fourth nymphal stage (N4 D3) to ensure an efficient knockdown of *LmKr-h1* during this nymphal stage. As a control condition, another group of 183 locusts was injected with dsRNA against *GFP* (*dsGFP*) following the same injection scheme. In our *L. migratoria* colony, we previously observed that the penultimate (N4) and final (N5) nymphal stage are lasting for 5 and 7 days, respectively. Female adult locusts are in the vitellogenic stage of their first gonadotrophic cycle 12 days (D12) after their final molt. As such, several time points during these developmental stages were chosen for tissue collection: day 4 for fourth nymphal female locusts (N4 D4), day 0 (N5 D0), 3 (N5 D3) and 6 (N5 D6) for fifth nymphal control locusts and day 0 (D0), 4 (D4), 8 (D8) and 12 (D12) for the adult (Ad) and adultoid (Ao) locusts.

Table 5.2: Oligonucleotide sequences of primers used for dsRNA synthesis. Oligonucleotide sequences indicated in 'bold' represent the T7 promoter sequences used for the preparation of dsRNA constructs.

dsRNA constructs	Forward primer	Reverse primer
LmKr-h1	5'- **TAATACGACTCACTATAGGGAGA** GAGAACCTGAGCGTGCACC -3'	5'- **TAATACGACTCACTATAGGGAGA** TGTGCACCTTGAGCTGCTT-3'
LmKr-h1_2	5'- **TAATACGACTCACTATAGGGAGA** ATGGTGGGCTACTTCAACGG-3'	5'- **TAATACGACTCACTATAGGGAGA** CCGCTCCTTGGTGTGGATG-3'
GFP	5'-**TAATACGACTCACTATAGGGAGA** AAGGTGATGCTACATACGGAA -3'	5'-**TAATACGACTCACTATAGGGAGA** ATCCCAGCAGCAGTTACAAAC-3'

Abbreviations: *Lm = Locusta migratoria; Kr-h1 = Krüppel-homolog 1*; *GFP = Green fluorescent protein.*

5.2.6 Observing ecdysis

The ecdysis of 83 *dsLmKr-h1* and 183 *dsGFP*-injected female locusts was closely observed. Starting from fourth nymphal locusts, synchronized on the day of ecdysis, the duration and type of each developmental stage were monitored in detail. Data were analyzed with a log-rank (Mantel–Cox) test using GraphPad Prism 6 (GraphPad Software Inc., San Diego, CA, USA).

5.2.7 Measurement of oocyte length

Oocytes at the base of the ovarioles, were carefully removed from the dissected ovaries of adult (*dsGFP* control) and adultoid (*dsKr-h1*) female locusts. Oocyte length was measured using millimeter graph paper. For 12 locusts per condition, the average size of three basal oocytes was calculated. Data were analyzed with a nonparametric Mann–Whitney test using GraphPad Prism 6 (GraphPad Software Inc., San Diego, CA, USA).

5.2.8 Microscopy and histological analysis

Images of randomly chosen ovaries and ovarioles dissected from adult (*dsGFP* control) and adultoid (*dsLmKr-h1*) females were obtained with a light microscope (Zeiss SteREO Discovery V8, Oberkochen, Germany) equipped with an AxioCam ICc3 camera using the AxioVision 4.7 (Carl Zeiss-Benelux, Oberkochen, Germany).

To investigate the presence of yolk and lipid droplets, oocyte sections were made according to Billen (2006). In brief, the dissected oocytes were fixed in 2% glutaraldehyde for 12 to 24 h where after the glutaraldehyde was replaced by sodium cacodylate buffer and postfixed in 2% osmium tetraoxide. Next, the samples were dehydrated in a graded acetone series and embedded in araldite. Semi-thin (1 µm) sections, obtained using a microtome (Leica EM UC6 microtome, Nussloch, Germany), were stained with methylene blue and thionine. The resulting oocyte sections were visualized using a light microscope (Zeiss Axio Imager Z1, Oberkochen, Germany) equipped with an AxioCam MRm camera (1388 × 1040 pixels) and the software program Zen 2012 (Bleu Edition: Carl Zeiss-Benelux, Oberkochen, Germany).

5.2.9 Observation of mating, egg deposition and hatching

Mating and oviposition events were monitored in adult (*dsGFP* control) and adultoid (*dsLmKr-h1*) female locusts, which were obtained in a follow-up experiment using the same injection scheme as described in §5.2.5. In this context, the following combinations were studied: 20 control males x control females, 20 control males x adultoid females and 14 adultoid males x adultoid females. On day 4 of the locusts' adult/adultoid life, the female locusts were separated from the males and transferred to individual cages where they were fed daily with freshly sprouted wheat leaves. On day 5 of the locusts' adult/adultoid life, one sexually mature virgin male was introduced to each female and mating (*i.e.,* actual connection between the male and female genitals) was monitored. If mating was observed within two hours of the male's introduction, the male was allowed to stay with the female for 24 h. Pots filled with a slightly humidified sand/turf mixture were supplied to the females to allow oviposition. These pots were checked daily for egg pods. The total number of deposited eggs per egg pod was counted to analyze fecundity. The percentage of hatchlings was determined to analyze fertility. If no mating was observed within two hours of the male's introduction, the male was removed, and another mating attempt was made the following day using a different virgin male. A log-rank (Mantel–Cox) test in GraphPad Prism 6 (GraphPad Software Inc., San Diego, CA, USA) was used to compare mating and egg deposition between adult and adultoid female locusts. Statistically significant differences in days between mating and egg laying, the number of eggs laid, days between egg laying and hatching and the number and percentage of hatchlings between the different conditions were found via a nonparametric Mann–Whitney test using GraphPad Prism 6 (GraphPad Software Inc., San Diego, CA, USA).

5.3 Results

5.3.1 Temporal transcript profiles of MEKRE93 and JH biosynthesis pathway components

In female locusts (*dsGFP*-injected control), we investigated the temporal profiles of the MEKRE93 pathway transcripts *LmKr-h1*, *LmE93* and *LmMet*, as well as these of *LmJHAMT* and *LmCYP15A1*, the enzymes catalyzing the two final steps in JH biosynthesis, by qRT-PCR analyses at different time points from day 4 of the fourth nymphal (N4 D4) until day 12 of the adult (Ad D12) stage (Figure 5.2). Relative *LmKr-h1* transcript levels were studied in the fat body, ovaries and CA. In the fat body, *LmKr-h1* was highly expressed at the end of the fourth nymphal stage (N4 D4). After molting to fifth nymphal locusts (N5 D0), *LmKr-h1* levels were significantly lower and stayed low at the following time point until initiating the adult molt (N5 D6 and Ad D0) when significant increases were observed (Figure 5.2A). A gradual increase in *LmKr-h1* expression was observed in the ovaries of adult females (Figure 5.2C), whereas in the CA (Figure 5.2B), reduced *LmKr-h1* levels were detected on the days of molting (N5 D0, Ad D0) and when the ovaries had entered the vitellogenic stage (Ad D12). At the two earliest time points, situated before and after the N4-N5 molt (N4 D4 and N5 D0), *LmE93* levels were low in both fat body and CA, but rose significantly during the final nymphal stage (N5 D3) (Figure 5.2D and E). In fat body, *LmE93* expression remained high at the different time points in the adult stage, while in the CA of the adult stage they gradually decreased towards day 12 after the final molt (Ad D12). In addition, *LmMet* expression levels in fat body were high on day 4 of the fourth nymphal stage (N4 D4) followed by a drop towards the fifth nymphal stage (N5 D0), after which they remained relatively constant at the following time points in this nymphal stage. In fat body of adult females, significantly lower *LmMe*t levels were detected on days 4 and 12 versus higher ones on days 0 and 8 (Figure 5.2G). *LmMet* expression levels measured in the CA showed a decreasing trend throughout the different time points of the final nymphal and adult stage. For checking the expression of two JH biosynthetic enzymes, the site of JH biosynthesis, *i.e.*, the CA, was selected. Both *LmJHAMT* and *LmCYP15A1* showed a significant increase in their expression after the transition from fifth nymphal to adult locusts (Ad D0), and *LmJHAMT* further increased on day four of the adult stage (Ad D4). The relative expression levels of both genes remained high at the time points observed during adult life (Figure 5.2F and I).

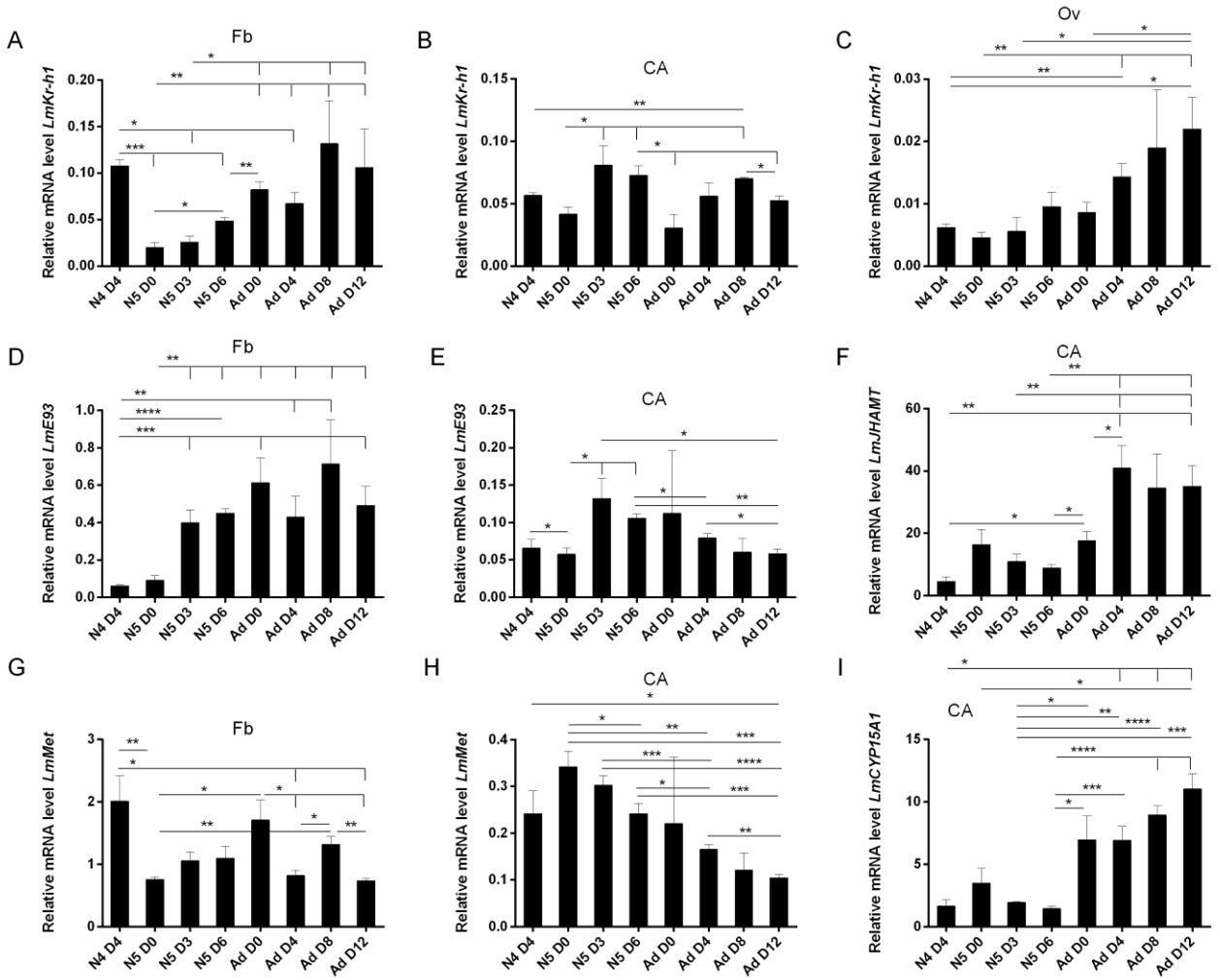

Figure 5.2: Transcript profiles of MEKRE93 and JH biosynthesis pathway components in control (*dsGFP* injected) female locusts during the last nymphal stages and the first gonadotrophic cycle. Relative levels of *LmKr-h1* (**A** + **B**)*, LmE93* (**D** + **E**) and *LmMet* (**G** + **H**) transcripts were determined in the fat body (**A** + **D** + **G**) and the CA (**B** + **E** + **H**) of control (*dsGFP*) females starting from day 4 in the fourth nymphal stage (N4 D4) until day 12 in the adult stage (Ad D12). Relative levels of *LmKr-h1* transcripts were also measured in the ovaries (**C**). Relative quantities of *LmJHAMT* (**F**) and *LmCYP15A1* (**I**) transcripts were measured in the CA. The data represent mean ± S.E.M. of four independent pools of three animals, run in duplicate and normalized to *rps13* + *CG13220*, *CG13220* + *TubA1* and *rp49* + *rps13* transcript levels for fat body, ovary and CA samples, respectively. Statistically significant differences between the measurements were found via a t-test on log-transformed data (with or without two-sided Welch's correction) and are indicated by (an) asterisk(s) (* $p < 0.05$; ** $p < 0.01$; *** $p < 0.001$; **** $p < 0.0001$).

5.3.2 Knockdown of *LmKr-h1* results in precocious development of external adult features

An initial RNAi pilot study was performed to eliminate the possibility of off-target effects and to verify the reproducibility of the phenotypic effects. Therefore, two distinct dsRNA constructs were designed (*dsLmKr-h1* and *dsLmKr-h1_2;* Figure 5.1). When tested within the same experimental setup, similar phenotypic effects were observed with both constructs. Next, the *dsLmKr-h1* construct was utilized in all further experiments.

The RNAi treatment, based on injections of *dsLmKr-h1* during the fourth nymphal stage (on D0 and D3), significantly affected development of *L. migratoria* (Figure 5.3). In total, 93% of the experimental locusts did not molt into the fifth nymphal stage, while 100% of the *dsGFP*-injected (control) locusts successfully completed this nymphal-to-nymphal molt (Figure 5.3A, B and C). Instead of molting into fifth nymphal locusts, most of the *dsLmKr-h1*-injected (experimental) animals molted into an adultoid phenotype, showing precocious development of adult features. These adultoids already had an adult color scheme as well as the presence of wings, although not fully extended and non-functional, while maintaining the physical body size of a fifth nymphal locust (Figure 5.3A). The animals that molted to the adultoid phenotype had remained in the fourth nymphal stage for a longer time than the *dsGFP*-injected (control) locusts that molted to the fifth nymphal stage: their N4 stage lasted for 6–8 days compared to 4–6 days, respectively (Figure 5.3C). Moreover, the adultoid insects did not undergo any further molts (Figure 5.3D). Apart from the adultoid phenotype, 29% of the *dsLmKr-h1-injected* (experimental) animals molted into an intermediate phenotype (Figure 5.3B), still having a nymphal color scheme, but with more developed wings (Figure 5.3A). These animals had remained in the fourth nymphal stage for 5 to 7 days before molting to their intermediate phenotype (Figure 5.3C). Unlike the adultoid phenotype, 20% of the intermediate phenotype locusts were still successfully completing the adult molt, while 100% of the control (*dsGFP*) and experimental (*dsLmKr-h1*) fifth nymphal locusts successfully completed the adult molt (Figure 5.3D).

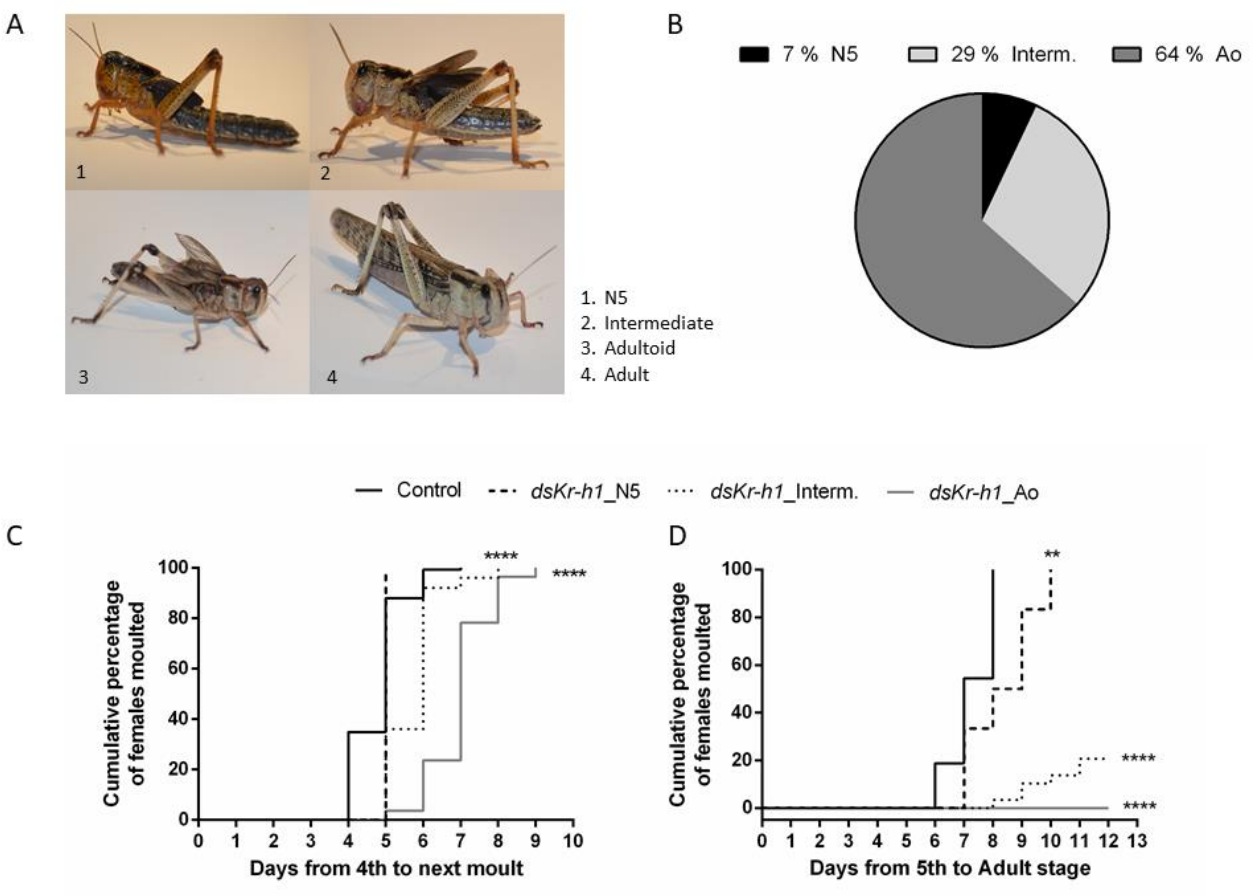

Figure 5.3. Phenotypes of *dsLmKr-h1*-injected female locusts and the timing of their ecdysis. The timing of ecdysis of 148 *dsGFP* (control) and 83 *dsLmKr-h1*-injected female locusts was observed starting from freshly molted fourth nymphal locusts. (**A**) Observed phenotypes of *dsGFP* (control) and/or *dsLmKr-h1*-injected locusts obtained after molting: (1) fifth nymphal stage (N5), (2) intermediate (Interm.), (3) adultoid (Ao), (4) adult (Ad). (**B**) A pie chart representing the percentages of phenotypes (N5, Interm, Ao) observed after molting of the *dsLmKr-h1-injected* fourth nymphal (N4) locusts. (**C**) The cumulative percentage of females that molted from the fourth nymphal to the fifth nymphal (control and *dsKr-h1*_N5) or to a precocious adult-like stage, classified as an intermediate (*dsKr-h1*_Interm.) or an adultoid phenotype (*dsKr-h1*_Ao). (**D**) The cumulative percentage of females that molted from N5, Interm. or Ao to the adult stage. Statistically significant differences (*p*) between the conditions were found via a log-rank (Mantel–Cox) test and are indicated by asterisks (** $p < 0.01$; **** $p < 0.0001$).

5.3.3 Transcript levels of MEKRE93 and JH biosynthesis pathway components in dsRNA-injected fourth nymphal and freshly molted fifth nymphal, adultoid and adult female locusts

Transcript levels of different components of the MEKRE93 pathway, as well as the enzymes catalyzing the two final steps of JH biosynthesis, were determined in different tissues on two developmental time points, *i.e*., day 4 of the fourth nymphal stage (N4 D4) and freshly molted fifth nymphal (N5 D0), adult (Ad D0) or adultoid (Ao D0) locusts (Figure 5.4). A significant downregulation of *LmKr-h1* transcript levels was measured in the fat body (44%) of fourth nymphal *dsLmKr-h1*-injected locusts, when compared with *dsGFP*-injected (control) locusts of the same age (N4 D4; Figure 5.4A). While in the ovaries (Figure 5.4C) no significant change in the transcript level was observed at this time point, a significant increase was noticed in the CA (Figure 5.4B). Interestingly, on the day of molting, *LmKr-h1* relative transcript levels were significantly higher in fat body and ovaries of adultoid locusts than fifth nymphal ones (Figure 5.4A and C), while no significant differences were observed in the CA (Figure 5.4B).

In comparison with *dsGFP*-injected (control) locusts, the *LmE93* mRNA levels were significantly higher in both fat body and CA of *dsLmKr-h1*-injected locusts on day 4 of the fourth nymphal stage (N4 D4). On the day of molting, the *LmE93* transcript levels in both tissues were significantly higher in adultoid (*dsLmKr-h1*) than in fifth nymphal locusts (*dsGFP* control), while no significant differences were observed between adultoid and adult locusts (Figure 5.4D and E). For *LmMet* mRNA levels, on the other hand, no significant changes were noticed with the single exception of a significantly lower level in the fat body of freshly molted fifth nymphal (*dsGFP* control) locusts (Figure 5.4G and H). When checking the expression levels of two JH biosynthetic enzymes, *LmJHAMT* and *LmCYP15A1* in the CA, no significant differences were observed between *dsLmKr-h1* and *dsGFP*-injected locusts on the time points that were analyzed (Figure 5.4F and I).

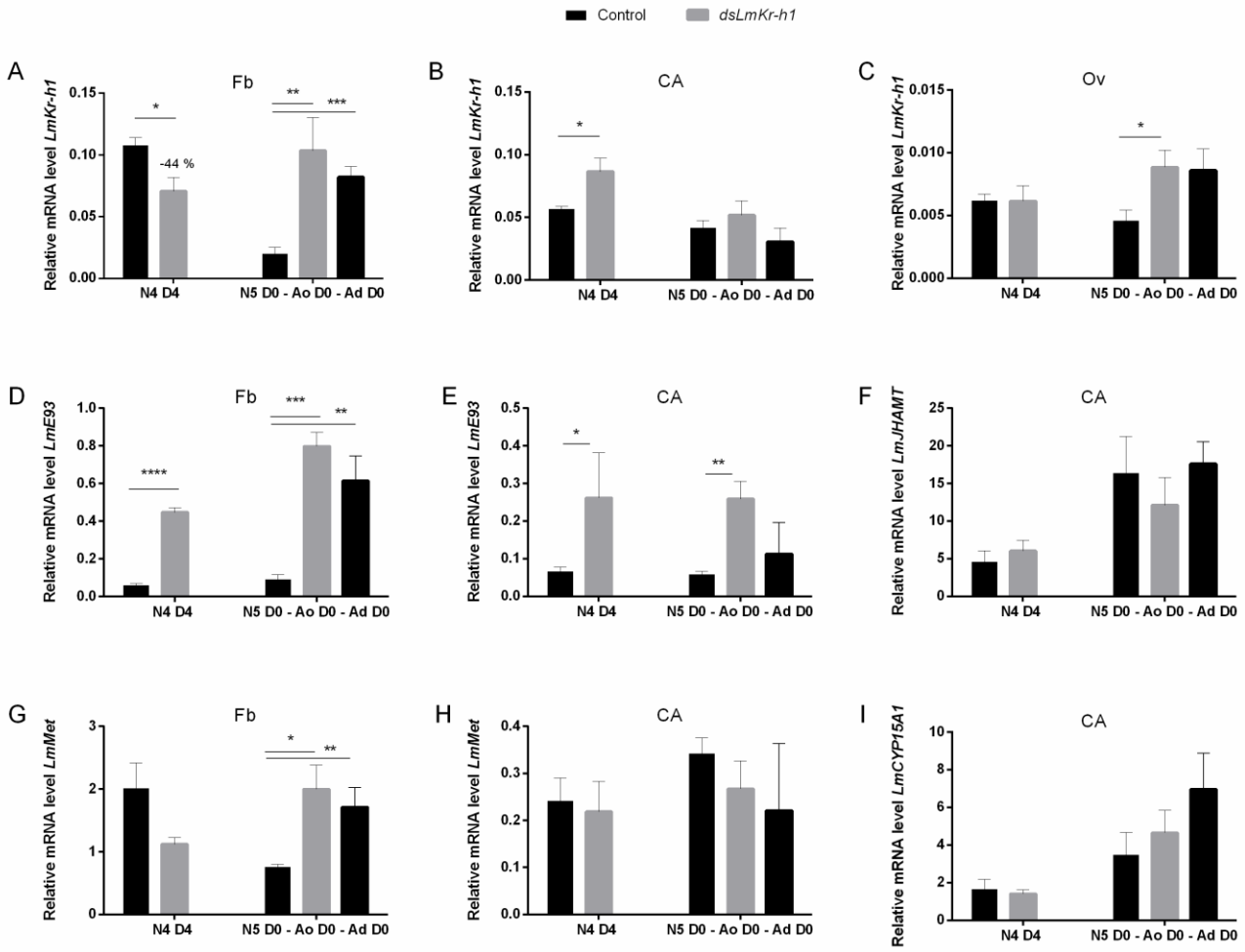

Figure 5.4: Relative transcript levels of MEKRE93 and JH biosynthesis pathway components in *dsLmKr-h1* or *dsGFP* injected female locusts. Relative *LmKr-h1* (**A** + **B**), *LmE93* (**D** + **E**) and *LmMet* (**G** + **H**) transcript levels were measured in the fat body (**A** + **D** + **G**) and the CA (**B** + **E** + **H**) of *dsLmKr-h1* (grey bars) and *dsGFP* (Control: black bars) injected 4-day-old fourth nymphal locusts (N4 D4), as well as in freshly moulted fifth nymphal (N5 D0), adultoid (Ao D0) and adult (Ad D0) female locusts. Relative *LmKr-h1* levels were also measured in the ovaries (**C**). Relative quantities of *LmJHAMT* (**F**) and *LmCYP15A1* (**I**) transcripts were measured in the CA. The data represent mean ± S.E.M. of four independent pools of three animals, run in duplicate and normalized to *rps13* + *CG13220*, *CG13220* + *TubA1* and *rp49* + *rps13* transcript levels for fat body, ovary and CA samples, respectively. Statistically significant differences between the measurements were found via a t-test on log-transformed data (with or without two-sided Welch's correction) and are indicated by (an) asterisk(s) (* $p < 0.05$; ** $p < 0.01$; *** $p < 0.001$; **** $p < 0.0001$).

5.3.4 The adultoid phenotype shows an accelerated ovarian maturation

To investigate the effect of the RNAi-mediated knockdown of *LmKr-h1* in fourth nymphal locusts on the later female reproductive physiology, adult (*dsGFP* control) and adultoid (*dsLmKr-h1*) locusts were dissected every four days (Figure 5.4A). Adultoid female locusts were in full vitellogenesis eight days after their precociously induced final molt (Ao D8). In comparison, eight days after their final molt (Ad D8) the adult females included in the same experiment had an average oocyte length of only 1.39 mm. Moreover, considering that a fifth nymphal stage preceded their adult molt, as illustrated in Figure 5.5A, the locusts of the control group (*dsGFP*)

were, in total, at least four days older than the adultoid (*dsLmKr-h1*) females. Adultoid females did not only develop faster but their ovaries also matured faster, as shown by the growth of their basal oocytes over time (Figure 5.5B). On day 4 of the adult stage, the average basal oocyte length measured 0.62 mm, while in adultoids this was 0.53 mm. Significantly accelerated growth was observed on day 8 of the adultoid phenotype with the average oocyte length of 3.88 mm, more than double the size of the basal oocytes in day 8 adults measuring 1.39 mm. A significant length difference was also observed between the basal oocytes in adultoids and adults on day 12 after the final molt. Ovaries were further dissected, cleaned by removing the attached fat body and imaged (Figure 5.5C-E' and M-O). Some adultoid females were already in their second gonadotrophic cycle, characterized by orange lesions at the base of the new basal oocyte. In addition to these orange lesions, multiple resorbing oocytes were observed (Figure 5.5D—E'). Upon dissection of the adultoid females, it became clear that, while most of these animals were unable to deposit their eggs, fully grown oocytes were filling the oviducts (Figure 5.5E). Transverse sections of terminal oocytes were examined. The sections clearly confirmed the presence of yolk (blue matrix) and lipid droplets (grey spheres) from as early as eight days after the final molt to adultoid (Figure 5.5F—H), whereas in the oocytes of adult (control) locusts, the presence of yolk and lipid droplets was only observed at day 12 (Figure 5.5K and L). In the resorbing oocytes of adultoids, a loss of yolk was observed (Figure 5.5I and I'). The oocytes found in the oviducts of adultoid locusts contained yolk and lipid droplets and were clearly surrounded by a chorion (Figure 5.5J).

Since yolk accumulation was observed relatively early in oocytes of adultoid (*dsLmKr-h1*) females, *LmVg* mRNA levels were analyzed in fat body samples during the first gonadotrophic cycle and compared to normal (*dsGFP* control) adult females (Figure 5.6). In the fat bodies of adultoid locusts, significantly higher *Vg* mRNA levels were observed for both *LmVg1* (Figure 5.6A) and *LmVg2* (Figure 5.6B) on days 8 and 12 after the final molt. When checking the temporal profiles of *LmVg* mRNA transcripts in fat body samples of adult and adultoid female locusts during their first gonadotrophic cycle (Figure 5.7), significantly higher *LmVg* mRNA levels were observed for both *LmVg1* (Figure 5.7A and C) and *LmVg2* (Figure 5.7B and D) on day 8 compared to day 4. Unlike adultoid females, *LmVg* mRNA levels in control adult females were still significantly increasing towards day 12 (Figure 5.7A and B).

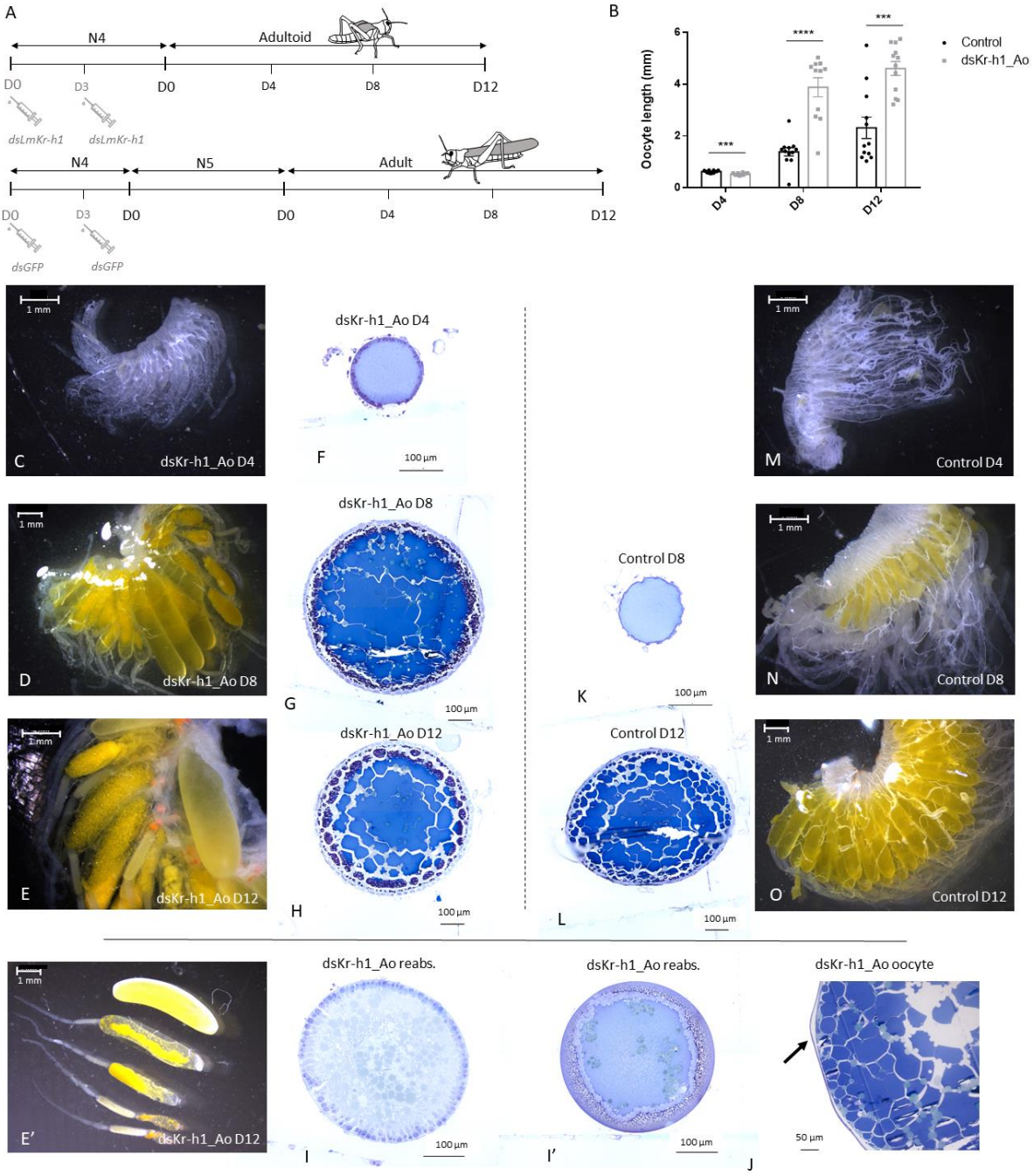

Figure 5.5. Ovarian maturation in adult and adultoid migratory locusts (*L. migratoria*). (**A**) Time scheme showing the different time points of dsRNA injection together with the duration of each developmental stage and the different time points chosen to dissect control adult (*dsGFP*) and adultoid (*dsLmKr-h1*) female locusts. (**B**) The oocyte length (mm) of adult (control: black bars) and adultoid (*dsKr-h1*_Ao: grey bars) female locusts was measured on day 4 (D4), day 8 (D8) and day 12 (D12) after the final molt. Each point represents the mean length of 3 randomly chosen basal oocytes (mean ± S.E.M). Statistically significant differences (*p*) were found via a nonparametric Mann–Whitney test and are indicated by asterisks (*** $p < 0.001$; **** $p < 0.0001$). (**C–E'** and **M–O**) Ovaries of 4-day-old (**C**), 8-day-old (**D**) and 12-day-old (**E,E'**) adultoid (*dsKr-h1*_Ao) locusts compared to 4-day-old (**M**), 8-day-old (**N**) and 12-day-old (**O**) adult locusts (control). Scale bars: 1 mm. (**F–L**) Histological sections of basal oocytes from 4-day-old (**F**), 8-day-old (**G**) and 12-day-old (**H**) adultoid (*dsKr-h1*_Ao) locusts compared to 8-day-old (**K**) and 12-day-old (**L**) adult locusts (control). Scale bar: 100 µm. (**I–J**) Histological sections of reabsorbing oocytes (**I, I'**) and an oocyte (**J**) found in the oviduct of an adultoid locust (*dsKr-h1*_Ao), with arrow (black) indicating the chorion. Scale bars: 100 µm (**I, I'**) and 50 µm (**J**).

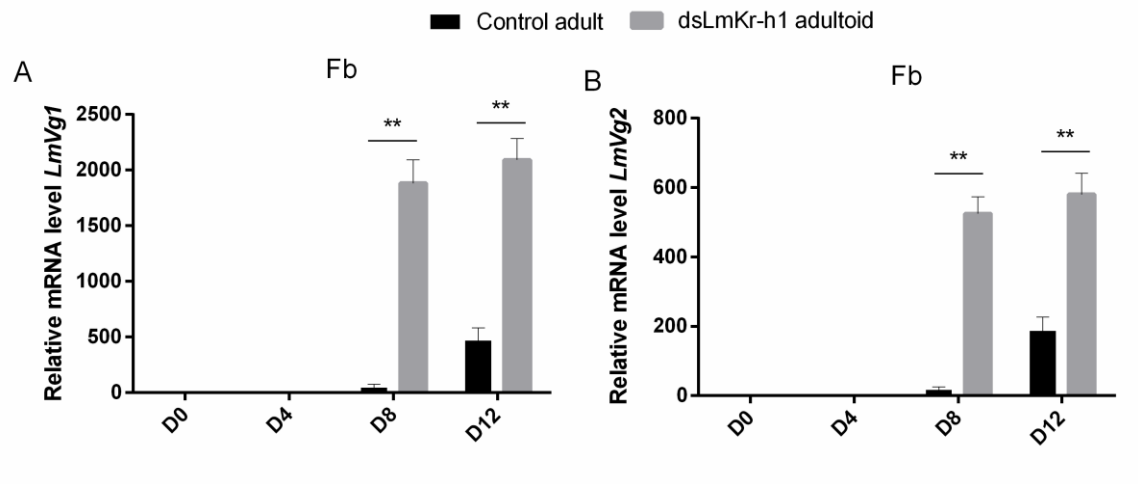

Figure 5.6. Relative *LmVg1* and *LmVg2* transcript levels in adult and adultoid females. Relative transcript levels of *LmVg1* (**A**) and *LmVg2* (**B**) in the fat body of freshly molted (D0), 4-day-old (D4), 8-day-old (D8) and 12-day-old (D12) adultoid (*dsLmKr-h1*) and adult (*dsGFP*: control) female locusts. The data represent mean ± S.E.M. of four independent pools of three animals, run in duplicate and normalized to *rps13* and *CG13220* transcript levels. Statistically significant differences between the measurements were found via a t-test on log-transformed data (with or without two-sided Welch's correction) and are indicated by asterisks (** $p < 0.01$).

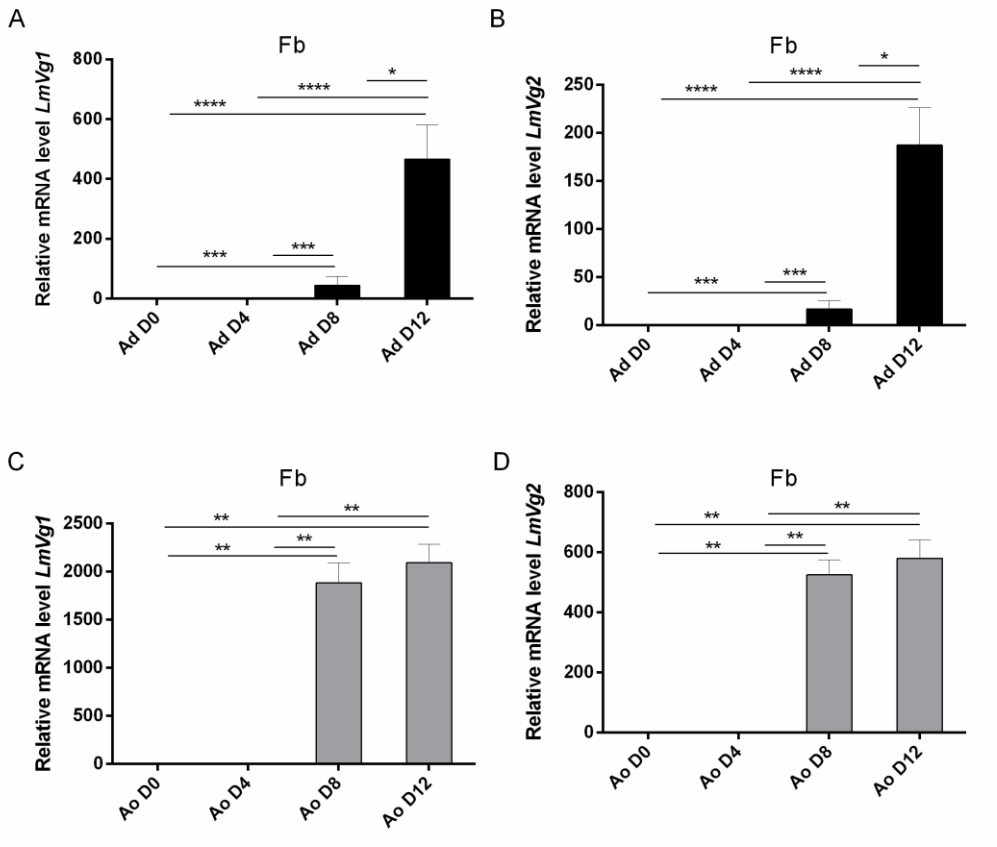

Figure 5.7: Relative *LmVg1* and *LmVg2* transcript levels of adult (*dsGFP* control) and adultoid (*dsLmKr-h1*) female locusts during the first gonadotrophic cycle. Relative transcript levels of *LmVg1* (**A** + **C**) and *LmVg2* (**B** + **D**) in the fat body of freshly moulted (D0), 4-day-old (D4), 8-day-old (D8) and 12-day-old (D12) adult (Ad: **A** + **B**) and adultoid (Ao: **C** + **D**) female locusts. The data represent mean ± S.E.M. of four independent pools of three animals, run in duplicate and

normalized to *rps13* and *CG13220* transcript levels. Statistically significant differences between successive time points were found via a t-test on log-transformed data (with or without two-sided Welch's correction) and are indicated (an) asterisk(s) (* $p < 0.05$; ** $p < 0.01$; *** $p < 0.001$; **** $p < 0.0001$).

5.3.5 Transcript levels of MEKRE93 and JH biosynthesis pathway components in adultoid females

The temporal expression profiles of genes encoding MEKRE93 and JH biosynthesis pathway components were monitored in the fat body, in the CA and in the ovaries of adultoid (*dsLmKr-h1*) female locusts (Figure 5.8). Figure 5.8 compares the expression levels at different time points after the final molt between adultoid (*dsLmKr-h1*) and adult (*dsGFP* control) female locusts. In the fat body of adultoid female locusts, *LmKr-h1* transcript levels significantly increased at day 8 (Figure 5.8A). At this time point a very pronounced increase was also observed in the ovaries (Figure S5C), whereas in the CA an increasing trend was observed from D4 to D12 (Figure 5.8B). When compared to adult females, the relative *LmKr-h1* mRNA levels of adultoid female locusts were significantly higher at different time points after the final molt: on days 4 and 12 in the fat body and day 12 in the CA (Figure 5.9A and B). In the fat body of adultoids, *LmE93* and *LmMet* mRNA levels were significantly higher on the day of molting (Ao D0) and then decreased on the following time point (Ao D4) (Figure 5.8D and G). Furthermore, when compared to days 0 and 4, a very pronounced decrease in the *LmE93* level was observed in the fat body of adultoids on day 8 (Ao D8) (Figure 5.8D). In the fat body of adult female locusts, a clear decreasing trend in the *LmE93* and *LmMet* expression profiles was not observed (Figure 5.1D and G). Therefore, in comparison to the adults, the adultoids had significantly lower *LmE93* and *LmMet* transcript levels in their fat body on day 8 after the final molt (Figure 5.9C and E). On the other hand, when compared to adult females, the adultoids had significantly higher *LmE93* transcript levels in the CA at some time points (D4 and D12), while for *LmMet* no significant differences were observed between adults and adultoids in these JH producing endocrine organs (Figure 5.9D and F). In a Pearson correlation calculation, the temporal profiles of the relative mRNA levels of *LmE93* and *LmMet* in the CA of control (*dsGFP*) adult females correlated well with these of adultoid (*dsLmKr-h1*) females (Figure 5.9D and F). For the two JH biosynthetic enzymes, *LmJHAMT* and *LmCYP15A1*, relative transcript levels tended to be higher in sexually maturing adultoid females (Figure 5.8F and I). When compared to adults, the adultoid females had significantly higher *LmCYP15A1* levels in their CA on day 8 after the final molt (Figure 5.9H).

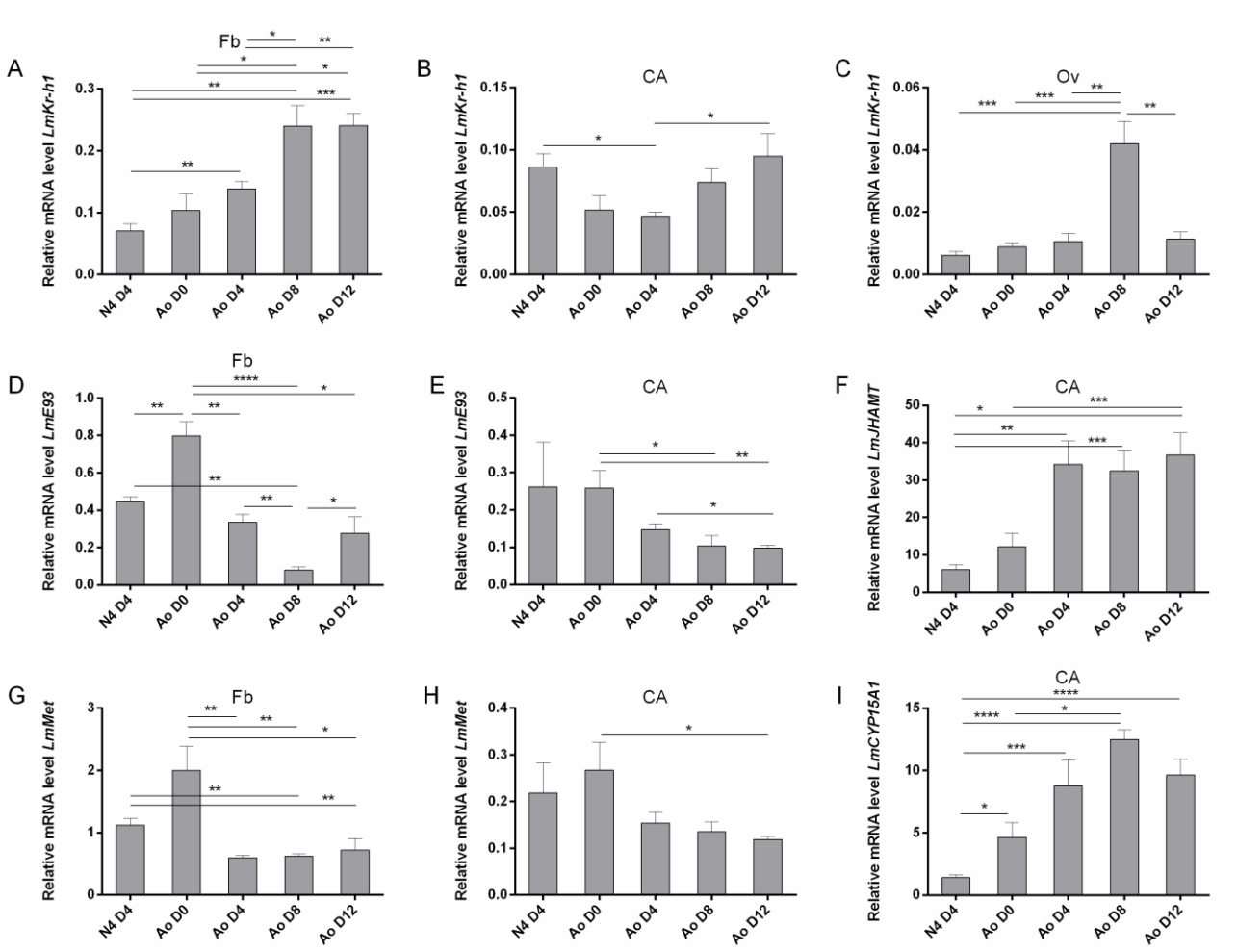

Figure 5.8: Relative transcript levels of MEKRE93 and JH biosynthesis pathway components in experimental (*dsLmKr-h1*) female locusts during the fourth nymphal stage and the first gonadotrophic cycle. Relative levels of *LmKr-h1* (**A** + **B**)*, LmE93* (**D** + **E**) and *LmMet* (**G** + **H**) transcripts were determined in the fat body (**A** + **D** + **G**) and the CA (**B** + **E** + **H**) of experimental (*dsLmKr-h1*) females starting from day 4 in the fourth nymphal stage (N4 D4) until day 12 in the adultoid stage (Ao D12). Relative *LmKr-h1* levels were also measured in the ovaries (**C**). Relative quantities of *LmJHAMT* (**F**) and *LmCYP15A1* (**I**) transcripts were measured in the CA. The data represent mean ± S.E.M. of four independent pools of three animals, run in duplicate and normalized to *rps13* + *CG13220*, *CG13220* + *TubA1* and *rp49* + *rps13* transcript levels for fat body, ovary and CA samples, respectively. Statistically significant differences between the measurements were found via a t-test on log-transformed data (with or without two-sided Welch's correction) and are indicated by (an) asterisk(s) (* $p < 0.05$; ** $p < 0.01$; *** $p < 0.001$; **** $p < 0.0001$).

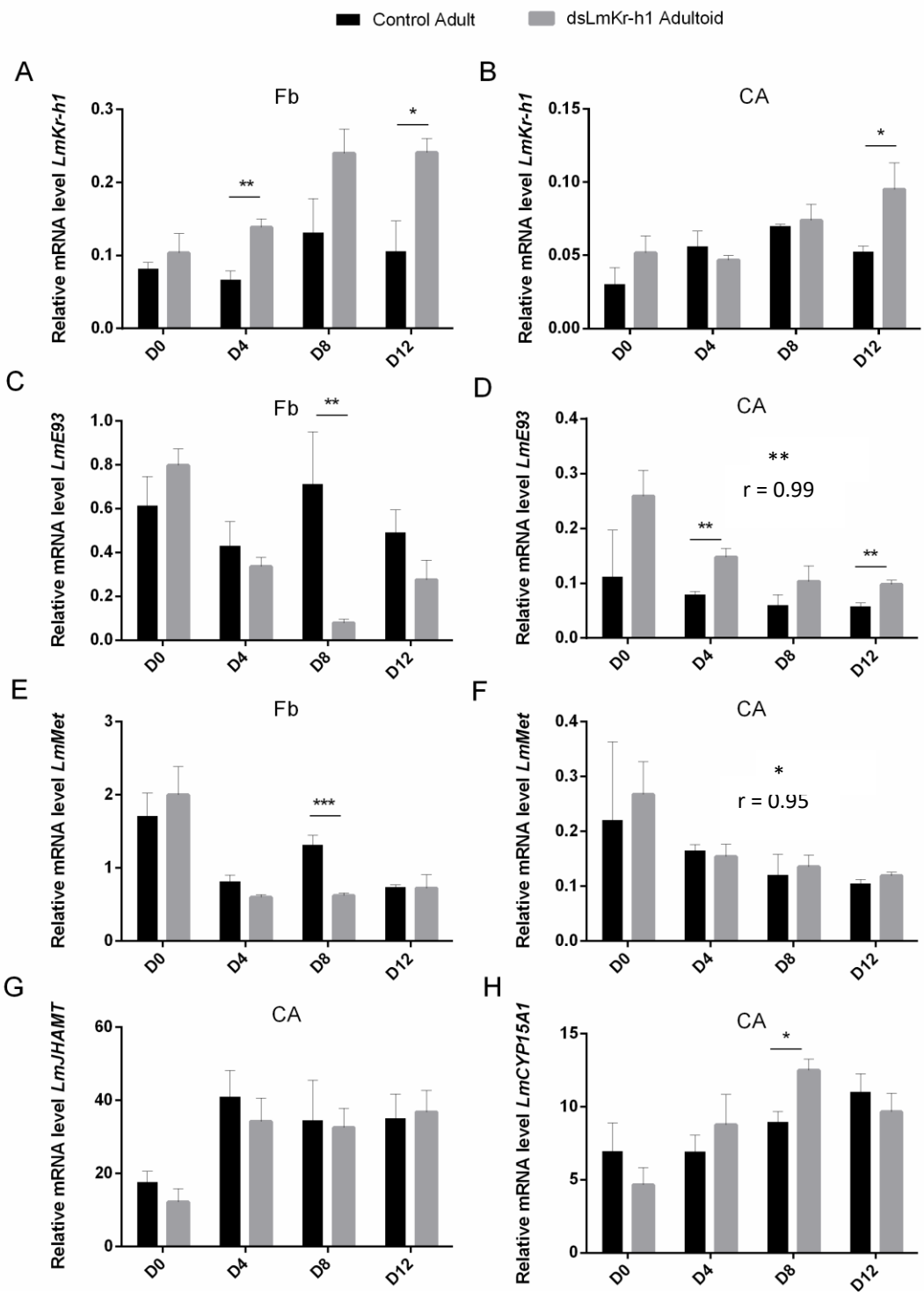

Figure 5.9. Relative transcript levels of MEKRE93 and JH biosynthesis pathway components in adult and adultoid *L. migratoria* females. Relative *LmKr-h1* (**A + B**)*, LmE93* (**C + D**) and *LmMet* (**E + F**) transcript levels were measured in the fat body (**A + C + D**) and the CA (**B + D + F**) of freshly molted (D0), 4-day-old (D4), 8-day-old (D8) and 12-day-old (D12) adultoid (*dsLmKr-h1*) and adult (*dsGFP*: control) female locusts. Relative *LmJHAMT* (**G**) and *LmCYP15A1* (**H**) transcript levels were measured in the CA as well. The data represent mean ± S.E.M. of four independent pools of three animals, run in duplicate and normalized to *rps13* + *CG13220* and *rp49* + *rps13* transcript levels for fat body and CA samples, respectively. Statistically significant differences between the measurements were found via a t-test on log-transformed data (with or without two-sided Welch's correction) and are indicated by (an) asterisk(s) (* $p < 0.05$; ** $p < 0.01$; *** $p < 0.001$). The correlation coefficient (r) between the transcript profiles of adult and adultoid locusts was obtained by a

Pearson correlation calculation. This coefficient is indicated above the figure panels where a significant correlation was observed [*p*-value is indicated by (an) asterisk(s) (* $p < 0.05$; ** $p < 0.01$)].

5.3.6 Transcript levels of Halloween genes and ecdysone receptor complex in adultoids and adults

Ovaries were collected every four days starting from freshly molted (D0) adultoid and adult locusts until day 12 (D12) after the final molt. Figure 5.10 compares the ovarian expression levels of *LmKr-h1*, the *Halloween* genes, *Spook* (*LmSpo*), *Phantom* (*LmPhm*), *Disembodied* (*LmDib*), *Shadow* (*LmSad*) and *Shade* (*LmShd*), which code for cytochrome P450 enzymes involved in ecdysteroid biosynthesis, as well as of the *LmEcR* and *LmRXR* genes, which encode the components of the ecdysone receptor complex, in adultoid (*dsLmKr-h1*) and adult (*dsGFP* control) female locusts at these different time points. Figures 5.11 and 5.12 show the temporal expression profiles for *Halloween* genes and ecdysone receptor components in ovaries of adult (*dsGFP* control) and adultoid (*dsLmKr-h1*) females, respectively.

In adult females, a significantly increased expression level was observed on day 12 (Ad D12) for *LmPhm*, while a similar temporal trend was also noticeable for *LmSpo* and *LmSad* (Figure 5.11A, B and D). For *LmShd* and *LmEcR* no significant changes in expression were observed (Figure 5.11E and F), while *LmDib* and *LmRXR* levels seemed to progressively decline at different time points after the final molt (Figure 5.11C and G). No correlations were found between adult and adultoid locusts for the temporal profiles of ovarian *LmKr-h1*, *LmSpo, LmPhm*, *LmDib*, *LmSad*, *LmShd*, *LmEcR* and *LmRXR* transcripts (Figure 5.10).

In comparison with freshly molted adultoid females (Ao D0), *LmPhm*, *LmEcR* and *LmRXR* transcript levels were significantly reduced on day 4 (Ao D4) after the final molt (Figure 5.12B, F and G). Furthermore, in these adultoids the *LmSpo, LmPhm, LmSad* and *LmEcR* genes showed significantly increased transcript levels on day 8 (Ao D8) (Figure 5.12A, B, D and F). At this time point, the rise of *LmSpo* and *LmPhm* levels in adultoids appeared very pronounced, as on day 8 (D8) the transcript levels for both *Halloween* genes were also significantly higher than in adult females (Figure 5.10B and C). A similar temporal profile was noticed when investigating *LmKr-h1* expression levels in the ovaries of adultoid locusts (Figure S5C and Figure 5.10A). For *LmDib* no significant changes in expression were observed between the different time points analyzed in the adultoids (Figure 5.12C). Nevertheless, in comparison with adult (control) females, a significantly higher *LmDib* mRNA level was observed on day 12 (D12) (Figure 5.10D). In addition, when compared to control adults, significantly lower *LmSpo, LmSad* and *LmRXR* transcript levels were detected in the adultoids on day 4 (D4) (Figure 5.10B, E and H). No significant differences in *LmShd* and *LmEcR* expression were observed between adult and adultoid females at the different time points (Figure 5.10F and G).

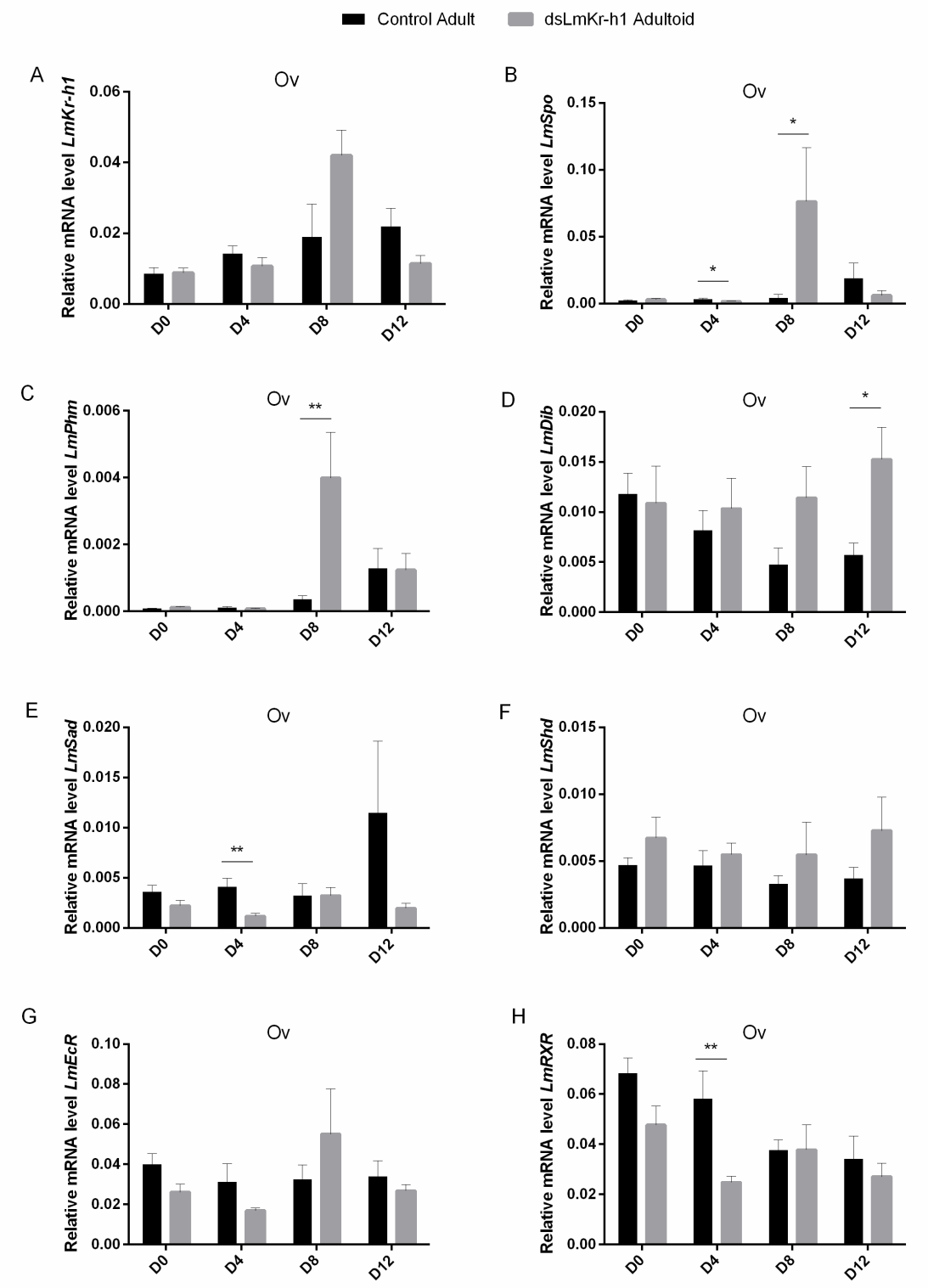

Figure 5.10. Relative transcript levels of *LmKr-h1*, several *Halloween* genes as well as *LmEcR and LmRXR* in ovaries of adult and adultoid *L. migratoria* females. Relative *LmKr-h1* (**A**)*, Spook* (*LmSpo*) (**B**)*, Phantom* (*LmPhm*) (**C**), *Disembodied* (*LmDib*) (**D**), *Shadow* (*LmSad*) (**E**), *Shade* (*LmShd*), (**F**)*, LmEcR* (**G**) and *LmRXR* (**H**) transcript levels were measured in the ovaries of freshly molted (D0), 4-day-old (D4), 8-day-old (D8) and 12-day-old (D12) adultoid (*dsLmKr-h1*) and adult (*dsGFP*: control) female locusts. The data represent mean ± S.E.M. of four independent pools of three animals, run in duplicate and normalized to *CG13220* and *TubA1* transcript levels. Statistically significant differences between the measurements were found via a t-test on log-transformed data (with or without two-sided Welch's correction) and are

indicated by (an) asterisk(s) (* $p < 0.05$; ** $p < 0.01$). With a Pearson correlation calculation, no significant correlations were found between transcript profiles of adult and adultoid locusts.

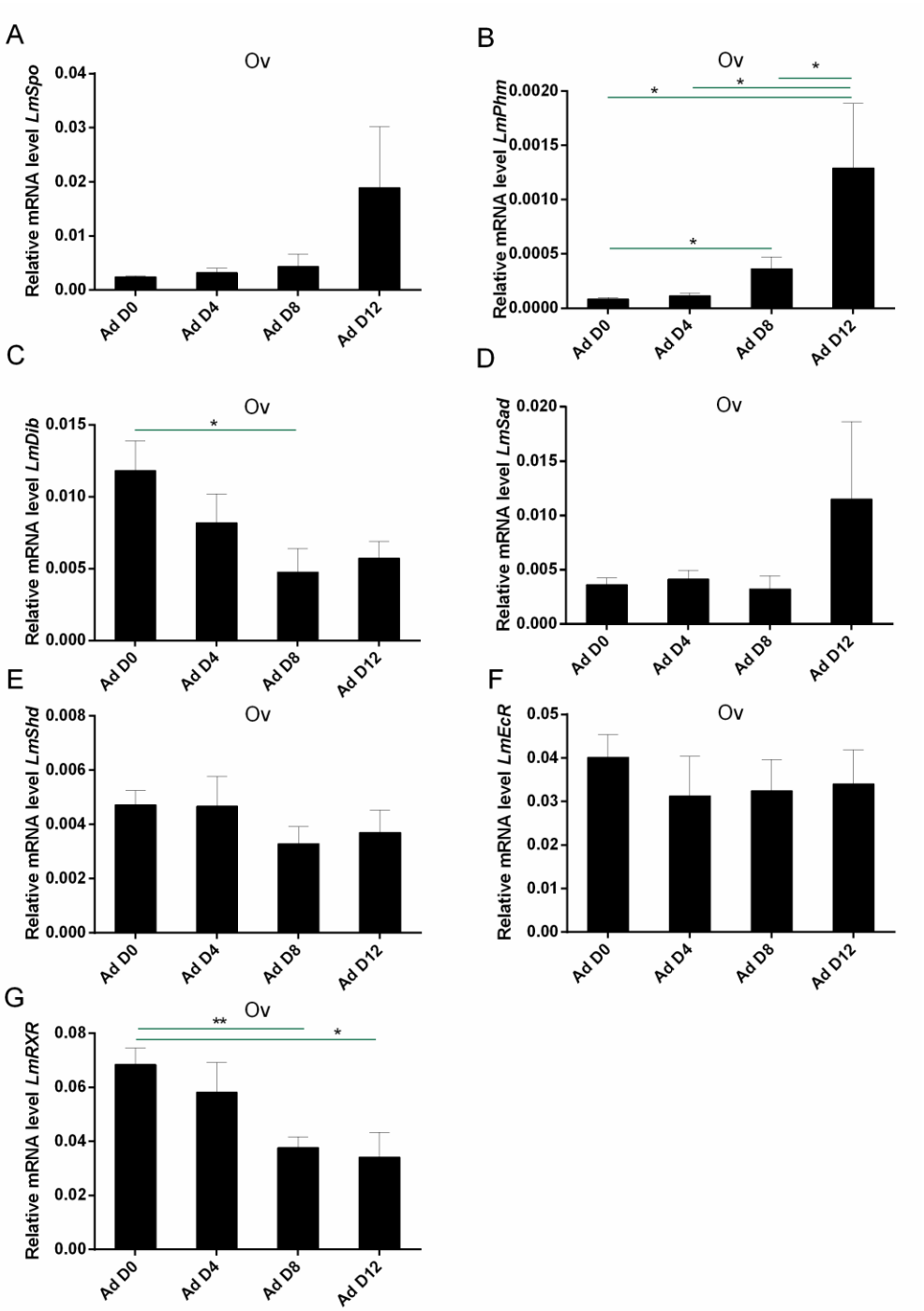

Figure 5.11: Relative transcript levels of several *Halloween* genes, as well as ecdysone receptor components *LmEcR and LmRXR,* during the first gonadotrophic cycle of adult (*dsGFP* control) female locusts. The relative quantities of *LmSpo* (**A**)*, LmPhm* (**B**), *LmDib* (**C**), *LmSad* (**D**), *LmShd* (**E**)*, LmEcR* (**F**) and *LmRXR* (**G**) transcripts were determined in the ovaries of control (*dsGFP*) adult females at 0 (Ad D0), 4 (Ad D4), 8 (Ad D8) and 12 (Ad D12) days after the final moult. The data represent mean ± S.E.M. of four independent pools of three animals, run in duplicate and normalized to *CG13220* and *TubA1* transcript levels. Statistically significant differences between the measurements were found via a t-test on log-transformed data (with or without two-sided Welch's correction) and are indicated by (an) asterisk(s) (* $p < 0.05$; ** $p < 0.01$).

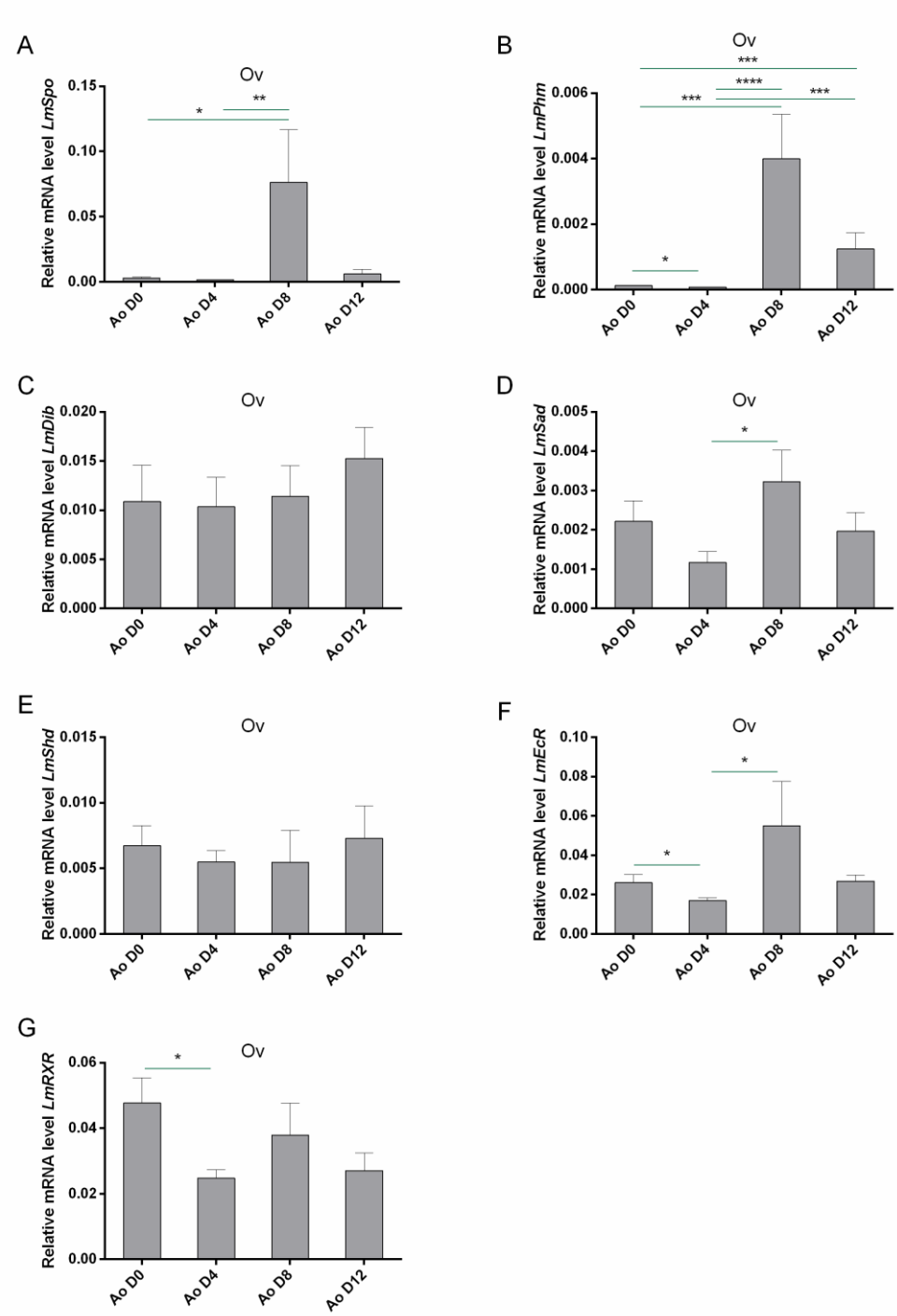

Figure 5.12: Relative transcript levels of several *Halloween* genes, as well as ecdysone receptor components *LmEcR and LmRXR,* during the first gonadotrophic cycle of adultoid (*dsLmKr-h1*) female locusts. The relative quantities of *LmSpo* (**A**)*, LmPhm* (**B**), *LmDib* (**C**), *LmSad* (**D**), *LmShd* (**E**)*, LmEcR* (**F**) and *LmRXR* (**G**) transcripts were determined in the ovaries of adultoid (*dsLmKr-h1*) females at 0 (Ao D0), 4 (Ao D4), 8 (Ao D8) and 12 (Ao D12) days after the final moult. The data represent mean ± S.E.M. of four independent pools of three animals, run in duplicate and normalized to *CG13220* and *TubA1* transcript levels. Statistically significant differences between measurements were found via a t-test on log-transformed data (with or without two-sided Welch's correction) and are indicated by (an) asterisk(s) (* $p < 0.05$; ** $p < 0.01$; *** $p < 0.001$; **** $p < 0.0001$).

5.3.7 Adultoid females have severe defects in mating and egg laying

Mating, fecundity and fertility were assessed in the adultoid (*dsLmKr-h1*) locusts in comparison with normal adults (*dsGFP* control). Therefore, the events of mating with a virgin adult male (showing an actual connection between the male and female genitals) and egg deposition were monitored for adult and adultoid females (Figure 5.13). We also registered the period between mating and oviposition, the incubation time from egg laying until hatching, as well as the numbers of eggs and hatchlings per egg pod that had been deposited by the females (Figure 5.14). Our results indicate that the mating process was significantly affected in the adultoid females. Adultoid females did not mate with virgin control males within the experimental timeframe (Figure 5.13A). In comparison, all control females mated successfully (Figure 5.13A). When paired with adultoid males, only a small fraction (14%) of the adultoid females was mating (Figure 5.13A and Figure 5.15A—C and G–H). Oviposition was also severely impaired, since only the adultoid females that had mated also deposited their eggs (Figure 5.13B and Figure 5.15D—F). Moreover, they deposited their eggs significantly earlier than the adult females (Figure 5.14A). Interestingly, the eggs deposited by the adultoid females appeared similar in size and shape to the ones obtained from adult females. However, the incubation period between egg laying and hatching was significantly longer (Figure 5.14B). Figure 5.14C shows the numbers of eggs and hatchlings per egg pod. Although adult and adultoid females did not significantly differ in the number of eggs they deposited per pod (fecundity), the number of hatchlings (fertility) was significantly lower for the offspring of adultoid locusts.

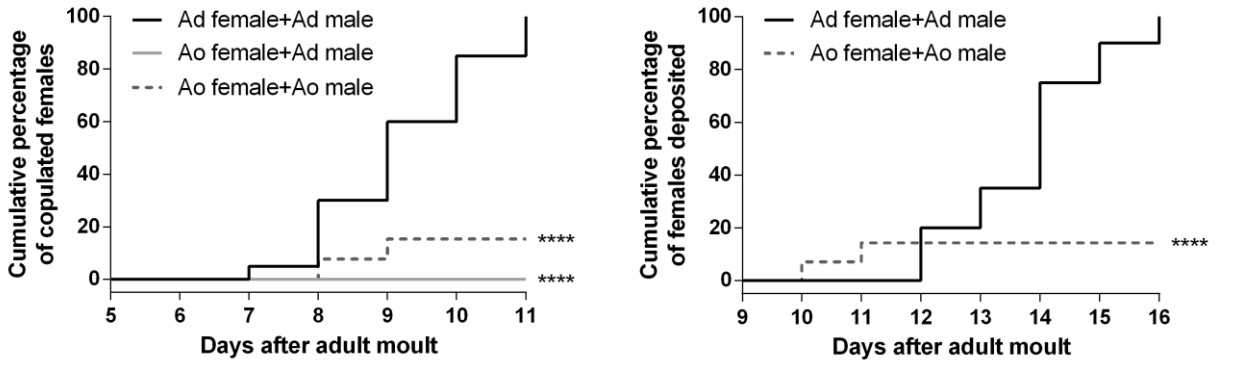

Figure 5.13. Mating and oviposition by adult and adultoid *L. migratoria* females. Mating and oviposition were observed for 20 adult (Ad) females (each combined with an adult male: 'Ad female + Ad male'), 20 adultoid (Ao) (each combined with an adult male: 'Ao female + Ad male') and 14 Ao (each combined with an adultoid male: 'Ao female + Ao male') females starting on day 5 of the adult (Ad) or adultoid (Ao) stage. (**A**) The cumulative percentage of mating females (achieving an actual connection between male and female genitals) and (**B**) the cumulative percentage of females that deposited eggs are shown. Since no mating was observed between adultoid females and adult males, the observation of oviposition was only made for the control condition, combining an adult female with an adult male, and the experimental condition, combining an adultoid female with an adultoid male. Statistically significant differences (p) between the control and experimental conditions were found via a log-rank (Mantel–Cox) test and are indicated by asterisks (**** $p < 0.0001$).

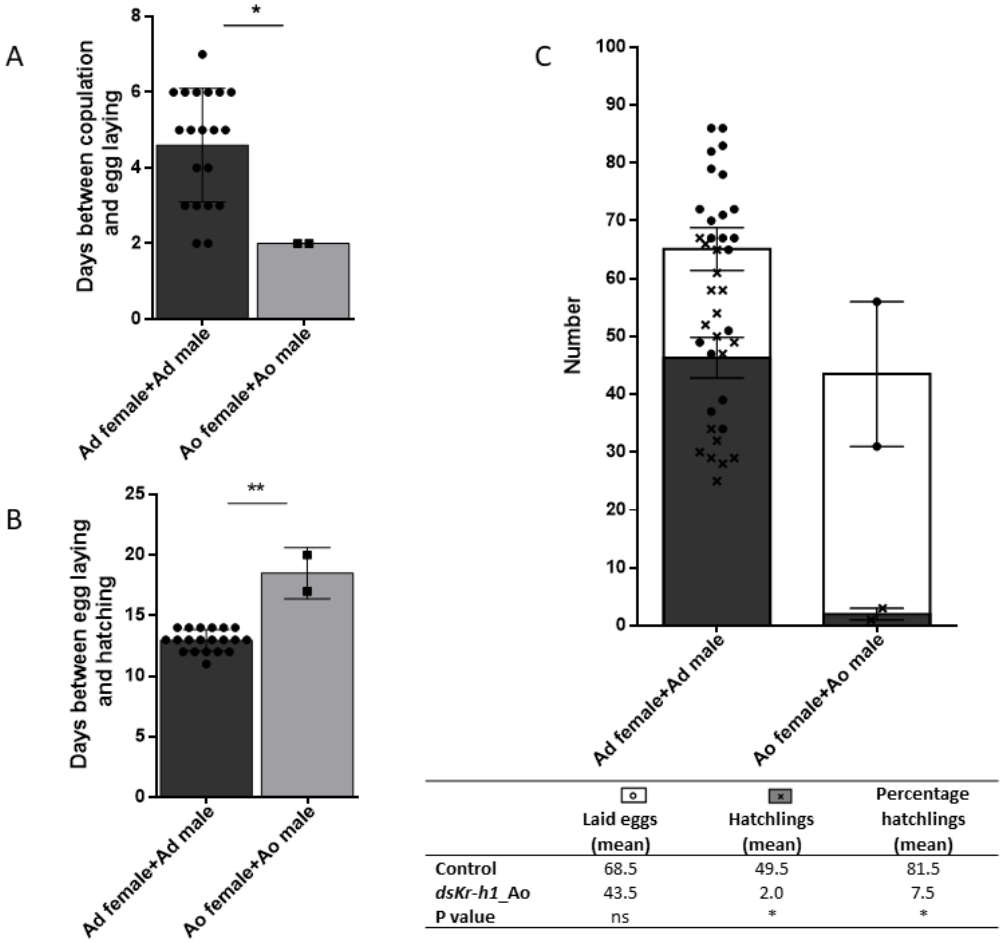

	Laid eggs (mean)	Hatchlings (mean)	Percentage hatchlings (mean)
Control	68.5	49.5	81.5
*dsKr-h1*_Ao	43.5	2.0	7.5
P value	ns	*	*

Figure 5.14: Time between mating and oviposition; incubation period between egg deposition and hatching; fecundity and fertility of adult (*dsGFP* control) and adultoid (*dsLmKr-h1*) *L. migratoria* females. Mating and oviposition were observed for 20 adult (Ad) (each combined with an adult male: 'Ad female + Ad male') and 14 adultoid (Ao) (each combined with an adultoid male: 'Ao female + Ao male') females starting on day 5 of their adult (Ad) or adultoid (Ao) stage. The periods (in number of days) between mating and oviposition (**A**), as well as between egg laying and hatching (**B**), were observed. The data represent mean ± S.E.M. for 20 adult ('Ad female + Ad male') and 2 adultoid ('Ao female + Ao male') females. Statistically significant differences (p) between the two conditions were found via a nonparametric Mann-Whitney test and are indicated by (an) asterisk(s) (* $p < 0.05$; ** $p < 0.01$). (**C**) The number of eggs per egg pod was counted, as well as the number of hatchlings. The data represent mean ± S.E.M. for 20 adult ('Ad female + Ad male') and 2 adultoid ('Ao female + Ao male') females, as well as the individual number of eggs (o) or hatchlings (x) per egg pod. Statistically significant differences (p) between the two conditions were found via a nonparametric Mann-Whitney test and are indicated by an asterisk (* $p < 0.05$).

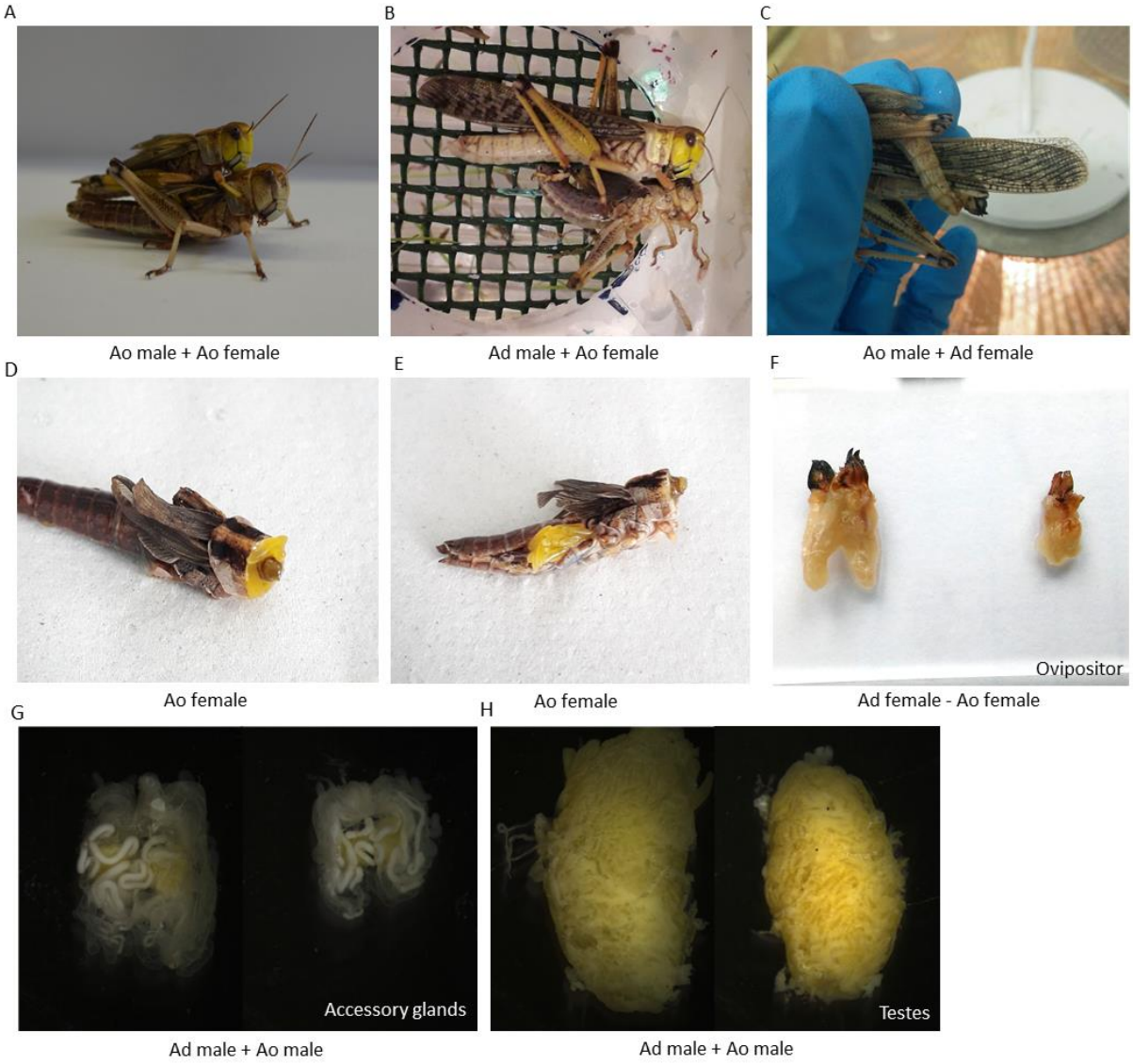

Figure 5.15: Mating and fecundity of adult (*dsGFP*) and adultoid (*dsKr-h1*) *L. migratoria*. The intention to mate as well as the actual connection between male and female genitalia were visually observed between adultoid (Ao) males and adultoid females (**A**), adult (Ad) control males and adultoid females (**B**), and adultoid males and adult control females (**C**). Adultoid females that were not successful in depositing their eggs were dissected. After decapitation (**D**) and making an incision in the abdomen (**E**), fully developed eggs were readily observed. (**F**) Dissected ovipositors from a control adult female (left) and an adultoid female (right). Dissected accessory glands (**G**) and testes (**H**) from a control adult male (left) and an adultoid male (right).

5.4 Discussion

5.4.1 *DsLmKr-h1* injections in fourth nymphal stage induced the developmental transition to adultoids

The migratory locust, *L. migratoria,* is a hemimetabolan insect that normally passes five nymphal stages before the adult, reproductive stage is reached. The final molt is characterized by an incomplete metamorphosis process, which results in development of functional wings and reproductive organs. In this study, a final molt was precociously induced by RNAi-mediated knockdown of *LmKr-h1*, a well-conserved transcription factor acting immediately downstream of the JH receptor Met, during the fourth nymphal stage (Figure 5.3). The adultoid phenotype resulting from this treatment displayed the coloration pattern that is typical for adults. On the other hand, its wings were not fully extended. Similar observations of precocious adult-like phenotypes were made after *Kr-h1* knockdown in several other hemimetabolan insect species, such as *B. germanica*, *R. prolixus*, *G. bimaculatus*, *N. lugens*, *C. lectularius* and *P. apterus* (Gujar and Palli, 2016a; Ishimaru et al., 2019; Konopova et al., 2011; K. L. Li et al., 2018; Lozano and Belles, 2014, 2011; Smykal et al., 2014a; Villalobos-Sambucaro et al., 2015).

Locusts were injected with *dsLmKr-h1* on the day of their molt to the fourth nymphal stage and a second injection was given 3 days later. One day later (N4 D4), a significant downregulation of the *LmKr-h1* transcript level was detected in the fat body (Figure 5.4A). On the day of the adultoid molt (Ao D0), the *LmKr-h1* levels were clearly much higher than in the *dsGFP*-injected (control) N5 condition and resembled the normal adult levels (Ad D0) (Figure 5.4A), suggesting that the effect of the knockdown was temporally restricted to the N4 stage. Similar studies in the common bed bug, *C. lectularius,* and the German cockroach, *B. germanica,* showed similar efficiencies of *Kr-h1* transcript knockdown (Gujar and Palli, 2016a; Lozano and Belles, 2011). The majority (64%) of the *dsLmKr-h1*-injected locusts developed into adultoids (Figure 5.3A and B). The presence of some fifth nymphal and intermediate phenotypes, as also observed by Lozano and Belles (2011) in *B. germanica* upon silencing *Kr-h1*, suggests some inter-individual variation in knockdown efficiency, which may account for the relatively mild reduction in the *LmKr-h1* transcript level that was measured in *dsLmKr-h1*-injected locusts on day 4 in the fourth nymphal stage (Lozano and Belles, 2011). A second injection in *B. germanica* was sufficient to obtain 100% adultoids, but this was not the case in the locusts of this study. The difficulty of obtaining adultoids with full efficiency (100%) was also noticed in the common bed bug, *C. lectularius.* When knocking down *Kr-h1* in the penultimate nymphal stage, only 31% of the dsRNA-injected insects developed precociously into adultoids (Gujar and Palli, 2016a). It is possible that the spatiotemporal characteristics of the RNAi-mediated knockdown influence its developmental outcome. In our study no downregulation of *LmKr-h1* was observed in the ovaries (Figure 5.4C), which can be explained by the previously described inefficient uptake of dsRNA into the follicle cells and oocytes (Ren et al., 2014; Wynant et al., 2012). Remarkably, a significantly increased *LmKr-h1* transcript level was detected in the CA (Figure 5.4B). This suggests the existence of a very dynamic and tissue-dependent regulation of this immediate early

JH response gene, which may explain why its downregulation was not maintained longer and even resulted in a compensatory effect within the CA. Still, the phenotypic effects obtained in this experiment were very obvious and fully in line with the well-established role of Kr-h1 in controlling the developmental timing of metamorphosis.

Expression of *Kr-h1* is known to be controlled by JH activity, downstream of Met, as previously reported for several insect species (Konopova et al., 2011; Lozano and Belles, 2011; Minakuchi et al., 2009, 2008b; Smykal et al., 2014b). Our qRT-PCR measurements indeed show that in *dsGFP*-injected control locusts, the expression of both *LmKr-h1* and *LmMet* in fat body was reduced on the day of molting to the fifth nymphal stage (N5 D0), followed by increased transcript levels of the adult specifier *Lm*E93 on the next time point that was analyzed (N5 D3) (Figure 5.2A, D and G). These temporal profiles are in agreement with the described role of these factors in the control of metamorphosis. Interestingly, for the *dsLmKr-h1*-injected locusts that developed into adultoids, the total duration of the fourth nymphal stage (from N4 D0 until the N4-adultoid transition) was on average two days longer than that of a normal fourth nymphal stage (5 days) and thus similar to that of a normal fifth nymphal stage (7 days) (Figure 5.3C). Moreover, none of the adultoids and only a small fraction of the intermediate phenotypes resulting from the *LmKr-h1* knockdown had any further molts (Figure 5.3D). These observations indicate that the transition process from N4-nymph to adultoid can indeed be considered as a precocious metamorphosis, at which the locusts were reprogrammed to stop increasing their body size and start investing more energy and nutrients in reproduction. Furthermore, clear differences in transcript levels of MEKRE93 pathway components were observed during this time. Normally, the expression levels of the adult specifier gene *E93* only start rising in the final nymphal stage, when JH titers drop and ecdysteroid titers rise, to ensure the final transition to the adult stage (Belles, 2019). A significant rise in *E93* levels was indeed observed on day three (N5 D3) in the control fifth nymphal locusts (Figure 5.1D and E). Therefore, the significantly higher *LmE93* levels that were detected in the *dsLmKr-h1*-injected locusts on day 4 of the fourth nymphal stage (Figure 5.4D and E) can explain the transition of the majority of these locusts into adultoids (Figure 5.3B). Ishimaru et al. (2019) also reported elevated *E93* transcript levels in premature *G. bimaculatus* adults after knocking down *Kr-h1*. A similar observation was made by Lozano and Belles (2011) who described that female fifth nymphal *B. germanica,* treated with *dsKr-h1*, required on average two to three days more to perform the next molt. *LmMet* expression measured in the fat body remained relatively stable on different time points during the fifth nymphal stage of control animals (Figure 5.1G). Similar temporal profiles were observed in *B. germanica*, *N. lugens* and *P. apterus*, with *Met* transcript levels staying relatively stable in nymphal whole body RNA samples, independently of JH titers (Konopova et al., 2011; Lin et al., 2015; Lozano and Belles, 2014; Smykal et al., 2014b). However, in the CA of locusts, the *LmMet* levels appeared to gradually decline over time (Figure 5.1H). Interestingly, in freshly molted adultoids the transcript levels of MEKRE93 pathway components were more similar to the ones observed in adults than

in fifth nymphal control locusts on the day of molting (Figure 5.4), emphasizing that the adult-like properties of the adultoid locusts were also noticeable at the molecular level.

5.4.2 Comparison between adultoid and adult female locusts during their first gonadotropic cycle

In the current study, we mainly focus on the reproductive physiology of the adultoid females and compare this with normal adult female locusts (*dsGFP*-injected control). In this context we also analyzed the transcript levels of several genes involved in hormone synthesis, signal transduction and vitellogenesis. Our data indicate that the adultoid females have the following characteristics:

5.4.2.1 An accelerated ovarian maturation

The adultoid females were characterized by an accelerated entry into the vitellogenic stage of the first gonadotrophic cycle (Figure 5.5). The first gonadotrophic cycle in the ovaries of female locusts can be divided in five stages: (i) an early growth period; (ii) the previtellogenic stage; (iii) the vitellogenic stage; (iv) the choriogenic stage and (v) ovulation and oviposition (Peel and Akam, 2007; Tobe and Pratt, 1975). It is clear from Figure 5.5 that the adultoid females entered the vitellogenic stage several days prior to the adult control locusts. This stage is characterized by patency of the follicular epithelium, allowing the passage of lipids and vitellogenins from the hemolymph to the developing basal oocytes, causing them to grow. Although the basal oocytes in adultoid ovaries were slightly smaller on day four after the final molt, they became much larger than these in adults on the subsequent time points (D8 and D12 in Figure 5.5B; Figure 5.5D versus 5.5N). To further confirm this early incorporation of yolk material, transverse sections of the oocytes were made (Figure 5.5F—L). Whereas in oocytes of adultoid locusts, proteins (blue matrix) and lipid droplets (greyish droplets) were already visible on day 8 after the final molt (Figure 5.5G), it took oocytes of adult locusts approximately four additional days to enter this stage (Figure 5.5L). In addition, some adultoid ovaries had then already entered the second gonadotrophic cycle and also contained resorbing oocytes (Figure 5.5D-E', I-I'). When the eggshell or chorion was formed, the basal oocytes took on a shiny appearance, then ovulation occurred and fully grown oocytes entered the lateral oviducts (Figure 5.5E). Morphological analysis of these oocytes confirmed the presence of a chorion (Figure 5.5J).

5.4.2.2 Associated changes in gene expression profiles in fat body and CA

Vitellogenin synthesis was monitored at the mRNA level on different time points in both adult and adultoid female locusts. When compared to adult females, the fat body of adultoids contained significantly higher levels of both *LmVg1* and *LmVg2* on days eight and twelve after the final molt (D8 and D12 in Figure 5.6). This timing is fully in line with the observed increase in length of the basal oocytes occurring in the adultoid female ovaries (Figure 5.5B). In addition, significantly higher transcript levels of the immediate early JH response

gene *LmKr-h*1 were also detected in fat body of adultoid females compared to control adult females (Figure 5.9A). The importance of JH signaling in regulating female vitellogenesis was previously confirmed in the migratory locust, *L. migratoria*. A study by Song et al. (2014) described reduced *Vg* gene expression in the fat body, lipid accumulation in the primary oocytes, as well as a strong inhibition of oocyte maturation upon silencing *LmMet* and *LmKr-h1*. These observations are corroborated by multiple other studies performed in numerous insect species (Gijbels et al., 2019; Gujar and Palli, 2016b; Guo et al., 2019, 2014; Liu et al., 2016; Ma et al., 2018; Marchal et al., 2014; Naghdi et al., 2016; Parthasarathy et al., 2010; Saiki et al., 2015; Smykal et al., 2014a; Villalobos-Sambucaro et al., 2015; J. L. Wang et al., 2017; Wu et al., 2018). In addition to the higher *LmKr-h1* transcript levels detected in fat body of adultoid females (Figure 5.8A), lower *LmE93* transcript levels were observed (Figure 5.8B), which may refer to the inhibitory effect of Kr-h1 on *E93* expression (Belles, 2019; Mao et al., 2019). *LmE93* expression was extremely low on day 8, when the adultoid females were in full vitellogenesis (D8 in Figure 5.9B). However, in fat body of normal adult females an inverse relationship between *LmKr-h1* and *LmE93* gene expression was not noticeable (Ad D0-D12 in Figure 5.1A and B), which may point at an important difference upstream in the regulation of these genes between adults and adultoids. In the CA, *LmJHAMT* and *LmCYP15A1* expression levels were increased in the adult/adultoid stages, which may refer to the important roles that are played by JH in reproduction (Figure 5.1F and I; Figure 5.8F and I). Moreover, the relative expression level of *LmCYP15A1* was higher on day 8 (Figure 5.9H) in the vitellogenic adultoid females, when compared with the control adult females. Multiple studies also reported on the increased expression of JH biosynthetic enzymes during the gonadotrophic cycle of two different locust species (Gijbels et al., 2019; Song et al., 2014), as well as several other insects (Kinjoh et al., 2007; Marchal et al., 2011b; Mayoral et al., 2009; Minakuchi et al., 2008a; Niwa et al., 2008; Parthasarathy et al., 2010; Sheng et al., 2008). During the maturation of reproductive organs and progression of the first gonadotrophic cycle, JH signaling is also crucial for the induction of polyploidy in the fat body cells, allowing for the massive metabolic conversion of stored energy and nutrients into yolk constituents, such as vitellogenins and lipids, which eventually will be incorporated into the basal oocytes during the vitellogenic phase (Guo et al., 2014; Wu et al., 2018).

5.4.2.3 Accelerated Kr-h1 *and* Halloween *gene expression in the ovary*

In addition to JH, ecdysteroids are playing an important role in the reproductive physiology of female locusts. Ecdysteroid biosynthesis mainly takes place in the follicular cell layer of the developing oocytes (Kappler et al., 1986; Lagueux et al., 1977). In a series of enzymatic reactions involving the *Halloween* genes, the steroid hormone precursor cholesterol is converted to 20E (Gilbert and Warren, 2005). When comparing female adultoids with control adults, significant differences in *Halloween* gene expression were observed on different time points after the final molt (Figure 5.10). In female adultoids, day 8 appeared to be a critical time point when a prominent peak of both *LmSpo* and *LmPhm* expression levels was observed (Figure 5.12A

and B). Where *Spo* is considered to catalyze the rate-limiting step, *Phm* is important in the conversion of ketodiol to ketotriol (Niwa et al., 2004; Ono et al., 2006; Warren et al., 2004). In agreement with the current study (Figure 5.11), Marchal et al. (2011a) also showed that the transcript levels of both *Halloween* genes were low in freshly molted adults and rose during the female reproductive cycle of the desert locust, *S. gregaria*. The observed elevated *LmSpo* and *LmPhm* transcript levels in the ovaries of adultoids on day 8 after their final molt, coinciding with the significantly increased *Kr-h1* levels in the same organs (Figure 5.8C), therefore once again reinforce our observations of an accelerated ovarian maturation in comparison with normal adult migratory locusts (D8 in Figure 5.10B and C). In addition to the accumulation of ecdysteroid conjugates in basal oocytes during vitellogenesis, acting as a source of ecdysteroids during embryonic development, ecdysteroid signaling also plays a role in choriogenesis, involving the heterodimeric nuclear receptor complex consisting of the ecdysone receptor (EcR) and the retinoid-X-receptor (RXR). An RNAi-mediated knockdown of *EcR/RXR* in the desert locust, *S. gregaria,* and the Pacific beetle cockroach, *D. punctata,* resulted in females incapable of initiating choriogenesis; basal oocytes reached their maximal length, after which they were resorbed, thereby affecting ovulation as well (Hult et al., 2015; Lenaerts et al., 2019b). These studies also suggested that EcR and RXR mediate critical ecdysteroid feedback to the CA, essential at the end of vitellogenesis for successful ovulation. In 1993, Belles et al. already suggested the existence of a crosstalk between JH and ecdysteroids in *B. germanica,* since ecdysteroids are responsible for the termination of the gonadotrophic cycle via lowering JH synthesis. In our study, the ovarian *LmEcR* and *LmRXR* transcript levels did not differ significantly on the observed time points during the vitellogenic stage between adult and adultoid female locusts (D8 and D12 in Figure 5.10G and H). Nevertheless, in adultoid ovaries, the *LmEcR* levels significantly increased at day eight, which may refer to the crucial role of ecdysteroid signaling in choriogenesis (Ao D8 in Figure 5.12F). These results can explain the normal appearance of the fully grown oocytes observed in adultoid females (Figure 5.5J).

5.4.2.4 Severe defects in mating and egg laying

None of the adultoid females effectively mated with virgin control males (Figure 5.13A). Since differences in body size and anatomy between adultoid and adult locusts (Figure 5.3A and Figure 5.15B) could have an adverse effect on mating success, adultoid females were also paired with adultoid males (Figure 5.15A). In addition, in this setup, mating was negatively affected when compared to control adult locusts (Figure 5.13A). To verify whether adultoid males were capable of mating, some were also paired with control females, eventually confirming that mating was physically possible (Figure 5.15C). The few adultoid females that were able to mate needed fewer days to deposit their eggs (Figure 5.13B and Figure 5.14A). However, it took the few hatchlings that were produced (7.5%) several days longer to emerge (Figure 5.14B and C). Remarkably, all adultoid females, even if they did not mate, attempted to oviposit, but the unmated ones did not succeed and subsequently died in the coming days. Dissection of their abdomens revealed ovaries full of mature

oocytes, some of them stuck in the oviducts and leaking yolk (Figure 5.15D and E). In *L. migratoria*, mating is known to induce physiological and endocrinological changes in the female resulting in appropriate maturation of the eggs and the subsequent deposition of fertile eggs in a suitable environment (Lange, 2009a). Mating in the kissing bug, *R. prolixus,* triggers the release of a myotropic peptide from the nervous system, resulting in ovulation and oviposition (Davey, 2007). In *Drosophila melanogaster*, the Sex Peptide is present in the seminal fluid and transferred from male to female upon mating; in the female fly, it triggers a recently described neural circuitry that controls egg laying (Wang et al., 2020). Therefore, the incapability of virgin adultoid *L. migratoria* females to oviposit might be due to the absence of such a physiological stimulus induced by mating. In addition, a recent study in the cricket, *G. bimaculatus,* where silencing *Kr-h1* resulted in adultoid females, described the occurrence of an abnormal ovipositor morphology (Ishimaru et al., 2019). Although the ovipositors of the adultoid female locusts had a normal anatomical appearance, their size was smaller when compared to the adult ones (Figure 5.15F). Since the eggs of adultoids had a similar size as the ones produced by adults, it is not unlikely that this may have caused great discomfort during oviposition. Finally, while the number of eggs per egg pod (fecundity) produced by the adultoid females was similar to that of adults, the number of hatchlings (fertility) was severely reduced. The reasons for this low fertility are not fully clear. We observed that adultoid males were eager to mate with an adultoid or adult female and noticed that their testes and accessory glands had a normal adult-like appearance (Figure 5.15G and H). However, we do not know how much sperm was transferred upon mating and how fertile it was. Therefore, the observed hatchlings either developed from fertilized eggs or were generated by parthenogenesis (Bergerard and Seugé, 1959; Pardo et al., 1995). Future dissections of adultoid male testes and adultoid female spermatheca, to verify the presence and transfer of sperm, would probably enable a more comprehensive interpretation of these data. Nevertheless, the fact that some eggs successfully hatched indicates that some adultoids were capable of generating offspring.

5.5 Conclusions

In conclusion, our findings show that the knockdown of *LmKr-h1* in the fourth nymphal stage resulted in an adultoid phenotype characterized by precocious development of adult features, an accelerated ovarian maturation and reduced mating (Figure 5.14). Only the few adultoid females capable of mating were also able to deposit their eggs successfully. Although the fecundity of the adultoid females did not seem to differ from that of control adults, the percentage of hatchlings was much lower.

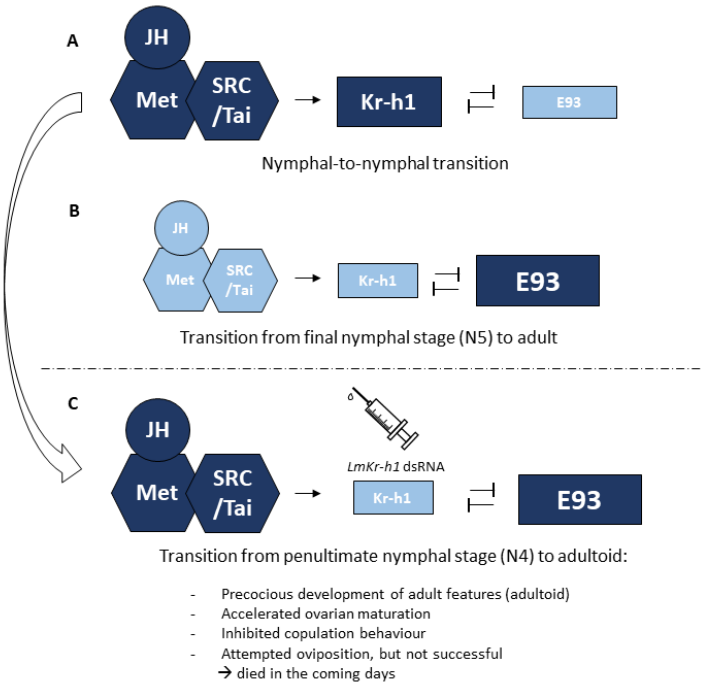

Figure 5.14: The MEKRE93 pathway in hemimetabolan metamorphosis. (A) During a nymphal-to-nymphal transition, JH (through Met/Tai) induces the expression of Kr-h1, a transcription factor which in turn, represses the expression of the adult specifier gene, *E93*. (B) A decline of JH production during the final nymphal stage (N5) interrupts the expression of Kr-h1 allowing a strong induction of E93 by ecdysone signalling, triggering the transition to adult (Belles and Santos, 2014). (C) Injection of dsRNA targeting *LmKr-h1* in penultimate nymphal *L. migratoria* results in adultoid stages.

Chapter 6: Juvenile hormone receptor Met is essential for ovarian maturation in *S. gregaria*

This chapter was based on:

Gijbels, M., Lenaerts, C., Vanden Broeck, J. and Marchal, E. (2019). Juvenile hormone receptor Met is essential for ovarian maturation in the desert locust, *Schistocerca gregaria*. Sci. Rep. 9, 10797.

6.1 Introduction

The classic insect hormones, juvenile hormones (JH) and ecdysteroids, play critical roles in insect postembryonic development. In juvenile insects ecdysteroids trigger the moulting process, while JH will determine the nature of the moult (Riddiford, 2012). These lipophilic hormones, together with nutritional cues, as well as signalling mechanisms directed by regulatory peptides, such as insulin-related peptides (IRP) and neuroparsins (NPs) also control the reproductive physiology of adult insects. However, the exact interplay between hormones and nutrition in this regulation may distinctly differ depending on the insect's specific feeding habits and reproductive strategies (Huybrechts, 2018; Roy et al., 2018). The role of JH as a master regulating gonadotropin in insect female reproduction is established in phylogenetically basal species, such as orthopterans (the insect order to which locusts belong), while ecdysteroids seem to have taken over this leading role in some lepidopteran and most dipteran species (Raikhel et al., 2005; Roy et al., 2018). In female locusts, JH, synthesized in the corpora allata (CA, part of the retrocerebral complex), stimulates vitellogenin (Vg) production in the fat body by activating *Vg* gene transcription (Wyatt et al., 1996). Furthermore, JH also binds membrane receptor sites in the ovarian follicular epithelium to initiate events that cause cells to shrink (Davey et al., 1993; Jing et al., 2018; Sevala, V.L. & Davey, 1989; Sevala et al., 1995; Sevale and Davey, 1993). This process, called patency, allows Vgs, which are mainly produced by the fat body and then released into the haemolymph, to be taken up by the developing oocyte. Recent ligature experiments in both *Locusta migratoria* and *S. gregaria* have shown the presence of an oviduct derived Patency Inducing Factor (PIF) involved in the initiation of patency in the terminal follicle via the pedicel. The action of PIF, for which the chemical structure is currently unknown, is clearly boosted by JH (Seidelmann et al., 2016). In adult female locusts, ecdysteroids produced in the ovarian follicular cell layer appear to induce meiotic re-initiation in the oocyte (Lanot et al., 1987). In addition, they are incorporated as conjugates into the eggs where they act as a source of ecdysteroids during embryogenesis (Isaac and Rees, 1984). These conjugates can bind vitellins, thereby preventing their leakage into the haemolymph (Isaac and Rees, 1984; Lagueux et al., 1981; Tawfik et al., 1999). Furthermore, ecdysteroid signalling via the nuclear receptor complex consisting of the ecdysone receptor and the retinoid-X-receptor/ultraspiracle, plays a role in choriogenesis in adult female desert locusts (Lenaerts et al., 2019a).

In contrast to the molecular basis of ecdysteroid action (as was reviewed by Roy et al. (2018)), the JH signalling pathway was only recently described with the characterization of the basic-helix-loop-helix (bHLH)/Per-Arnt-Sim (PAS) transcription factor, Methoprene-tolerant (Met). First described in *Drosophila melanogaster* as a factor involved in the resistance to the commercial Insect Growth Regulator (IGR) Methoprene (Wilson and Fabian, 1986), the affinity binding study by Charles et al. (2011) ultimately confirmed the function of Met as JH receptor. Upon JH binding, the Met-Met homodimer dissociates and becomes accessible to other bHLH-PAS proteins such as Taiman, a steroid receptor co-activator, which

induces the expression of JH response genes (Godlewski et al., 2006; Song et al., 2014). RNA interference (RNAi) studies in the red flour beetle, *Tribolium castaneum*, the German cockroach, *Blattella germanica*, and the fire bug, *Pyrrhocoris apterus* have demonstrated the importance of Met and its downstream transcription factor krüppel-homolog 1 (Kr-h1) in the anti-metamorphic effects of JH (Konopova et al., 2011; Konopova and Jindra, 2007; Lozano and Belles, 2014; Smykal et al., 2014a; Villalobos-Sambucaro et al., 2015). Moreover, RNAi studies in multiple insect species have confirmed the conserved function of Met and Kr-h1 as key players in JH signalling in adults as well. The pleiotropic JH acts via Met and Kr-h1 to control different processes in adults, such as vitellogenesis in the fat body, lipid accumulation in the primary oocyte, regulation of mating and sex pheromone production (Bilen et al., 2013; Gujar and Palli, 2016b; Lin et al., 2015; Liu et al., 2016; Ma et al., 2018; Marchal et al., 2014; Naghdi et al., 2016; Parthasarathy et al., 2010; Saiki et al., 2015; Sheng et al., 2011; Smykal et al., 2014a; J. L. Wang et al., 2017; X. Wang et al., 2017; Zou et al., 2013). Importantly, in another locust species, the migratory locust, *L. migratoria*, the molecular basis of JH action in reproduction is well established (Song et al., 2014; Z. Wang et al., 2017). The RNAi-mediated knockdown of *Met* and *Kr-h1* prevents *Vg* expression in the fat body, ovarian development, lipid accumulation and patency in the oocyte. Several molecular players involved in fat body polyploidy, DNA replication and apoptosis, as well as in the folding of Vg proteins and patency have since then been identified (Guo et al., 2014; Luo et al., 2017; Z. Wu et al., 2016). However the interplay with other hormonal pathways and nutritional signalling in locust species remains unknown.

Our study focuses on the role of Met, the nuclear receptor that mediates JH signalling, in the female reproductive physiology of the desert locust, Schistocerca gregaria. The insulin signalling pathway (ISP), sensing nutrient status, plays a crucial role in the trade-off between reproduction and survival in insects, positively controlling vitellogenesis and oocyte growth (Lenaerts et al., 2019c; Mirth et al., 2019). Whether or not the ISP acts via a mediator action of ecdysteroids and JH remains ambiguous as evidenced by contradictory reports in different insect orders. Most likely, IRP, ecdysteroids and JH are involved in an intricate cross-talk, in which the insect's nutritional status is a crucial determinant of this cross-talk's output. For a more in depth summary on this topic, the reader is referred to Badisco et al. (2013), Van Wielendaele et al. (2013) and Roy et al. (2018). In the desert locust, *S. gregaria,* silencing *SgIRP* negatively affects *Vg* transcript levels and oocyte growth (Badisco et al., 2011). Since JH initiates vitellogenesis in this species, these earlier results from our lab suggest communication between both pathways. This same study showed that knockdown of the *S. gregaria NPs* (*SgNPs*) increases *SgVg* transcription, resulting in bigger oocytes. This finding was in line with the initial discovery of the first locust NP, a peptide purified from the pars intercerebralis-corpora cardiaca (CC) neurohaemal complex, which was shown to act as an anti-gonadotrophic factor, contrary to the effects of JH (Badisco et al., 2007; Girardie et al., 1998, 1989). Locust NPs belong to a conserved family of arthropod peptides, but they were also reported to share sequence similarity with the binding region of vertebrate insulin-like growth factor binding proteins (IGFBP) (Badisco

et al., 2007) and *Sg*NP4 was shown to be capable of interacting with *Sg*IRP *in vitro* (Badisco et al., 2008). Using RNAi, we demonstrate that the JH receptor Met is crucial for the initiation of ovarian maturation and vitellogenesis, and that its key role is situated within a complex hormonal network involved in the control of reproduction in *S. gregaria*.

6.2 Materials and methods

6.2.1 Rearing of animals

The desert locusts, *S. gregaria*, were reared under crowded conditions as previously described in §4.2.1. Sand/turf pots, into which eggs were deposited by mated females, were set apart once a week in clean cages.

6.2.2 Tissue collection

The tissues of interest were dissected as previously described in §4.2.2. For the tissue and temporal expression profile of the genes of interest, tissues were collected in three pools of ten animals each. Tissues for the RNAi experiment were collected in four pools consisting of five animals each. The collected tissues were used in an RNA extraction protocol or stored at -80 °C until further processing.

6.2.3 RNA extraction and cDNA synthesis

Fat body, ovaries, muscles and midgut of female adult locusts as well as the male reproductive system (testes + AGs) were pooled in MagNA Lyser Green Beads Tubes (Roche) and homogenized using a MagNA Lyser instrument (20 s, 5000 rpm; Roche). Subsequently, total RNA was extracted using the RNeasy Lipid Tissue Kit (Qiagen) according to the manufacturer's protocol as described in §3.2.3.1. To prevent genomic DNA contamination, an on-column DNase digestion (RNase-free DNase set, Qiagen) was performed. Total RNA of the small sized tissues (CA/CC complex, PGs and suboesophageal ganglion (SOG)) was extracted using the RNAqueous-Micro Kit (Ambion) according to the manufacturer's protocol, including the optional DNase step. Quality and concentration of the resulting RNA samples was measured using a Nanodrop spectrophotometer (Nanodrop ND-1000, Thermo Fisher Scientific Inc.). For each RNA sample, equal amounts of RNA (1000 ng for brain, fat body, ovaries, muscles, midgut, testes and AGs and 200 ng for PGs, CA/CC complex and SOG) were transcribed in subsequent cDNA synthesis using a mix of random hexamers and oligo(dT) primers according to the manufacturer's protocol (PrimeScript™ RT Reagent Kit, TaKaRa, Invitrogen Life Technologies). The obtained cDNA was diluted ten-fold with Milli-Q water (Millipore).

6.2.4 Quantitative real-time PCR

Prior to quantitative real-time PCR (qRT-PCR) transcript profiling, optimal housekeeping genes were selected using geNorm software (Vandesompele et al., 2002). Therefore, several previously described housekeeping genes (Van Hiel et al., 2009) were tested for their stability in the designed experiment and β-actin and EF1α

appeared to be most stable in the studied samples. Primer Express software (Applied Biosystems) was used to design qRT-PCR primers for the different target genes (Table 6.1). Subsequent primer validation and qRT-PCR reactions were performed as previously described in §2.2.5.

Table 6.1: Oligonucleotide sequences of primers used for qRT-PCR.

Reference/ target genes	Forward primer	Reverse primer
SgAct	5'- AATTACCATTGGTAACGAGCGATT -3'	5'- TGCTTCCATACCCAGGAATGA -3'
SgEF1α	5'- GATGCTCCAGGCCACAGAGA -3'	5'- TGCACAGTCGGCCTGTGAT -3'
SgMet	5'- GGTGCCTGAAGAGGAAGAAA -3'	5'- ATGGAGGTGATGAAGGAGAAAG -3'
SgKr-h1	5'- CTCCAAGACGTTCATCCAGAG -3'	5'- TGCTTGGAGCAGGTGAAG -3'
SgIRP	5'- CCGTGGCAACTACAACACCAT -3'	5'- TCCGCGTCCGACACATCT -3'
SgNP3	5'- GCGGAATCGGCATGGA -3'	5'- TCACAGAGCAACCGGAACATT -3'
SgNP4	5'- TGGCGACTCTCCAGTGCTT -3'	5'- TGACACATTCATTCCTCTTCTGACA -3'
SgVg1	5'- CCGCTGAACATCACTGCAAT -3'	5'- ACTTGGGCCAAATGGATGAG -3'
SgVg2	5'- GCTACCCGCAATCTGTAAAATACA -3'	5'- CGACTGTGAAAGGGCATTGA -3'
SgCYP15A1	5'- AAAGCAACTTCATCATTCACAGATG -3'	5'- CAGAGCCAGCCATGAACAAA -3'
SgJHAMT	5'- CGGAGCAAAGGCAAGCA -3'	5'- CCACTTCACCGCCTGGTTT -3'
SgSpo	5'- CAACATCTTCACCAGCTACATGTG -3'	5'- GGGTCGTCGTAGTCGAAGGA -3'
SgPhm	5'- CGCAGAGCCCGGACAAC -3'	5'- CGAACATGTCGGCCATGA -3'
SgShd	5'- CCGCCGTCATTGACTTCATA -3'	5'- GTGAGCTCCCAAGCGTGG -3'
SgVKR	5'- GCATCTTGGCATTGATTTGCTA -3'	5'- GGAATCTCCCATTTGTCAAGAGTT -3'

Abbreviations: *Sg = Schistocerca gregaria*, *Act = β-actin*; *EF1α = Elongation factor 1α*; *Met = Methoprene-tolerant*; *Kr-h1 = Krüppel-homolog 1*; *IRP = Insulin-related peptide*; *NP = Neuroparsin*; *Vg = Vitellogenin*; *CYP15A1 = Cytochrome P450 enzyme 15A1 (methyl farnesoate epoxidase)*; *JHAMT = Juvenile hormone acid methyltransferase*; *Spo = Spook*; *Phm = Phantom*; *Shd = Shade*; *VKR = Venus Kinase Receptor.*

All qRT-PCR results were normalized to both the *β-actin* and *EF1α* transcript levels and calculated relative to the transcript level in a calibrator sample according to the comparative Ct method ($\Delta\Delta$Ct) (Vandesompele et al., 2002). qRT-PCR was used to determine the tissue and temporal distributions of the genes of interest in the adult stage. Therefore, cDNA samples were used from adult female locusts, except for the male AGs and testes. Moreover, statistically significant differences between the *dsSgMet* injected and control adult female locusts were found via a t-test on the log transformed data (with or without two-sided Welch's correction) using GraphPad Prism 6 (GraphPad Software Inc.). Correlation coefficients between temporal expression profiles of the genes of interest were found via a Pearson correlation calculation using GraphPad Prism 6 (GraphPad Software Inc.).

6.2.5 RNA interference experiments

DsRNA constructs were prepared using Ambion's MEGAScript RNAi kit following the manufacturer's protocol and as previously described by Lenaerts et al. (2017). In short, a linear transcript with 5' T7 promotor sequences was used in a high yield RNA transcription reaction. Linear transcripts for the targets of interest were PCR amplified using REDTaq DNA polymerase (Sigma), *S. gregaria* fat body cDNA and the primers given in Table 6.2. The amplicons were sequenced to confirm target specificity and used in a high-yield RNA

transcription reaction using T7 RNA polymerase. ssRNA and DNA were further removed in a nuclease digestion step. The resulting dsRNA was analysed on gel and using the Nanodrop spectrophotometer for integrity, quality and concentration.

Table 6.2: Oligonucleotide sequences of primers used for dsRNA synthesis. Bases indicated in 'bold' represent the T7 promotor sequences used in the preparation of dsRNA constructs.

RNAi constructs	F-primer	R-primer
SgMet	5'- **TAATACGACTCACTATAGGGAGA** AATGAGCCGTTTGGCAGTTCCAC -3'	5'- **TAATACGACTCACTATAGGGAGA** GGCGGTGCAGCACTCATAGC -3'
SgMet2	5'- **TAATACGACTCACTATAGGGAGA** GCTATGAGTGCTGCACCGCC -3'	5'- **TAATACGACTCACTATAGGGAGA** AAGAGGCAGGCCACTAGGTT -3'
GFP	5'-**TAATACGACTCACTATAGGGAGA** AAGGTGATGCTACATACGGAA -3'	5'-**TAATACGACTCACTATAGGGAGA** ATCCCAGCAGCAGTTACAAAC-3'

Abbreviations: *Sg = Schistocerca gregaria*, *Met = Methoprene-tolerant*; *GFP = Green fluorescent peptide.*

Newly moulted adult female locusts, synchronized on the day of ecdysis, were injected with 8 µl dsRNA against *SgMet* (500 ng dsRNA/locust, diluted in *S. gregaria* ringer). A second and third boost injection was given on days four and eight after final moult to ensure a lasting knockdown of target gene mRNA levels. A second group of control locusts was injected with dsRNA against *GFP* following the same injection scheme. From previous observations of our *S. gregaria* colony, it is known that female adults are fully in the vitellogenic stage of oocyte maturation 12 days after their final moult. Therefore, all the tissues and samples of interest were dissected and collected on this day. In a follow-up experiment, the same injection scheme was followed and copulation behaviour and oviposition were observed. Starting on day 8, the female locusts were transferred to individual cages, supplied with oats and fed daily with fresh cabbage. On day 10 of the females' adult life, one sexually mature virgin male was introduced into the separate cages and mating behaviour and copulation (actual connection between male and female genitalia) was registered. If no copulation was observed within two hours of the male's introduction, the male was removed and another mating was attempted the following day with another virgin male. After mating, pots filled with a humid sand/turf mixture were supplied to the females to allow oviposition. These pots were checked daily for egg pods. Statistically significant differences between the two conditions were found via a log-rank (Mantel-Cox) test using GraphPad Prism 6 (GraphPad Software Inc.).

6.2.6 Measurement of oocyte length

Terminal oocytes, *i.e.* oocytes at the base of the ovarioles, were carefully removed from the dissected ovaries and their length was measured using millimetre graph paper. Statistically significant differences between the *dsSgMet* injected and control adult female locusts were found via a nonparametric Mann-Whitney test using GraphPad Prism 6 (GraphPad Software Inc.).

6.2.7 Microscopy and histological analysis

Images of the dissected ovaries and ovarioles as well as of the oocyte sections of *dsSgMet* and *dsGFP* (*GFP* dsRNA) treated animals were made as previously described by Lenaerts et al. (2017).

6.2.8 Ecdysteroid measurements using an enzyme immunoassay

Female locusts were pierced behind the hind leg on the dorsal side allowing haemolymph to flow out. 10 µl of haemolymph was collected from each adult female using a glass capillary tube, immediately transferred to 90 µl of 100 % ethanol and stored at -20 °C until further processing as described in §3.2.10.

One ovarium of each female locust was dissected and transferred to 1 ml of 100 % ethanol after which it was stored at -20 °C until further processing. These ovarium samples were homogenized using a bar sonicator and subsequently for 10 min at 60 °C. After centrifugation at 10 000 g (10 min), the supernatants were transferred to a fresh Eppendorf tube and the remaining pellets were re-extracted twice by adding 1 ml of 100 % ethanol. Combined extracts were dried in a SpeedVac concentrator and redissolved in 1 ml of 70 % ethanol and 1 ml of 100 % hexane in order to remove the apolar lipids and as such obtain optimal EIA measurements. Both 'free' and total ecdysteroid levels were determined where the 'free' ecdysteroids are non-conjugated. The total ecdysteroid levels were determined after enzymatic conversion of the conjugated ecdysteroids into 'free' ecdysteroids.

Ecdysteroid titers in *S. gregaria* haemolymph and ovaries were measured using an EIA, modified from Porcheron et al. (1989) and discussed by Pascual et al. (1995) and Lafont et al. (2012). In brief a peroxidase conjugate of 20E is used as tracer together with rabbit L2 polyclonal antibodies against ecdysteroids. Both serum and tracer were a kind gift by Prof. J.P. Delbecque (Université de Bordeaux, France).

The resulting absorbance values were compared to the calibration curve obtained with 20E as a standard. Since the data were normally distributed upon log transformation, a t-test (with or without two-sided Welch's correction) was performed using GraphPad Prism 6 (GraphPad Software Inc.) to test for statistically significant differences between the data.

6.3 Results and discussion

6.3.1 Description of the relative transcript levels of the genes of interest

SgMet (accession number: MK855050) shows a wide tissue distribution profile. Its expression in 10-day-old adult locusts is mainly observed in the male accessory glands (AGs), CA, fat body, prothoracic glands (PGs) and (flight) muscles (Fig. 6.1). *SgMet* transcript levels remain relatively stable in the fat body of adult female locusts throughout the first gonadotrophic cycle (Fig. 6.2A), a situation which is similar to what was reported on the expression of *Met* during the reproductive cycle of the pacific beetle cockroach, *Diploptera punctata* and the German cockroach, *B. germanica* (Marchal et al., 2014; Naghdi et al., 2016). Also the relative *Met* mRNA levels measured in the complete body of the cotton bollworm, *Helicoverpa armigera,* and the red flour beetle, *Tribolium castaneum,* remain stable during adult female development (Ma et al., 2018; Parthasarathy et al., 2010). On the other hand, the temporal profile of the relative mRNA levels of the downstream transcription factor *SgKr-h1* correlate well with the transcript levels of two *Vg* genes (Fig. 6.2A). Since *Sg*Kr-h1 is a transcription factor acting directly downstream of the JH receptor Met, *SgKr-h1* transcript levels can be considered as a measure for Met-mediated JH signalling activity, as was previously described for *B. germanica*, *D. melanogaster* and *T. castaneum* (Lozano and Belles, 2011; Minakuchi et al., 2009, 2008b). The *SgVg* developmental profile shows a clear increasing trend which starts on day 6, when the basal oocytes enter their vitellogenic stage of maturation, and continues to increase until day 16, when these oocytes almost reach their maximal length. The population of animals from which these samples were taken, completed their first gonadotrophic cycle with oviposition around day 18 (Fig. 6.2B).

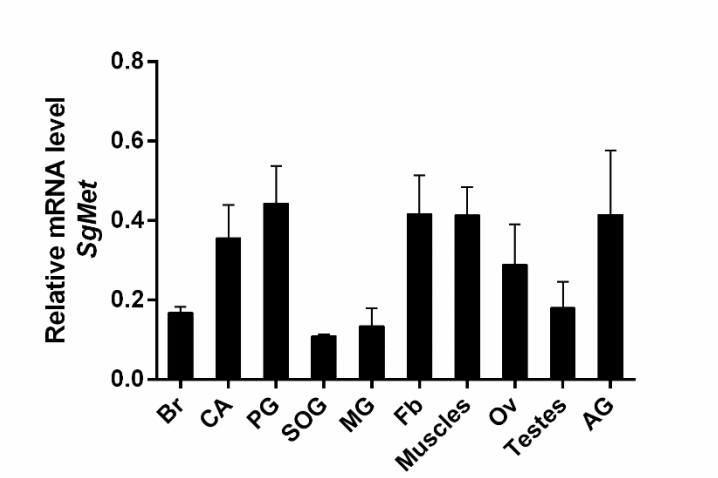

Figure 6.1: **Tissue distribution profile of the relative transcript levels of *SgMet***. Tissues were dissected from 10-day-old adult female locusts, except for the male gonads and accessory glands. The data represent mean ± S.E.M. of three independent pools of ten animals, run in duplicate and normalized to *β-actin* and *EF1α* transcript levels. Abbreviations X-axis: Br = Brain; CA = Corpora allata; PG = Prothoracic glands; SOG = Suboesophageal ganglion; MG = Midgut; Fb = Fat body; Ov = Ovaries; AG = Accessory glands.

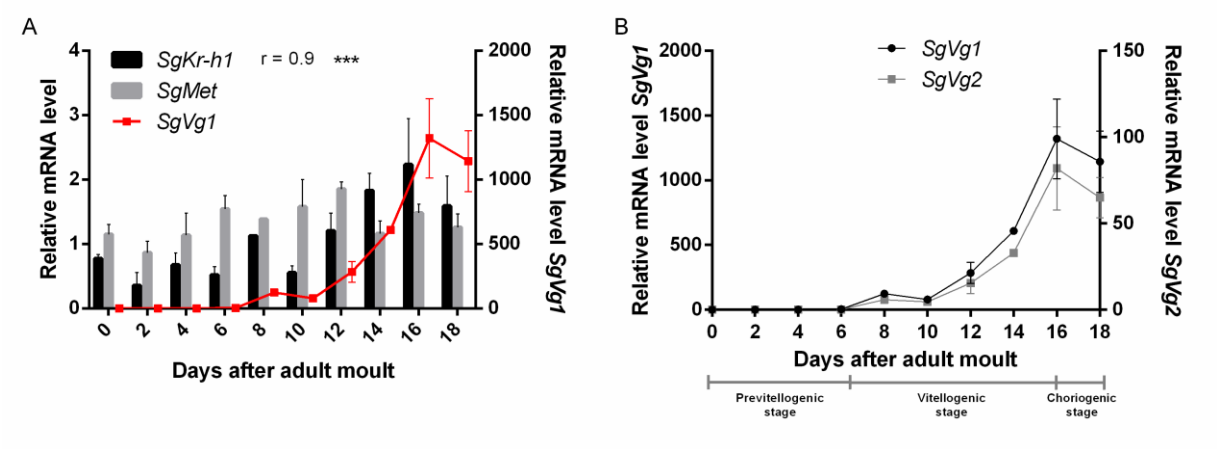

Figure 6.2: Relative transcript levels of *SgMet*, *SgKr-h1* and *SgVgs* in the fat body throughout the first gonadotrophic cycle. (A) *SgMet* + *SgKr-h1* and (B) *SgVg1* + *SgVg2* relative transcript levels were determined in the fat body of adult females throughout the first gonadotropic cycle (day 0 until day 18). (B) The different stages in which the first gonadotrophic cycle can be divided are included as well. *SgVg1* mRNA are given in A), similar temporal profiles for both *SgVg1* and *SgVg2* mRNA levels were observed as shown in B). The data represent mean ± S.E.M. of three independent pools of ten animals, run in duplicate and normalized to *β-actin* and *EF1α* transcript levels. The correlation coefficient (r) between the measurements was found via a Pearson correlation calculation. P-values are indicated by asterisks (*** = $p < 0.001$).

6.3.2 Knockdown of the JH receptor *Met* affects expression of the downstream signalling component *Kr-h1* and of JH biosynthetic enzymes

In order to verify the reproducibility of the results obtained, and to eliminate the possibility of off-target effects, two separate *dsSgMet* (*SgMet* dsRNA) constructs were designed and tested in the same experimental setup, which resulted in similar phenotypic observations.

The knockdown efficiency of the systemic RNAi of *SgMet* was assessed in different tissues on day 12 after adult eclosion (Fig. 6.3). A significant downregulation was measured in the CA/CC complex (61 %) and fat body (51 %). However, *SgMet* levels were not downregulated in the ovaries. This can be explained by the previously described inefficient uptake of dsRNA into the follicle cells and oocytes of the desert locust (Ren et al., 2014; Wynant et al., 2012). In both the CA/CC complexes and the fat body, relative mRNA levels of *SgKr-h1* were shown to be significantly reduced with 88 % and 73 % respectively, upon silencing *SgMet* (Fig. 6.4A, B). Relative *SgKr-h1* mRNA levels were not affected in the ovaries as *SgMet* was not effectively silenced in this tissue (Fig. 6.4C). These findings confirm the transcription factor *SgKr-h1* to be situated downstream of *SgMet*.

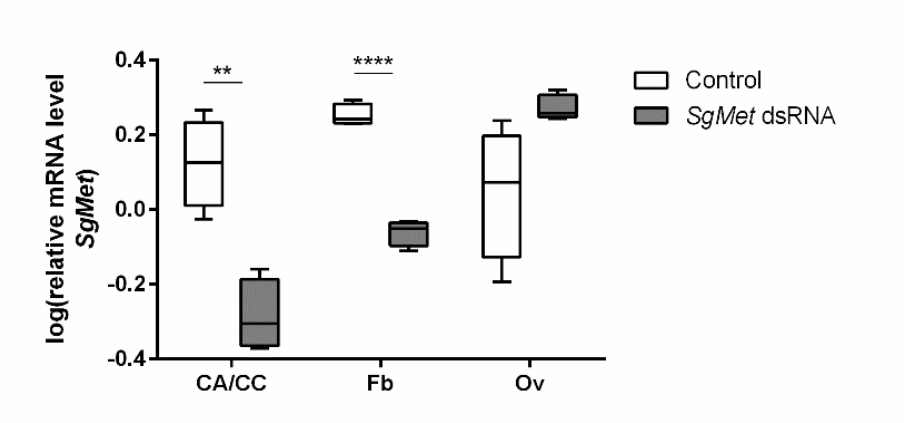

Figure 6.3: Knockdown efficiency of *SgMet* dsRNA injections. The knockdown efficiency of *SgMet* dsRNA injections was assessed in three different tissues on day 12 after adult eclosion, *i.e.* CA/CC complex, fat body and ovaries. The data (log transformed) are shown as box plots (min to max) of four independent pools of five animals, run in duplicate and normalized to *β-actin* and *EF1α* transcript levels. Statistical significant differences between the measurements were found via a t-test (with or without two-sided Welch's correction) and are indicated by asterisks (** = p < 0.01; **** = p < 0.0001).

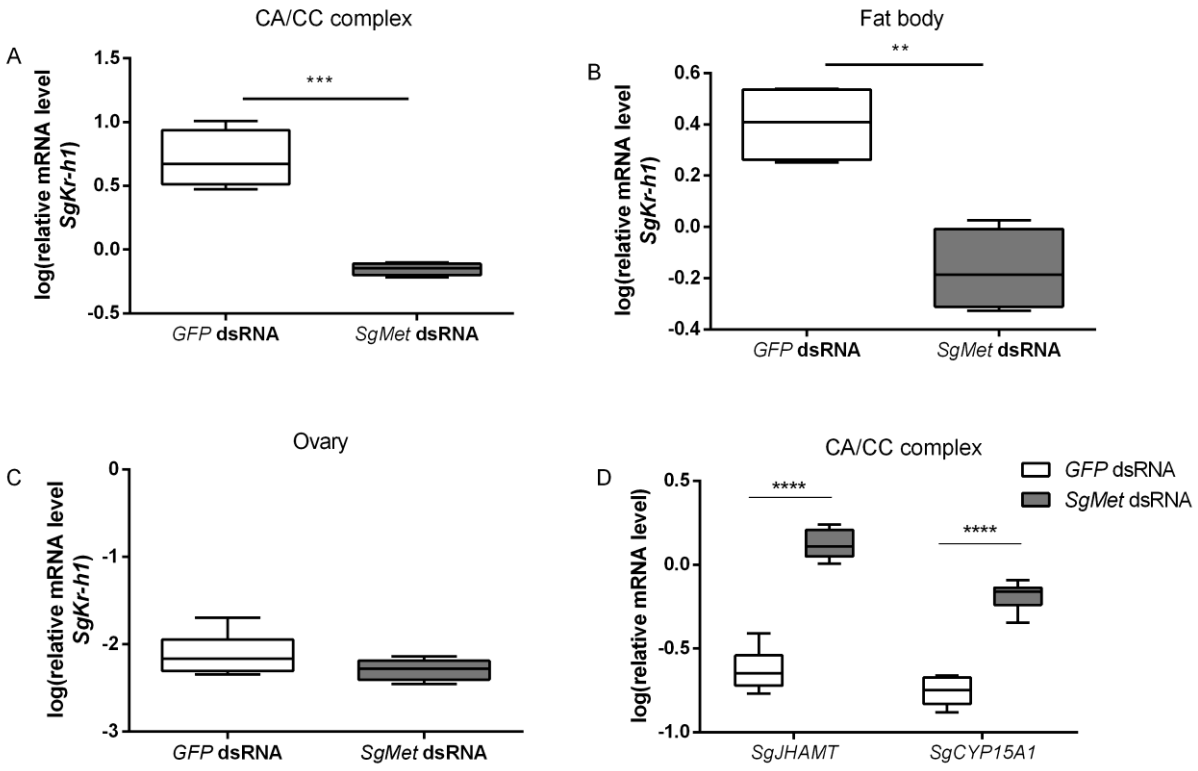

Figure 6.4: Relative transcript levels of *SgKr-h1* and two JH synthesis genes upon *dsSgMet* injections. Relative *SgKr-h1* transcript levels were measured in (A) the CA/CC complex, (B) the fat body and (C) the ovaries of 12-day-old *dsSgMet* or *dsGFP* injected adult female locusts. (D) Relative *SgJHAMT* and *SgCYP15A1* transcript levels were measured in the CA/CC complex as well. The data (log transformed) are shown as box plots (min to max) of four independent pools of five animals, run in duplicate and normalized to *β-actin* and *EF1α* transcript levels. Statistically significant differences (p) between the measurements were found, after a log transformation, via a t-test (with or without two-sided Welch's correction) and are indicated by asterisks (** = p < 0.01; *** = p < 0.001**** = p < 0.0001).

The effect of silencing *SgMet* was also studied in the CA, the site of JH biosynthesis. Previous work already characterized the genes encoding the enzymes catalysing the penultimate and ultimate steps in the JH biosynthetic pathway of the desert locust (Marchal et al., 2011b). Juvenile hormone acid methyl transferase (JHAMT) methylates farnesoic acid to methylfarnesoate (MF) and is known to act as the rate-limiting enzyme in JH biosynthesis (Huang et al., 2015; Marchal et al., 2011b; Mayoral et al., 2009; Shinoda and Itoyama, 2003). The ultimate step in the pathway is catalysed by the cytochrome P450 enzyme CYP15A1 which epoxidizes MF to the active hormone, JHIII. Our current results show that silencing the JH receptor causes upregulation of the transcripts that code for the JH biosynthetic enzymes, *SgJHAMT* and *SgCYP15A1* (Fig. 6.4D), by 550 % and 370 %, respectively. Upon dissection of the CA, it also became apparent that silencing *SgMet* resulted in larger sized CA, again suggesting an increase in activity of these JH producing glands (Fig. 6.5). Our data are in accordance with a recent study in the linden bug, *P. apterus*, where a rise in the circulating JH levels was observed upon silencing *Met* (Smykal et al., 2014a). It can thus be hypothesized that in the CA *Sg*Met acts as a JH sensor involved in a negative feedback loop that keeps JH biosynthesis and CA activity under control, a homeostatic mechanism similar to what is often observed in endocrine gland regulation (Hejnikova et al., 2016).

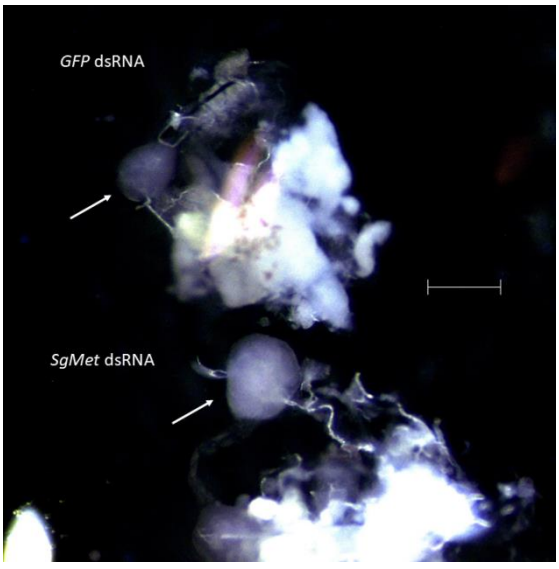

Figure 6.5: **Comparing gland sizes of dissected CA between control and experimental adult female locusts.** The CA/CC complex of 12-day-old control and *SgMet* dsRNA injected female locusts was dissected where after CA gland sizes (indicated by an arrow) were compared. Scale bar = 1 mm.

6.3.3 *SgMet* is crucial for initiating ovarian maturation, vitellogenesis and reproductive behavior

It should be noted that the locust reproductive cycle is strongly determined by environmental factors, which can cause variation in the exact timing. The first gonadotrophic cycle is therefore usually divided in different stages instead of exact time periods: i) an early growth period during which the oocytes only reach a length of 0.8-0.9 mm; ii) the previtellogenic stage, during which oocytes grow until they reach a length of 1.8 mm;

iii) the vitellogenic stage starting from 1.8 mm, characterized by patency, the shrinkage of the follicular epithelial cells, allowing passage of lipids and vitellogenin from the haemolymph into the developing oocytes, causing oocytes to grow until they reach about 7.5 mm; iv) egg shell formation during the choriogenic stage and v) ovulation and oviposition (Peel and Akam, 2007; Tobe and Pratt, 1975). It is clear from Figure 6.6J that the *SgMet* knockdown animals never enter the (pre)vitellogenic stage as the oocytes do not appear to have increased in length after 12 days in the adult stage when compared to newly moulted adult females. As such, it became evident that ovarian maturation was arrested by silencing *SgMet* (Fig. 6.6A-F). The ovaries of 12-day-old *dsSgMet* injected locusts remained arrested in a very immature, previtellogenic stage (Fig. 6.6A, B), still resembling the ovaries of freshly moulted control locusts (D0) (Fig. 6.6E, F). To further verify whether or not yolk materials were incorporated, transverse sections of oocytes were made (Fig. 6.6G, H). In oocytes of *dsGFP* injected control locusts, Vgs (blue matrix) as well as lipid droplets (greyish droplets) were visible. The accumulation of Vgs and lipid droplets was not observed in the *SgMet* knockdown animals. Moreover, when studying these sections, no patency of the follicular cell layer was observed even though higher JH levels might circulate in the haemolymph (due to the higher relative mRNA levels of *JHAMT* and *CYP15A1*; Fig. 6.4D). Our observations are similar to the lack of patency observed in both *L. migratoria* and *D. punctata* treated with *dsMet* which could not be rescued by treatment with methoprene (Marchal et al., 2014; Song et al., 2014). Patency was long thought to be initiated by JH acting on membrane receptors in the ovary (Davey et al., 1993; Jing et al., 2018; Sevala, V.L. & Davey, 1989; Sevala et al., 1995; Sevale and Davey, 1993). The recent report by Seidelmann et al. (2016) suggests that PIF, an as yet unidentified oviduct derived factor, is responsible for the initiation of patency in locusts and that its action is boosted by JH. As no Vg was observable in oocytes of locusts where *SgMet* was knocked down, we analysed *SgVg* mRNA levels in fat body samples from *dsSgMet* versus *dsGFP* injected locusts on day 12 of the first gonadotrophic cycle (Fig. 6.6I). Silencing *SgMet* very obviously resulted in much lower relative *Vg* mRNA levels for both *SgVg1* and *SgVg2*, for which transcript levels during the first gonadotrophic cycle of wild type locusts are shown in Figure 6.1C. In control knockdown animals, a large variation in basal oocyte lengths exists. Some of the control locusts were already in their second gonadotrophic cycle, characterised by orange lesions at the base of the new basal oocyte. In the *SgMet* knockdown locusts, it was evident that ovarian maturation was arrested. Oocytes longer than 1.5 mm were never observed, suggesting oocyte maturation could not be completed, even after 12 days in the adult stage (Fig. 6.6J). Moreover, dissection of the *SgMet* females at the end of the copulation experiment 22 days after adult eclosion revealed a continued arrest of oocyte development. It is apparent that JH-Met signalling is a common pathway regulating female vitellogenesis as evidenced by RNAi studies in different insect species, such as *T. castaneum*, *Colaphellus bowringi*, *Cimex lectularius*, *B. germanica*, *D. punctata*, *Aedes aegypti*, *H. armigera*, *R. prolixus*, *Reticulitermes speratus*, *P. apterus* and *L. migratoria* (Gujar and Palli, 2016b; Guo et al., 2019, 2014; Liu et al., 2016; Ma et al., 2018; Marchal et al., 2014; Naghdi et al., 2016; Parthasarathy et al., 2010; Saiki et al., 2015; Smykal et al., 2014a; Villalobos-Sambucaro et al., 2015; J. L. Wang et al., 2017; Wu et al., 2018).

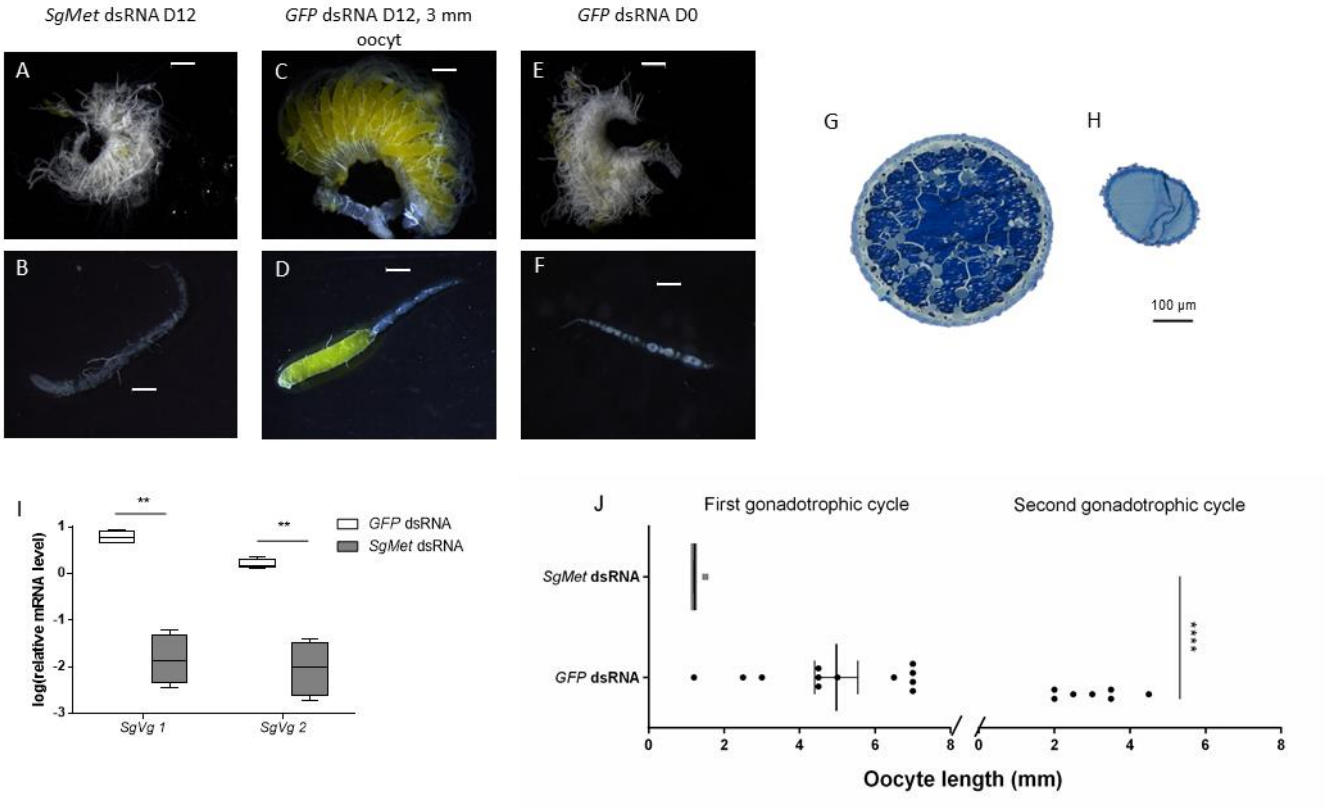

Figure 6.6: Arrest of ovarian maturation after silencing *SgMet*. Ovaries (A, C, E) and single ovarioles (B, D, F) of 12-day-old *dsSgMet* injected locusts (A, B), 12-day-old *dsGFP* injected (control) locusts (C, D) and freshly moulted (D0) control locusts (E, F). Scale bars: 1 mm. (G - H) Histological sections of 12-day-old (G) control and (H) *dsSgMet* injected locust oocytes. Scale bar: 100 µm. (I) Relative transcript levels of *SgVg1* and *SgVg2* in the fat body of 12-day-old *dsSgMet* injected and control female locusts. The data (log transformed) are shown as box plots (min to max) of four independent pools of five animals, run in duplicate and normalized to *β-actin* and *EF1α* transcript levels. Statistically significant differences (p) were found, after a log transformation, via a t-test (with or without two-sided Welch's correction) and are indicated by asterisks (** = $p < 0.01$). (J) The oocyte length (mm) of 12-day-old control and *dsSgMet* treated female locusts was observed. Each point represents the mean length of 3 randomly chosen oocytes (mean ± S.E.M). Statistically significant differences (p) were found via a nonparametric Mann-Whitney test and are indicated by asterisks (**** = $p < 0.0001$).

Met knockdown in female bed bugs (*C. lectularius*) also caused a reduced number of eggs deposited (Gujar and Palli, 2016b). In our study, an effect on copulation behaviour as well as on oviposition was witnessed. Where control females all copulated on day 15, a delay was seen in the *dsSgMet* injected individuals (Fig. 6.7A). Moreover, none of these experimental locusts was capable of depositing their eggs within the set experimental timeframe (Fig. 6.7B), likely the result of incomplete oocyte maturation (Fig. 6.6J) and no increase in survival was observed in any of the knockdown experiments.

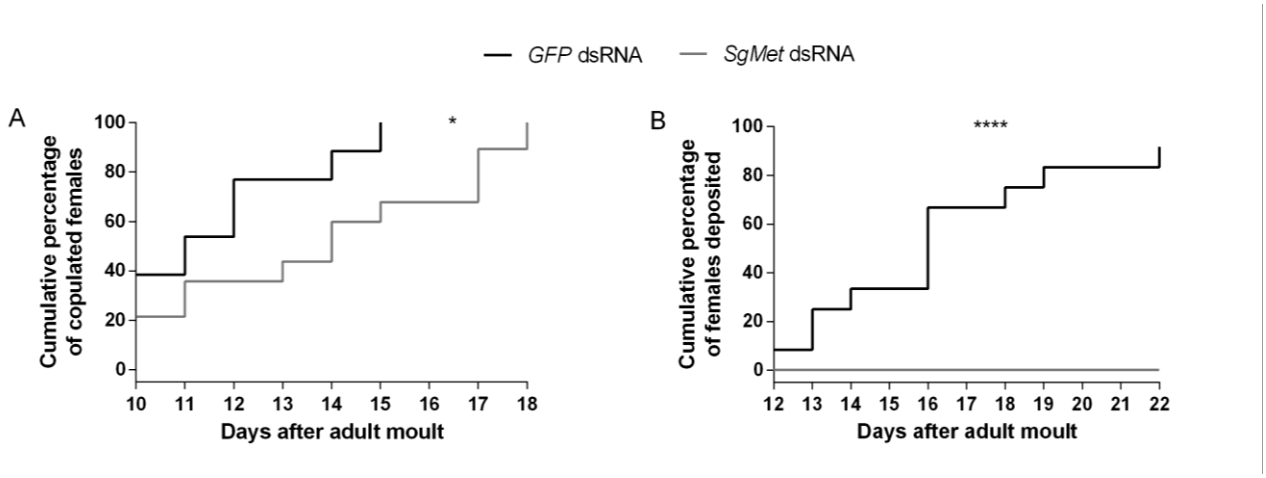

Figure 6.7: Copulation behaviour and oviposition of *dsSgMet* injected locusts. Copulation behaviour and post-copulation effects were observed from 12 individuals per condition starting on day 8 of the adult stage. (A) The cumulative percentage of copulating females (actual connection between male and female genitalia) and (B) the cumulative percentage of eggs deposited by the females are showed. Statistically significant differences (p) between the two conditions were found via a log-rank (Mantel-Cox) test and are indicated by asterisks (* = p = < 0.05; **** = p = < 0.0001).

6.3.4 *SgMet* is also crucial for ovarian ecdysteroid biosynthesis

In vitellogenic female locusts, the developing basal oocytes also incorporate 'free' and conjugated ecdysteroids, while a rise in the circulating ecdysteroid levels can be observed in the haemolymph, as described previously (Marchal et al., 2011a; Van Wielendaele et al., 2012). The majority of the ecdysteroids produced by the follicle cell layer are incorporated in the growing oocytes as conjugates. Only a small fraction is stored in the oocytes as 'free' ecdysteroids. An enzyme immunoassay (EIA) was used to determine the effect of *SgMet* knockdown on ecdysteroid levels in the developing oocytes and the haemolymph. Silencing *SgMet* resulted in a significantly reduced level of both circulating and ovarian ecdysteroids (expressed in 20E equivalents) compared to the control locusts (Fig. 6.8A-C). Ecdysteroid biosynthesis in adult locusts mainly takes place in the follicle cell layer of the developing oocytes (Kappler et al., 1986; Lagueux et al., 1977) where the steroid hormone precursor cholesterol is converted to 20E in a series of enzymatic reactions involving the *Halloween* genes, first characterized in *D. melanogaster* (Gilbert and Warren, 2005). Three of these *Halloween* genes, *i.e. Spook* (*Spo*), *Phantom* (*Phm*) and *Shade* (*Shd*), encoding cytochrome P450 enzymes were already functionally characterized in *S. gregaria* (Marchal et al., 2012, 2011a). *SgSpo*, encoding an enzyme acting in the Black Box of the ecdysteroid biosynthetic pathway, is considered to catalyse the rate-limiting step. *SgShd* is important in the conversion of ecdysone to the active hormone, 20E. In adult locusts, relative mRNA levels of all three are highest in the ovaries and degenerating PGs. The reduced level of circulating and ovarian ecdysteroids in the *dsSgMet* treated animals is also evidenced in the ovarian transcript levels of both *SgSpo* and *SgPhm* (Fig. 6.8D). Our data indicate that the initiation of ecdysteroid biosynthesis by the reproductive organs is situated downstream of the JH-mediated initiation of oocyte growth and vitellogenesis. The start of ecdysteroidogenesis in locusts may be directed by a nutritional state-dependent

factor binding to the Venus Kinase Receptor (VKR), a receptor tyrosine kinase as evidenced by a recent study by Lenaerts et al. (2017). Knockdown of *SgVKR* in adult females results in reduced oocyte size, ovarian and circulating ecdysteroid levels. Relative transcript levels of several *Halloween* genes were negatively affected. Downregulation of *SgMet* resulted in a significant reduction of relative *SgVKR* transcript levels in the ovary (Fig. 6.9A). In the mosquito, *A. aegypti*, the ligand for this receptor is the Ovarian Ecdysteroidogenic Hormone (OEH), an 83 AA long peptide released from medial neurosecretory cells in the mosquito brain upon blood feeding which induces the ovaries to produce ecdysteroids. These ecdysteroids, as in other higher insects, will stimulate the fat body to produce yolk protein (Brown et al., 1998; Vogel et al., 2015). Interestingly, OEH is considered as a member of the neuroparsin family, which possesses a typical, conserved pattern of Cys residues (Badisco et al., 2007). Most insects seem to encode a single NP gene, while in some species, such as *D. melanogaster*, no NP has been discovered (Badisco et al., 2013). However, in *S. gregaria* four *SgNP* precursor transcripts are found, for which transcript profiling studies were performed in the past (Claeys et al., 2006b, 2005). In gregarious locusts, transcripts for *SgNP1* and *SgNP2* are predominantly detected in the brain; whereas *SgNP3* and *SgNP4* are also detected in female fat body and ovaries. As previous research from our lab and current data in Figure 6.10A, B show, transcripts of *SgNP3* and *SgNP4* are highly regulated during the first gonadotrophic cycle, suggesting these peptides play a role in reproductive physiology. A decline of both *SgNP3* and *SgNP4* transcripts was observed approximately at the time when *SgVg* transcript levels started rising in the fat body. In the *dsMet* treated animals the relative mRNA levels of both *SgNP3* and *SgNP4* are higher compared to the control animals in fat body, while the relative transcript level of *SgNP4* is also increased in the ovary (see Fig. 6.11 and Fig. 6.9B). At present, it is still unclear whether the changes in *SgNP3* and *SgNP4* expression are caused by changes in JH signalling or to indirect effects via other regulatory pathways that have been affected in the *dsMet* treated locusts. JH injection into the haemocoel of day 5 adult female locusts results in an increase of *SgNP3* and *SgNP4* transcript levels in both female fat body and ovary (Claeys et al., 2006a). In our current study, we observe that *SgMet* expression in the ovary is not significantly influenced by the systemic knockdown, which could be due to weaker RNAi sensitivity (Wynant et al., 2012) and/or stronger compensatory effects in this tissue. In the CA, we observe another kind of compensatory effect resulting in significantly increased expression of JH biosynthetic enzymes. So, it could be that these compensatory effects may also have resulted in increased ovarian *SgNP4* levels. However, this does not explain why both *SgNP3* and *SgNP4* transcript levels are strongly increased in the fat body, since in this tissue knockdown of *SgMet* and reduced JH signalling are clearly evidenced by significantly reduced transcript levels of *SgMet* and *SgKrh1*, respectively. Another receptor that may be involved in causing the observed changes in *SgNP* transcript levels is *Sg*VKR. In the current study, we show that *SgVKR* transcript levels are significantly reduced in *dsMet* treated desert locusts. The observed effect on *SgNP* transcript levels might be due to these reduced *SgVKR* levels, since Lenaerts et al. (2017) have shown that knockdown of *SgVKR* resulted in increased *SgNP3* and *SgNP4* levels in locusts. Nevertheless, the occurrence of other currently unknown mechanisms cannot be ruled out.

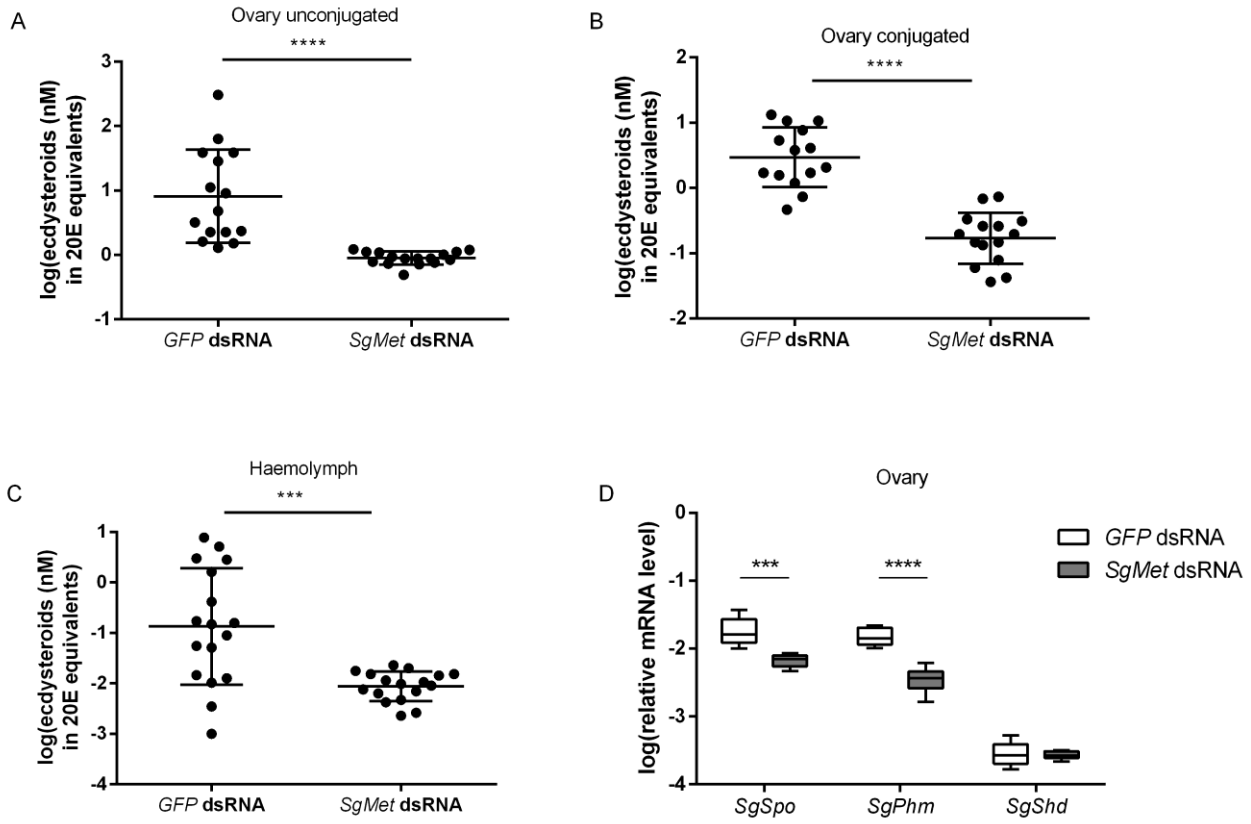

Figure 6.8: Ecdysteroid levels and expression of *Halloween* genes upon silencing of *SgMet* in adult female locusts. Ecdysteroid levels (20E equivalents in nM) as well as *Halloween* gene expression were measured in 12-day-old female control and experimental locusts; (A) non-conjugated ovarian ecdysteroid levels, (B) conjugated ovarian ecdysteroid levels and (C) haemolymph ecdysteroid levels. Each point (log transformed) represents a measurement (mean ± S.E.M). (D) Relative expression levels of three *Halloween* genes, *i.e. SgSpo, SgPhm* and *SgShd* were measured in the ovaries of 12-day-old *dsSgMet* injected female locusts. The data (log transformed) are shown as box plots (min to max) of four independent pools of five animals, run in duplicate and normalized to *β-actin* and *EF1α* transcript levels. (A-D) Statistically significant differences (p) between the measurements were found, after a log transformation, via a t-test (with or without two-sided Welch's correction) and indicated by asterisks (*** = $p < 0.001$, **** = $p < 0.0001$).

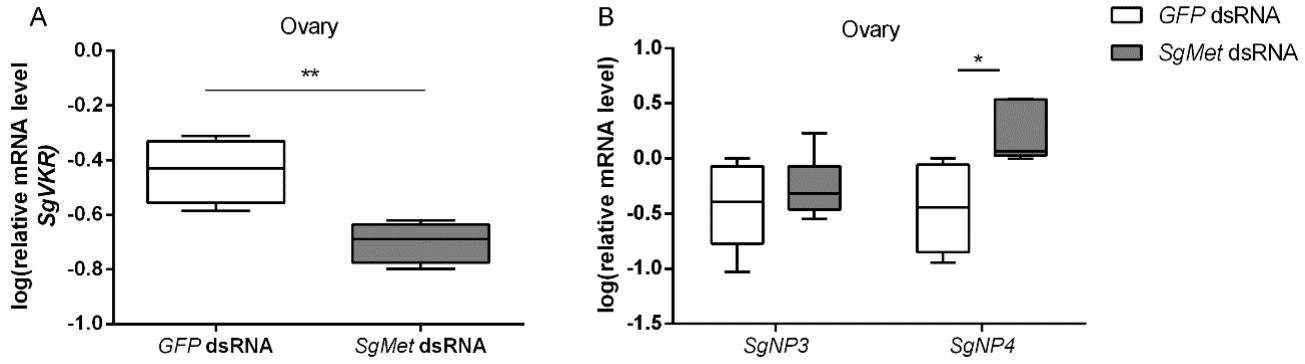

Figure 6.9: *SgVKR*, *SgNP3* and *SgNP4* relative transcript levels. Relative expression level of (A) *SgVKR* and (B) *SgNP3* + *SgNP4* was measured in the ovaries of 12-day-old *SgMet* dsRNA treated locusts and control locusts. The data (log

transformed) are shown as box plots (min to max) of four independent pools of five animals, run in duplicate and normalized to *β-actin* and *EF1α* transcript levels. Statistical significant differences (p) between the measurements were found, after a log transformation, via a t-test (with or without two-sided Welch's correction) and are indicated by asterisks (** = $p < 0.01$).

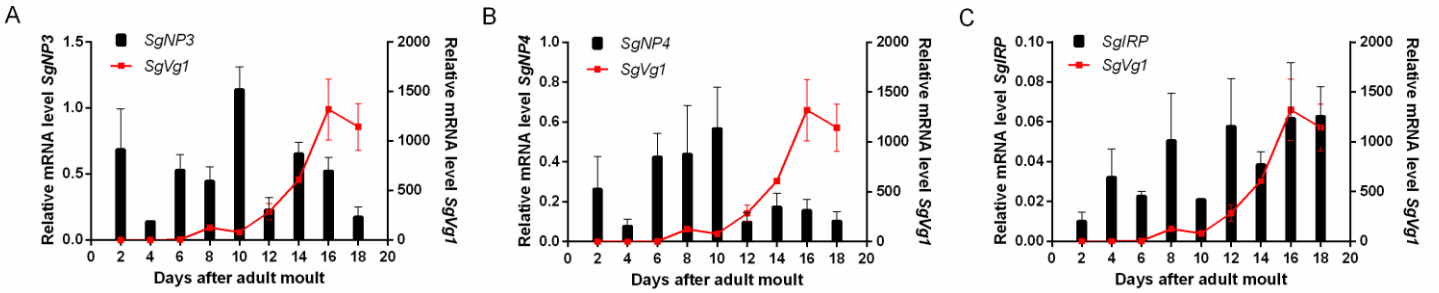

Figure 6.10: Relative transcript levels of *SgNP3*, *SgNP4* and *SgIRP* throughout the first gonadotrophic cycle. (A) *SgNP3*, (B) *SgNP4* and (C) *SgIRP* relative transcript levels were determined in the fat body of freshly moulted adult females (day 0 until day 18). *SgVg1* expression is included as well. Samples were collected every other day during the first gonadotrophic cycle. The data represent mean ± S.E.M. of three independent pools of ten animals, run in duplicate and normalized to *β-actin* and *EF1α* transcript levels.

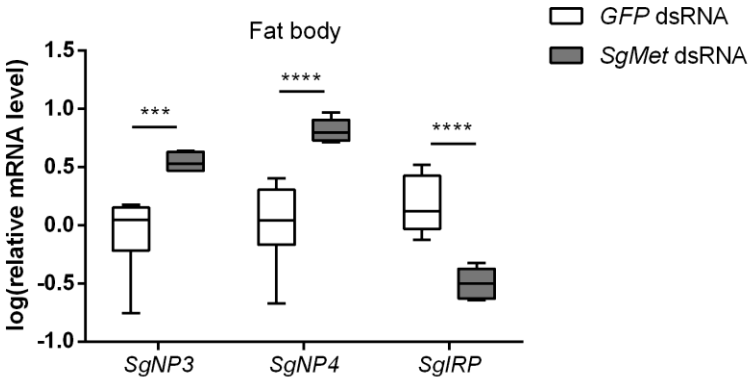

Figure 6.11: JH receptor knockdown alters the levels of neuroparsin and insulin-related peptide precursor transcripts. Relative *SgNP3*, *SgNP4* and *SgIRP* transcript levels were measured in the fat body of 12-day-old *dsSgMet* injected female locusts. The data (log transformed) are shown as box plots (min to max) of four independent pools of five animals, run in duplicate and normalized to *β-actin* and *EF1α* transcript levels. Statistically significant differences (p) between the measurements were found, after a log transformation, via a t-test (with or without two-sided Welch's correction) and are indicated by asterisks (*** = $p < 0.001$; **** = $p < 0.0001$).

6.3.5 Knockdown of JH receptor Met alters expression of *insulin-related peptide* and *neuroparsin precursor* genes in an opposite way

Previous research has shown that IRP has a gonadotropic role, while NPs have an anti-gonadotropic role in the female reproductive physiology of locusts. Studies in *S. gregaria* revealed that an increase in *SgIRP*

transcript levels can be observed during specific reproductive events such as vitellogenesis and intensive growth of the oocytes (Girardie et al., 1987). The effect of this peptide was later evidenced in an RNAi-mediated study in *S. gregaria* by Badisco et al. (2011) showing lower *SgVg* transcript levels and smaller oocytes compared to control animals upon ds*IRP* injections. Playing a vital role as nutritional sensor, the ISP has been described in different insect species as having a gonadotropic effect. In dipterans, insulin-like peptides (ILPs) are involved in stimulating egg production and affecting germ line cyst development rate as well as progression through vitellogenesis (Brown et al., 2008; Gulia-Nuss et al., 2011; LaFever and Drummond-Barbosa, 2005). In the yellow fever mosquito, *A. aegypti,* ILP3 stimulates yolk uptake by the developing oocytes (Brown et al., 2008). Moreover, insulin signalling is also required to induce vitellogenin production in the fat body (Roy et al., 2007) and to stimulate ecdysteroid production in the ovaries (Wen et al., 2010). Furthermore, *D. melanogaster* female ISP mutants generally show reduced vitellogenesis (Tu et al., 2002). In addition, mutations in the insulin receptor result in a decrease of JH synthesis suggesting the involvement of the ISP in the regulation of JH biosynthesis (Tatar et al., 2001; Tu et al., 2005). In the red flour beetle, *T. castaneum*, it was shown that JH is able to regulate ILP synthesis, which in turn regulates Vg synthesis (Sheng et al., 2011). In the adult female beetles, both JH and feeding are crucial in the onset of ILP production in the fat body and brain after which ILPs will trigger the Vg synthesis through removal of a Vg transcriptional repressor (Parthasarathy et al., 2010; Parthasarathy and Palli, 2011; Sheng et al., 2011). RNAi of the insulin receptor in *B. germanica* adult females resulted in a reduction in JH biosynthesis, *Vg* expression and ovarian development (Abrisqueta et al., 2014). On the other hand, silencing of *SgNP*s in the RNAi-mediated study by Badisco et al. (2011) resulted in higher *SgVg* transcript levels and bigger oocytes in 12-day-old female locusts. This anti-gonadotropic action of NPs has also been proven in *L. migratoria* (Girardie et al., 1987).

Our current results show that during the locust's first gonadotrophic cycle, a decrease in relative *SgNP3* and *SgNP4* transcript levels coincides with an increase in relative *SgIRP* expression in the locust fat body (Fig. 6.10). Also in the *dsSgMet* treated females, a significant increase in *SgNP*3 and *SgNP4* expression was measured in the fat body. *SgIRP* expression on the other hand decreased (Fig. 6.6). This clearly indicates a consistent cross-talk between *SgNP* and *SgIRP* signalling downstream of JH.

All the above mentioned effects observed upon *SgMet* silencing are summarized in Figure 6.12.

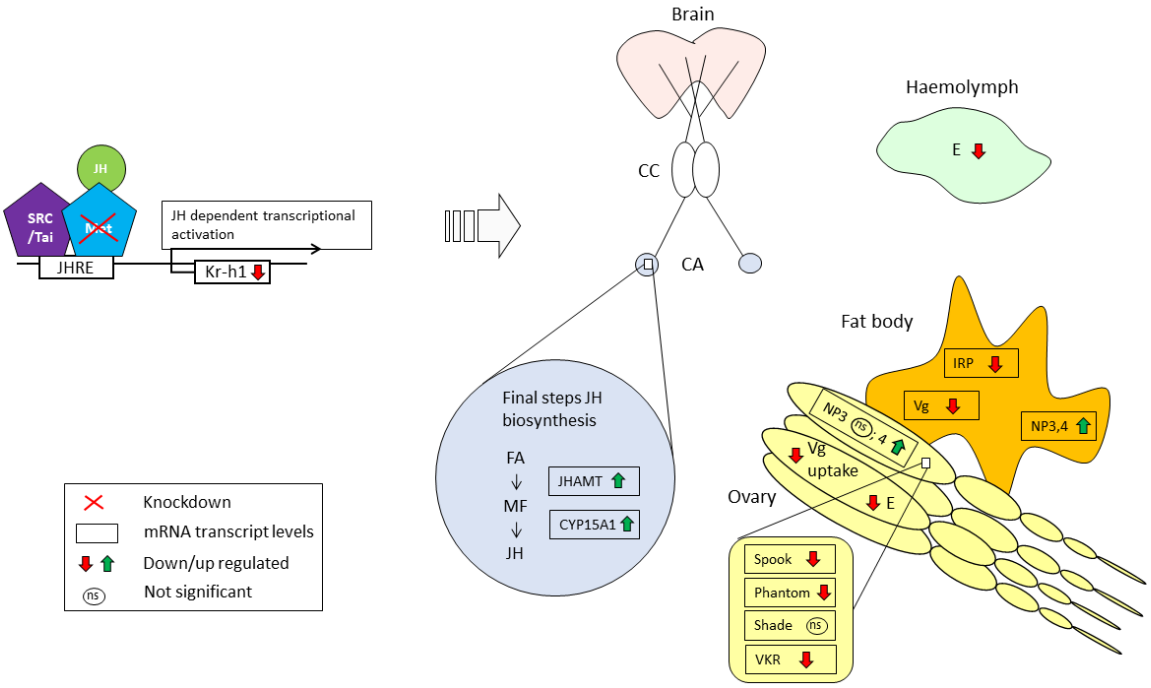

Figure 6.12: A schematic of the different effects upon *SgMet* silencing. All the effects observed upon *SgMet* silencing are summarized. Effects on the relative mRNA transcript levels are shown in rectangular boxes with arrowheads indicating down or up regulation upon *SgMet* knockdown. CA = Corpora allata; CC = Corpora cardiaca; CYP15A1 = Cytochrome P450 enzyme 15A1; FA = Farnesoic acid; E = Ecdysteroid; IRP = Insulin-related peptide; JH = Juvenile hormone; JHAMT = Juvenile hormone acid methyl transferase; Kr-h1 = Krüppel-homolog 1; Met = Methoprene-tolerant; MF = methylfarnesoate; NP = Neuroparsin; ns = not significant; SRC/Tai = Steroid receptor coactivator/Taiman; Vg = Vitellogenin.

6.4 Conclusion

Our results show that the knockdown of *SgMet* in female locusts results in a failure to initiate vitellogenin expression in the fat body as well as oocyte growth in the ovaries. These *dsSgMet* treated animals are still able to copulate, albeit later, but they do not oviposit. Our study also indicates that upon *SgMet* knockdown some *SgNP* transcripts are significantly upregulated in the locust fat body, while the *SgIRP* levels are downregulated. In fact, these observations appear to be very well in line with their previously reported opposing roles in the control of reproduction. Furthermore, we show that *SgMet* knockdown strongly influences the expression of JH biosynthesis enzymes in the CA, as well as of ecdysteroid biosynthesis enzymes in the ovary, as evidenced by lower ovarian concentrations of both free and conjugated ecdysteroids. In conclusion, our study sheds more light on the essential role of the JH receptor *SgMet*, as well as on the interdependencies between different endocrine pathways involved in the control of reproduction in female desert locusts.

Chapter 7: General conclusions, discussion and future perspectives

The classic insect hormones, JH and 20E, are crucial regulators of the insect's life cycle (Riddiford, 2012). Besides playing an important role in post-embryonic development, they also coordinate reproduction in adult insects. Also in the locust species, *S. gregaria* and *L. migratoria*, the regulatory role of these hormones in moulting, metamorphosis and reproduction is corroborated. However, the functional interactions with other hormonal signalling pathways still remain unclear. Moreover, recently, the importance of miRNAs in regulating key insect processes was established. The discovery of these non-coding RNAs has added an additional level of complexity, at which different signalling pathways may functionally interact. In a variety of organisms, from plants to mammals, it has also been shown that miRNAs are present in extracellular fluids. In insects, the study of extracellular (ex-)miRNAs still is an underexplored, but very intriguing research area. In this thesis, we have clearly shown the presence of ex-miRNAs in the cell-free conditioned media of two *Drosophila* cell lines, as well as in haemolymph of fifth nymphal locusts (*L. migratoria*). Moreover, experiments with mimics for some of these miRNAs have resulted in severe disruption of post-embryonic development in the migratory locust. This thesis forms a solid basis for future research on the role of both JH/20E and miRNAs and their functional interactions in insects. In addition, this work may also reveal new leads for development of more selective insect control methods.

7.1 The presence of extracellular miRNAs

While regulatory RNA pathways have commonly been described at an intracellular level, studies investigating extracellular RNA species constitute a new and interesting research field. MiRNA molecules have already been observed in the biological fluids of a wide variety of organisms (Buck et al., 2014; Cai et al., 2018b; Castoldi et al., 2016; Dhahbi et al., 2016; Etheridge et al., 2013; Guo et al., 2013; Li et al., 2012; Makarova et al., 2015; Sohel, 2016; Zhao et al., 2019). Their encapsulation in extracellular vesikels (EVs) or their inclusion in complexes with proteins of the Argonaute (Ago) family makes these extracellular miRNAs (ex-miRNAs) extremely stable, capable of withstanding the high RNase activities that often occur in extracellular environments (Arroyo et al., 2011; Buck et al., 2014; Cai et al., 2018b; Castoldi et al., 2016; Sohel, 2016; Turchinovich et al., 2015; Valadi et al., 2007; Zhao et al., 2019).

Our study described in chapter two (Van den Brande et al., 2018) together with the study of Mingels et al. (2020) are the only two that reported on the occurrence of ex-miRNAs in insects within similar fractions as already described in mammals, plants and des (Arroyo et al., 2011; Buck et al., 2014; Cai et al., 2018b; Castoldi et al., 2016; Duguet et al., 2020; Sohel, 2016; Turchinovich et al., 2015; Valadi et al., 2007; Zhao et al., 2019). We demonstrated the presence of ex-miRNAs in EVs and EAgo-1 in the cell-free culture media of two *Drosophila* cell lines. Moreover, evidence for selective miRNA secretion in EVs, as already suggested for mammalian systems (Shurtleff et al., 2016; Turchinovich et al., 2011), was obtained as well. Mingels et al. (2020) demonstrated the presence of ex-miRNAs, amongst a wide variety of small non-coding RNAs, in EVs of *Tribolium castaneum* TcA cells. Moreover, they found that EVs containing dsRNA-specific siRNAs can

trigger RNAi in recipient cells. Furthermore, we have also demonstrated the presence of ex-miRNAs in haemolymph of migratory locusts (*L. migratoria*) in the fifth nymphal stage, as described in chapter three. The abundances of 43 miRNAs significantly differed between haemolymph samples characterized by low (N5 D2 and N5 D3) *versus* high (N5 D6 and N5 D7) ecdysteroid levels. To our knowledge, this is the first report on the differential occurrence of ex-miRNAs throughout the moulting cycle of an insect.

Altogether, these observations point towards a possible role of ex-miRNAs, and probably other extracellular small non-coding RNA molecules, in intercellular communication in insects, a hitherto underexplored research topic (Dhahbi et al., 2016; Guo et al., 2013; Wang et al., 2018). Besides intercellular communication, the role of ex-miRNAs in cross-kingdom communication also constitutes an interesting field, especially when opting for biotechnological applications. It has become apparent that in plant-insect interactions, both plants and insects use miRNAs to regulate their biological processes. The use of miRNA mimics in transgenic plants to target insect genes has many potential applications in agriculture. However, the study of the involvement of miRNAs in these reciprocal interactions is in its infancy (C. Li et al., 2018; Sattar and Thompson, 2016).

7.2 Regulation of moulting and metamorphosis

The migratory locust, *L. migratoria*, and the desert locust, *S. gregaria*, are hemimetabolous insects that in their gregarious phase normally go through five nymphal stages before the adult, reproductive stage is reached. The final moult is induced by 20E in absence of JH and is characterized by an incomplete metamorphosis process resulting in the development of functional wings and reproductive organs (Riddiford, 2012). In this thesis, we have established the importance of Kr-h1 and E93 in the anti-metamorphic effects of JH and in promoting metamorphosis, respectively.

As described in chapter four, silencing of the adult specifier *E93* in late nymphal *S. gregaria* causes the development of supernumerary nymphs. Silencing of *LmKr-h1* in penultimate nymphal *L. migratoria*, as described in chapter five, resulted in premature adults. Similar observations of supernumerary nymphal and precocious adult-like phenotypes were made in several other hemimetabolan insect species after *E93* and *Kr-h1* knockdown, respectively (Gujar and Palli, 2016a; Ishimaru et al., 2019; Konopova et al., 2011; K. L. Li et al., 2018; Lozano and Belles, 2014, 2011; Smykal et al., 2014b; Ureña et al., 2014; Villalobos-Sambucaro et al., 2015). Besides the described phenotypic characteristics, as well as the affected period of transition, clear differences in transcript levels of MEKRE93 and JH biosynthesis pathway components were also observed during this time. Moreover, a temporal shift in the ecdysteroid profile in haemolymph, together with altered transcript levels of the *Halloween* genes and ecdysteroid receptor components, are in agreement with the observed phenotypes.

Although ecdysone signalling allows a strong induction of E93, which triggers metamorphosis, the exact interplay between the MEKRE93 signalling pathway and other hormonal factors still needs to be elucidated. Figure 7.1 summarizes the MEKRE93 pathway in hemimetabolan metamorphosis together with suggested interactions with other signalling pathways, as discussed throughout this thesis.

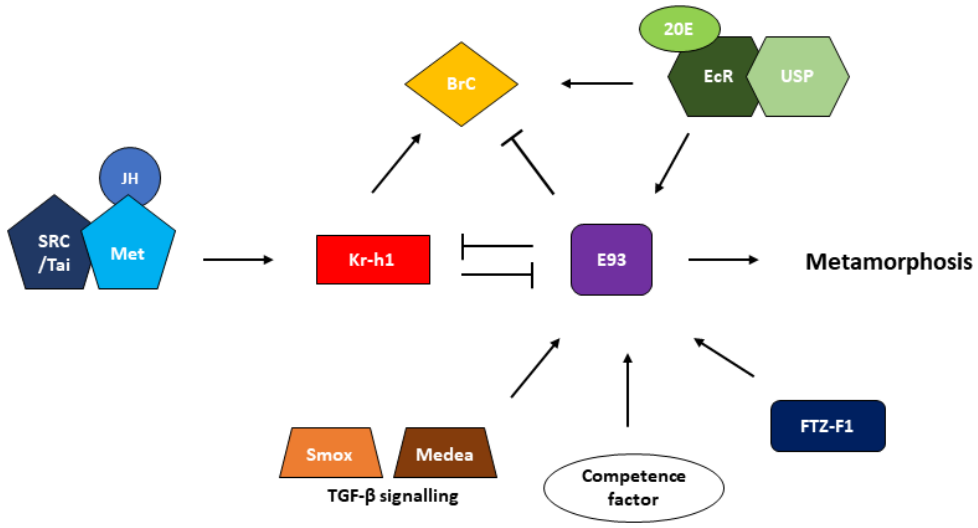

Figure 7.1: The MEKRE93 pathway with suggested functional interactions in hemimetabolan metamorphosis. During the nymphal-to-nymphal transitions, JH (through Met-Tai) induces the expression of Kr-h1, which in turn, represses the expression of *E93*. The decline of JH production during the final nymphal stage interrupts the expression of Kr-h1 allowing a strong induction of E93 by ecdysone signalling, which triggers the transition from nymph to adult (Belles and Santos, 2014). Br-C is mainly involved in promoting the growth of wing primordia (Erezyilmaz et al., 2006; Huang et al., 2013; Konopova et al., 2011). The expression of E93 at the beginning of the final nymphal stage is also co-activated by Smox-Medea (two components of the TGF-β signalling pathway) (Santos et al., 2016), a competence factor (Hironaka and Morishita, 2017) and FTZ-F1 (Kamsoi and Belles, 2020). Abbreviations: JH = Juvenile hormone; SRC/Tai = Steroid receptor coactivator/Taiman; Met = Methoprene-tolerant; Kr-h1 = Krüppel-homolog 1; BrC = Broad Complex; 20E = 20-hydroxyecdysone; EcR = Ecdysone Receptor; USP = Ultraspiracle; TGF-β = Transforming Growth Factor-β; FTZ-F1 = Fushi Tarazu Factor-1.

Even though the transcriptional regulation of ecdysteroid and MEKRE93 pathway components has been extensively studied, little is known about its regulation at the post-transcriptional level. miRNAs have already been demonstrated to target genes in the ecdysone and JH cascade, thereby regulating these processes (Belles, 2017; Gomez-Orte and Belles, 2009; Ling et al., 2014; Sokol et al., 2008; Wu et al., 2017), although more research will be crucial for examining the regulatory role of multiple miRNAs in post-embryonic development of insects. In this thesis, we have reported on the importance of a few miRNAs in the metamorphic transition of *L. migratoria* nymphs (chapter three). Using systemic RNAi to silence the expression of *LmDicer-1* during the fifth nymphal stage, we disrupted the nymphal-to-adult moult, confirming a crucial role of miRNAs during metamorphosis. Moreover, mimicking *Lmi*-miR-13b-3p, *Lmi*-bantam-3p and *Lmi*-miR-306-5p (agomiRs) in late nymphal *L. migratoria* severely affected the period of transition. Moreover,

many miRNA agomiR-injected locusts appeared to be unable to shed their old cuticle and eventually died. Altogether, these results support a role for miRNAs as important players in the metamorphic transition in *L. migratoria*.

7.3 Regulation of female reproductive physiology

Besides regulating the process of moulting, ecdysteroids and JH also act as endocrine regulators of reproduction. In female insects, JH is known to act as the primary regulator of ovarian development and vitellogenesis by regulating the synthesis of Vgs in the fat body (Wyatt and Davey, 1996) and subsequently ensuring the uptake of Vgs by the developing oocytes (Davey et al., 1993; Jing et al., 2018; Sevala, V.L. & Davey, 1989; Sevala et al., 1995). Ecdysteroids, produced in the ovarian follicular cell layer, appear to have multiple fates. They induce meiotic re-initiation in the oocyte (Lanot et al., 1987), are incorporated as conjugates into the growing oocytes where they act as a source of ecdysteroids during embryogenesis (Isaac and Rees, 1984) and bind to vitellins, thereby preventing their leakage into the haemolymph (Isaac and Rees, 1984; Lagueux et al., 1981; Tawfik et al., 1999).

The premature or 'adultoid' phenotype of the migratory locust, obtained through silencing of *LmKr-h1* in the penultimate nymphal stage, shows an accelerated ovarian maturation and vitellogenesis as described in chapter five. These observations coincide with clear differences in expression of MEKRE93 and JH biosynthesis pathway components. Furthermore, adultoid females show elevated expression of *Halloween* genes in the ovaries, reinforcing our observations of an accelerated ovarian maturation in comparison with normal adult migratory locusts. This is the first study that reports on the molecular basis of the reproductive development of premature adult insects. Prior to this thesis, only descriptive observations of the reproductive organs were available (Gujar and Palli, 2016b; Ishimaru et al., 2019; Jin et al., 2014; Konopova et al., 2011; K. L. Li et al., 2018).

As described in chapter six, the juvenile hormone receptor Met is essential for ovarian maturation, vitellogenesis and associated ecdysteroid biosynthesis in adult female *S. gregaria.* Moreover, evidence was found for a feedback of *SgMet* on the JH biosynthesis pathway. As evidenced by RNAi studies in different insect species, JH-Met signalling is a common pathway regulating female vitellogenesis (Gujar and Palli, 2016b; Guo et al., 2019, 2014; Liu et al., 2016; Ma et al., 2018; Marchal et al., 2014; Naghdi et al., 2016; Parthasarathy et al., 2010; Saiki et al., 2015; Smykal et al., 2014a; Villalobos-Sambucaro et al., 2015; J. L. Wang et al., 2017; Wu et al., 2018). However, possible interactions between JH and other signalling pathways are still poorly understood. In this thesis, the existence of an intricate regulatory interplay between different hormonal factors was shown, as silencing *SgMet* resulted in a significant decrease of *SgIRP* and increase of *SgNP 3* and *4* transcript levels. These observations are very well in line with the previously reported opposing

roles of these hormones in the control of reproduction (Badisco et al., 2011; Girardie et al., 1987), but it is still unclear whether the changes in expression are caused by changes in JH signalling or to indirect effects via other regulatory pathways that were affected in the *dsMet*-treated locusts.

7.4 MEKRE93 pathway components as molecular targets of novel insect control agents

When taking into account the urgent need for greener and more locust selective control strategies, E93, Kr-h1 and Met are very promising candidate targets since severe defects on survival and reproduction were witnessed. As discussed in chapter four, many supernumerary N6 and all supernumerary N7 nymphal stages eventually died due to problems in shedding their old cuticle. Premature adults on the other hand are characterised by a final moult, but subsequently died at the end of the first gonadotropic cycle due to problems in oviposition (chapter five). *DsSgMet*-injected females showed severe defects in mating and egg laying (chapter six). MiRNAs, as reported in chapter three, constitute an additional level of control, which may also be exploited for pest management purposes. Applying two or more pesticides with different modes of action may minimize/delay existing pest resistance.

7.5 General discussion and future perspectives

The aims of this thesis were to investigate the possible roles of (i) miRNAs, including ex-miRNAs, and (ii) JH signalling pathway components in regulating key processes in locust post-embryonic development, in particular metamorphosis and reproduction, as well as (iii) their functional interactions with different pathways. Answers to these questions are reported in this thesis, but it is evident that novel questions for further research have also arisen from this work.

7.5.1 MiRNAs regulating postembryonic development

7.5.1.1 Optimisation of purification methods for ex-miRNA containing fractions

We have shown the presence of ex-miRNAs in extracellular conditioned media of insect cells. More specifically, ex-miRNAs are identified in different fractions (namely EVs and EAgo-1) of extracellular media of cultured *Drosophila* cells (Van den Brande et al., 2018). Yet, it is still unclear if ex-miRNAs reside in other fractions as well. Ex-miRNA interactions with insect lipoproteins (lipophorins), for example, have not yet been investigated, although our lab demonstrated that lipophorins can also associate with dsRNA (Wynant et al., 2014a). In order to isolate insect lipophorins, a density-based ultracentrifugation approach was used. Currently, an antibody against apolipophorin-I is available in our research group, which may offer a possibility to immunoprecipitate lipophorin-RNA complexes as well. In this way, a possible contamination of the lipophorin fraction with EVs having a similar density can be avoided. Moreover, the EV fraction consists of a combination of exosomes and microvesicles. It might be of interest to investigate these EV subtypes to

determine in which subtypes ex-miRNAs reside and moreover, if miRNAs are selectively loaded, but their separation will require further method optimisation. In general, for investigation of the different ex-miRNA containing fractions, an optimisation of purification procedures will be needed. These procedures, in their turn, will open new avenues to study the potential role(s) of ex-miRNAs in intercellular communication in insects, an intriguing research topic since in several organisms, including mammals, nematodes and plants, a functional transfer of miRNAs by EVs and lipoproteins has already been demonstrated (Buck et al., 2014; Cai et al., 2018b; Duguet et al., 2020; Hunter et al., 2008; Lotvall and Valadi, 2007; Shurtleff et al., 2016; Sohel, 2016; Turchinovich et al., 2011; Valadi et al., 2007; Zhao et al., 2019).

7.5.1.2 Ex-miRNA containing fractions regulating the transition from juvenile to adult

For revealing the possible role(s) of ex-miRNAs in regulating insect post-embryonic development, further studies will have to be explored. More specifically, the possible role of ex-miRNAs in regulating the transition from juvenile locusts to fully reproductive adults deserves more detailed attention. With optimised isolation and purification procedures, it would be feasible to separate different ex-miRNA containing fractions from early and late fifth nymphal locusts. First, small RNA sequencing on these different fractions would then reveal which miRNAs are associated with these different fractions. Some miRNAs might perhaps be associated with a specific ex-miRNA containing fraction, when compared to others. Interestingly, our research group already provided evidence for selective miRNA secretion in EVs derived from *Drosophila* cell cultures (Van den Brande et al., 2018). For instance, in future experiments the ex-miRNA containing fractions isolated from late fifth nymphal locusts could subsequently be injected in early fifth nymphal locusts. Via close monitoring of the ecdysis process, a possible role of ex-miRNAs in regulating moulting and metamorphosis may be studied. Considering the limited functional information available on these fractions, different outcomes might be plausible:

i) The early fifth nymphal locusts, injected with ex-miRNA containing fractions isolated from late fifth nymphal locusts, may die shortly after the injection. Toxicity might explain this outcome, particularly when sudden death would also be observed in control locusts injected with fractions obtained from the same stage. This could perhaps occur if, during the separation of fractions, ‘toxic’ solvents or products were introduced. In this case, although the fractions would be dissolved in locust Ringer solution, toxic effects might still occur. Besides toxicity caused by injecting remnants of ‘toxic’ solvents/products, a sudden overload in ex-miRNA containing fractions may perhaps also result in mortality. However, all these effects would be revealed when including appropriate control conditions.

ii) No differences may be observed upon the injection. As it is often the case with negative results, this outcome might be explained in several ways. It may mean that locusts do not functionally transfer

ex-miRNAs for controlling this process, despite the fact that functional transfer of ex-miRNAs has already been reported in several other organisms and processes (Buck et al., 2014; Cai et al., 2018b; Hunter et al., 2008; Lotvall and Valadi, 2007; Shurtleff et al., 2016; Sohel, 2016; Turchinovich et al., 2011; Valadi et al., 2007; Zhao et al., 2019). However, other reasons may still apply. For instance, the injected early fifth nymphal locusts are not yet responsive to the signals present in late fifth nymphal locusts. Research on locusts already showed that, when injecting dsRNA, the exact timing can be crucial. Moreover, a critical weight needs to be attained by (some) insects before they successfully complete their adult moult (Hironaka and Morishita, 2017).

iii) The early fifth nymphal locusts, injected with ex-miRNA containing fractions isolated from late fifth nymphal locusts, remain in the fifth nymphal stage for a shorter time compared to control locusts, but do not successfully complete the adult moult. In this case, a functional transfer of miRNAs is plausible, however, the injected early fifth nymphal locusts are perhaps not yet fully responsive to the signals of late fifth nymphal locusts explaining the failed transition to adult.

iv) The early fifth nymphal locusts, injected with ex-miRNA containing fractions isolated from late fifth nymphal locusts, remain in the fifth nymphal stage for a shorter time than the control locusts and successfully complete the adult moult. When observing this outcome, it can be assumed that locusts are capable of functionally transferring ex-miRNAs. Furthermore, injecting the ex-miRNA containing fractions does not result in any toxicity issues and the early fifth nymphal locusts seem to be responsive to the signals of late fifth nymphal locusts.

Considering the crucial role of miRNAs in regulating key insect processes, the existence of a functional transport of ex-miRNAs in locusts, as already demonstrated in several other organisms and processes, is more than likely (Buck et al., 2014; Cai et al., 2018b; Hunter et al., 2008; Lotvall and Valadi, 2007; Shurtleff et al., 2016; Sohel, 2016; Turchinovich et al., 2011; Valadi et al., 2007; Zhao et al., 2019). However, before unravelling the role of ex-miRNAs in the moulting process of locusts, several possible issues regarding toxicity and unresponsiveness of these early fifth nymphal locusts would have to be tackled first. Optimising the experimental setup by determining ideal injection conditions and timepoints would be of crucial importance. With the proposed experiments, the possible role of ex-miRNAs in regulating the moulting process of locusts may be investigated. Besides answering the question if a functional transport of ex-miRNAs in locusts is present, the question whether this functional transfer is fraction dependent may be answered as well. For instance, in mammals, a functional transfer of miRNAs by EVs and lipoproteins is already demonstrated (Lotvall and Valadi, 2007; Valadi et al., 2007), whereas the presence of extracellular complexes of ex-miRNAs with Ago seems to be cell waste related (Turchinovich et al., 2011; Turchinovich and Burwinkel, 2012). Furthermore, small RNA sequencing data would give more information regarding the identity of the ex-

miRNAs involved. Nevertheless, since this is a hitherto underexplored research area in insects, experimental optimisation and troubleshooting will probably be required in order to properly elucidate the potential role(s) of ex-miRNAs in insects.

7.5.1.3 The use of miRNA a(nta)gomiRs in elucidating metamorphosis

Besides focussing on the ex-miRNA containing fractions, the small RNA-seq reads obtained from fifth nymphal *L. migratoria* haemolymph samples characterized by low (N5 D2 and N5 D3) *versus* high (N5 D6 and N5 D7) ecdysteroid levels are also worth building on in future work. We already demonstrated a significant role for *Lmi*-miR-13b-3p, *Lmi*-bantam-3p *and Lmi*-miR-306-5p in metamorphosis of *L. migratoria*, but undoubtedly, other miRNAs of interest still reside in these data. However, including several optimization steps would benefit our research. Optimizing the experimental setup by determining the ideal dose of a(nta)gomiR injection, as well as the ideal injection timepoints will be of crucial importance. Next, when miRNA agomiRs were injected in fifth nymphal *L. migratoria*, no clear differences in transcript levels of target mRNAs were observed as explained in chapter three. However, in order to verify if a miRNA effectively interacts with the predicted mRNA, an *in vitro* functional analysis can be included. In short, a fusion construct, consisting of the miRNA binding site (for example the 3' UTR of a mRNA), downstream of a reporter gene (luciferase or GFP), can be used. Interaction of a miRNA with the binding site would then cause an inhibition of the reporter expression and result in reduced fluorescence (GFP) or luminescence (luciferase). In this way, the interaction between miRNAs and their predicted target sites can be studied. Moreover, in addition to qRT-PCR, Western Blot analysis, using antibodies against the target mRNA encoded protein, may enable a more comprehensive interpretation of the data.

7.5.2 Regulation of moulting and female reproductive success

7.5.2.1 Identification of JH signalling cascade components

In this thesis, we focussed on the MEKRE93 pathway components in regulating metamorphosis and reproduction in two locust species. We demonstrated that locusts behave in a similar way with what is currently known from studies in other hemimetabolan species. Downregulation of *Kr-h1* in penultimate nymphal *L. migratoria* resulted in precocious development of adult features whereas downregulating *E93* in final nymphal *S. gregaria* gave rise to a supernumerary nymphal phenotype. Moreover, a complete block in ovarian development was illustrated upon knocking down *Met* in adult female *S. gregaria* whereas an accelerated ovarian maturation was observed in adultoid (*dsLmKr-h1*) female *L. migratoria*. Although the function of MEKRE93 pathway components in regulating moulting and female reproductive physiology is confirmed, little is known about the existence of possible analogous or homologous genes. Particularly, since knocking down *Met* in penultimate nymphal *L. migratoria* did not result in the desired adultoid phenotype as observed in *dsKr-h1* injected locusts (unpublished data). Even though the lack of a phenotype could be

explained by differences in the efficiency of knocking down *Met* and *Kr-h1*, it also raises the question whether still other JH receptors might be present. Recently, the existence of a membrane receptor for JH was suggested (Davey, 2000; P. Liu et al., 2015). Nevertheless, this membrane receptor is not yet functionally characterised. It would be important to identify this hypothetical JH membrane receptor in order to understand how both intracellular and membrane receptors of JH interact to regulate moulting and reproduction in insects. Taiman (Tai), also known as steroid receptor co-activator, was identified as an additional component required for JH dependent transcription of genes (Godlewski et al., 2006; Z. Wang et al., 2017). However, Met may engage in JH-dependent interactions with multiple distinct partners, each time regulating a different aspect of insect biology. With this assumption, new interesting questions arise: i) how many partners are there, ii) how does Met discriminate among them and iii) what are the biological functions of each protein complex?

Another explanation for the observed differences upon *Met* and *Kr-h1* knockdown in locusts may be the existence of multiple downstream targets of Met. Next to Kr-h1, the *juvenile hormone esterase* gene was reported as another JH-inducible gene in *Tribolium* larvae (Minakuchi et al., 2009; Zhang et al., 2011). In *Drosophila*, the *E75A* gene appears to be under dual hormonal regulation and can be activated by either JH or ecdysone (Dubrovsky et al., 2004). The studies by Mao et al. (2020) and Saha et al. (2019) reported on the crucial role of both *Kr-h1* and *Hairy* in mediating JH signalling in the brown planthopper, *N. lugens* and in the mosquito, *A. aegypti*. Furthermore, several studies report on the role of JH in promoting cell polyploidization and chaperones activity for *L. migratoria* vitellogenesis and egg production. Wu et al. (2018) reported that JH regulates the expression of *cyclin-dependent kinase 6* and *adenovirus E2 factor-1*, the core mediators in cell cycle progression. Moreover, Wu et al. (2018) demonstrated the regulatory role of JH on the expression of *78-kDa glucose-regulated protein*, one of the most abundant chaperones in the endoplasmic reticulum folding newly synthesized peptides. Guo et al. (2014) suggested that the JH-receptor complex acts on *mini-chromosome maintenance 4* and *7* to regulate DNA replication and polyploidy for vitellogenesis and oocyte maturation. Two years later, the involvement of Cell-division-cycle 6 in the JH pathway was indicated as well (Z. Wu et al., 2016). These JH-inducible genes are worth investigating in locusts, but the question whether, apart from these genes, still other transcription factors mediate JH signalling downstream of Met, remains to be answered as well. When scanning the genomes of both *L. migratoria* and *S. gregaria*, no similar genes or homologs of the MEKRE93 pathway components are found, but a more in-depth study is recommended. Besides scanning the genomes, the *L. migratoria* and *S. gregaria* transcriptomes can also be browsed, scanning the MEKRE93 pathway components in order to find transcripts of different lengths. These transcripts can subsequently be loaded into a conserved domain search checking for potentially different outcomes. When checking for possible isoforms, specific software is available (*e.g*. AUGUSTUS) predicting splicing based on a reference genome. In this way, we may get an idea if and where alternative splicing can occur and subsequently if isoforms do exist.

Altogether, we can conclude that, although the MEKRE93 pathway is already investigated intensively, more than likely other (unknown) factors may influence this pathway. Moreover, we speculate that these factors may differ depending on the insect's stage (nymph/adult), feeding habits, environmental stressors, *etc*. Future knockdown experiments of the targets of interest (other JH receptors and JH-inducible genes), would probably enable a better interpretation of these data.

7.5.2.2 Functional interactions with other signalling pathways

Investigating functional interactions with other signalling pathways would be of great value as well. The question how the moulting process and female reproductive physiology in locusts is exactly regulated is still to be answered. For sure, an intricate interplay between different hormonal pathways is present, but how these pathways interact with each other remains to be elucidated (Figure 7.1). When focussing on moulting, monitoring the expression of *Broad-Complex* (*Br-C*) in response to JH titres would probably be of interest. In holometabolan insects, JH acts through Met to regulate *Kr-h1* and *Br-C*. While Met and Kr-h1 prevent precocious metamorphosis (Konopova and Jindra, 2007; Minakuchi et al., 2009), Br-C specifies the pupal stage (Kiss et al., 1988; Konopova and Jindra, 2008; Parthasarathy et al., 2008; Suzuki et al., 2008; Uhlirova et al., 2003; Zhou and Riddiford, 2002). The function of Br-C in post-embryonic development of hemimetabolan insects, including locusts, is poorly understood. Br-C seems to be required for anisometric growth of the larval wing pads of the milkweed bug, *Oncopeltus fasciatus* (Erezyilmaz et al., 2006), but no function is related to metamorphosis. It would be interesting to also investigate *Br-C* expression in adultoid and supernumerary nymphal phenotypes, as aberrations in wing development were observed in these animals. Moreover, a temporal profile of relative *Br-C* transcript levels throughout the different nymphal stages of *L. migratoria* and *S. gregaria* would give more insights in the possible role of *Br-C* in post-embryonic development. Besides studying Br-C in regulating the growth of larval wing pads, functional interactions with other signalling pathways are also worth being investigated in more detail. While JH determines the nature of the moult, ecdysteroids trigger the moulting process and activate a neuropeptide signalling cascade, which in turn regulates ecdysis at the end of the moulting cycle. For a more in depth review on the neuroendocrine regulation of ecdysis, the reader is referred to Zitnan and Adams (2012). As we observed moulting defects when knocking down *Kr-h1* and *E93* in nymphal *L. migratoria* and *S. gregaria,* respectively, the question arises whether this neuroendocrine signalling cascade was affected. In a next experiment, more focus on ecdysis might contribute to a better understanding of the observed moulting defects. Ecdysis triggering hormone (ETH), eclosion hormone (EH) and crustacean cardioactive peptide (CCAP) are candidate genes for this study. Especially ETH is worth investigating in more detail, as Lenaerts et al. (2017) already showed its crucial role in regulating ecdysis in *S. gregaria*.

When focussing on female reproductive physiology, unravelling the possible role(s) of ETH in adult female locusts may also be worth investigating. ETH was originally discovered and characterized as a peptide produced in epitracheal glands, that functions as the signal initiating ecdysis in juvenile insects. Recently, Meiselman et al. (2017) reported that ETH also plays a role in adult *D. melanogaster* through promoting JH biosynthesis and subsequently reproduction, since JH titres, ovary size, egg production and yolk deposition in mature oocytes were reduced upon negatively affecting ETH signalling. In both *L. migratoria* and *S. gregaria*, an oviduct derived Patency Inducing Factor (PIF) is involved in the initiation of patency in the terminal follicle via the pedicel and its action is boosted by JH (Seidelmann et al., 2016). Therefore, analysing relative *PIF* transcript levels in control and knockdown locusts would probably contribute to a better understanding of the process of oocyte maturation. *Greglin*, a gene coding for Kazal-type protease inhibitor, is also demonstrated to play a significant role in the female reproductive physiology of locusts. Knockdown of *Greglin* in adult female *L. migratoria* resulted in blocked oocyte maturation, arrested ovarian growth and shrunken follicular epithelium as well as declines in egg number and hatchability (Guo et al., 2019). The ISP plays a crucial role in the trade-off between reproduction and survival in insects, but whether this role of the ISP is mediated by JH and/or 20E, or *vice versa,* remains unclear. Studying the ISP in knockdown locusts in more detail may contribute to elucidating the intricate cross-talk between IRP, JH and 20E. Studying the functional interactions with other signalling pathways would most likely result in the identification of new candidate genes that are worthy of thorough investigation. Via RNAi-mediated knockdown studies, the role of these genes can be studied in more detail.

7.5.2.3 Elucidating the supernumerary nymphal phenotype in more detail

Supernumerary nymphal stages were observed upon knocking down *SgE93* in late nymphal *S. gregaria*. Besides clear differences in expression levels of the MEKRE93 pathway components *E93* and *Kr-h1*, a temporal shift in the ecdysteroid profile in haemolymph was observed, as well as altered transcript levels of *SgSpo*, *SgEcR* and *SgRXR*. However, it was difficult to properly investigate the supernumerary nymphal stages as a reliable control, *i.e*. a sixth nymphal control stage, was missing. Interestingly, the study of solitarious locusts may solve this issue, since for locusts in the (extreme) solitary phase an additional moult has been observed, *i.e.* a moult to a sixth and final nymphal stage. Nevertheless, we need to keep in mind that these locusts would then be solitarious and therefore differ in many aspects from gregarious locusts.

As *S. gregaria* and *L. migratoria* belong to the same family, but to a different subfamily, it would also be interesting to investigate the function of *E93* in the migratory locust. Downregulating *LmE93* in *L. migratoria* results in similar supernumerary stages (Figure 7.2; unpublished data). These observations point towards a conserved role of the MEKRE93 pathway components in locusts. However, the molecular consequences of an RNAi-mediated silencing of *LmE93* are still to be elucidated in detail.

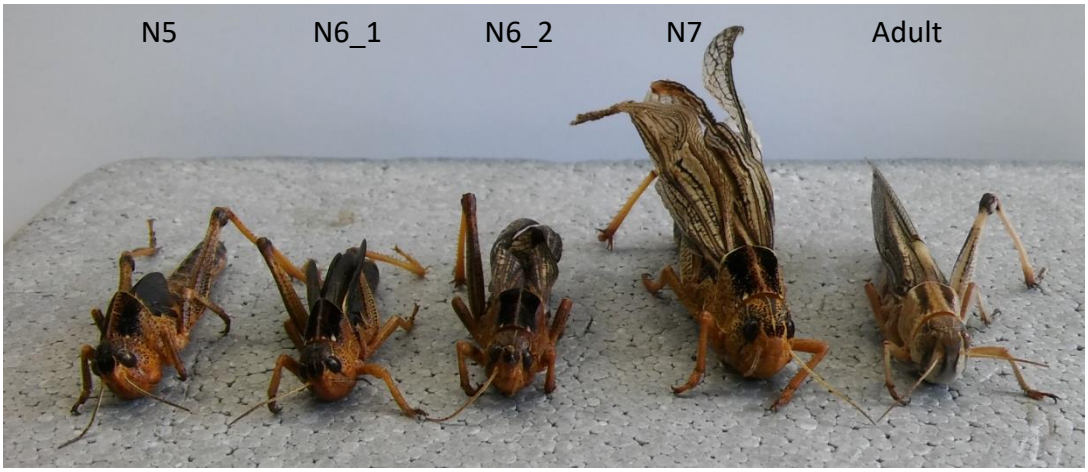

Figure 7.2: Representation of the final fifth (N5) to adult stage, including the observed supernumerary nymphal stages (N6 and N7) obtained upon silencing *LmE93*. The final nymphal stage (N5), the adult stage and two supernumerary nymphal stages (N6 and N7) that were observed upon injection of *dsLmE93* are shown.

7.5.2.4 Unravelling the story behind the adultoid reproductive physiology

Via downregulating *Kr-h1* in penultimate nymphal *L. migratoria,* an adultoid phenotype was observed, characterised by an accelerated ovarian maturation. These adultoid females, however, had major difficulties in copulating with virgin control males and in depositing their eggs successfully. In order to explain these severe defects in mating and oviposition, a follow-up experiment closely observing male and female genitals, as well as mating behaviour and oviposition (monitoring of attempts as well as successful copulation/egg laying) may be planned. Different experimental outcomes are plausible and may be explained as follows:

i) Adultoid females lack essential signals (or the responsiveness to these signals) to successfully copulate and/or oviposit. Adult locusts (*dsGFP* control group) were approximately four days older than the adultoid females, because their adult moult was preceded by a fifth larval stage. In addition, adultoid females are also classified as an adult-like phenotype showing precocious development of adult features, raising the question whether they are all fully capable of inducing and/or responding to all signals necessary to successfully copulate and/or oviposit.

ii) Adultoid females are physiologically competent of producing and responding to all signals needed for successful copulation and oviposition, but an abnormal size/morphology of their external genitals causes severe defects in mating and oviposition.

iii) Adultoid females lack essential signals (or the responsiveness to these signals) to successfully copulate and/or oviposit and have an abnormal genital size/morphology. These physiological and anatomical defects would then explain the inability of (most) adultoid females to copulate and oviposit.

The reasons mentioned above may explain why we observed defects in oviposition in adultoid females. Although all females did ovulate and attempted to deposit their eggs, only two females, which had succeeded in mating, effectively deposited their eggs. It has been reported that copulation in *L. migratoria* induces physiological and endocrinological changes in the female resulting in appropriate maturation of the eggs and the subsequent deposition of fertile eggs in a suitable environment (Lange, 2009a). Still, the exact reasons why most of the adultoid females did not copulate and oviposit remain elusive. The observed reproductive defects may either be due to an incapability of adultoid females to induce and/or respond to signals necessary to successfully copulate/oviposit, or to an abnormal size/morphology of the external genitals. Although we did not observe clear morphological defects, we did not study their detailed structure, musculature or innervation. We currently hypothesize that the clearly reduced ovipositor size, while the eggs were similar in size to these in adult females, may already have caused major difficulties in egg deposition. The proposed follow-up experiments could help in elucidating remaining questions. In addition, it may also be of interest to further investigate the reproductive characteristics of adultoid males.

7.5.3 Quantification of JH titers

An up and running protocol to quantify JH titers would benefit all future experiments. Currently, many research groups try to assess the involvement of JH signaling in regulating certain processes by measuring the transcript levels of the downstream immediate early gene *Kr-h1,* and/or by analysing the expression levels of genes involved in JH biosynthesis, such as *JHAMT* and *CYP15A1*, the enzymes catalysing the last two steps, with JHAMT acting as the main rate-limiting enzyme (Huang et al., 2015; Marchal et al., 2011b; Mayoral et al., 2009; Shinoda and Itoyama, 2003). Moreover, comparing CA gland sizes may offer additional evidence, since CA that have high JH biosynthetic activity are larger in size when compared to glands with reduced activity. Although these parameters allow for making strong assumptions, quantifying JH titres would directly help in interpreting functional data. Although different JH quantification methods have been described in literature, it is very difficult to accurately quantify JH in biological samples. Recently, an extraction protocol followed by a high-performance liquid chromatography-electrospray ionisation-mass spectrometry/mass spectrometry (HPLC-ESI-MS/MS) analysis has generated high expectations, because it has increased sensitivity and reproducibility while reducing the analysis time for JHIII detection. For a detailed description of this procedure, the reader is referred to Ramirez et al. (2016). JH levels are not solely dependent on JH biosynthesis, JH degradation plays an important role as well. In this context, it would be of great value to also determine JH esterase activity. Using the JH esterase activity assay, as described by Gu and Zera (1994), the JH degrading activity in haemolymph can be calculated. However, when measuring JH metabolising activities in other tissues than the haemolymph, a more complicated assay is needed because other tissues also contain JH-epoxide hydrolase in addition to JH esterase. Quantifying JH titers, JH biosynthetic enzyme expression and JH esterase activity would shed more light on the observed compensatory effects upon

knocking down JH pathway related genes. For instance, the observed accelerated ovarian maturation upon knocking down *Kr-h1* in penultimate nymphal *L. migratoria*, can perhaps be related to elevated JH titers. Although *Kr-h1* relative transcript levels are significantly higher, the effect on expression of JH biosynthesis genes is less clear (with only *CYP15A1* showing higher relative transcript levels). Using the above-mentioned protocol to quantify JH titers, temporal changes of JH in relation to the accelerated ovarian maturation may be analysed. The JH esterase activity protocol would also give more insights on the possible role of JH degradation in the temporal dynamics of JH titres in relation to the observed phenotypes.

7.5.4 dsRNA and miRNAs as novel insect control agents

RNAi has provided a novel and powerful reverse genetics tool for identifying gene functions, but has also shown great potential in pest management (Cai et al., 2018a; Kim et al., 2015; Mamta and Rajam, 2017; Nandety et al., 2015). A promising area is the development of transgenic crops expressing dsRNA against key genes of insect pests (Baum et al., 2007; Gordon and Waterhouse, 2007; Head et al., 2017; Yan et al., 2020). When taking into account the major problems that are still caused by migrating locust swarms in many countries worldwide, RNAi-based strategies targeting JH signalling pathway components that proved to be crucial for locust development and reproduction would probably be also a very effective means to control locust population growth, swarm formation and expansion.

Locusts usually live a solitary lifestyle, making them relatively harmless as they do not cause severe crop damage. However, under certain environmental conditions, the population can build up rapidly, forming enormous insect armies eating everything on their path (Symmons and Cressman, 2001). Metamorphosis and reproduction are two vital insect processes playing a crucial role in locust swarm formation. Using RNAi, we aimed at elucidating the role of the MEKRE93 pathway components. These components were indeed found to be essential in regulating metamorphosis and reproduction. In turn, this knowledge could now be used in the search for more locust-selective control strategies. In fact, the commercialisation of several Insect Growth Regulators (IGRs) has proven that the search for new insecticides, screened for biochemical/physiological targets that are specific to the pest species, is possible (Grafton-Cardwell et al., 2005; Smagghe et al., 2002; Sundaram et al., 1998; Ware and Whitacre, 2003). Many of these IGRs are analogs of the classic insect hormones, JH and 20E, the key players in developmental-physiological processes in insects. In locusts, these hormones and their signalling pathway components are implicated in control of metamorphosis and reproduction. Moreover, many plant species possess compounds with JH hormone disrupter activity. Plant JH disrupter diterpenes disrupt insect development by interfering with the JH-mediated formation of JH receptor complexes (Lee et al., 2015; Oh et al., 2017; Shin et al., 2018). An advantage of using the RNAi technology would be that unique sequence regions in the gene of interest can be selected, thereby increasing the specificity (to avoid targeting other genes and species) of the approach.

The use of artificial miRNA a(nta)gomiRs targeting JH and/or ecdysteroid signalling pathway components may also contribute to the future discovery of novel locust control strategies. Via regulating gene expression at the post-transcriptional level, miRNAs constitute an additional level of control. The study by Yogindran and Rajam (2020) nicely illustrates the potential of miRNAs in controlling the lepidopteran pest, *Helicoverpa armigera*. In all probability, more studies uncovering the possible role of miRNAs as a pest control strategy will be published in the near future.

7.5.5 The limitations of RNAi

Although RNAi technology has important applications in the field, there are also limitations (as reviewed by Vogel et al. (2019)). The use of RNAi only leads to a partial and temporal reduction of gene expression. Moreover, RNAi might also lead to off-target effects and is not inherited in locusts (Nandety et al., 2015). Furthermore, the efficiency of the induced RNAi response may vary between species and even between tissues within the same organism (Belles, 2010; Wynant et al., 2014b; Xu et al., 2016). In line with the study of Wynant et al. (2012), we observed an inefficient knockdown in the female reproductive system of *dsLmKr-h1*- and *dsSgMet*-treated locusts. The exact nature of this variable efficiency remains to be discovered, but tissue or cell-type dependent differences in dsRNA-degrading activity, in dsRNA-uptake mechanisms and in expression of core components of the cell-autonomous RNAi-machinery would probably have an important impact. Packaging dsRNA in such a way that it is protected against degradation and uptake is facilitated could solve the main problems encountered by insufficient RNAi sensitivity. This may be achieved through the use of dsRNA delivery systems (Vogel et al., 2019).

Gene editing by 'Clustered Interspaced Short Palindromic Repeat' (CRISPR) technology could represent an alternative, but more time-consuming research strategy. This method is based on an adaptive mechanism through which bacterial and archaeal species can resist invading viruses and phages or plasmids. The system has been classified into three major types (I, II and III) based on the CRISPR-associated (*Cas*) gene and CRISPR sequence. The most explored for genome editing to date is the type II CRISPR-Cas system which involves only one Cas9 protein that forms a complex with CRISPR RNA and trans-activating CRISPR RNA. Cas9 can cleave target genes when the functional complex recognizes the proton spacer-adjacent motif (PAM) sequence NGG (N is A, T, C or G). Due to its high specificity and applicability, CRISPR/Cas9-mediated gene editing has been employed in a multitude of organisms and cells. Although CRISPR/Cas9 has fallen behind its exploding popularity in mammalian studies, CRISPR/Cas9 applications in insects have been reported increasingly (as reviewed by Sun et al. (2017) and Taning et al. (2017)). The studies by Li et al. (2016) and Guo et al. (2020) nicely illustrate the potential of the CRISPR/Cas9 technology in the migratory locust, *L. migratoria*, opening new avenues to study gene functions.

References

Abdel-latief, M., Hoffmann, K.H., 2010. Neuropeptide regulators of the juvenile hormone biosynthesis (*in vitro*) in the beetle, *Tenebrio molitor* (coleoptera, tenebrionidae). Arch. Insect Biochem. Physiol. 74, 135–146. https://doi.org/10.1002/arch.20359

Abdel-Latief, M., Hoffmann, K.H., 2014. Functional activity of allatotropin and allatostatin in the pupal stage of a holometablous insect, *Tribolium castaneum* (Coleoptera, Tenebrionidae). Peptides 53, 172–184. https://doi.org/10.1016/j.peptides.2013.10.007

Abrisqueta, M., Süren-Castillo, S., Maestro, J.L., 2014. Insulin receptor-mediated nutritional signalling regulates juvenile hormone biosynthesis and vitellogenin production in the German cockroach. Insect Biochem. Mol. Biol. 49, 14–23. https://doi.org/10.1016/j.ibmb.2014.03.005

Acuña, S.M., Floeter-Winter, L.M., Muxel, S.M., 2020. MicroRNAs: Biological Regulators in Pathogen-Host Interactions. Cells 9, 1–25. https://doi.org/10.3390/cells9010113

Agawa, Y., Sarhan, M., Kageyama, Y., Akagi, K., Takai, M., Hashiyama, K., Wada, T., Handa, H., Iwamatsu, A., Hirose, S., Ueda, H., 2007. *Drosophila* Blimp-1 is a transient transcriptional repressor that controls timing of the ecdysone-induced developmental pathway. Mol. Cell. Biol. 27, 8739–8747. https://doi.org/10.1128/MCB.01304-07

Akat, K.M., Moore-McGriff, D., Morozov, P., Brown, M., Gogakos, T., Correa Da Rosa, J., Mihailovic, A., Sauer, M., Ji, R., Ramarathnam, A., Totary-Jain, H., Williams, Z., Tuschl, T., Schulze, P.C., 2014. Comparative RNA-sequencing analysis of myocardial and circulating small RNAs in human heart failure and their utility as biomarkers. Proc. Natl. Acad. Sci. 111, 11151–11156. https://doi.org/10.1073/pnas.1401724111

Altschul, S.F., Gish, W., Miller, W., Myers, E.W., Lipman, D.J., 1990. Basic local alignment search tool. J. Mol. Biol. 215, 403–410. https://doi.org/10.1016/S0022-2836(05)80360-2

Amanda, M., Bajracharya, S.D., Yuen, P.S.T., Zhou, H., Star, R.A., Illei, G.G., Alevizos, Ll., 2010. Exosomes from Human Saliva as a Source of microRNA Biomarkers. Oral Dis. 16, 34–38. https://doi.org/10.1111/j.1601-0825.2009.01604.x.Exosomes

Ambros, V., 2004. The functions of animal microRNAs. Nature 431, 350–355. https://doi.org/10.1038/nature02871

Aravin, A., Lagos-Quintana, M., Yalcin, A., 2003. The Small RNA Profile during *Drosophila melanogaster* Development. Dev. Cell 5, 337–350. https://doi.org/10.1016/S1534-5807(03)00228-4

Aribi, N., Pitoizet, N., Quennedey, A., Delbecque, J.P., 1997. 2-Deoxyecdysone is a circulating ecdysteroid in the beetle *Zophobas atratus*. Biochim. Biophys. Acta - Gen. Subj. 1335, 246–252. https://doi.org/10.1016/S0304-4165(96)00144-4

Arroyo, J.D., Chevillet, J.R., Kroh, E.M., Ruf, I.K., Pritchard, C.C., Gibson, D.F., Mitchell, P.S., Bennett, C.F., Pogosova-Agadjanyan, E.L., Stirewalt, D.L., Tait, J.F., Tewari, M., 2011. Argonaute2 complexes carry a population of circulating microRNAs independent of vesicles in human plasma. Proc. Natl. Acad. Sci. 108, 5003–5008. https://doi.org/10.1073/pnas.1019055108

Asgari, S., 2013. MicroRNA functions in insects. Insect Biochem. Mol. Biol. 43, 388–397. https://doi.org/10.1016/j.ibmb.2012.10.005

Audsley, N., Vandersmissen, H.P., Weaver, R., Dani, P., Matthews, J., Down, R., Vuerinckx, K., Kim, Y.J., Vanden Broeck, J., 2013. Characterisation and tissue distribution of the PISCF allatostatin receptor in the red flour beetle, *Tribolium castaneum*. Insect Biochem. Mol. Biol. 43, 65–74. https://doi.org/10.1016/j.ibmb.2012.09.007

Audsley, N., Weaver, R.J., Edwards, J.P., 1999. The significance of *Manduca sexta* allatostatin in the tomato moth *Lacanobia oleracea*. Ann. N. Y. Acad. Sci. 897, 330–341. https://doi.org/10.1111/j.1749-6632.1999.tb07903.x

Badisco, L., Claeys, I., Van Hiel, M., Clynen, E., Huybrechts, J., Vandersmissen, T., Van Soest, S., Vanden Bosch, L., Simonet, G., Broeck, J. Vanden, 2008. Purification and characterization of an insulin-related peptide in the desert locust, *Schistocerca gregaria*: Immunolocalization, cDNA cloning, transcript profiling and interaction with neuroparsin. J. Mol. Endocrinol. 40, 137–150. https://doi.org/10.1167/JME-07-0161

Badisco, L., Claeys, I., Van Loy, T., Van Hiel, M., Franssens, V., Simonet, G., Broeck, J. Vanden, 2007. Neuroparsins, a family of conserved arthropod neuropeptides. Gen. Comp. Endocrinol. 153, 64–71.

https://doi.org/10.1016/j.ygcen.2007.03.008

Badisco, L., Marchal, E., Van Wielendaele, P., Verlinden, H., Vleugels, R., Vanden Broeck, J., 2011. RNA interference of insulin-related peptide and neuroparsins affects vitellogenesis in the desert locust *Schistocerca gregaria*. Peptides 32, 573–580. https://doi.org/10.1016/j.peptides.2010.11.008

Badisco, L., Van Wielendaele, P., Vanden Broeck, J., 2013. Eat to reproduce: a key role for the insulin signaling pathway in adult insects. Front. Physiol. 4, 1–16. https://doi.org/10.3389/fphys.2013.00202

Baehrecke, E.H., Thummel, C.S., 1995. The Drosophila *E93* Gene from the 93F Early Puff Displays Stage- and Tissue-Specific Regulation by 20-Hydroxyecdysone. Dev. Biol. 171, 85–97. https://doi.org/10.1006/dbio.1995.1262

Bartel, D.P., 2004. MicroRNAs: Genomics, Biogenesis, Mechanism, and Function. Cell 116, 281–297. https://doi.org/10.1016/S0092-8674(04)00045-5

Baum, J.A., Bogaert, T., Clinton, W., Heck, G.R., Feldmann, P., Ilagan, O., Johnson, S., Plaetinck, G., Munyikwa, T., Pleau, M., Vaughn, T., Roberts, J., 2007. Control of coleopteran insect pests through RNA interference. Nat. Biotechnol. 25, 1322–1326. https://doi.org/10.1038/nbt1359

Behr, M., Hoch, M., 2005. Identification of the novel evolutionary conserved obstructor multigene family in invertebrates. FEBS Lett. 579, 6827–6833. https://doi.org/10.1016/j.febslet.2005.11.021

Behura, S.K., Whitfield, C.W., 2010. Correlated expression patterns of microRNA genes with age-dependent behavioural changes in honeybee. Insect Mol. Biol. 19, 431–439. https://doi.org/10.1111/j.1365-2583.2010.01010.x

Bejarano, F., Smibert, P., Lai, E.C., 2010. miR-9a prevents apoptosis during wing development by repressing *Drosophila* LIM-only. Dev. Biol. 338, 63–73. https://doi.org/10.1016/j.ydbio.2009.11.025

Belles, X., 2019. Krüppel homolog 1 and E93: The doorkeeper and the key to insect metamorphosis. Arch. Insect Biochem. Physiol. e21609, 1–8. https://doi.org/10.1002/arch.21609

Belles, X., 2017. MicroRNAs and the evolution of insect metamorphosis. Annu. Rev. Entomol. 62, 111–125. https://doi.org/10.1146/annurev-ento-031616-034925

Belles, X., 2010. Beyond Drosophila: RNAi in vivo and functional genomics in insects. Annu. Rev. Entomol. 55, 111–128. https://doi.org/10.1146/annurev-ento-112408-085301

Belles, X., Cassier, P., Cerdá, X., Pascual, N., André, M., Rósso, Y., Piulachs, M.D., 1993. Induction of choriogenesis by 20-hydroxyecdysone in the german cockroach. Tissue Cell 25, 195–204. https://doi.org/10.1016/0040-8166(93)90019-H

Belles, X., Piulachs, M.D., 2015. Ecdysone signalling and ovarian development in insects: From stem cells to ovarian follicle formation. Biochim. Biophys. Acta - Gene Regul. Mech. 1849, 181–186. https://doi.org/10.1016/j.bbagrm.2014.05.025

Belles, X., Santos, C.G., 2014. The MEKRE93 (Methoprene tolerant-Krüppel homolog 1-E93) pathway in the regulation of insect metamorphosis, and the homology of the pupal stage. Insect Biochem. Mol. Biol. 52, 60–68. https://doi.org/10.1016/j.ibmb.2014.06.009

Bendena, W.G., Hui, J.H.L., Chin-Sang, I., Tobe, S.S., 2020. Neuropeptide and microRNA regulators of juvenile hormone production. Gen. Comp. Endocrinol. 295, 113507. https://doi.org/10.1016/j.ygcen.2020.113507

Berezikov, E., 2011. Evolution of microRNA diversity and regulation in animals. Nat. Rev. Genet. 12, 846–860. https://doi.org/10.1038/nrg3079

Bergerard, J., Seugé, J., 1959. La parthénogenèse accidentelle chez *Locusta migratoria L*. Bull Biol Fr Belg 93, 16–37.

Bernstein, E., Caudy, A.A., Hammond, S.M., Hannon, G.J., 2001. Role for a bidentate ribonuclease in the initiation step of RNA interference. Nature 409, 363–366. https://doi.org/10.1038/35053110

Bilen, J., Atallah, J., Azanchi, R., Levine, J.D., Riddiford, L.M., 2013. Regulation of onset of female mating and sex pheromone production by juvenile hormone in *Drosophila melanogaster*. Proc. Natl. Acad. Sci. U. S. A. 110, 18321–18326. https://doi.org/10.1073/pnas.1318119110

Billen, J., 2006. Morphology and ultrastructure of the Dufour gland in workers of social wasps (Hymenoptera, Vespidae). Arthropod Struct. Dev. 35, 77–84. https://doi.org/10.1016/j.asd.2006.01.002

Brown, M.R., Clark, K.D., Gulia, M., Zhao, Z., Garczynski, S.F., Crim, J.W., Suderman, R.J., Strand, M.R., 2008. An insulin-like peptide regulates egg maturation and metabolism in the mosquito *Aedes aegypti*. Proc. Natl. Acad. Sci. 105, 5716–5721. https://doi.org/10.1073/pnas.0800478105

Brown, M.R., Graf, R., Swiderek, K.M., Fendley, D., Stracker, T.H., Champagne, D.E., Lea, A.O., 1998.

Identification of a steroidogenic neurohormone in female mosquitoes. J. Biol. Chem. 273, 3967–3971. https://doi.org/10.1074/jbc.273.7.3967

Buck, A.H., Coakley, G., Simbari, F., McSorley, H.J., Quintana, J.F., Le Bihan, T., Kumar, S., Abreu-Goodger, C., Lear, M., Harcus, Y., Ceroni, A., Babayan, S.A., Blaxter, M., Ivens, A., Maizels, R.M., 2014. Exosomes secreted by nematode parasites transfer small RNAs to mammalian cells and modulate innate immunity. Nat. Commun. 5, 5488. https://doi.org/10.1038/ncomms6488

Butenandt, A., Karlson, P., 1954. Über die Isolierung eines Metamorphose-Hormons der Insekten in kristallisierter Form. Zeitschrift fur Naturforsch. - Sect. B J. Chem. Sci. 9, 389–391. https://doi.org/10.1515/znb-1954-0601

Cai, Q., He, B., Kogel, K.H., Jin, H., 2018a. Cross-kingdom RNA trafficking and environmental RNAi — nature's blueprint for modern crop protection strategies. Curr. Opin. Microbiol. 46, 58–64. https://doi.org/10.1016/j.mib.2018.02.003

Cai, Q., Qiao, L., Wang, M., He, B., Lin, F.M., Palmquist, J., Huang, S. Da, Jin, H., 2018b. Plants send small RNAs in extracellular vesicles to fungal pathogen to silence virulence genes, Science. https://doi.org/10.1126/science.aar4142

Carlone, M., Sestito, D., 2020. "There's nothing left" – Sardinian farmland stripped by locust swarms [WWW Document]. CGTN. URL https://newseu.cgtn.com/news/2020-06-25/-There-s-nothing-left-Sardinian-farmland-stripped-by-locust-swarms-RzaYxkBVuw/index.html (accessed 8.14.20).

Castoldi, M., Kordes, C., Sawitza, I., Häussinger, D., 2016. Isolation and characterization of vesicular and non-vesicular microRNAs circulating in sera of partially hepatectomized rats. Sci. Rep. 6, 31869. https://doi.org/10.1038/srep31869

Caygill, E.E., Johnston, L.A., 2008. Temporal Regulation of Metamorphic Processes in *Drosophila* by the let-7 and miR-125 Heterochronic MicroRNAs. Curr. Biol. 18, 943–950. https://doi.org/10.1016/j.cub.2008.06.020

Chafino, S., López-Escardó, D., Benelli, G., Kovac, H., Casacuberta, E., Franch-Marro, X., Kathirithamby, J., Martín, D., 2018. Differential expression of the adult specifier E93 in the strepsipteran *Xenos vesparum Rossi* suggests a role in female neoteny. Sci. Rep. 8, 14176. https://doi.org/10.1038/s41598-018-32611-y

Chafino, S., Ureña, E., Casanova, J., Casacuberta, E., Franch-Marro, X., Martín, D., 2019. Upregulation of *E93* gene expression acts as the trigger for metamorphosis independently of the threshold size in the beetle *Tribolium castaneum*. Cell Rep. 27, 1039–1049. https://doi.org/10.1016/j.celrep.2019.03.094

Chapman, R.F., 2012. The Insects: Structure and Function, in: Cambridge University Press. p. 5th ed.

Charles, J.-P., Iwema, T., Epa, V.C., Takaki, K., Rynes, J., Jindra, M., 2011. Ligand-binding properties of a juvenile hormone receptor, Methoprene-tolerant. Proc. Natl. Acad. Sci. U. S. A. 108, 21128–21133. https://doi.org/10.1073/pnas.1116123109

Chávez, V.M., Marqués, G., Delbecque, J.P., Kobayashi, K., Hollingsworth, M., Burr, J., Natzle, J.E., O'Connor, M.B., 2000. The *Drosophila disembodied* gene controls late embryonic morphogenesis and codes for a cytochrome P450 enzyme that regulates embryonic ecdysone levels. Development 127, 4115–4126. https://doi.org/8223268

Chawla, G., Sokol, N.S., 2011. MicroRNAs in *Drosophila* development. Int. Rev. Cell Mol. Biol. 286, 1–65. https://doi.org/10.1016/B978-0-12-385859-7.00001-X

Chen, J., Liang, Z., Liang, Y., Pang, R., Zhang, W., 2013. Conserved microRNAs miR-8-5p and miR-2a-3p modulate chitin biosynthesis in response to 20-hydroxyecdysone signaling in the brown planthopper, *Nilaparvata lugens*. Insect Biochem. Mol. Biol. 43, 839–848. https://doi.org/10.1016/j.ibmb.2013.06.002

Chen, X., Ba, Y., Ma, L., Cai, X., Yin, Y., Wang, K., Guo, J., Zhang, Yujing, Chen, J., Guo, X., Li, Q., Li, X., Wang, W., Zhang, Yan, Wang, Jin, Jiang, X., Xiang, Y., Xu, C., Zheng, P., Zhang, Juanbin, Li, R., Zhang, H., Shang, X., Gong, T., Ning, G., Wang, Jun, Zen, K., Zhang, Junfeng, Zhang, C.Y., 2008. Characterization of microRNAs in serum: A novel class of biomarkers for diagnosis of cancer and other diseases. Cell Res. 18, 997–1006. https://doi.org/10.1038/cr.2008.282

Claeys, I., Breugelmans, B., Simonet, G., Franssens, V., Van Soest, S., Vanden Broeck, J., 2006a. Regulation of *Schistocerca gregaria* neuroparsin transcript levels by juvenile hormone and 20-hydroxyecdysone. Arch. Insect Biochem. Physiol. 62, 107–115. https://doi.org/10.1002/arch.20127

Claeys, I., Breugelmans, B., Simonet, G., Soest, S. Van, Sas, F., De Loof, A., Broeck, J. Vanden, 2006b.

Neuroparsin transcripts as molecular markers in the process of desert locust (*Schistocerca gregaria*) phase transition. Biochem. Biophys. Res. Commun. 341, 599–606. https://doi.org/10.1016/j.bbrc.2006.01.011

Claeys, I., Simonet, G., Breugelmans, B., Van Soest, S., Franssens, V., Sas, F., De Loof, A., Vanden Broeck, J., 2005. Quantitative real-time RT-PCR analysis in desert locusts reveals phase dependent differences in neuroparsin transcript levels. Insect Mol. Biol. 14, 415–422. https://doi.org/10.1111/j.1365-2583.2005.00572.x

Claeys, I., Simonet, G., Poels, J., Van Loy, T., Vercammen, L., De Loof, A., Vanden Broeck, J., 2002. Insulin-related peptides and their conserved signal transduction pathway. Peptides 23, 807–816. https://doi.org/10.1016/S0196-9781(01)00666-0

Coast, G.M., Schooley, D.A., 2011. Toward a consensus nomenclature for insect neuropeptides and peptide hormones. Peptides 32, 620–631. https://doi.org/10.1016/j.peptides.2010.11.006

Corsten, M.F., Dennert, R., Jochems, S., Kuznetsova, T., Devaux, Y., Hofstra, L., Wagner, D.R., Staessen, J.A., Heymans, S., Schroen, B., 2010. Circulating MicroRNA-208b and MicroRNA-499 reflect myocardial damage in cardiovascular disease. Circ. Cardiovasc. Genet. 3, 499–506. https://doi.org/10.1161/CIRCGENETICS.110.957415

Creemers, E.E., Tijsen, A.J., Pinto, Y.M., 2012. Circulating MicroRNAs. Circ. Res. 110, 483–495. https://doi.org/10.1161/circresaha.111.247452

Cristino, A.S., Tanaka, E.D., Rubio, M., Piulachs, M.D., Belles, X., 2011. Deep sequencing of organ- and stage-specific micrornas in the evolutionarily basal insect *Blattella germanica* (L.) (Dictyoptera, Blattellidae). PLoS One 6, e19350. https://doi.org/10.1371/journal.pone.0019350

Cruz, J., Mané-Padrós, D., Bellés, X., Martín, D., 2006. Functions of the ecdysone receptor isoform-A in the hemimetabolous insect *Blattella germanica* revealed by systemic RNAi *in vivo*. Dev. Biol. 279, 158–171. https://doi.org/10.1016/j.ydbio.2006.06.048

Czech, B., Zhou, R., Erlich, Y., Brennecke, J., Binari, R., Villalta, C., Gordon, A., Perrimon, N., Hannon, G.J., 2009. Hierarchical Rules for Argonaute Loading in *Drosophila*. Mol. Cell 36, 445–456. https://doi.org/10.1016/j.molcel.2009.09.028

Davey, K., 2007. The interaction of feeding and mating in the hormonal control of egg production in *Rhodnius prolixus*. J. Insect Physiol. 53, 208–215. https://doi.org/10.1016/j.jinsphys.2006.10.002

Davey, K.G., 2000. The modes of action of juvenile hormones: Some questions we ought to ask. Insect Biochem. Mol. Biol. 30, 663–669. https://doi.org/10.1016/S0965-1748(00)00037-0

Davey, K.G., Sevala, V.L., Gordon, D.R.B., 1993. The action of juvenile hormone and antigonadotropin on the follicle cells of *Locusta migratoria*. Invertebr. Reprod. Dev. 24, 39–45. https://doi.org/10.1080/07924259.1993.9672329

Davis, M.B., Carney, G.E., Robertson, A.E., Bender, M., 2005. Phenotypic analysis of EcR-A mutants suggests that EcR isoforms have unique functions during *Drosophila* development. Dev. Biol. 282, 385–396. https://doi.org/10.1016/j.ydbio.2005.03.019

De Mendonça, R.L., Bouton, D., Bertin, B., Escriva, H., Noël, C., Vanacker, J.M., Cornette, J., Laudet, V., Pierce, R.J., 2002. A functionally conserved member of the FTZ-F1 nuclear receptor family from *Schistosoma mansoni*. Eur. J. Biochem. 269, 5700–5711. https://doi.org/10.1046/j.1432-1033.2002.03287.x

Defelipe, L.A., Dolghih, E., Roitberg, A.E., Nouzova, M., Mayoral, J.G., Noriega, F.G., Turjanski, A.G., 2011. Juvenile hormone synthesis: “esterify then epoxidize” or “ epoxidize then esterify” ? Insights from the structural characterization of juvenile hormone acid methyltransferase. Insect Biochem. Mol. Biol. 41, 228–235. https://doi.org/10.1016/j.ibmb.2010.12.008

Delić, D., Eisele, C., Schmid, R., Baum, P., Wiech, F., Gerl, M., Zimdahl, H., Pullen, S.S., Urquhart, R., 2016. Urinary exosomal miRNA signature in type II diabetic nephropathy patients. PLoS One 11, e0150154. https://doi.org/10.1371/journal.pone.0150154

Denli, A.M., Tops, B.B.J., Plasterk, R.H.A., Ketting, R.F., Hannon, G.J., 2004. Processing of primary microRNAs by the Microprocessor complex. Nature 432, 231–235. https://doi.org/10.1038/nature03049

Deveci, D., Martin, F.A., Leopold, P., Romero, N.M., 2019. AstA Signaling Functions as an Evolutionary Conserved Mechanism Timing Juvenile to Adult Transition. Curr. Biol. 29, 813–822. https://doi.org/10.1016/j.cub.2019.01.053

Dhahbi, J.M., Atamna, H., Li, R., Yamakawa, A., Guerrero, N., Lam, H.T., Mote, P., Spindler, S.R., 2016. MicroRNAs circulate in the hemolymph of *Drosophila* and accumulate relative to tissue micrornas in an

age-dependent manner. Genomics Insights 28, 29–39. https://doi.org/10.4137/GEI.S38147

Dubrovsky, E.B., Dubrovskaya, V.A., Berger, E.M., 2004. Hormonal regulation and functional role of *Drosophila* E75A orphan nuclear receptor in the juvenile hormone signaling pathway. Dev. Biol. 268, 258–270. https://doi.org/10.1016/j.ydbio.2004.01.009

Duguet, T.B., Soichot, J., Kuzyakiv, R., Malmström, L., Tritten, L., 2020. Extracellular Vesicle-Contained microRNA of *C. elegans* as a Tool to Decipher the Molecular Basis of Nematode Parasitism. Front. Cell. Infect. Microbiol. 10, 217. https://doi.org/10.3389/fcimb.2020.00217

Edgar, R.C., 2004. MUSCLE: Multiple sequence alignment with high accuracy and high throughput. Nucleic Acids Res. 32, 1792–1797. https://doi.org/10.1093/nar/gkh340

El-Khoury, V., Pierson, S., Kaoma, T., Bernardin, F., Berchem, G., 2016. Assessing cellular and circulating miRNA recovery: the impact of the RNA isolation method and the quantity of input material. Sci. Rep. 6, 19529. https://doi.org/10.1038/srep19529

Elliott, K.L., Chan, K.K., Teesch, L., Clor, O., Stay, B., 2009. Identification of Phe-Gly-Leu-amide type allatostatin-7 in *Reticulitermes flavipes*: Its localization in tissues and relation to juvenile hormone synthesis. Peptides 30, 495–506. https://doi.org/10.1016/j.peptides.2008.06.020

Ellwanger, D.C., Büttner, F.A., Mewes, H.W., Stümpflen, V., 2011. The sufficient minimal set of miRNA seed types. Bioinformatics 27, 1346–1350. https://doi.org/10.1093/bioinformatics/btr149

Enright, A.J., John, B., Gaul, U., Tuschl, T., Sander, C., Marks, D.S., 2003. MicroRNA targets in *Drosophila*. Genome Biol. 5, R1. https://doi.org/10.1186/gb-2003-5-1-r1

Epstein, Y., Perry, N., Volin, M., Zohar-Fux, M., Braun, R., Porat-Kuperstein, L., Toledano, H., 2017. MiR-9a modulates maintenance and ageing of Drosophila germline stem cells by limiting N-cadherin expression. Nat. Commun. 8, 600. https://doi.org/10.1038/s41467-017-00485-9

Erezyilmaz, D.F., Riddiford, L.M., Truman, J.W., 2006. The pupal specifier broad directs progressive morphogenesis in a direct-developing insect. Proc. Natl. Acad. Sci. U. S. A. 103, 6925–6930. https://doi.org/10.1073/pnas.0509983103

Etheridge, A., Gomes, C.P.C., Pereira, R.W., Galas, D., Wang, K., 2013. The complexity, function, and applications of RNA in circulation. Front. Genet. 4, 1–8. https://doi.org/10.3389/fgene.2013.00115

Ewer, J., 2005. How the ecdysozoan changed its coat. PLoS Biol. 3, e349. https://doi.org/10.1371/journal.pbio.0030349

Fire, A., Xu, S., Montgomery, M.K., Kostas, S.A., Driver, S.E., Mello, C.C., 1998. Potent and specific genetic interference by double-stranded RNA in *Caenorhabditis elegans*. Nature 391, 806–811. https://doi.org/10.1038/35888

Food and Agriculture Organization of the United Nations, 2020a. GIEWS Update, South America, Outbreaks of locusts could threaten wheat and barley crops in Argentina, Brazil and Uruguay.

Food and Agriculture Organization of the United Nations, 2020b. FAO Regional Office for Africa [WWW Document]. URL http://www.fao.org/africa/news/detail-news/en/c/1306167/ (accessed 11.13.20).

Food and Agriculture Organization of the United Nations, 2015. FAO Desert Locust Information Service (DLIS) Helps countries to control Desert Locust.

Food and Agriculture Organization of the United Nations, 2013. Response to the locust plague. Three-year Programme 2013–2016.

Freitas, F.C.P., Pires, C. V., Claudianos, C., Cristino, A.S., Simões, Z.L.P., 2017. MicroRNA-34 directly targets pair-rule genes and cytoskeleton component in the honey bee. Sci. Rep. 7, 40884. https://doi.org/10.1038/srep40884

Fromm, B., Billipp, T., Peck, L.E., Johansen, M., Tarver, J.E., King, B.L., Newcomb, J.M., Sempere, L.F., Flatmark, K., Hovig, E., Peterson, K.J., 2015. A Uniform System for the Annotation of Vertebrate microRNA Genes and the Evolution of the Human microRNAome. Annu. Rev. Genet. 49, 213–242. https://doi.org/10.1146/annurev-genet-120213-092023

Gijbels, M., Lenaerts, C., Vanden Broeck, J., Marchal, E., 2019. Juvenile hormone receptor Met is essential for ovarian maturation in the desert locust, *Schistocerca gregaria*. Sci. Rep. 9, 10797. https://doi.org/10.1038/s41598-019-47253-x

Gijbels, M., Schellens, S., Schellekens, T., Bruyninckx, E., Marchal, E., Vanden Broeck, J., 2020. Precocious downregulation of Krüppel-homolog 1 in the migratory locust, *Locusta migratoria*, gives rise to an adultoid phenotype with accelerated ovarian development but disturbed mating and oviposition. Int. J. Mol. Sci. 21, 6058.

Gilbert, L.I., Rybczynski, R., Warren, J.T., 2002. Control and Biochemical Nature of the Ecdysteroidogenic Pathway. Annu. Rev. Entomol. 47, 883–916. https://doi.org/10.1146/annurev.ento.47.091201.145302

Gilbert, L.I., Warren, J.T., 2005. A Molecular Genetic Approach to the Biosynthesis of the Insect Steroid Molting Hormone. Vitam. Horm. https://doi.org/10.1016/S0083-6729(05)73002-8

Girardie, J., Boureme, D., Couillaud, F., Tamarelle, M., Girardie, a., 1987. Anti-juvenile effect of neuroparsin A, a neuroprotein isolated from locust corpora cardiaca. Insect Biochem. 17, 977–983. https://doi.org/10.1016/0020-1790(87)90106-5

Girardie, J., Girardie, A., 1996. Lom OMP, a putative ecdysiotropic factor for the ovary in *Locusta migratoria*. J. Insect Physiol. 42, 215–221. https://doi.org/10.1016/0022-1910(95)00097-6

Girardie, J., Girardie, A., Huet, J.C., Pernollet, J.C., 1989. Amino acid sequence of locust neuroparsins. FEBS Lett. 245, 4–8. https://doi.org/10.1016/0014-5793(89)80179-6

Girardie, J., Huet, J.C., Atay-Kadiri, Z., Ettaouil, S., Delbecque, J.P., Fournier, B., Pernollet, J.C., Girardie, A., 1998. Isolation, sequence determination, physical and physiological characterization of the neuroparsins and ovary maturing parsins of *Schistocerca gregaria*. Insect Biochem. Mol. Biol. 28, 641–650.

Girardie, J., Richard, O., Huet, J. -C, Nespoulous, C., Van Dorsellaer, A., Pernollet, J. -C, 1991. Physical characterization and sequence identification of the ovary maturating parsin: A new neurohormone purified from the nervous corpora cardiaca of the African locust (Locusta migratoria migratorioides). Eur. J. Biochem. 202, 1121–1126. https://doi.org/10.1111/j.1432-1033.1991.tb16479.x

Godlewski, J., Wang, S., Wilson, T.G., 2006. Interaction of bHLH-PAS proteins involved in juvenile hormone reception in *Drosophila*. Biochem. Biophys. Res. Commun. 342, 1305–1311. https://doi.org/10.1016/j.bbrc.2006.02.097

Gomez-Orte, E., Belles, X., 2009. MicroRNA-dependent metamorphosis in hemimetabolan insects. Proc. Natl. Acad. Sci. U. S. A. 106, 21678–82. https://doi.org/10.1073/pnas.0907391106

Goodman, W.G., Granger, N.A., 2005. The Juvenile Hormones, in: Comprehensive Molecular Insect Science. pp. 319–408. https://doi.org/10.1016/B0-44-451924-6/00039-9

Gordon, K.H.J., Waterhouse, P.M., 2007. RNAi for insect-proof plants. Nat. Biotechnol. 25, 1231. https://doi.org/10.1038/nbt1107-1231

Grafton-Cardwell, E.E., Godfrey, L.D., Chaney, W.E., Bentley, W.J., 2005. Various novel insecticides are less toxic to humans, more specific to key pests. Calif. Agric. 59, 29–34. https://doi.org/10.3733/ca.v059n01p29

Gregory, R.I., Yan, K., Amuthan, G., Chendrimada, T., Doratotaj, B., Cooch, N., Shiekhattar, R., 2004. The Microprocessor complex mediates the genesis of microRNAs. Nature 432, 235–240. https://doi.org/10.1038/nature03120

Griebler, M., Westerlund, S.A., Hoffmann, K.H., Meyering-Vos, M., 2008. RNA interference with the allatoregulating neuropeptide genes from the fall armyworm *Spodoptera frugiperda* and its effects on the JH titer in the hemolymph. J. Insect Physiol. 54, 997–1007. https://doi.org/10.1016/j.jinsphys.2008.04.019

Griffiths-Jones, 2018. miRBase [WWW Document]. URL http://mirbase.org/ (accessed 3.22.20).

Griffiths-Jones, S., Grocock, R.J., van Dongen, S., Bateman, A., Enright, A.J., 2006. miRBase: microRNA sequences, targets and gene nomenclature. Nucleic Acids Res. 34, D140–D144. https://doi.org/10.1093/nar/gkj112

Gu, X., Zera, A.J., 1994. Developmental profiles and characteristics of hemolymph juvenile hormone esterase, general esterase and juvenile hormone binding in the cricket, *Gryllus assimilis*. Comp. Biochem. Physiol. -- Part B Biochem. 1078, 553–560. https://doi.org/10.1016/0305-0491(94)90184-8

Gujar, H., Palli, S.R., 2016a. Krüppel homolog 1 and E93 mediate Juvenile hormone regulation of metamorphosis in the common bed bug, *Cimex lectularius*. Sci. Rep. 6, 26092. https://doi.org/10.1038/srep26092

Gujar, H., Palli, S.R., 2016b. Juvenile hormone regulation of female reproduction in the common bed bug, *Cimex lectularius*. Sci. Rep. 6, 1–10. https://doi.org/10.1038/srep35546

Gulia-Nuss, M., Robertson, A.E., Brown, M.R., Strand, M.R., 2011. Insulin-like peptides and the target of rapamycin pathway coordinately regulate blood digestion and egg maturation in the mosquito *Aedes aegypti*. PLoS One 6, e20401. https://doi.org/10.1371/journal.pone.0020401

Guo, W., Wu, Z., Song, J., Jiang, F., Wang, Z., Deng, S., Walker, V.K., Zhou, S., 2014. Juvenile hormone-receptor

complex acts on mcm4 and mcm7 to promote polyploidy and vitellogenesis in the migratory locust. PLoS Genet. 10, 1–14. https://doi.org/10.1371/journal.pgen.1004702

Guo, W., Wu, Z., Yang, L., Cai, Z., Zhao, L., Zhou, S., 2019. Juvenile hormone-dependent Kazal-type serine protease inhibitor Greglin safeguards insect vitellogenesis and egg production. FASEB J. 33, 917–927. https://doi.org/10.1096/fj.201801068R

Guo, X., Su, S., Skogerboe, G., Dai, S., Li, W., Li, Z., Liu, F., Ni, R., Guo, Y., Chen, S., Zhang, S., Chen, R., 2013. Recipe for a busy bee: MicroRNAs in honey bee caste determination. PLoS One 8, e81661. https://doi.org/10.1371/journal.pone.0081661

Guo, X., Yu, Q., Chen, D., Wei, J., Yang, P., Yu, J., Wang, X., Kang, L., 2020. 4-Vinylanisole is an aggregation pheromone in locusts. Nature 584, 584–588. https://doi.org/10.1038/s41586-020-2610-4

He, K., Sun, Y., Xiao, H., Ge, C., Li, F., Han, Z., 2017. Multiple miRNAs jointly regulate the biosynthesis of ecdysteroid in the holometabolous insects, *Chilo suppressalis*. RNA 23, 1817–1833. https://doi.org/10.1261/rna.061408.117

Head, G.P., Carroll, M.W., Evans, S.P., Rule, D.M., Willse, A.R., Clark, T.L., Storer, N.P., Flannagan, R.D., Samuel, L.W., Meinke, L.J., 2017. Evaluation of SmartStax and SmartStax PRO maize against western corn rootworm and northern corn rootworm: efficacy and resistance management. Pest Manag. Sci. 73, 1883–1899. https://doi.org/10.1002/ps.4554

Hejnikova, M., Paroulek, M., Hodkova, M., 2016. Decrease in Methoprene tolerant and Taiman expression reduces juvenile hormone effects and enhances the levels of juvenile hormone circulating in males of the linden bug *Pyrrhocoris apterus*. J. Insect Physiol. 93–94, 72–80. https://doi.org/10.1016/j.jinsphys.2016.08.009

Hetru, C., Li, K.W., Buler, P., Laguex, M., Hoffmann, J.A., 1991. Isolation and structural characterization of an insulin-related molecule, a predominant neuropeptide from Locusta migratoria. Eur. J. Biochem. 201, 495–499. https://doi.org/10.1111/j.1432-1033.1991.tb16308.x

Hietter, H., Van Dorsselaer, A., Green, B., Denoroy, L., Hoffmann, J., Luu, B., 1990. Isolation and structure elucidation of a novel 5-kDa peptide from neurohaemal lobes of the corpora cardiaca of *Locusta migratoria* (Insecta, Orthoptera). Eur. J. Biochem. 187, 241–247. https://doi.org/10.1111/j.1432-1033.1990.tb15301.x

Hill, R.J., Billas, I.M.L., Bonneton, F., Graham, L.D., Lawrence, M.C., 2013. Ecdysone receptors: from the Ashburner model to structural biology. Annu. Rev. Entomol. 58, 251–271. https://doi.org/10.1146/annurev-ento-120811-153610

Hironaka, K. ichi, Morishita, Y., 2017. Adaptive significance of critical weight for metamorphosis in holometabolous insects. J. Theor. Biol. 417, 68–83. https://doi.org/10.1016/j.jtbi.2017.01.014

Hoang, D.T., Chernomor, O., Von Haeseler, A., Minh, B.Q., Vinh, L.S., 2018. UFBoot2: Improving the ultrafast bootstrap approximation. Mol. Biol. Evol. 35, 518–522. https://doi.org/10.1093/molbev/msx281

Huang, J., Marchal, E., Hult, E.F., Tobe, S.S., 2015. Characterization of the juvenile hormone pathway in the viviparous cockroach, *Diploptera punctata*. PLoS One 10, e0117291. https://doi.org/10.1371/journal.pone.0117291

Huang, J.H., Lozano, J., Belles, X., 2013. Broad-complex functions in postembryonic development of the cockroach *Blattella germanica* shed new light on the evolution of insect metamorphosis. Biochim. Biophys. Acta - Gen. Subj. 1830, 2178–2187. https://doi.org/10.1016/j.bbagen.2012.09.025

Huet, F., Ruiz, C., Richards, G., 1995. Sequential gene activation by ecdysone in *Drosophila melanogaster*: the hierarchical equivalence of early and early late genes. Development 121, 1195–1204.

Hult, E.F., Huang, J., Marchal, E., Lam, J., Tobe, S.S., 2015. RXR/USP and EcR are critical for the regulation of reproduction and the control of JH biosynthesis in *Diploptera punctata*. J. Insect Physiol. 9, 15. https://doi.org/10.1016/j.jinsphys.2015.04.006

Hunter, M.P., Ismail, N., Zhang, X., Aguda, B.D., Lee, E.J., Yu, L., Xiao, T., Schafer, J., Lee, M.L.T., Schmittgen, T.D., Nana-Sinkam, S.P., Jarjoura, D., Marsh, C.B., 2008. Detection of microRNA expression in human peripheral blood microvesicles. PLoS One 3, e3694. https://doi.org/10.1371/journal.pone.0003694

Hussain, M., Asgari, S., 2014. MicroRNAs as mediators of insect host-pathogen interactions and immunity. J. Insect Physiol. 70, 151–158. https://doi.org/10.1016/j.jinsphys.2014.08.003

Hussain, M., Asgari, S., 2010. Functional Analysis of a Cellular MicroRNA in Insect Host-Ascovirus Interaction. J. Virol. 84, 612–620. https://doi.org/10.1128/jvi.01794-09

Huybrechts, R., 2018. Endocrine Control of Reproduction, Insects, in: Reference Module in Life Sciences. pp.

1–8.
Huybrechts, R., De Loof, A., 1977. Induction of vitellogenin synthesis in male *Sarcophaga bullata* by ecdysterone. J. Insect Physiol. 23, 1359–1362. https://doi.org/10.1016/0022-1910(77)90158-5
Isaac, R.E., Rees, H.H., 1984. Isolation and identification of ecdysteroid phosphates and acetylecdysteroid phosphates from developing eggs of the locust, *Schistocerca gregaria*. Biochem. J. 221, 459–64.
Ishimaru, Y., Tomonari, S., Watanabe, T., Noji, S., Mito, T., 2019. Regulatory mechanisms underlying the specification of the pupal-homologous stage in a hemimetabolous insect. Philos. Trans. R. Soc. B Biol. Sci. 374, 20190225. https://doi.org/10.1098/rstb.2019.0225
Jansons, I.S., Cusson, M., McNeil, J.N., Tobe, S.S., Bendena, W.G., 1996. Molecular characterization of a cDNA from *Pseudaletia unipuncta* encoding the *Manduca sexta* allatostatin peptide (Mas-AST). Insect Biochem. Mol. Biol. 26, 767–773. https://doi.org/10.1016/S0965-1748(96)00023-9
Javidi, M.A. mi., Ahmadi, A.H. ossei., Bakhshinejad, B., Nouraee, N., Babashah, S., Sadeghizadeh, M., 2014. Cell-free microRNAs as cancer biomarkers: the odyssey of miRNAs through body fluids. Med. Oncol. 31, 295. https://doi.org/10.1007/s12032-014-0295-y
Jayachandran, B., Hussain, M., Asgari, S., 2013. An insect trypsin-like serine protease as a target of microRNA: Utilization of microRNA mimics and inhibitors by oral feeding. Insect Biochem. Mol. Biol. 43, 398–406. https://doi.org/10.1016/j.ibmb.2012.10.004
Jin, M., Xue, J., Yao, Y., Lin, X., 2014. Molecular characterization and functional analysis of Krüppel-homolog 1 (Kr-h1) in the brown planthopper, *Nilaparvata lugens* (Stål). J. Integr. Agric. 13, 1972–1981. https://doi.org/10.1016/S2095-3119(13)60654-1
Jindra, M., Palli, S.R., Riddiford, L.M., 2013. The Juvenile Hormone Signaling Pathway in Insect Development. Annu. Rev. Entomol. 58, 181–204. https://doi.org/10.1146/annurev-ento-120811-153700
Jing, Y.-P., An, H., Zhang, S., Wang, N., Zhou, S., 2018. Protein kinase C mediates juvenile hormone-dependent phosphorylation of Na+/K+-ATPase to induce ovarian follicular patency for yolk protein uptake. J. Biol. Chem. 293, 20112–20122. https://doi.org/10.1074/jbc.RA118.005692
Joly, P., Joly, L., Halbwachs, M., 1956. Contrôle humoral du développement chez *Locusta migratoria*. Ann. Sci. nat. Zool. 18, 256–261.
Kamsoi, O., Belles, X., 2020. E93-depleted adult insects preserve the prothoracic gland and molt again. bioRxiv.
Kaneko, Y., Hiruma, K., 2015. Allatotropin inhibits juvenile hormone biosynthesis by the corpora allata of adult *Bombyx mori*. J. Insect Physiol. 80, 15–21. https://doi.org/10.1016/j.jinsphys.2015.01.005
Kaneko, Y., Hiruma, K., 2014. Short neuropeptide F (sNPF) is a stage-specific suppressor for juvenile hormone biosynthesis by corpora allata, and a critical factor for the initiation of insect metamorphosis. Dev. Biol. 393, 312–319. https://doi.org/10.1016/j.ydbio.2014.07.014
Kang, D.S., Denlinger, D.L., Sim, C., 2014. Suppression of allatotropin simulates reproductive diapause in the mosquito Culex pipiens. J. Insect Physiol. 64, 48–53. https://doi.org/10.1016/j.jinsphys.2014.03.005
Kappler, C., Goltzené, F., Lagueux, M., Hetru, C., Hoffmann, J.A., 1986. Role of the follicle cells and the oocytes in ecdysone biosynthesis and esterification in vitellogenic females of *Locusta migratoria*. Int. J. Invertebr. Reprod. Dev. 9, 17–34. https://doi.org/10.1080/01688170.1986.10510177
Karim, F.D., Thummel, C.S., 1992. Temporal coordination of regulatory gene expression by the steroid hormone ecdysone. EMBO J. 11, 4083–4093. https://doi.org/10.1002/j.1460-2075.1992.tb05501.x
Karlson, P., 1996. On the hormonal control of insect metamorphosis " A historical review. Int. J. Dev. Biol. 96, 93–96.
Karres, J.S., Hilgers, V., Carrera, I., Treisman, J., Cohen, S.M., 2007. The conserved microRNA miR-8 tunes atrophin levels to prevent neurodegeneration in *Drosophila*. Cell 131, 136–145. https://doi.org/10.1016/j.cell.2007.09.020
Kataoka, H., Toschi, A., Li, J.P., Carney, R.L., Schooley, D.A., Kramer, S.J., 1989. Identification of an allatotropin from adult *Manduca sexta*. Science (80-.). 243, 1481–1483. https://doi.org/10.1126/science.243.4897.1481
Kawano, Y., Iwata, S., Kawada, J.I., Gotoh, K., Suzuki, M., Torii, Y., Kojima, S., Kimura, H., Ito, Y., 2013. Plasma viral MicroRNA profiles reveal potential biomarkers for chronic active epstein-barr virus infection. J. Infect. Dis. 208, 771–779. https://doi.org/10.1093/infdis/jit222
Kayukawa, T., Jouraku, A., Ito, Y., Shinoda, T., 2017. Molecular mechanism underlying juvenile hormone-mediated repression of precocious larval-adult metamorphosis. Proc. Natl. Acad. Sci. U. S. A. 114, 1057–

1062. https://doi.org/10.1073/pnas.1615423114

Khvorova, A., Reynolds, A., Jayasena, S.D., 2003. Functional siRNAs and miRNAs exhibit strand bias. Cell 115, 209–216. https://doi.org/10.1016/S0092-8674(03)00801-8

Kikukawa, S., Tobe, S.S., 1986. Critical periods for juvenile hormone sensitivity during larval life of female Diploptera punctata. J. Insect Physiol. 32, 1035-1039,1041-1042. https://doi.org/10.1016/0022-1910(86)90123-X

Kim, V.N., Han, J., Siomi, M.C., 2009. Biogenesis of small RNAs in animals. Nat. Rev. Mol. Cell Biol. 10, 126–139. https://doi.org/10.1038/nrm2632

Kim, Y.H., Soumaila Issa, M., Cooper, A.M.W., Zhu, K.Y., 2015. RNA interference: Applications and advances in insect toxicology and insect pest management. Pestic. Biochem. Physiol. 120, 109–117. https://doi.org/10.1016/j.pestbp.2015.01.002

Kinjoh, T., Kaneko, Y., Itoyama, K., Mita, K., Hiruma, K., Shinoda, T., 2007. Control of juvenile hormone biosynthesis in *Bombyx mori*: Cloning of the enzymes in the mevalonate pathway and assessment of their developmental expression in the *corpora allata*. Insect Biochem. Mol. Biol. 37, 808–818. https://doi.org/10.1016/j.ibmb.2007.03.008

Kiss, I., Beaton, A.H., Tardiff, J., Fristrom, D., Fristrom, J.W., 1988. Interactions and developmental effects of mutations in the Broad-Complex of *Drosophila melanogaster*. Genetics 118, 247–259.

Klowden, M.J., 2008. Physiological systems in insects (2nd edition), in: Elsevier Academic Press. p. 688.

Knight, S.W., Bass, B.L., 2001. A Role for the RNase III Enzyme DCR-1 in RNA Interference and Germ Line Development in *Caenorhabditis elegans*. Science (80-.). https://doi.org/10.1126/science.1062039

Kolliopoulou, A., Santos, D., Taning, C.N.T., Wynant, N., Vanden Broeck, J., Smagghe, G., Swevers, L., 2019. PIWI pathway against viruses in insects. Wiley Interdiscip. Rev. RNA 10. https://doi.org/10.1002/wrna.1555

Konopova, B., Jindra, M., 2008. Broad-Complex acts downstream of Met in juvenile hormone signaling to coordinate primitive holometabolan metamorphosis. Development 135, 559–568. https://doi.org/10.1242/dev.016097

Konopova, B., Jindra, M., 2007. Juvenile hormone resistance gene *Methoprene-tolerant* controls entry into metamorphosis in the beetle *Tribolium castaneum*. Proc. Natl. Acad. Sci. U. S. A. 104, 10488–10493. https://doi.org/10.1073/pnas.0703719104

Konopova, B., Smykal, V., Jindra, M., 2011. Common and distinct roles of juvenile hormone signaling genes in metamorphosis of holometabolous and hemimetabolous insects. PLoS One 6, e28728. https://doi.org/10.1371/journal.pone.0028728

Koppers-Lalic, D., Hackenberg, M., Bijnsdorp, I. V., van Eijndhoven, M.A.J., Sadek, P., Sie, D., Zini, N., Middeldorp, J.M., Ylstra, B., de Menezes, R.X., Würdinger, T., Meijer, G.A., Pegtel, D.M., 2014. Nontemplated nucleotide additions distinguish the small RNA composition in cells from exosomes. Cell Rep. 8, 1649–1658. https://doi.org/10.1016/j.celrep.2014.08.027

Kramer, S.J., Toschi, A., Miller, C.A., Kataoka, H., Quistad, G.B., Li, J.P., Carney, R.L., Schooley, D.A., 1991. Identification of an allatostatin from the tobacco hornworm *Manduca sexta*. Proc. Natl. Acad. Sci. U. S. A. 88, 9458–9462. https://doi.org/10.1073/pnas.88.21.9458

Krol, J., Loedige, I., Filipowicz, W., 2010. The widespread regulation of microRNA biogenesis, function and decay. Nat. Rev. Genet. 11, 597–610. https://doi.org/10.1038/nrg2843

Krüger, J., Rehmsmeier, M., 2006. RNAhybrid: MicroRNA target prediction easy, fast and flexible. Nucleic Acids Res. 1, W451–W454. https://doi.org/10.1093/nar/gkl243

Kucherenko, M.M., Shcherbata, H.R., 2013. Steroids as external temporal codes act via miRNAs and cooperate with cytokines in differential neurogenesis. Fly (Austin). 7, 173–183. https://doi.org/10.4161/fly.25241

LaFever, L., Drummond-Barbosa, D., 2005. Direct control of germline stem cell division and cyst growth by neural insulin in *Drosophila*. Science (80-.). 309, 1071–1073. https://doi.org/10.1126/science.1111410

Lafont, R., Dauphin-Villemant, C., Warren, J.T., Rees, H., 2012. Ecdysteroid chemistry and biochemistry, in: Insect Endocrinology. Elsevier, pp. 106–176. https://doi.org/10.1016/B978-0-12-384749-2.10004-4

Lagos-Quintana, M., Rauhut, R., Lendeckel, W., Tuschl, T., 2001. Identification of novel genes coding for small expressed RNAs. Science (80-.). 294, 853–858. https://doi.org/10.1126/science.1064921

Lagueux, M., Harry, P., Hoffmann, J.A., 1981. Ecdysteroids are bound to vitellin in newly laid eggs of *Locusta*. Mol. Cell. Endocrinol. 24, 325–338. https://doi.org/10.1016/0303-7207(81)90007-1

Lagueux, M., Hirn, M., Hoffmann, J.A., 1977. Ecdysone during ovarian development in *Locusta migratoria*. J. Insect Physiol. 23, 109–119. https://doi.org/10.1016/0022-1910(77)90116-0

Laguex, M., Lwoff, L., Meister, M., Goltzené, F., Hoffmann, J.A., 1990. cDNAs from neurosecretory cells of brains of Locusta migratoria (Insecta, Orthoptera) encoding a novel member of the superfamily of insulins. Eur. J. Biochem. 187, 249–254. https://doi.org/10.1111/j.1432-1033.1990.tb15302.x

Lange, A.B., 2009a. Neural mechanisms coordinating the female reproductive system in the locust. Front. Biosci. 14, 4401–4415. https://doi.org/10.2741/3536

Lange, A.B., 2009b. The female reproductive system and control of oviposition in *locusta migratoria* migratorioides. Can. J. Zool. 87, 649–661. https://doi.org/10.1139/Z09-063

Lange, A.B., Alim, U., Vandersmissen, H.P., Mizoguchi, A., Broeck, J. Vanden, Orchard, I., 2012. The distribution and physiological effects of the myoinhibiting peptides in the kissing bug, *Rhodnius prolixus*. Front. Neurosci. 6. https://doi.org/10.3389/fnins.2012.00098

Lange, A.B., da Silva, R., 2007. Neural and hormonal control of muscular activity of the spermatheca in the locust, *Locusta migratoria*. Peptides 28, 174–184. https://doi.org/10.1016/j.peptides.2006.08.028

Lanot, R., Thiebold, J., Lagueux, M., Goltzene, F., Hoffmann, J.A., 1987. Involvement of ecdysone in the control of meiotic reinitiation in oocytes of *Locusta migratoria* (Insecta , Orthoptera). Dev. Biol. 121, 174–181.

Laterza, O.F., Lim, L., Garrett-Engele, P.W., Vlasakova, K., Muniappa, N., Tanaka, W.K., Johnson, J.M., Sina, J.F., Fare, T.L., Sistare, F.D., Glaab, W.E., 2009. Plasma microRNAs as sensitive and specific biomarkers of tissue injury. Clin. Chem. 55, 1977–1983. https://doi.org/10.1373/clinchem.2009.131797

Lee, C.Y., Wendel, D.P., Reid, P., Lam, G., Thummel, C.S., Baehrecke, E.H., 2000. E93 directs steroid-triggered programmed cell death in *Drosophila*. Mol. Cell 6, 433–443. https://doi.org/10.1016/S1097-2765(00)00042-3

Lee, R.C., Ambros, V., 2001. An extensive class of small RNAs in *Caenorhabditis elegans*. Science (80-.). 294, 862–864. https://doi.org/10.1126/science.1065329

Lee, R.C., Feinbaum, R.L., Ambros, V., 1993. The *C. elegans* heterochronic gene lin-4 encodes small RNAs with antisense complementarity to lin-14. Cell 75, 843–854. https://doi.org/10.1016/0092-8674(93)90529-Y

Lee, S.H., Oh, H.W., Fang, Y., An, S.B., Park, D.S., Song, H.H., Oh, S.R., Kim, S.Y., Kim, S., Kim, N., Raikhel, A.S., Je, Y.H., Shin, S.W., 2015. Identification of plant compounds that disrupt the insect juvenile hormone receptor complex. Proc. Natl. Acad. Sci. U. S. A. 112, 1733–1738. https://doi.org/10.1073/pnas.1424386112

Lenaerts, Cynthia, Cools, D., Verdonck, R., Verbakel, L., Vanden Broeck, J., Marchal, E., 2017. The ecdysis triggering hormone system is essential for successful moulting of a major hemimetabolous pest insect, *Schistocerca gregaria*. Sci. Rep. 7, 46502. https://doi.org/10.1038/srep46502

Lenaerts, C., Marchal, E., Peeters, P., Vanden Broeck, J., 2019a. The ecdysone receptor complex is essential for the reproductive success in the female desert locust, *Schistocerca gregaria*. Sci. Rep. 9, 15. https://doi.org/10.1038/s41598-018-36763-9

Lenaerts, C., Marchal, E., Peeters, P., Vanden Broeck, J., 2019b. The ecdysone receptor complex is essential for the reproductive success in the female desert locust, *Schistocerca gregaria*. Sci. Rep. 9, 15. https://doi.org/10.1038/s41598-018-36763-9

Lenaerts, C., Monjon, E., Van Lommel, J., Verbakel, L., Vanden Broeck, J., 2019c. Peptides in insect oogenesis. Curr. Opin. Insect Sci. https://doi.org/10.1016/j.cois.2018.08.007

Lenaerts, C., Palmans, J., Marchal, E., Verdonck, R., Vanden Broeck, J., 2017. Role of the venus kinase receptor in the female reproductive physiology of the desert locust, *Schistocerca gregaria*. Sci. Rep. 7, 1–12. https://doi.org/10.1038/s41598-017-11434-3

Lenaerts, C., Van Wielendaele, P., Peeters, P., Vanden Broeck, J., Marchal, E., 2016. Ecdysteroid signalling components in metamorphosis and development of the desert locust, Schistocerca gregaria. Insect Biochem. Mol. Biol. 75, 10–23. https://doi.org/10.1016/j.ibmb.2016.05.003

Li, C., Wong, A.Y.P., Wang, S., Jia, Q., Chuang, W.P., Bendena, W.G., Tobe, S.S., Yang, S.H., Chung, G., Chan, T.F., Lam, H.M., Bede, J.C., Hui, J.H.L., 2018. MiRNA-mediated interactions in and between plants and insects. Int. J. Mol. Sci. 19, 3239. https://doi.org/10.3390/ijms19103239

Li, H., Huang, S., Guo, C., Guan, H., Xiong, C., 2012. Cell-free seminal mRNA and microRNA exist in different forms. PLoS One 7, e34566. https://doi.org/10.1371/journal.pone.0034566

Li, J., Cai, Y., Ye, L., Wang, S., Che, J., You, Z., Yu, J., Zhong, B., 2014. MicroRNA expression profiling of the fifth-

instar posterior silk gland of *Bombyx mori*. BMC Genomics 15, 410. https://doi.org/10.1186/1471-2164-15-410

Li, K.L., Yuan, S.Y., Nanda, S., Wang, W.X., Lai, F.X., Fu, Q., Wan, P.J., 2018. The Roles of E93 and Kr-h1 in Metamorphosis of *Nilaparvata lugens*. Front. Physiol. 9, 1677. https://doi.org/10.3389/fphys.2018.01677

Li, M. zhen, Xiao, H. mei, He, K., Li, F., 2019. Progress and prospects of noncoding RNAs in insects. J. Integr. Agric. 18, 729–747. https://doi.org/10.1016/S2095-3119(18)61976-8

Li, X., Carthew, R.W., 2005. A microRNA mediates EGF receptor signaling and promotes photoreceptor differentiation in the *Drosophila* eye. Cell 123, 1276–1277. https://doi.org/10.1016/j.cell.2005.10.040

Li, X., Guo, L., Zhou, X., Gao, X., Liang, P., 2015. MiRNAs regulated overexpression of ryanodine receptor is involved in chlorantraniliprole resistance in *Plutella xylostella* (L.). Sci. Rep. 5, 14095. https://doi.org/10.1038/srep14095

Li, Yiping, Hernandez-Martinez, S., Fernandez, F., Mayoral, J.G., Topalis, P., Priestap, H., Perez, M., Navare, A., Noriega, F.G., 2006. Biochemical, molecular, and functional characterization of PISCF-allatostatin, a regulator of juvenile hormone biosynthesis in the mosquito Aedes aegypti. J. Biol. Chem. 281, 34048–34055. https://doi.org/10.1074/jbc.M606341200

Li, Yan, Wang, F., Lee, J.A., Gao, F.B., 2006. MicroRNA-9a ensures the precise specification of sensory organ precursors in Drosophila. Genes Dev. 20, 2793–2805. https://doi.org/10.1101/gad.1466306

Li, Y., Zhang, J., Chen, D., Yang, P., Jiang, F., Wang, X., Kang, L., 2016. CRISPR/Cas9 in locusts: Successful establishment of an olfactory deficiency line by targeting the mutagenesis of an odorant receptor co-receptor (Orco). Insect Biochem. Mol. Biol. 79, 27–35. https://doi.org/10.1016/j.ibmb.2016.10.003

Lin, X., Yao, Y., Wang, B., 2015. Methoprene-tolerant (Met) and Krüpple-homologue 1 (Kr-h1) are required for ovariole development and egg maturation in the brown plant hopper. Sci. Rep. 5, 1–9. https://doi.org/10.1038/srep18064

Ling, L., Ge, X., Li, Z., Zeng, B., Xu, J., Aslam, A.F.M., Song, Q., Shang, P., Huang, Y., Tan, A., 2014. MicroRNA Let-7 regulates molting and metamorphosis in the silkworm, *Bombyx mori*. Insect Biochem. Mol. Biol. 53, 13–21. https://doi.org/10.1016/j.ibmb.2014.06.011

Ling, L., Kokoza, V.A., Zhang, C., Aksoy, E., Raikhel, A.S., 2017. MicroRNA-277 targets insulin-like peptides 7 and 8 to control lipid metabolism and reproduction in *Aedes aegypti* mosquitoes. Proc. Natl. Acad. Sci. U. S. A. 114, E8017–E8024. https://doi.org/10.1073/pnas.1710970114

Liu, P., Peng, H.J., Zhu, J., 2015. Juvenile hormone-activated phospholipase C pathway enhances transcriptional activation by the methoprene-tolerant protein. Proc. Natl. Acad. Sci. U. S. A. 112, E1871–E1879. https://doi.org/10.1073/pnas.1423204112

Liu, W., Li, Y., Zhu, L., Zhu, F., Lei, C.L., Wang, X.P., 2016. Juvenile hormone facilitates the antagonism between adult reproduction and diapause through the *methoprene-tolerant* gene in the female *Colaphellus bowringi*. Insect Biochem. Mol. Biol. 74, 50–60. https://doi.org/10.1016/j.ibmb.2016.05.004

Liu, X., Dai, F., Guo, E., Li, K., Ma, L., Tian, L., Cao, Y., Zhang, G., Palli, S.R., Li, S., 2015. 20-Hydroxyecdysone (20E) primary response gene *E93* modulates 20E signaling to promote *Bombyx* larval-pupal metamorphosis. J. Biol. Chem. 290, 27370–27383. https://doi.org/10.1074/jbc.M115.687293

Lorenz, M.W., Kellner, R., Hoffmann, K.H., 1995. A family of neuropeptides that inhibit juvenile hormone biosynthesis in the cricket, *Gryllus bimaculatus*. J. Biol. Chem. 270, 201103–201108. https://doi.org/10.1074/jbc.270.36.21103

Lotvall, J., Valadi, H., 2007. Cell to cell signalling via exosomes through esRNA. Cell Adh. Migr. 1, 156–158. https://doi.org/10.4161/cam.1.3.5114

Lozano, J., Belles, X., 2014. Role of methoprene-tolerant (Met) in adult morphogenesis and in adult ecdysis of *Blattella germanica*. PLoS One 9, e103614. https://doi.org/10.1371/journal.pone.0103614

Lozano, J., Belles, X., 2011. Conserved repressive function of Krüppel homolog 1 on insect metamorphosis in hemimetabolous and holometabolous species. Sci. Rep. 1, 1–7. https://doi.org/10.1038/srep00163

Lozano, J., Montañez, R., Bellesa, X., 2015. MiR-2 family regulates insect metamorphosis by controlling the juvenile hormone signaling pathway. Proc. Natl. Acad. Sci. U. S. A. 112, 3740–3745. https://doi.org/10.1073/pnas.1418522112

Lucas, K.J., Roy, S., Ha, J., Gervaise, A.L., Kokoza, V.A., Raikhel, A.S., 2015. MicroRNA-8 targets the wingless signaling pathway in the female mosquito fat body to regulate reproductive processes. Proc. Natl. Acad. Sci. U. S. A. 112, 1440–1445. https://doi.org/10.1073/pnas.1424408112

Lum, L., Yao, S., Mozer, B., Rovescalli, A., Kessler, D. Von, Nirenberg, M., Beachy, P.A., 2003. Identification of Hedgehog Pathway Components by RNAi in Drosophila Cultured Cells. Science (80-.). 299, 2039–2045.

Lund, E., 2004. Nuclear Export of MicroRNA Precursors. Science (80-.). 303, 95–98. https://doi.org/10.1126/science.1090599

Luo, M., Li, D., Wang, Z., Guo, W., Kang, L., Zhou, S., 2017. Juvenile hormone differentially regulates two Grp78 genes encoding protein chaperones required for insect fat body cell homeostasis and vitellogenesis. J. Biol. Chem. 292, 8823–8834. https://doi.org/10.1074/jbc.M117.780957

Ma, L., Zhang, W., Liu, C., Chen, L., Xu, Y., Xiao, H., Liang, G., 2018. Methoprene-Tolerant (Met) is indispensable for larval metamorphosis and female reproduction in the cotton bollworm *Helicoverpa armigera*. Front. Physiol. 9, 1–12.

Makarova, J.A., Shkurnikov, M.U., Turchinovich, A.A., Tonevitsky, A.G., Grigoriev, A.I., 2015. Circulating MicroRNAs. Biochem. 80, 1117–1126. https://doi.org/10.1161/circresaha.111.247452

Makarova, J.A., Shkurnikov, M.U., Wicklein, D., Lange, T., Samatov, T.R., Turchinovich, A.A., Tonevitsky, A.G., 2016. Intracellular and extracellular microRNA: An update on localization and biological role. Prog. Histochem. Cytochem. 51, 33–49. https://doi.org/10.1016/j.proghi.2016.06.001

Mamta, B., Rajam, M. V., 2017. RNAi technology: a new platform for crop pest control. Physiol. Mol. Biol. Plants 23, 487–501. https://doi.org/10.1007/s12298-017-0443-x

Mao, Y., Li, Y., Gao, H., Lin, X., 2020. Krüppel homologue 1 interacts directly with Hairy and regulates ecdysis in the brown planthopper. Insect Mol. Biol. 29, 293–300. https://doi.org/10.1111/imb.12635

Mao, Y., Li, Y., Gao, H., Lin, X., 2019. The direct interaction between E93 and Kr-h1 mediated their antagonistic effect on ovary development of the brown planthopper. Int. J. Mol. Sci. 20, 2431. https://doi.org/10.3390/ijms20102431

Marchal, E., Badisco, L., Verlinden, H., Vandersmissen, T., Van Soest, S., Van Wielendaele, P., Vanden Broeck, J., 2011a. Role of the *Halloween* genes, *Spook* and *Phantom* in ecdysteroidogenesis in the desert locust, *Schistocerca gregaria*. J. Insect Physiol. 57, 1240–1248. https://doi.org/10.1016/j.jinsphys.2011.05.009

Marchal, E., Hult, E.F., Huang, J., Pang, Z., Stay, B., Tobe, S.S., 2014. Methoprene-tolerant (met) knockdown in the adult female cockroach, *Diploptera punctata* completely inhibits ovarian development. PLoS One 9, e106737. https://doi.org/10.1371/journal.pone.0106737

Marchal, E., Verlinden, H., Badisco, L., Van Wielendaele, P., Vanden Broeck, J., 2012. RNAi-mediated knockdown of *Shade* negatively affects ecdysone-20-hydroxylation in the desert locust, *Schistocerca gregaria*. J. Insect Physiol. 58, 890–896. https://doi.org/10.1016/j.jinsphys.2012.03.013

Marchal, E., Zhang, J., Badisco, L., Verlinden, H., Hult, E.F., Van Wielendaele, P., Yagi, K.J., Tobe, S.S., Vanden Broeck, J., 2011b. Final steps in juvenile hormone biosynthesis in the desert locust, *Schistocerca gregaria*. Insect Biochem. Mol. Biol. 41, 219–227. https://doi.org/10.1016/j.ibmb.2010.12.007

Martín, D., Maestro, O., Cruz, J., Mané-Padrós, D., Bellés, X., 2006. RNAi studies reveal a conserved role for RXR in molting in the cockroach *Blattella germanica*. J. Insect Physiol. 52, 410–416. https://doi.org/10.1016/j.jinsphys.2005.12.002

Mayoral, J.G., Nouzova, M., Yoshiyama, M., Shinoda, T., Hernandez-Martinez, S., Dolghih, E., Turjanski, A.G., Roitberg, A.E., Priestap, H., Perez, M., Mackenzie, L., Li, Y., Noriega, F.G., 2009. Molecular and functional characterization of a juvenile hormone acid methyltransferase expressed in the *corpora allata* of mosquitoes. Insect Biochem. Mol. Biol. 39, 31–37. https://doi.org/10.1016/j.ibmb.2008.09.010

McDonald, M.K., Capasso, K.E., Ajit, S.K., 2013. Purification and microRNA Profiling of Exosomes Derived from Blood and Culture Media. J. Vis. Exp. 76, 1–7. https://doi.org/10.3791/50294

Meiselman, M., Lee, S.S., Tran, R.T., Dai, H., Ding, Y., Rivera-Perez, C., Wijesekera, T.P., Dauwalder, B., Noriega, F.G., Adams, M.E., 2017. Endocrine network essential for reproductive success in *Drosophila melanogaster*. Proc. Natl. Acad. Sci. U. S. A. 114, E3849–E3858. https://doi.org/10.1073/pnas.1620760114

Mello, T.R.P., Aleixo, A.C., Pinheiro, D.G., Nunes, F.M.F., Bitondi, M.M.G., Hartfelder, K., Barchuk, A.R., Simões, Z.L.P., 2014. Developmental regulation of ecdysone receptor (*EcR*) and EcR-controlled gene expression during pharate-adult development of honeybees (*Apis mellifera*). Front. Genet. 5, 455. https://doi.org/10.3389/fgene.2014.00445

Minakuchi, C., Namiki, T., Shinoda, T., 2009. *Krüppel homolog 1*, an early juvenile hormone-response gene downstream of *Methoprene-tolerant*, mediates its anti-metamorphic action in the red flour beetle *Tribolium castaneum*. Dev. Biol. 325, 341–350. https://doi.org/10.1016/j.ydbio.2008.10.016

Minakuchi, C., Namiki, T., Yoshiyama, M., Shinoda, T., 2008a. RNAi-mediated knockdown of *juvenile hormone acid O-methyltransferase* gene causes precocious metamorphosis in the red flour beetle *Tribolium castaneum*. FEBS J. 275, 2919–2931. https://doi.org/10.1111/j.1742-4658.2008.06428.x

Minakuchi, C., Zhou, X., Riddiford, L.M., 2008b. Krüppel homolog 1 (Kr-h1) mediates juvenile hormone action during metamorphosis of *Drosophila melanogaster*. Mech. Dev. 125, 91–105. https://doi.org/10.1016/j.mod.2007.10.002

Mingels, L., Wynant, N., Santos, D., Peeters, P., Gansemans, Y., Billen, J., Van Nieuwerburgh, F., Vanden Broeck, J., 2020. Extracellular vesicles spread the RNA interference signal of *Tribolium castaneum* TcA cells. Insect Biochem. Mol. Biol. 122, 103377. https://doi.org/10.1016/j.ibmb.2020.103377

Mirth, C.K., Nogueira Alves, A., Piper, M.D., 2019. Turning food into eggs: insights from nutritional biology and developmental physiology of *Drosophila*. Curr. Opin. Insect Sci. 31, 49–57. https://doi.org/10.1016/j.cois.2018.08.006

Mitchell, P.S., Parkin, R.K., Kroh, E.M., Fritz, B.R., Wyman, S.K., Pogosova-Agadjanyan, E.L., Peterson, A., Noteboom, J., O'Briant, K.C., Allen, A., Lin, D.W., Urban, N., Drescher, C.W., Knudsen, B.S., Stirewalt, D.L., Gentleman, R., Vessella, R.L., Nelson, P.S., Martin, D.B., Tewari, M., 2008. Circulating microRNAs as stable blood-based markers for cancer detection. Proc. Natl. Acad. Sci. 105, 10513–10518. https://doi.org/10.1073/pnas.0804549105

Miyoshi, K., Okada, T.N., Siomi, H., Siomi, M.C., 2009. Characterization of the miRNA-RISC loading complex and miRNA-RISC formed in the Drosophila miRNA pathway. RNA 15, 1282–91. https://doi.org/10.1261/rna.1541209

Morgan, E.D., Poole, C.F., 1976. The pattern of ecdysone levels during development in the desert locust, *Schistocerca gregaria*. J. Insect Physiol. 22, 885–889. https://doi.org/10.1016/0022-1910(76)90260-2

Mou, X., Duncan, D.M., Baehrecke, E.H., Duncan, I., 2012. Control of target gene specificity during metamorphosis by the steroid response gene *E93*. Proc. Natl. Acad. Sci. U. S. A. 109, 2949–2954. https://doi.org/10.1073/pnas.1117559109

Nagasawa, H., Guo, F., Zhong, X.C., Xia, B.Y., Wang, Z.S., Qui, X.J., Wei, D.Y., Chen, E.I., Wang, J.Z., Suzuki, A., Isogai, A., Hori, Y., Tamura, S., Ishizaki, H., 1980. Large-scale purification of prothoracicotropic hormone of the silkworm (*Bombyx mori*)). Sci. Sin. 23, 1053–1060. https://doi.org/10.1360/ya1980-23-8-1053

Nagasawa, H., Kataoka, H., Hori, Y., Isogai, A., Tamura, S., Suzuki, A., Guo, F., Zhong, X., Mizoguchi, A., Fujishita, M., Takahashi, S.Y., Ohnishi, E., Ishizaki, H., 1984a. Isolation and some characterization of the prothoracicotropic hormone from *Bombyx mori*. Gen. Comp. Endocrinol. 53, 143–152. https://doi.org/10.1016/0016-6480(84)90234-X

Nagasawa, H., Kataoka, H., Isogai, A., Tamura, S., Suzuki, Akinori, Ishizaki, H., Mizoguchi, A., Fujiwara, Y., Suzuki, Atsushi, 1984b. Amino-terminal amino acid sequence of the silkworm prothoracicotropic hormone: Homology with insulin. Science (80-.). 226, 1344–1345. https://doi.org/10.1126/science.226.4680.1344

Naghdi, M., Maestro, J.-L., Belles, X., Bandani, A., 2016. Transduction of the vitellogenic signal of juvenile hormone by Methoprene-tolerant in the cockroach *Blattella germanica* (L.) (Dictyoptera, Blattellidae). Arthropods 5, 130–136.

Nandety, R.S., Kuo, Y.W., Nouri, S., Falk, B.W., 2015. Emerging strategies for RNA interference (RNAI) applications in insects. Bioengineered 6, 8–19. https://doi.org/10.4161/21655979.2014.979701

Neuhäuser, T., Sorge, D., Stay, B., Hoffmann, K.H., 1994. Responsiveness of the adult cricket (*Gryllus bimaculatus* and *Acheta domesticus*) retrocerebral complex to allatostatin-1 from a cockroach, *Diploptera punctata*. J. Comp. Physiol. B 164, 23–31. https://doi.org/10.1007/BF00714567

Nguyen, L.T., Schmidt, H.A., Von Haeseler, A., Minh, B.Q., 2015. IQ-TREE: A fast and effective stochastic algorithm for estimating maximum-likelihood phylogenies. Mol. Biol. Evol. 32, 268–274. https://doi.org/10.1093/molbev/msu300

Nijhout, H.F., 1979. Stretch-induced moulting in *Oncopeltus fasciatus*. J. Insect Physiol. 25, 277–281. https://doi.org/10.1016/0022-1910(79)90055-6

Ninova, M., Ronshaugen, M., Griffiths-Jones, S., 2016. MicroRNA evolution, expression, and function during short germband development in Tribolium castaneum. Genome Res. 26, 85–96. https://doi.org/10.1101/gr.193367.115

Niwa, R., Matsuda, T., Yoshiyama, T., Namiki, T., Mita, K., Fujimoto, Y., Kataoka, H., 2004. CYP306A1, a cytochrome P450 enzyme, is essential for ecdysteroid biosynthesis in the prothoracic glands of *Bombyx*

and *Drosophila*. J. Biol. Chem. 279, 35942–35949. https://doi.org/10.1074/jbc.M404514200

Niwa, R., Niimi, T., Honda, N., Yoshiyama, M., Itoyama, K., Kataoka, H., Shinoda, T., 2008. Juvenile hormone acid O-methyltransferase in *Drosophila melanogaster*. Insect Biochem. Mol. Biol. 38, 714–720. https://doi.org/10.1016/j.ibmb.2008.04.003

Niwa, R., Niwa, Y.S., 2014. Enzymes for ecdysteroid biosynthesis: their biological functions in insects and beyond. Biosci. Biotechnol. Biochem. 78, 1283–92. https://doi.org/10.1080/09168451.2014.942250

Nouzova, M., Brockhoff, A., Mayoral, J.G., Goodwin, M., Meyerhof, W., Noriega, F.G., 2012. Functional characterization of an allatotropin receptor expressed in the corpora allata of mosquitoes. Peptides 34, 201–208. https://doi.org/10.1016/j.peptides.2011.07.025

Oh, H.W., Yun, C.S., Jeon, J.H., Kim, J.A., Park, D.S., Ryu, H.W., Oh, S.R., Song, H.H., Shin, Y., Jung, C.S., Shin, S.W., 2017. Conifer Diterpene Resin Acids Disrupt Juvenile Hormone-Mediated Endocrine Regulation in the Indian Meal Moth *Plodia interpunctella*. J. Chem. Ecol. 43, 703–711. https://doi.org/10.1007/s10886-017-0861-9

Ohno, C.K., Ueda, H., Petkovich, M., 1994. The *Drosophila* nuclear receptors FTZ-F1 alpha and FTZ-F1 beta compete as monomers for binding to a site in the fushi tarazu gene. Mol. Cell. Biol. 14, 3166–3175. https://doi.org/10.1128/mcb.14.5.3166

Okamura, K., Ishizuka, A., Siomi, H., Siomi, M.C., 2004. Distinct roles for Argonaute proteins in small RNA-directed RNA cleavage pathways. Genes Dev. 18, 1655–1666. https://doi.org/10.1101/gad.1210204

Okamura, K., Liu, N., Lai, E.C., 2009. Distinct Mechanisms for MicroRNA Strand Selection by *Drosophila* Argonautes. Mol. Cell 36, 431–444. https://doi.org/10.1016/j.molcel.2009.09.027

Ono, H., Rewitz, K.F., Shinoda, T., Itoyama, K., Petryk, A., Rybczynski, R., Jarcho, M., Warren, J.T., Marqués, G., Shimell, M.J., Gilbert, L.I., O'Connor, M.B., 2006. Spook and Spookier code for stage-specific components of the ecdysone biosynthetic pathway in Diptera. Dev. Biol. 298, 555–570. https://doi.org/10.1016/j.ydbio.2006.07.023

Pardo, M.C., López-León, M.D., Cabrero, J., Camacho, J.P.M., 1995. Cytological and developmental analysis of tychoparthenogenesis in *Locusta migratoria*. Heredity (Edinb). 75, 485–494. https://doi.org/10.1038/hdy.1995.165

Parthasarathy, R., Palli, S.R., 2011. Molecular analysis of nutritional and hormonal regulation of female reproduction in the red flour beetle, *Tribolium castaneum*. Insect Biochem. Mol. Biol. 41, 294–305. https://doi.org/10.1016/j.ibmb.2011.01.006

Parthasarathy, R., Sun, Z., Bai, H., Palli, S.R., 2010. Juvenile hormone regulation of vitellogenin synthesis in the red flour beetle, *Tribolium castaneum*. Insect Biochem. Mol. Biol. 40, 405–414. https://doi.org/10.1016/j.ibmb.2010.03.006

Parthasarathy, R., Tan, A., Bai, H., Palli, S.R., 2008. Transcription factor broad suppresses precocious development of adult structures during larval-pupal metamorphosis in the red flour beetle, *Tribolium castaneum*. Mech. Dev. 125, 299–313. https://doi.org/10.1016/j.mod.2007.11.001

Parvy, J.P., Blais, C., Bernard, F., Warren, J.T., Petryk, A., Gilbert, L.I., O'Connor, M.B., Dauphin-Villemant, C., 2005. A role for βFTZ-F1 in regulating ecdysteroid titers during post-embryonic development in *Drosophila melanogaster*. Dev. Biol. 282, 84–94. https://doi.org/10.1016/j.ydbio.2005.02.028

Pascual, N., Belles, X., Delbecque, J.P., Hua, Y.J., Koolman, J., 1995. Quantification of Ecdysteroids by Immunoassay: Comparison of Enzyme Immunoassay and Radioimmunoassay. Zeitschrift fur Naturforsch. - Sect. C J. Biosci. 50, 862–867. https://doi.org/10.1515/znc-1995-11-1219

Peel, A.D., Akam, M., 2007. The dynamics of yolk deposition in the desert locust *Schistocerca gregaria*. J. Insect Physiol. 53, 436–443. https://doi.org/10.1016/j.jinsphys.2007.01.005

Peel, D.J., Milner, M.J., 1990. The diversity of cell morphology in cloned cell lines derived from *Drosophila* imaginal discs. Dev. Biol. 198, 479–482.

Pener, M.P., Simpson, S.J., 2009. Locust Phase Polyphenism: An Update. Adv. In Insect Phys. 36, 1–272. https://doi.org/10.1016/S0065-2806(08)36001-9

Peter, M.E., 2010. Targeting of mRNAs by multiple miRNAs: The next step. Oncogene 29, 2161–2164. https://doi.org/10.1038/onc.2010.59

Petryk, A., Warren, J.T., Marques, G., Jarcho, M.P., Gilbert, L.I., Kahler, J., Parvy, J.-P., Li, Y., Dauphin-Villemant, C., O'Connor, M.B., 2003. *Shade* is the *Drosophila* P450 enzyme that mediates the hydroxylation of ecdysone to the steroid insect molting hormone 20-hydroxyecdysone. Proc. Natl. Acad. Sci. 100, 13773–13780. https://doi.org/10.1073/pnas.2336088100

Porcheron, P., Moriniere, M., Grassi, J., Pradelles, P., 1989. Development of an enzyme immunoassay for ecdysteroids using acetylcholinesterase as label. Insect Biochem. 19, 117–122. https://doi.org/10.1016/0020-1790(89)90081-4

Pratt, G.E., Farnsworth, D.E., Siegel, N.R., Fok, K.F., Feyereisen, R., 1989. Identification of an allatostatin from adult *Diploptera punctata*. Biochem. Biophys. Res. Commun. 163, 1243–1247. https://doi.org/10.1016/0006-291X(89)91111-X

Rabinowits, G., Gerçel-Taylor, C., Day, J.M., Taylor, D.D., Kloecker, G.H., 2009. Exosomal microRNA: A diagnostic marker for lung cancer. Clin. Lung Cancer 10, 42–46. https://doi.org/10.3816/CLC.2009.n.006

Raikhel, a S., Brown, M.R., Belles, X., 2005. Hormonal control of reproductive processes. Compr. Mol. insect Sci. 3, 433–491. https://doi.org/10.1016/B0-44-451924-6/00040-5

Ramirez, C.E., Nouzova, M., Benigni, P., Quirke, J.M.E., Noriega, F.G., Fernandez-Lima, F., 2016. Fast, ultra-trace detection of juvenile hormone III from mosquitoes using mass spectrometry. Talanta 159, 371–378. https://doi.org/10.1016/j.talanta.2016.06.041

Ren, D., Cai, Z., Song, J., Wu, Z., Zhou, S., 2014. DsRNA uptake and persistence account for tissue-dependent susceptibility to RNA interference in the migratory locust, *Locusta migratoria*. Insect Mol. Biol. 23, 175–184. https://doi.org/10.1111/imb.12074

Riddiford, L.M., 2012. How does juvenile hormone control insect metamorphosis and reproduction? Gen. Comp. Endocrinol. 179, 477–484. https://doi.org/10.1016/j.ygcen.2012.06.001

Rodriguez, A., Griffiths-Jones, S., Ashurst, J.L., Bradley, A., 2004. Identification of mammalian microRNA host genes and transcription units. Genome Res. 14, 1902–1910. https://doi.org/10.1101/gr.2722704

Roush, S., Slack, F.J., 2008. The let-7 family of microRNAs. Trends Cell Biol. 18, 505–516. https://doi.org/10.1016/j.tcb.2008.07.007

Roussi, A., 2020. The Battle to contain gigantic locust swarms. Nature 579, 330.

Roy, S., Hansen, I., Raikhel, A., 2007. Effect of insulin and 20-hydroxyecdysone in the fat body of the yellow fever mosquito, *Aedes aegypti*. Insect Biochem. Mol. Biol. 37, 1317–26. https://doi.org/10.1016/j.ibmb.2007.08.004

Roy, S., Saha, T.T., Zou, Z., Raikhel, A.S., 2018. Regulatory Pathways Controlling Female Insect Reproduction. Annu. Rev. Entomol. 63, 489–511. https://doi.org/10.1146/annurev-ento-020117-043258

Rubio, M., de Horna, A., Belles, X., 2012. MicroRNAs in metamorphic and non-metamorphic transitions in hemimetabolan insect metamorphosis. BMC Genomics 13, 386. https://doi.org/10.1186/1471-2164-13-386

Saha, T.T., Roy, S., Pei, G., Dou, W., Zou, Z., Raikhel, A.S., 2019. Synergistic action of the transcription factors Krüppel homolog 1 and Hairy in juvenile hormone/Methoprene-tolerant-mediated gene-repression in the mosquito *Aedes aegypti*. PLoS Genet. 15, e1008443. https://doi.org/10.1371/journal.pgen.1008443

Saiki, R., Gotoh, H., Toga, K., Miura, T., Maekawa, K., 2015. High juvenile hormone titre and abdominal activation of JH signalling may induce reproduction of termite neotenics. Insect Mol. Biol. 24, 432–441. https://doi.org/10.1111/imb.12169

Saleh, M.-C., van Rij, R.P., Hekele, A., Gillis, A., Foley, E., O'Farrell, P.H., Andino, R., 2006. The endocytic pathway mediates cell entry of dsRNA to induce RNAi silencing. Nat. Cell Biol. 8, 793–802.

Santos, C.G., Fernandez-Nicolas, A., Belles, X., 2016. Smads and insect hemimetabolan metamorphosis. Dev. Biol. 417, 104–113. https://doi.org/10.1016/j.ydbio.2016.07.006

Sattar, S., Thompson, G.A., 2016. Small RNA regulators of plant-hemipteran interactions: Micromanagers with versatile roles. Front. Plant Sci. 7, 1241. https://doi.org/10.3389/fpls.2016.01241

Sayed, A.S.M., Xia, K., Salma, U., Yang, T., Peng, J., 2014. Diagnosis, prognosis and therapeutic role of circulating miRNAs in cardiovascular diseases. Hear. Lung Circ. 23, 503–510. https://doi.org/10.1016/j.hlc.2014.01.001

Schneider, I., 1972. Cell lines derived from late embryonic stages of *Drosophila melanogaster*. J. Embryol. Exp. Morphol. 27, 353–365.

Schoofs, L., Holman, G.M., Hayes, T.K., Nachman, R.J., De Loof, A., 1991. Isolation, identification and synthesis of locustamyoinhibiting peptide (LOM-MIP), a novel biologically active neuropeptide from *Locusta migratoria*. Regul. Pept. 36, 111–119. https://doi.org/10.1016/0167-0115(91)90199-Q

Schoofs, L., Veelaert, D., Broeck, J. Vanden, De Loof, A., 1996. Immunocytochemical distribution of Locustamyoinhibiting peptide (Lom-MIP) in the nervous system of *Locusta migratoria*. Regul. Pept. 63, 171–179. https://doi.org/10.1016/S0167-0115(96)00040-7

Schwarz, D.S., Hutvágner, G., Du, T., Xu, Z., Aronin, N., Zamore, P.D., 2003. Asymmetry in the assembly of the RNAi enzyme complex. Cell 115, 199–208. https://doi.org/10.1016/S0092-8674(03)00759-1

Seidelmann, K., Helbing, C., Göbeler, N., Weinert, H., 2016. Sequential oogenesis is controlled by an oviduct factor in the locusts *Locusta migratoria* and *Schistocerca gregaria*: Overcoming the doctrine that patency in follicle cells is induced by juvenile hormone. J. Insect Physiol. 90, 1–7. https://doi.org/10.1016/j.jinsphys.2016.03.008

Sevala, V.L. & Davey, K.G., 1989. Action of juvenile hormone on the follicle cells of *Rhodnius prolixus*: Evidence for a novel regulatory mechanism involving protein kinase C. Experientia 45, 355–356.

Sevala, V.L., Davey, K.G., Prestwich, G.D., 1995. Photoaffinity labeling and characterization of a juvenile hormone binding protein in the membranes of follicle cells of *Locusta migratoria*. Insect Biochem. Mol. Biol. 25, 267–273. https://doi.org/10.1016/0965-1748(94)00065-P

Sevale, V.L., Davey, K.G., 1993. Juvenile hormone dependent phosphorylation of a 100 kDa polypeptide is mediated by protein kinase C in the follicle cells of *Rhodnius prolixus*. Invertebr. Reprod. Dev. 23, 189–193. https://doi.org/10.1080/07924259.1993.9672314

Sheng, Z., Ma, L., Cao, M.X., Jiang, R.J., Li, S., 2008. Juvenile hormone acid methyl transferase is a key regulatory enzyme for juvenile hormone synthesis in the eri silkworm, *Samia cynthica ricini*. Arch. Insect Biochem. Physiol. 69, 143–154. https://doi.org/10.1002/arch.20268

Sheng, Z., Xu, J., Bai, H., Zhu, F., Palli, S.R., 2011. Juvenile hormone regulates vitellogenin gene expression through insulin-like peptide signaling pathway in the red flour beetle, *Tribolium castaneum*. J. Biol. Chem. 286, 41924–41936. https://doi.org/10.1074/jbc.M111.269845

Shin, S.W., Jeon, J.H., Jeong, S.A., Kim, J.A., Park, D.S., Shin, Y., Oh, H.W., 2018. A plant diterpene counteracts juvenile hormone-mediated gene regulation during *Drosophila melanogaster* larval development. PLoS One 13, e0200706. https://doi.org/10.1371/journal.pone.0200706

Shinoda, T., Itoyama, K., 2003. Juvenile hormone acid methyltransferase: a key regulatory enzyme for insect metamorphosis. Proc. Natl. Acad. Sci. U. S. A. 100, 11986–11991. https://doi.org/10.1073/pnas.2134232100

Shurtleff, M.J., Temoche-Diaz, M.M., Karfilis, K. V., Ri, S., Schekman, R., 2016. Y-box protein 1 is required to sort microRNAs into exosomes in cells and in a cell-free reaction. Elife 5, 1–23. https://doi.org/10.7554/eLife.19276

Siomi, H., Siomi, M.C., 2009. On the road to reading the RNA-interference code. Nature 457, 396–404. https://doi.org/10.1038/nature07754

Smagghe, G., Dhadialla, T.S., Lezzi, M., 2002. Comparative toxicity and ecdysone receptor affinity of nonsteroidal ecdysone agonists and 20-hydroxyecdysone in Chironomus tentans. Insect Biochem. Mol. Biol. 32, 187–192. https://doi.org/10.1016/S0965-1748(01)00109-6

Smykal, V., Bajgar, A., Provaznik, J., Fexova, S., Buricova, M., Takaki, K., Hodkova, M., Jindra, M., Dolezel, D., 2014a. Juvenile hormone signaling during reproduction and development of the linden bug, *Pyrrhocoris apterus*. Insect Biochem. Mol. Biol. 45, 69–76. https://doi.org/10.1016/j.ibmb.2013.12.003

Smykal, V., Daimon, T., Kayukawa, T., Takaki, K., Shinoda, T., Jindra, M., 2014b. Importance of juvenile hormone signaling arises with competence of insect larvae to metamorphose. Dev. Biol. 390, 221–230. https://doi.org/10.1016/j.ydbio.2014.03.006

Sohel, M.H., 2016. Extracellular/circulating microRNAs: release mechanisms, functions and challenges. Achiev. Life Sci. 10, 175–186. https://doi.org/10.1016/j.als.2016.11.007

Sokol, N.S., Ambros, V., 2005. Mesodermally expressed *Drosophila* microRNA-1 is regulated by Twist and is required in muscles during larval growth. Genes Dev. 19, 2343–2354. https://doi.org/10.1101/gad.1356105

Sokol, N.S., Xu, P., Jan, Y.N., Ambros, V., 2008. *Drosophila* let-7 microRNA is required for remodeling of the neuromusculature during metamorphosis. Genes Dev. 22, 1591–1596. https://doi.org/10.1101/gad.1671708

Song, J., Li, W., Zhao, H., Gao, L., Fan, Y., Zhou, S., 2018. The microRNAs let 7 and mir 278 regulate insect metamorphosis and oogenesis by targeting the juvenile hormone early response gene *Krüppel homolog*. Dev. 145, 170670. https://doi.org/10.1242/dev.170670

Song, J., Wu, Z., Wang, Z., Deng, S., Zhou, S., 2014. Krüppel-homolog 1 mediates juvenile hormone action to promote vitellogenesis and oocyte maturation in the migratory locust. Insect Biochem. Mol. Biol. 52, 94–101. https://doi.org/10.1016/j.ibmb.2014.07.001

Stay, B., Zhang, J.R., Tobe, S.S., 2002. Methyl farnesoate and juvenile hormone production in embryos of *Diploptera punctata* in relation to innervation of corpora allata and their sensitivity to allatostatin. Peptides 23, 1981–1990. https://doi.org/10.1016/S0196-9781(02)00185-7

Stephen, S., 2019. "Biblical" swarm of locusts plague Italian farmlands in worst infestation since WWII [WWW Document]. Fox News. URL https://www.foxnews.com/world/biblical-locusts-italy-sardinia-farmers (accessed 8.14.20).

Stork, N.E., 2018. How Many Species of Insects and Other Terrestrial Arthropods Are There on Earth? Annu. Rev. Entomol. 63, 31–45. https://doi.org/10.1146/annurev-ento-020117-043348

Sugahara, R., Tanaka, S., Shiotsuki, T., 2017. RNAi-mediated knockdown of SPOOK reduces ecdysteroid titers and causes precocious metamorphosis in the desert locust *Schistocerca gregaria*. Dev. Biol. 429, 71–80. https://doi.org/10.1016/j.ydbio.2017.07.007

Suh, Y.S., Bhat, S., Hong, S.H., Shin, M., Bahk, S., Cho, K.S., Kim, S.W., Lee, K.S., Kim, Y.J., Jones, W.D., Yu, K., 2015. Genome-wide microRNA screening reveals that the evolutionary conserved miR-9a regulates body growth by targeting sNPFR1/NPYR. Nat. Commun. 6, 7693. https://doi.org/10.1038/ncomms8693

Sun, D., Guo, Z., Liu, Y., Zhang, Y., 2017. Progress and prospects of CRISPR/Cas systems in insects and other arthropods. Front. Physiol. 8, 608. https://doi.org/10.3389/fphys.2017.00608

Sundaram, M., Palli, S.R., Krell, P.J., Sohi, S.S., Dhadialla, T.S., Retnakaran, A., 1998. Basis for selective action of a synthetic molting hormone agonist, RH- 5992 on lepidopteran insects. Insect Biochem. Mol. Biol. 28, 693–704. https://doi.org/10.1016/S0965-1748(98)00035-6

Suzuki, Y., Truman, J.W., Riddiford, L.M., 2008. The role of broad in the development of *Tribolium castaneum*: Implications for the evolution of the holometabolous insect pupa. Development 135, 569–577. https://doi.org/10.1242/dev.015263

Symmons, P.M., Cressman, K., 2001. Desert Locust Guidelines, Biology and behaviour, in: Food and Agriculture Organization of the United Nations. pp. 1–43.

Szopa, T.M., 1980. The role of the accessory reproductive glands and genital ducts in egg pod formation in female in *Schistocerca gregaria*. J. Insect Physiol. 27, 23–29.

Tang, Y., He, H., Qu, X., Cai, Y., Ding, W., Qiu, L., Li, Y., 2019. RNA interference-mediated knockdown of the transcription factor *Krüppel homologue 1* suppresses vitellogenesis in *Chilo suppressalis*. Insect Mol. Biol. 29, 1–10. https://doi.org/10.1111/imb.12617

Taning, C.N.T., Van Eynde, B., Yu, N., Ma, S., Smagghe, G., 2017. CRISPR/Cas9 in insects: Applications, best practices and biosafety concerns. J. Insect Physiol. 98, 245–257. https://doi.org/10.1016/j.jinsphys.2017.01.007

Tassetto, M., Kunitomi, M., Andino, R., 2017. Circulating Immune Cells Mediate a Systemic RNAi-Based Adaptive Antiviral Response in *Drosophila*. Cell 169, 314-325.e13. https://doi.org/10.1016/j.cell.2017.03.033

Tatar, M., Kopelman, A., Epstein, D., Tu, M.P., Yin, C.M., Garofalo, R.S., 2001. A mutant *Drosophila* insulin receptor homolog that extends life-span and impairs neuroendocrine function. Science 292, 107–110. https://doi.org/10.1126/science.1057987

Tawfik, A.I., Mat'hová, A., Sehnal, F., Ismail, S.H., 1996. Haemolymph ecdysteroids in the solitary and gregarious larvae of *Schistocerca gregaria*. Arch. Insect Biochem. Physiol. 31, 427–438. https://doi.org/10.1002/(SICI)1520-6327(1996)31:4<427::AID-ARCH5>3.0.CO;2-S

Tawfik, A.I., Tanaka, Y., Tanaka, S., 2002. Possible involvement of ecdysteroids in photoperiodically induced suppresion of ovarian development in a Japanese strain of the migratory locust, *Locusta migratoria*. J. Insect Physiol. https://doi.org/10.1016/S0022-1910(02)00058-6

Tawfik, A.I., Treiblmayr, K., Hassanali, A., Osir, E.O., 2000. Time-course haemolymph juvenile hormone titres in solitarious and gregarious adults of *Schistocerca gregaria*, and their relation to pheromone emission, CA volumetric changes and oocyte growth. J. Insect Physiol. 46, 1143–1150. https://doi.org/10.1016/S0022-1910(99)00225-5

Tawfik, A.I., Vedrová, A., Sehnal, F., 1999. Ecdysteroids during ovarian development and embryogenesis in solitary and gregarious *Schistocerca gregaria*. Arch. Insect Biochem. Physiol. 41, 134–143. https://doi.org/10.1002/(SICI)1520-6327(1999)41:3<134::AID-ARCH4>3.0.CO;2-6

Taylor, D.D., Gercel-Taylor, C., 2008. MicroRNA signatures of tumor-derived exosomes as diagnostic biomarkers of ovarian cancer. Gynecol. Oncol. 110, 13–21. https://doi.org/10.1016/j.ygyno.2008.04.033

Thadani, R., Tammi, M.T., 2006. MicroTar: Predicting microRNA targets from RNA duplexes. BMC Bioinformatics 7, S20. https://doi.org/10.1186/1471-2105-7-S5-S20

Thompson, B.J., Cohen, S.M., 2006. The Hippo Pathway Regulates the bantam microRNA to Control Cell Proliferation and Apoptosis in *Drosophila*. Cell 126, 767–774. https://doi.org/10.1016/j.cell.2006.07.013

Tobe, S.S., Pratt, G.E., 1975. *Corpus allatum* activity *in vitro* during ovarian maturation in the desert locust, *Schistocerca gregaria*. J. Exp. Biol. 62, 611–627.

Tomoyasu, Y., Miller, S.C., Tomita, S., Schoppmeier, M., Grossmann, D., Bucher, G., 2008. Exploring systemic RNA interference in insects: A genome-wide survey for RNAi genes in *Tribolium*. Genome Biol. 9, 10. https://doi.org/10.1186/gb-2008-9-1-r10

Tsui, N.B.Y., Ng, E.K.O., Lo, Y.M.D., 2002. Stability of endogenous and added RNA in blood specimens, serum, and plasma. Clin. Chem. 48, 1647–1653.

Tu, M.P., Yin, C.M., Tatar, M., 2005. Mutations in insulin signaling pathway alter juvenile hormone synthesis in Drosophila melanogaster. Gen. Comp. Endocrinol. 142, 347–356. https://doi.org/10.1016/j.ygcen.2005.02.009

Tu, M.P., Yin, C.M., Tatar, M., 2002. Impaired ovarian ecdysone synthesis of *Drosophila melanogaster* insulin receptor mutants. Aging Cell 1, 158–160. https://doi.org/10.1046/j.1474-9728.2002.00016.x

Turchinovich, A., Burwinkel, B., 2012. Distinct AGO1 and AGO2 associated miRNA profiles in human cells and blood plasma. RNA Biol. 9, 1066–1075. https://doi.org/10.4161/rna.21083

Turchinovich, A., Tonevitsky, A.G., Burwinkel, B., 2016. Extracellular miRNA: A Collision of Two Paradigms. Trends Biochem. Sci. 41, 883–892. https://doi.org/10.1016/j.tibs.2016.08.004

Turchinovich, A., Tonevitsky, A.G., Cho, W.C., Burwinkel, B., 2015. Check and mate to exosomal extracellular miRNA: new lesson from a new approach. Front. Mol. Biosci. 2, 10–12. https://doi.org/10.3389/fmolb.2015.00011

Turchinovich, A., Weiz, L., Langheinz, A., Burwinkel, B., 2011. Characterization of extracellular circulating microRNA. Nucleic Acids Res. 39, 7223–7233. https://doi.org/10.1093/nar/gkr254

Uhlirova, M., Foy, B.D., Beaty, B.J., Olson, K.E., Riddiford, L.M., Jindra, M., 2003. Use of Sindbis virus-mediated RNA interference to demonstrate a conserved role of Broad-Complex in insect metamorphosis. Proc. Natl. Acad. Sci. U. S. A. 100, 15607–15612. https://doi.org/10.1073/pnas.2136837100

Ureña, E., Chafino, S., Manjón, C., Franch-Marro, X., Martín, D., 2016. The occurrence of the holometabolous pupal stage requires the interaction between E93, Krüppel-Homolog 1 and Broad-Complex. PLoS Genet. 12, e1006020. https://doi.org/10.1371/journal.pgen.1006020

Ureña, E., Manjón, C., Franch-Marro, X., Martín, D., 2014. Transcription factor E93 specifies adult metamorphosis in hemimetabolous and holometabolous insects. Proc. Natl. Acad. Sci. U. S. A. 111, 7024–7029. https://doi.org/10.1073/pnas.1401478111

Uvarov, B., 1977. Grasshoppers and locusts. A handbook of general acridology. Volume 2. Behaviour, ecology, biogeography, population dynamics., Centre for Overseas Pest Research.

Uvarov, B.P., 1921. A Revision of the Genus Locusta, L. (= Pachytylus, Fieb.), with a New Theory as to the Periodicity and Migrations of Locusts. Bull. Entomol. Res. 12, 135–163. https://doi.org/10.1017/S0007485300044989

Valadi, H., Ekström, K., Bossios, A., Sjöstrand, M., Lee, J.J., Lötvall, J.O., 2007. Exosome-mediated transfer of mRNAs and microRNAs is a novel mechanism of genetic exchange between cells. Nat. Cell Biol. 9, 654–659. https://doi.org/10.1038/ncb1596

Van den Brande, S., Gijbels, M., Wynant, N., Santos, D., Mingels, L., Gansemans, Y., Van Nieuwerburgh, F., Vanden Broeck, J., 2018. The presence of extracellular microRNAs in the media of cultured *Drosophila cells*. Sci. Rep. 8, 17312. https://doi.org/10.1038/s41598-018-35531-z

Van der Valk, H., Del Castello, R., Cressman, K., Monard, A., Eriksson, H., Ammati, M., Bartoleschi, P., De Brouwer, B., Gazza, S., Everts, J., 2006. Fighting the Locusts... Safely, Pesticides in Desert Locust Control: Balancing Risks Against Benefits. Food Agric. Organ. United Nations. https://doi.org/10.1665/1082-6467(2001)010[0277:RPIDAM]2.0.CO;2

Van Hiel, M.B., Van Wielendaele, P., Temmerman, L., Van Soest, S., Vuerinckx, K., Huybrechts, R., Vanden Broeck, J., Simonet, G., 2009. Identification and validation of housekeeping genes in brains of the desert locust *Schistocerca gregaria* under different developmental conditions. BMC Mol. Biol. 10, 1–10. https://doi.org/10.1186/1471-2199-10-56

Van Wielendaele, P., Badisco, L., Vanden Broeck, J., 2013. Neuropeptidergic regulation of reproduction in insects. Gen. Comp. Endocrinol. 188, 23–34. https://doi.org/10.1016/j.ygcen.2013.02.005

Van Wielendaele, P., Dillen, S., Marchal, E., Badisco, L., Vanden Broeck, J., 2012. CRF-like diuretic hormone negatively affects both feeding and reproduction in the desert locust, *Schistocerca gregaria*. PLoS One 7, e31425. https://doi.org/10.1371/journal.pone.0031425

Vandesompele, J., De Preter, K., Pattyn, F., Poppe, B., Van Roy, N., De Paepe, A., Speleman, F., 2002. Accurate normalization of real-time quantitative RT-PCR data by geometric averaging of multiple internal control genes. Genome Biol. 3, 0034.1-0034.11. https://doi.org/10.1186/gb-2002-3-7-research0034

Varghese, J., Cohen, S.M., 2007. microRNA miR-14 acts to modulate a positive autoregulatory loop controlling steroid hormone signaling in *Drosophila*. Genes Dev. 21, 2277–2282. https://doi.org/10.1101/gad.439807

Verlinden, H., Gijbels, M., Lismont, E., Lenaerts, C., Vanden Broeck, J., Marchal, E., 2015. The pleiotropic allatoregulatory neuropeptides and their receptors: A mini-review. J. Insect Physiol. 80, 2–14. https://doi.org/10.1016/j.jinsphys.2015.04.004

Verlinden, H., Sterck, L., Li, J., Li, Z., Yssel, A., Gansemans, Y., Verdonck, R., Holtof, M., Song, H., Behmer, S.T., Sword, G.A., Matheson, T., Ott, S.R., Deforce, D., Van Nieuwerburgh, F., Van de Peer, Y., Vanden Broeck, J., 2020. First draft genome assembly of the desert locust, *Schistocerca gregaria*. F1000Research 9, 775. https://doi.org/10.12688/f1000research.25148.1

Verlinden, H., Vleugels, R., Zels, S., Dillen, S., Lenaerts, C., Crabbé, K., Spit, J., Vanden Broeck, J., 2014. Receptors for neuronal or endocrine signalling molecules as potential targets for the control of insect pests. Adv. In Insect Phys. 46, 167–303. https://doi.org/10.1016/B978-0-12-417010-0.00003-3

Villalobos-Sambucaro, M.J., Riccillo, F.L., Calderón-Fernández, G.M., Sterkel, M., Diambra, L.A., Ronderos, J.R., 2015. Genomic and functional characterization of a *methoprene-tolerant* gene in the kissing-bug *Rhodnius prolixus*. Gen. Comp. Endocrinol. 216, 1–8. https://doi.org/10.1016/j.ygcen.2015.04.018

Villarroya-Beltri, C., Gutiérrez-Vázquez, C., Sánchez-Cabo, F., Pérez-Hernández, D., Vázquez, J., Martin-Cofreces, N., Martinez-Herrera, D.J., Pascual-Montano, A., Mittelbrunn, M., Sánchez-Madrid, F., 2013. Sumoylated hnRNPA2B1 controls the sorting of miRNAs into exosomes through binding to specific motifs. Nat. Commun. 4, 2980. https://doi.org/10.1038/ncomms3980

Vodovar, N., Saleh, M.C., 2012. Of Insects and Viruses: The Role of Small RNAs in Insect Defence. Adv. In Insect Phys. 42, 1–36.

Vogel, E., Santos, D., Mingels, L., Verdonckt, T.W., Broeck, J. Vanden, 2019. RNA interference in insects: Protecting beneficials and controlling pests. Front. Physiol. 9, 1912. https://doi.org/10.3389/fphys.2018.01912

Vogel, K.J., Brown, M.R., Strand, M.R., 2015. Ovary ecdysteroidogenic hormone requires a receptor tyrosine kinase to activate egg formation in the mosquito *Aedes aegypti*. Proc. Natl. Acad. Sci. 112, 5057–5062. https://doi.org/10.1073/pnas.1501814112

Vojtech, L., Woo, S., Hughes, S., Levy, C., Ballweber, L., Sauteraud, R.P., Strobl, J., Westerberg, K., Gottardo, R., Tewari, M., Hladik, F., 2014. Exosomes in human semen carry a distinctive repertoire of small non-coding RNAs with potential regulatory functions. Nucleic Acids Res. 42, 7290–7304. https://doi.org/10.1093/nar/gku347

Vuerinckx, K., Verlinden, H., Lindemans, M., Broeck, J. Vanden, Huybrechts, R., 2011. Characterization of an allatotropin-like peptide receptor in the red flour beetle, *tribolium castaneum*. Insect Biochem. Mol. Biol. 41, 815–822. https://doi.org/10.1016/j.ibmb.2011.06.003

Waldron, J.A., Newbury, S.F., 2012. The roles of microRNAs in wing imaginal disc development in *Drosophila*. Biochem. Soc. Trans. 40, 891–895.

Wang, C., Zhang, J., Tobe, S.S., Bendena, W.G., 2012. Defining the contribution of select neuropeptides and their receptors in regulating sesquiterpenoid biosynthesis by *Drosophila melanogaster* ring gland/corpus allatum through RNAi analysis. Gen. Comp. Endocrinol. 176, 347–353. https://doi.org/10.1016/j.ygcen.2011.12.039

Wang, F., Wang, K., Forknall, N., Patrick, C., Yang, T., Parekh, R., Bock, D., Dickson, B.J., 2020. Neural circuitry linking mating and egg laying in *Drosophila females*. Nature 579, 101–105. https://doi.org/10.1038/s41586-020-2055-9

Wang, J.L., Saha, T.T., Zhang, Y., Zhang, C., Raikhel, A.S., 2017. Juvenile hormone and its receptor methoprene-tolerant promote ribosomal biogenesis and vitellogenesis in the *Aedes aegypti* mosquito.

J. Biol. Chem. 292, 10306–10315. https://doi.org/10.1074/jbc.M116.761387

Wang, S.F., Li, C., Sun, G., Zhu, J., Raikhel, A.S., 2002. Differential expression and regulation by 20-hydroxyecdysone of mosquito ecdysteroid receptor isoforms A and B. Mol. Cell. Endocrinol. 196, 29–42. https://doi.org/10.1016/S0303-7207(02)00225-3

Wang, X., Guo, B., Li, Q., Peng, J., Yang, Z., Wang, A., Li, D., Hou, Z., Lv, K., Kan, G., Cao, H., Wu, H., Song, J., Pan, X., Sun, Q., Ling, S., Li, Yuheng, Zhu, M., Zhang, P., Peng, S., Xie, X., Tang, T., Hong, A., Bian, Z., Bai, Y., Lu, A., Li, Yinghui, He, F., Zhang, G., Li, Yingxian, 2013. MiR-214 targets ATF4 to inhibit bone formation. Nat. Med. 19, 93–100. https://doi.org/10.1038/nm.3026

Wang, X., Hou, Y., Saha, T.T., Pei, G., Raikhel, A.S., Zou, Z., 2017. Hormone and receptor interplay in the regulation of mosquito lipid metabolism. Proc. Natl. Acad. Sci. U. S. A. 114, E2709–E2718. https://doi.org/10.1021/ie50289a006

Wang, Y., Li, D., Liu, X., Li, T., Ma, E., Fan, R., Zhang, J., 2015. Molecular characterization and RNAi-based functional analysis of Obstructor family genes in *Locusta migratoria*. Sci. Agric. Sin. 48, 73–82.

Wang, Y.L., Yang, M.L., Jiang, F., Zhang, J.Z., Kang, L., 2013. MicroRNA-dependent development revealed by RNA interference-mediated gene silencing of *LmDicer1* in the migratory locust. Insect Sci. 20, 53–60. https://doi.org/10.1111/j.1744-7917.2012.01542.x

Wang, Z., Yang, L., Song, J., Kang, L., Zhou, S., 2017. An isoform of Taiman that contains a PRD-repeat motif is indispensable for transducing the vitellogenic juvenile hormone signal in *Locusta migratoria*. Insect Biochem. Mol. Biol. 82, 31–40. https://doi.org/10.1016/j.ibmb.2017.01.009

Wang, Z.Z., Ye, X.Q., Shi, M., Li, F., Wang, Z.H., Zhou, Y.N., Gu, Q.J., Wu, X.T., Yin, C.L., Guo, D.H., Hu, R.M., Hu, N.N., Chen, T., Zheng, B.Y., Zou, J.N., Zhan, L.Q., Wei, S.J., Wang, Y.P., Huang, J.H., Fang, X.D., Strand, M.R., Chen, X.X., 2018. Parasitic insect-derived miRNAs modulate host development. Nat. Commun. 9, 2205. https://doi.org/10.1038/s41467-018-04504-1

Ware, G.W., Whitacre, D.M., 2003. The pesticide book. MeistroPRO, Willoughby, OH.

Warren, J.T., O'Connor, M.B., Gilbert, L.I., 2009. Studies on the black box: Incorporation of 3-oxo-7-dehydrocholesterol into ecdysteroids by *Drosophila melanogaster* and *Manduca sexta*. Insect Biochem. Mol. Biol. https://doi.org/10.1016/j.ibmb.2009.08.004

Warren, J.T., Petryk, A., Marques, G., Jarcho, M., Parvy, J.-P., Dauphin-Villemant, C., O'Connor, M.B., Gilbert, L.I., 2002. Molecular and biochemical characterization of two P450 enzymes in the ecdysteroidogenic pathway of *Drosophila melanogaster*. Proc. Natl. Acad. Sci. 99, 11043–11048. https://doi.org/10.1073/pnas.162375799

Warren, J.T., Petryk, A., Marqués, G., Parvy, J.P., Shinoda, T., Itoyama, K., Kobayashi, J., Jarcho, M., Li, Y., O'Connor, M.B., Dauphin-Villemant, C., Gilbert, L.I., 2004. *Phantom* encodes the 25-hydroxylase of *Drosophila melanogaster* and *Bombyx mori*: A P450 enzyme critical in ecdysone biosynthesis. Insect Biochem. Mol. Biol. 34, 991–1010. https://doi.org/10.1016/j.ibmb.2004.06.009

Weaver, R.J., Audsley, N., 2009. Neuropeptide regulators of juvenile hormone synthesis: Structures, functions, distribution, and unanswered questions. Ann. N. Y. Acad. Sci. 1163, 316–329. https://doi.org/10.1111/j.1749-6632.2009.04459.x

Wei, Y., Chen, S., Yang, P., Ma, Z., Kang, L., 2009. Characterization and comparative profiling of the small RNA transcriptomes in two phases of locust. Genome Biol. 10, R6. https://doi.org/10.1186/gb-2009-10-1-r6

Wen, Z., Gulia, M., Clark, K.D., Dhara, A., Crim, J.W., Strand, M.R., Brown, M.R., 2010. Two insulin-like peptide family members from the mosquito *Aedes aegypti* exhibit differential biological and receptor binding activities. Mol. Cell. Endocrinol. 328, 47–55. https://doi.org/10.1016/j.mce.2010.07.003

Wigglesworth, V.B., 1936. The function of the Corpus allatum in the growth and reproduction of *Rhodnius prolixus* (Hemiptera). Q. J. Microsc. Sci. s2-79, 91–121.

Wigglesworth, V.B., 1934. The Physiology of Ecdysis in *Rhodnius Prolixus* (Hemiptera). II. Factors controlling Moulting and "Metamorphosis." Q. J. Microsc. Sci. 77, 193–221.

Wilson, T.G., Fabian, J., 1986. A *Drosophila melanogaster* mutant resistant to a chemical analog of juvenile hormone. Dev. Biol. 118, 190–201. https://doi.org/10.1016/0012-1606(86)90087-4

Woodhead, A.P., Stay, B., Seidel, S.L., Khan, M.A., Tobe, S.S., 1989. Primary structure of four allatostatins: neuropeptide inhibitors of juvenile hormone synthesis. Proc. Natl. Acad. Sci. U. S. A. 86, 5997–6001. https://doi.org/10.1073/pnas.86.15.5997

Wu, P., Jiang, X., Guo, X., Li, L., Chen, T., 2016. Genome-wide analysis of differentially expressed microrna in *bombyx mori* infected with nucleopolyhedrosis virus. PLoS One 11, e0165865.

https://doi.org/10.1371/journal.pone.0165865

Wu, W., Xiong, W., Li, C., Zhai, M., Li, Y., Ma, F., Li, B., 2017. MicroRNA-dependent regulation of metamorphosis and identification of microRNAs in the red flour beetle, *Tribolium castaneum*. Genomics 109, 362–373. https://doi.org/10.1016/j.ygeno.2017.06.001

Wu, Z., Guo, W., Xie, Y., Zhou, S., 2016. Juvenile hormone activates the transcription of cell-division-cycle 6 (Cdc6) for polyploidy-dependent insect vitellogenesis and oogenesis. J. Biol. Chem. 291, 5418–5427. https://doi.org/10.1074/jbc.M115.698936

Wu, Z., Guo, W., Yang, L., He, Q., Zhou, S., 2018. Juvenile hormone promotes locust fat body cell polyploidization and vitellogenesis by activating the transcription of Cdk6 and E2f1. Insect Biochem. Mol. Biol. 102, 1–10. https://doi.org/10.1016/j.ibmb.2018.09.002

Wyatt, G.R., Braun, R.P., Zhang, J., 1996. Priming effect in gene activation by juvenile hormone in locust fat body. Arch. Insect Biochem. Physiol. 32, 633–640. https://doi.org/Doi 10.1002/(Sici)1520-6327(1996)32:3/4<633::Aid-Arch34>3.0.Co;2-B

Wyatt, G.R., Davey, K.G., 1996. Cellular and Molecular Actions of Juvenile Hormone. II. Roles of Juvenile Hormone in Adult Insects. Adv. In Insect Phys. 26, 1–155. https://doi.org/10.1016/S0065-2806(08)60030-2

Wynant, N., Duressa, T.F., Santos, D., Van Duppen, J., Proost, P., Huybrechts, R., Vanden Broeck, J., 2014a. Lipophorins can adhere to dsRNA, bacteria and fungi present in the hemolymph of the desert locust: A role as general scavenger for pathogens in the open body cavity. J. Insect Physiol. 64, 7–13. https://doi.org/10.1016/j.jinsphys.2014.02.010

Wynant, N., Santos, D., Vanden Broeck, J., 2017. The evolution of animal Argonautes: evidence for the absence of antiviral AGO Argonautes in vertebrates. Sci. Rep. 7, 9230. https://doi.org/10.1038/s41598-017-08043-5

Wynant, N., Santos, D., Vanden Broeck, J., 2014b. Biological Mechanisms Determining the Success of RNA Interference in Insects. Int. Rev. Cell Mol. Biol. 312, 139–167. https://doi.org/10.1016/B978-0-12-800178-3.00005-1

Wynant, N., Verlinden, H., Breugelmans, B., Simonet, G., Vanden Broeck, J., 2012. Tissue-dependence and sensitivity of the systemic RNA interference response in the desert locust, *Schistocerca gregaria*. Insect Biochem. Mol. Biol. 42, 911–917. https://doi.org/10.1016/j.ibmb.2012.09.004

Xu, J., Wang, X.F., Chen, P., Liu, F.T., Zheng, S.C., Ye, H., Mo, M.H., 2016. RNA interference in moths: Mechanisms, applications, and progress. Genes (Basel). 7, 88. https://doi.org/10.3390/genes7100088

Yamanaka, N., Rewitz, K.F., O 'Connor, M.B., 2013. Ecdysone Control of Developmental Transitions: Lessons from *Drosophila* Research. Annu. Rev. Entomol. 58, 497–516. https://doi.org/10.1146/annurev-ento-120811-153608

Yamanaka, N., Yamamoto, S., Žitňan, D., Watanabe, K., Kawada, T., Satake, H., Kaneko, Y., Hiruma, K., Tanaka, Y., Shinoda, T., Kataoka, H., 2008. Neuropeptide receptor transcriptome reveals unidentified neuroendocrine pathways. PLoS One 3, e3048. https://doi.org/10.1371/journal.pone.0003048

Yan, S., Ren, B., Zeng, B., Shen, J., 2020. Improving RNAi efficiency for pest control in crop species. Biotechniques 68, 283–290. https://doi.org/10.2144/BTN-2019-0171

Yang, J.-S., Phillips, M.D., Betel, D., Mu, P., Ventura, A., Siepel, A.C., Chen, K.C., Lai, E.C., 2011. Widespread regulatory activity of vertebrate microRNA* species. RNA 17, 312–326. https://doi.org/10.1261/rna.2537911

Yang, M., Wei, Y., Jiang, F., Wang, Y., Guo, X., He, J., Kang, L., 2014. MicroRNA-133 Inhibits Behavioral Aggregation by Controlling Dopamine Synthesis in Locusts. PLoS Genet. 10, e1004206. https://doi.org/10.1371/journal.pgen.1004206

Ylla, G., Fromm, B., Piulachs, M.D., Belles, X., 2016. The microRNA toolkit of insects. Sci. Rep. 6, 37736. https://doi.org/10.1038/srep37736

Yogindran, S., Rajam, M.V., 2020. Host-derived artificial miRNA-mediated silencing of ecdysone receptor gene provides enhanced resistance to *Helicoverpa armigera* in tomato. Genomics in press. https://doi.org/10.1016/j.ygeno.2020.10.004

Yu, X., Zhou, Q., Li, S.C., Luo, Q., Cai, Y., Lin, W.C., Chen, H., Yang, Y., Hu, S., Yu, J., 2008. The silkworm (*Bombyx mori*) microRNAs and their expressions in multiple developmental stages. PLoS One 3, e2997. https://doi.org/10.1371/journal.pone.0002997

Zaim, M., Guillet, P., 2002. Alternative insecticides: An urgent need. Trends Parasitol.

https://doi.org/10.1016/S1471-4922(01)02220-6

Zhang, Q., Xu, J., Chen, Q., Chen, X., Zen, K., Zhang, C.Y., 2013. Selective secretion of microRNA in CNS system. Protein Cell 4, 243–247. https://doi.org/10.1007/s13238-013-3006-0

Zhang, Y., Zhao, B., Roy, S., Saha, T.T., Kokoza, V.A., Li, M., Raikhel, A.S., 2016. MicroRNA-309 targets the Homeobox gene SIX4 and controls ovarian development in the mosquito Aedes aegypti. Proc. Natl. Acad. Sci. U. S. A. 113, E4828–E4836. https://doi.org/10.1073/pnas.1609792113

Zhang, Y., Zhou, X., Ge, X., Jiang, J., Li, M., Jia, S., Yang, X., Kan, Y., Miao, X., Zhao, G., Li, F., Huang, Y., 2009. Insect-specific microRNA involved in the development of the silkworm Bombyx mori. PLoS One 4, e4677. https://doi.org/10.1371/journal.pone.0004677

Zhang, Y.L., Huang, Q.X., Yin, G.H., Lee, S., Jia, R.Z., Liu, Z.X., Yu, N.T., Pennerman, K.K., Chen, X., Guo, A.P., 2015. Identification of microRNAs by small RNA deep sequencing for synthetic microRNA mimics to control *Spodoptera exigua*. Gene 557, 215–221. https://doi.org/10.1016/j.gene.2014.12.038

Zhang, Z., Xu, J., Sheng, Z., Sui, Y., Palli, S.R., 2011. Steroid receptor co-activator is required for juvenile hormone signal transduction through a bHLH-PAS transcription factor, methoprene tolerant. J. Biol. Chem. 286, 8437–8447. https://doi.org/10.1074/jbc.M110.191684

Zhao, B., Lucas, K.J., Saha, T.T., Ha, J., Ling, L., Kokoza, V.A., Roy, S., Raikhel, A.S., 2017. MicroRNA-275 targets sarco/endoplasmic reticulum Ca2+adenosine triphosphatase (SERCA) to control key functions in the mosquito gut. PLoS Genet. 13, e1006943. https://doi.org/10.1371/journal.pgen.1006943

Zhao, C., Sun, X., Li, L., 2019. Biogenesis and function of extracellular miRNAs. ExRNA 1, 1–9. https://doi.org/10.1186/s41544-019-0039-4

Zhao, X., Gou, X., Qin, Z., Li, D., Wang, Y., Ma, E., Li, S., Zhang, J., 2017. Identification and expression of cuticular protein genes based on *Locusta migratoria* transcriptome. Sci. Rep. 7, 4562. https://doi.org/10.1038/srep45462

Zhou, Q., Li, M., Wang, Xiaoyan, Li, Q., Wang, T., Zhu, Q., Zhou, X., Wang, Xin, Gao, X., Li, X., 2011. Immune-related microRNAs are abundant in breast milk exosomes. Int. J. Biol. Sci. 8, 118–123. https://doi.org/10.7150/ijbs.8.118

Zhou, X., Riddiford, L.M., 2002. Broad specifies pupal development and mediates the “status quo” action of juvenile hormone on the pupal-adult transformation in *Drosophila* and *Manduca*. Development 129, 2259–2269.

Zitnan, D., Adams, M.E., 2012. Neuroendocrine Regulation of Ecdysis, in: Insect Endocrinology. pp. 253–309. https://doi.org/10.1016/B978-0-12-384749-2.10007-X

Zou, Z., Saha, T.T., Roy, S., Shin, S.W., Backman, T.W.H., Girke, T., White, K.P., Raikhel, A.S., 2013. Juvenile hormone and its receptor, methoprene-tolerant, control the dynamics of mosquito gene expression. Proc. Natl. Acad. Sci. U. S. A. 110, E2173–E2181. https://doi.org/10.1073/pnas.1305293110

Publications and awards

Articles in internationally peer-reviewed scientific journals

Gijbels, M., Schellens, S., Verdonckt, T.W., Bruyninckx, E. and Vanden Broeck, J. (2020). RNAi-mediated knockdown of transcription factor E93 in nymphs of the desert locust (*Schistocerca gregaria*) inhibits adult morphogenesis and results in supernumerary juvenile stages. International Journal of Molecular Sciences, 21: 7518. doi: 10.3390/ijms21207518

Gijbels, M., Schellens, S., Schellekens, T., Bruyninckx, E., Marchal, E. and Vanden Broeck, J. (2020). Precocious downregulation of Krüppel-homolog 1 in the migratory locust, *Locusta migratoria*, gives rise to an adultoid phenotype with accelerated ovarian development but disturbed mating and oviposition. International Journal of Molecular Sciences, 61: 6058. doi: 10.3390/ijms21176058

Gijbels, M., Lenaerts, C., Vanden Broeck, J. and Marchal, E. (2019). Juvenile hormone receptor Met is essential for ovarian maturation in the desert locusts, *Schistocerca gregaria*. Scientific Reports, 9: 10797. doi: 10.1038/s41598-019-47253-x

Van den Brande, S*., **Gijbels, M***., Wynant, N., Santos, D., Mingels, L., Gansemans, Y., Van Nieuwerburgh, F. and Vanden Broeck, J. (2018). The presence of extracellular microRNAs in the media of cultured *Drosophila* cells. Scientific Reports, 8: 17312. doi: 10.1038/s41598-018-35531-z (***equally contributing first authors**)

Verlinden, H., **Gijbels, M.**, Lismont, E., Lenaerts, C., Vanden Broeck, J., Marchal, E. (2015). The pleiotropic allatoregulatory neuropeptides and their receptors: A mini-review. Journal of Insect Physiology, 80: 2-14. doi: 10.1016/j.jinsphys.2015.04.004

Article on the preprint server for biology

Holtof, M., **Gijbels, M.**, Van Lommel, J., DeKempeneer, E., Nicolaï, B.M., Vanden Broeck, J. and Marchal, E. (2020). Crucial role of Juvenile Hormone receptor components Methoprene-tolerant and Taiman in sexual maturation of adult male desert locusts (*Schistocerca gregaria*). https://t.co/LXMThRjIIb #bioRxiv. doi: 10.1101/2020.09.01.277558

Reports of communications at international scientific conferences, symposia and meetings

Gijbels, M., Marchal, E., Vanden Broeck, J. (2016). Cross-talk of juvenile hormone, ecdysteroids and insulin during reproduction of the desert locust, *Schistocerca gregaria*. 28th Conference of European Comparative Endocrinologists, 21-25 August 2016, Leuven, Belgium. (Poster presentation)

Marchal, E., Lenaerts, C., **Gijbels, M.**, Van Wielendaele, P., Vanden Broeck, J. (2016). Cross-talk between the ecdysteroid, insulin and juvenile hormone pathway in the desert locust, *Schistocerca gregaria*. XXV International Congress of Entomology, 25-30 September 2016, Orlando, Florida, USA. (Oral presentation)

Awards

The ESCE Young Investigator Award for the **best poster presentation** at CECE 2016, 28th Conference of European Comparative Endocrinologists, 21-25 August 2016, Leuven, Belgium.

Appendices

Supplementary Figure 1 Chapter 2

Immunoblot analysis on EVs and EAgo-1 immunoprecipitates. (**A**) EVs of both cell lines were subjected to immunoblot analysis for three common EV markers, which were clearly detected in the EV fractions purified from the extracellular media of both cell lines. (**B**) EAgo-1 IP was performed on the conditioned S2 and Cl.8 media as described in Methods section, but eluted in lithium dodecyl sulfate (LDS) instead of Qiazol. After elution, S2 and Cl.8 IP products were subjected to immunoblot analysis for EAgo-1, which was clearly detected in both IP products. Full-length blots of Fig. 1. Abbreviations: L: Seeblue Prestained 2 Protein Standard (Thermo Fisher); + : positive control sample (in this case, a protein extract of respectively Cl.8 and S2 cells); IP: Detection of EAgo-1 after immunoprecipitation. Both in the Cl.8 and S2 samples, we detect two additional bands at approximately 55 and 29 kDa, representing co-eluted antibody chains (heavy and light). IP*: Elution performed using Glycine buffer at different concentrations as a pilot experiment.

A) **B)**

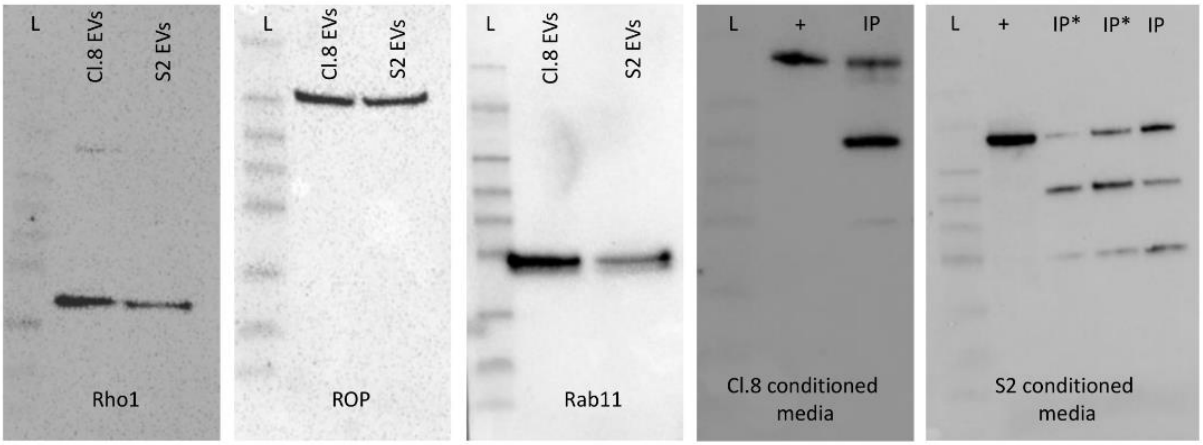

Supplementary Figure 2 Chapter 2

miRNA cDNA synthesis. Equal amounts of small RNA were used for cDNA synthesis using the qScript™ microRNA cDNA Synthesis Kit (Quanta Bio) following the manufacturer's protocol. This protocol includes polyadenylation of the miRNAs in a poly(A) polymerase reaction followed by cDNA synthesis using an oligo-dT containing adapter primer. This adapter primer allows amplification of cDNAs in quantitative real-time PCR (qRT-PCR) reactions due to a unique sequence at its 5' end.

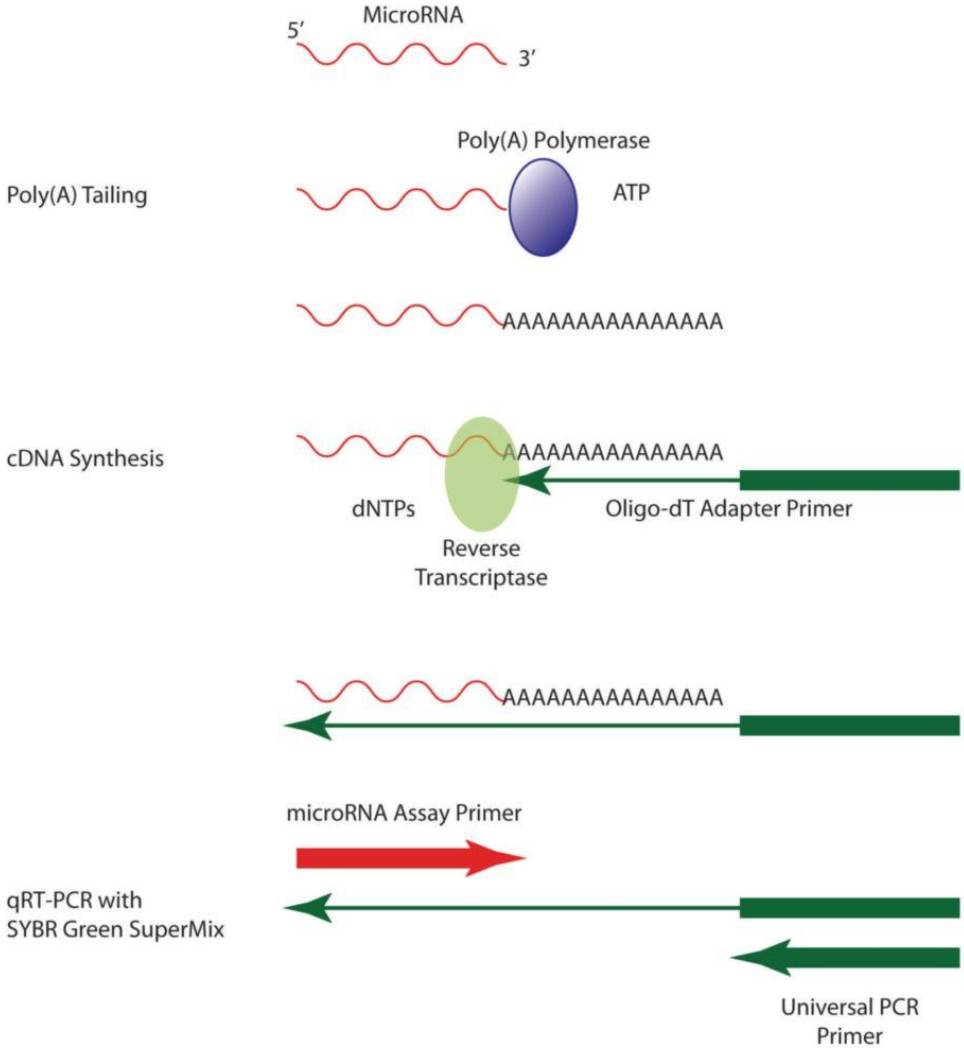

Supplementary Table Chapter 2

S2 small RNA sequencing data. Small RNA sequencing was executed on 3 biological replicates of S2 cells and EVs. Differential expression analysis was performed using edgeR. Amount of nucleotides (nt) and raw reads are included in the table.

Replicate 1 S2 Cells

MiRNA	nt	Reads	MiRNA	nt	Reads
dme-bantam-3p	23	13431	dme-miR-996-5p	22	32
dme-miR-184-3p	22	7316	dme-miR-282-5p	24	31
dme-miR-8-3p	23	3774	dme-miR-11-5p	22	29
dme-bantam-5p	23	3706	dme-miR-965-5p	23	27
dme-miR-14-3p	22	2560	dme-miR-8-5p	22	20
dme-miR-33-5p	21	1870	dme-miR-989-5p	23	20
dme-miR-9b-5p	23	891	dme-miR-2a-1-5p	22	18
dme-miR-34-5p	24	827	dme-miR-308-5p	22	18
dme-miR-276a-3p	22	696	dme-miR-980-3p	22	18
dme-miR-7-5p	23	456	dme-miR-317-5p	22	16
dme-miR-11-3p	21	392	dme-miR-92a-5p	22	15
dme-miR-277-3p	23	372	dme-miR-973-5p	25	15
dme-miR-2a-2-5p	21	329	dme-miR-980-5p	24	14
dme-miR-995-3p	21	316	dme-miR-281-2-5p	22	13
dme-miR-283-5p	22	198	dme-miR-34-3p	23	13
dme-miR-2b-2-5p	23	195	dme-miR-2a-3p	23	11
dme-miR-375-3p	22	190	dme-miR-9381-5p	20	10
dme-miR-279-3p	22	185	dme-miR-9388-3p	22	8
dme-miR-14-5p	22	184	dme-miR-1007-3p	22	7
dme-miR-2b-3p	23	151	dme-miR-1012-3p	23	7
dme-miR-9c-5p	22	147	dme-miR-4956-5p	22	7
dme-miR-305-3p	23	144	dme-miR-1003-3p	22	6
dme-miR-306-5p	22	127	dme-miR-263a-5p	24	6
dme-miR-999-3p	22	100	dme-miR-275-5p	23	6
dme-miR-970-3p	21	92	dme-miR-313-5p	22	6
dme-miR-190-5p	24	83	dme-miR-4911-3p	22	6
dme-miR-275-3p	23	83	dme-let-7-5p	21	5
dme-miR-305-5p	23	78	dme-miR-13b-2-5p	24	5
dme-miR-317-3p	24	67	dme-miR-184-5p	21	5
dme-miR-996-3p	22	54	dme-miR-289-5p	26	5
dme-miR-9b-3p	22	46	dme-miR-306-3p	22	5
dme-miR-988-5p	22	43	dme-miR-998-5p	22	5
dme-miR-12-5p	23	38	dme-miR-9a-5p	23	5
dme-miR-986-5p	22	38	dme-miR-304-5p	23	4
dme-miR-13b-3p	22	36	dme-miR-4976-5p	22	4
dme-miR-10404-5p	22	35	dme-miR-954-5p	21	4
dme-miR-277-5p	21	32	dme-miR-1002-5p	24	3

MiRNA	nt	Reads	MiRNA	nt	Reads
dme-miR-1010-5p	21	3	dme-miR-1-3p	22	1
dme-miR-279-5p	26	3	dme-miR-219-3p	22	1
dme-miR-311-5p	23	3	dme-miR-2489-3p	22	1
dme-miR-5-5p	23	3	dme-miR-2501-5p	23	1
dme-miR-6-3-5p	23	3	dme-miR-281-1-5p	23	1
dme-miR-9373-3p	21	3	dme-miR-284-5p	26	1
dme-miR-9382-5p	21	3	dme-miR-285-5p	23	1
dme-miR-957-3p	22	3	dme-miR-286-3p	23	1
dme-miR-970-5p	24	3	dme-miR-303-3p	22	1
dme-miR-979-5p	23	3	dme-miR-310-5p	23	1
dme-miR-981-3p	22	3	dme-miR-312-5p	23	1
dme-miR-988-3p	22	3	dme-miR-314-5p	26	1
dme-miR-989-3p	21	3	dme-miR-316-3p	22	1
dme-miR-995-5p	22	3	dme-miR-31a-5p	23	1
dme-miR-12-3p	22	2	dme-miR-33-3p	22	1
dme-miR-210-3p	23	2	dme-miR-3642-5p	22	1
dme-miR-2279-5p	22	2	dme-miR-4912-5p	23	1
dme-miR-2491-3p	18	2	dme-miR-4919-3p	21	1
dme-miR-2496-3p	22	2	dme-miR-4939-3p	21	1
dme-miR-2496-5p	24	2	dme-miR-4940-5p	22	1
dme-miR-274-3p	23	2	dme-miR-4941-5p	21	1
dme-miR-274-5p	23	2	dme-miR-4947-5p	23	1
dme-miR-278-5p	23	2	dme-miR-4948-5p	22	1
dme-miR-310-3p	22	2	dme-miR-4949-3p	22	1
dme-miR-311-3p	22	2	dme-miR-4956-3p	22	1
dme-miR-318-3p	22	2	dme-miR-4957-3p	21	1
dme-miR-3642-3p	22	2	dme-miR-4957-5p	22	1
dme-miR-4909-3p	23	2	dme-miR-4958-3p	22	1
dme-miR-4942-3p	22	2	dme-miR-4961-5p	22	1
dme-miR-4958-5p	22	2	dme-miR-4965-5p	21	1
dme-miR-4963-3p	22	2	dme-miR-4969-3p	22	1
dme-miR-4985-3p	22	2	dme-miR-4969-5p	24	1
dme-miR-9370-3p	22	2	dme-miR-4974-3p	22	1
dme-miR-9370-5p	22	2	dme-miR-4979-5p	22	1
dme-miR-960-5p	22	2	dme-miR-4981-3p	21	1
dme-miR-976-5p	22	2	dme-miR-4986-5p	23	1
dme-miR-982-5p	23	2	dme-miR-4987-3p	21	1
dme-miR-984-5p	23	2	dme-miR-6-2-5p	23	1
dme-miR-987-3p	20	2	dme-miR-7-3p	22	1
dme-miR-990-3p	24	2	dme-miR-79-3p	22	1
dme-miR-1001-3p	22	1	dme-miR-92b-3p	22	1
dme-miR-1007-5p	23	1	dme-miR-92b-5p	23	1
dme-miR-1013-3p	20	1	dme-miR-9376-3p	21	1
dme-miR-1016-3p	21	1	dme-miR-9377-3p	21	1
dme-miR-11182	22	1	dme-miR-9380-3p	22	1

MiRNA	nt	Reads
dme-miR-9380-5p	22	1
dme-miR-955-5p	23	1
dme-miR-956-3p	23	1
dme-miR-960-3p	22	1
dme-miR-961-3p	22	1
dme-miR-963-5p	24	1
dme-miR-966-5p	21	1
dme-miR-967-3p	23	1
dme-miR-969-5p	21	1
dme-miR-974-3p	22	1
dme-miR-983-5p	22	1
dme-miR-986-3p	22	1
dme-miR-991-3p	22	1
dme-miR-993-3p	23	1

Replicate 2 S2 Cells

MiRNA	nt	Reads	MiRNA	nt	Reads
dme-miR-184-3p	22	17861	dme-miR-4976-5p	22	9
dme-miR-14-3p	22	2273	dme-miR-92b-3p	22	9
dme-miR-276a-3p	22	1051	dme-miR-252-5p	22	8
dme-miR-8-3p	23	951	dme-miR-283-5p	22	8
dme-bantam-3p	23	751	dme-miR-1000-3p	22	7
dme-miR-34-5p	24	657	dme-miR-2493-3p	23	7
dme-bantam-5p	23	607	dme-miR-4948-5p	22	7
dme-miR-33-5p	21	446	dme-miR-970-5p	24	7
dme-miR-14-5p	22	422	dme-miR-1003-3p	22	6
dme-miR-275-3p	23	421	dme-miR-306-3p	22	6
dme-miR-11-3p	21	216	dme-miR-313-5p	22	6
dme-miR-2b-3p	23	214	dme-miR-318-3p	22	6
dme-miR-317-3p	24	176	dme-miR-9377-3p	21	6
dme-miR-279-3p	22	129	dme-miR-996-3p	22	6
dme-miR-9b-5p	23	115	dme-miR-998-5p	22	6
dme-miR-970-3p	21	102	dme-miR-12-5p	23	5
dme-miR-980-5p	24	89	dme-miR-263a-5p	24	5
dme-miR-306-5p	22	84	dme-miR-289-5p	26	5
dme-miR-995-3p	21	76	dme-miR-4958-5p	22	5
dme-miR-277-3p	23	70	dme-miR-184-5p	21	4
dme-miR-11-5p	22	65	dme-miR-278-3p	22	4
dme-miR-34-3p	23	65	dme-miR-281-1-5p	23	4
dme-miR-7-5p	23	61	dme-miR-282-5p	24	4
dme-miR-2a-2-5p	21	49	dme-miR-375-3p	22	4
dme-miR-305-3p	23	41	dme-miR-9388-3p	22	4
dme-miR-988-3p	22	36	dme-miR-973-5p	25	4
dme-miR-2b-2-5p	23	28	dme-miR-980-3p	22	4
dme-miR-8-5p	22	25	dme-miR-990-3p	24	4
dme-miR-999-3p	22	20	dme-miR-1002-5p	24	3
dme-miR-279-5p	26	18	dme-miR-263b-3p	22	3
dme-miR-2a-3p	23	16	dme-miR-277-5p	21	3
dme-miR-9c-5p	22	16	dme-miR-308-5p	22	3
dme-miR-965-5p	23	15	dme-miR-310-3p	22	3
dme-miR-996-5p	22	15	dme-miR-310-5p	23	3
dme-miR-275-5p	23	14	dme-miR-4956-5p	22	3
dme-miR-9381-5p	20	14	dme-miR-4963-3p	22	3
dme-miR-9b-3p	22	14	dme-miR-9371-5p	22	3
dme-miR-317-5p	22	11	dme-miR-9376-3p	21	3
dme-miR-988-5p	22	11	dme-miR-9381-3p	22	3
dme-miR-1012-3p	23	10	dme-miR-954-5p	21	3
dme-miR-281-2-5p	22	10	dme-miR-1003-5p	21	2
dme-miR-2a-1-5p	22	10	dme-miR-13b-2-5p	24	2
dme-miR-305-5p	23	10	dme-miR-2496-5p	24	2
dme-miR-13b-3p	22	9	dme-miR-2c-3p	23	2
dme-miR-190-5p	24	9	dme-miR-4911-3p	22	2

MiRNA	nt	Reads	MiRNA	nt	Reads
dme-miR-4941-3p	24	2	dme-miR-4962-5p	24	1
dme-miR-4948-3p	22	2	dme-miR-4968-3p	22	1
dme-miR-4957-3p	21	2	dme-miR-4969-3p	22	1
dme-miR-4968-5p	22	2	dme-miR-4969-5p	24	1
dme-miR-4973-5p	21	2	dme-miR-4985-3p	22	1
dme-miR-4987-5p	23	2	dme-miR-6-3p	22	1
dme-miR-5-5p	23	2	dme-miR-7-3p	22	1
dme-miR-92a-3p	22	2	dme-miR-9370-5p	22	1
dme-miR-9376-5p	23	2	dme-miR-9373-5p	21	1
dme-miR-9382-3p	22	2	dme-miR-9375-3p	22	1
dme-miR-966-5p	21	2	dme-miR-959-5p	21	1
dme-miR-979-5p	23	2	dme-miR-960-3p	22	1
dme-miR-986-3p	22	2	dme-miR-960-5p	22	1
dme-miR-986-5p	22	2	dme-miR-963-5p	24	1
dme-miR-995-5p	22	2	dme-miR-965-3p	22	1
dme-miR-9a-5p	23	2	dme-miR-974-3p	22	1
dme-miR-1006-3p	23	1	dme-miR-979-3p	21	1
dme-miR-1009-3p	23	1	dme-miR-981-5p	22	1
dme-miR-10404-5p	22	1	dme-miR-989-3p	21	1
dme-miR-125-3p	21	1	dme-miR-991-3p	22	1
dme-miR-1-3p	22	1	dme-miR-991-5p	22	1
dme-miR-219-3p	22	1	dme-miR-992-5p	22	1
dme-miR-2489-3p	22	1			
dme-miR-2495-3p	24	1			
dme-miR-2496-3p	22	1			
dme-miR-276b-3p	22	1			
dme-miR-280-5p	27	1			
dme-miR-281-3p	23	1			
dme-miR-286-5p	22	1			
dme-miR-304-3p	22	1			
dme-miR-307a-3p	23	1			
dme-miR-3641-3p	22	1			
dme-miR-3641-5p	20	1			
dme-miR-3642-5p	22	1			
dme-miR-3645-3p	21	1			
dme-miR-4913-3p	23	1			
dme-miR-4941-5p	21	1			
dme-miR-4950-5p	22	1			
dme-miR-4954-3p	21	1			
dme-miR-4957-5p	22	1			
dme-miR-4958-3p	22	1			

Replicate 3 S2 Cells

MiRNA	nt	Reads	MiRNA	nt	Reads
dme-miR-184-3p	22	13865	dme-miR-281-2-5p	22	8
dme-miR-14-3p	22	1403	dme-miR-996-3p	22	8
dme-miR-276a-3p	22	867	dme-miR-92b-3p	22	7
dme-miR-8-3p	23	792	dme-miR-263a-5p	24	6
dme-bantam-3p	23	692	dme-miR-275-5p	23	6
dme-bantam-5p	23	444	dme-miR-277-5p	21	6
dme-miR-34-5p	24	443	dme-miR-184-5p	21	5
dme-miR-33-5p	21	415	dme-miR-970-5p	24	5
dme-miR-275-3p	23	358	dme-miR-1003-3p	22	4
dme-miR-14-5p	22	335	dme-miR-13b-3p	22	4
dme-miR-2b-3p	23	212	dme-miR-281-3p	23	4
dme-miR-11-3p	21	191	dme-miR-282-5p	24	4
dme-miR-279-3p	22	128	dme-miR-318-3p	22	4
dme-miR-317-3p	24	105	dme-miR-995-5p	22	4
dme-miR-9b-5p	23	95	dme-miR-1002-5p	24	3
dme-miR-306-5p	22	85	dme-miR-12-5p	23	3
dme-miR-980-5p	24	76	dme-miR-279-5p	26	3
dme-miR-277-3p	23	75	dme-miR-281-1-5p	23	3
dme-miR-2a-2-5p	21	70	dme-miR-4987-5p	23	3
dme-miR-995-3p	21	64	dme-miR-9a-5p	23	3
dme-miR-7-5p	23	62	dme-miR-1000-3p	22	2
dme-miR-970-3p	21	57	dme-miR-10404-5p	22	2
dme-miR-11-5p	22	54	dme-miR-1-3p	22	2
dme-miR-34-3p	23	49	dme-miR-278-3p	22	2
dme-miR-305-3p	23	42	dme-miR-289-5p	26	2
dme-miR-2b-2-5p	23	23	dme-miR-308-5p	22	2
dme-miR-4948-5p	22	22	dme-miR-313-5p	22	2
dme-miR-8-5p	22	21	dme-miR-31a-5p	23	2
dme-miR-988-3p	22	21	dme-miR-33-3p	22	2
dme-miR-996-5p	22	15	dme-miR-9381-5p	20	2
dme-miR-9b-3p	22	15	dme-miR-9388-3p	22	2
dme-miR-263b-3p	22	13	dme-miR-998-5p	22	2
dme-miR-317-5p	22	12	dme-let-7-5p	21	1
dme-miR-999-3p	22	12	dme-miR-100-5p	22	1
dme-miR-283-5p	22	11	dme-miR-1007-3p	22	1
dme-miR-2a-1-5p	22	11	dme-miR-124-3p	23	1
dme-miR-965-5p	23	11	dme-miR-2279-5p	22	1
dme-miR-2a-3p	23	10	dme-miR-2496-3p	22	1
dme-miR-305-5p	23	10	dme-miR-2501-5p	23	1
dme-miR-1012-3p	23	9	dme-miR-2535b-3p	22	1
dme-miR-190-5p	24	9	dme-miR-283-3p	21	1
dme-miR-2493-3p	23	9	dme-miR-2c-3p	23	1
dme-miR-252-5p	22	9	dme-miR-304-5p	23	1
dme-miR-988-5p	22	9	dme-miR-306-3p	22	1
dme-miR-9c-5p	22	9	dme-miR-310-3p	22	1

MiRNA	nt	Reads
dme-miR-4941-3p	24	1
dme-miR-4956-5p	22	1
dme-miR-4958-5p	22	1
dme-miR-4963-3p	22	1
dme-miR-4965-3p	22	1
dme-miR-4969-5p	24	1
dme-miR-4973-5p	21	1
dme-miR-79-3p	22	1
dme-miR-9372-3p	23	1
dme-miR-9377-3p	21	1
dme-miR-9382-3p	22	1
dme-miR-9382-5p	21	1
dme-miR-9383-5p	22	1
dme-miR-965-3p	22	1
dme-miR-966-5p	21	1
dme-miR-967-5p	21	1
dme-miR-973-5p	25	1
dme-miR-986-5p	22	1
dme-miR-990-3p	24	1

Replicate 1 S2 Extracellular Vesicles

MiRNA	nt	Reads	MiRNA	nt	Reads
dme-miR-184-3p	22	5307	dme-miR-988-5p	22	19
dme-miR-375-3p	22	1562	dme-miR-92a-5p	22	18
dme-bantam-3p	23	330	dme-miR-316-3p	22	17
dme-miR-10-5p	22	280	dme-miR-2491-5p	22	15
dme-miR-276a-3p	22	247	dme-miR-2494-3p	24	15
dme-miR-9381-5p	20	201	dme-miR-2500-3p	22	15
dme-miR-14-5p	22	193	dme-miR-2c-5p	25	15
dme-bantam-5p	23	164	dme-miR-305-3p	23	14
dme-miR-34-5p	24	161	dme-miR-957-3p	22	14
dme-miR-8-3p	23	154	dme-miR-277-5p	21	13
dme-miR-33-5p	21	127	dme-miR-4982-5p	21	13
dme-miR-124-5p	23	125	dme-miR-984-5p	23	13
dme-miR-989-3p	21	103	dme-miR-190-3p	22	12
dme-miR-277-3p	23	93	dme-miR-986-5p	22	12
dme-miR-9b-5p	23	89	dme-miR-190-5p	24	11
dme-miR-100-3p	22	86	dme-miR-307a-3p	23	11
dme-miR-2b-3p	23	78	dme-miR-263a-5p	24	10
dme-miR-970-3p	21	78	dme-miR-289-5p	26	10
dme-miR-11-3p	21	74	dme-miR-317-5p	22	10
dme-miR-275-3p	23	74	dme-miR-9372-3p	23	10
dme-miR-279-3p	22	61	dme-miR-1000-3p	22	9
dme-miR-984-3p	20	59	dme-miR-281-3p	23	9
dme-miR-14-3p	22	58	dme-miR-307b-5p	22	9
dme-miR-308-3p	22	58	dme-miR-927-3p	22	9
dme-miR-306-5p	22	54	dme-miR-954-3p	21	9
dme-miR-4949-3p	22	54	dme-miR-1010-5p	21	8
dme-miR-2283-5p	23	53	dme-miR-11182	22	8
dme-miR-989-5p	23	46	dme-miR-3645-5p	21	8
dme-miR-9377-3p	21	42	dme-miR-954-5p	21	8
dme-miR-133-5p	23	41	dme-miR-1003-5p	21	7
dme-miR-995-3p	21	41	dme-miR-979-5p	23	7
dme-miR-7-5p	23	36	dme-miR-932-5p	22	6
dme-miR-9370-3p	22	35	dme-miR-999-3p	22	6
dme-miR-312-5p	23	30	dme-miR-1-3p	22	5
dme-miR-4969-5p	24	28	dme-miR-280-5p	27	5
dme-miR-9c-5p	22	28	dme-miR-282-5p	24	5
dme-miR-283-5p	22	26	dme-miR-31b-5p	22	5
dme-miR-283-3p	21	25	dme-miR-4947-5p	23	5
dme-miR-279-5p	26	24	dme-miR-4948-5p	22	5
dme-miR-9379-5p	21	24	dme-miR-4967-3p	22	5
dme-miR-313-5p	22	23	dme-miR-4983-3p	22	5
dme-miR-4963-3p	22	23	dme-miR-8-5p	22	5
dme-miR-4958-5p	22	20	dme-miR-965-5p	23	5
dme-miR-317-3p	24	19	dme-miR-990-3p	24	5
dme-miR-9372-5p	24	19	dme-miR-996-5p	22	5

MiRNA	nt	Reads	MiRNA	nt	Reads
dme-miR-iab-8-5p	23	5	dme-miR-2280-5p	22	2
dme-let-7-5p	21	4	dme-miR-2495-5p	22	2
dme-miR-1004-3p	22	4	dme-miR-2499-3p	24	2
dme-miR-12-5p	23	4	dme-miR-278-3p	22	2
dme-miR-2282-3p	22	4	dme-miR-286-5p	22	2
dme-miR-274-3p	23	4	dme-miR-2a-2-5p	21	2
dme-miR-2a-1-5p	22	4	dme-miR-304-5p	23	2
dme-miR-2a-3p	23	4	dme-miR-305-5p	23	2
dme-miR-4916-3p	22	4	dme-miR-309-3p	22	2
dme-miR-4970-5p	22	4	dme-miR-318-3p	22	2
dme-miR-4974-5p	22	4	dme-miR-34-3p	23	2
dme-miR-7-3p	22	4	dme-miR-4911-3p	22	2
dme-miR-9380-3p	22	4	dme-miR-4944-5p	22	2
dme-miR-9380-5p	22	4	dme-miR-4954-3p	21	2
dme-miR-982-5p	23	4	dme-miR-4956-5p	22	2
dme-miR-985-3p	22	4	dme-miR-4963-5p	21	2
dme-miR-988-3p	22	4	dme-miR-4964-3p	23	2
dme-miR-992-3p	22	4	dme-miR-4965-3p	22	2
dme-miR-996-3p	22	4	dme-miR-4973-3p	22	2
dme-miR-2493-5p	21	3	dme-miR-4978-5p	21	2
dme-miR-2497-5p	25	3	dme-miR-4987-5p	23	2
dme-miR-281-2-5p	22	3	dme-miR-6-3p	22	2
dme-miR-288-3p	23	3	dme-miR-9376-3p	21	2
dme-miR-2b-2-5p	23	3	dme-miR-9378-3p	22	2
dme-miR-310-5p	23	3	dme-miR-9384-5p	22	2
dme-miR-4952-5p	23	3	dme-miR-956-5p	24	2
dme-miR-4962-3p	23	3	dme-miR-972-5p	21	2
dme-miR-4984-5p	25	3	dme-miR-974-3p	22	2
dme-miR-929-3p	21	3	dme-miR-976-5p	22	2
dme-miR-92b-3p	22	3	dme-miR-980-5p	24	2
dme-miR-961-3p	22	3	dme-miR-iab-4-3p	24	2
dme-miR-966-5p	21	3	dme-miR-1001-5p	21	1
dme-miR-973-5p	25	3	dme-miR-1010-3p	24	1
dme-miR-980-3p	22	3	dme-miR-1011-3p	23	1
dme-miR-995-5p	22	3	dme-miR-1014-5p	22	1
dme-miR-9a-5p	23	3	dme-miR-1015-3p	22	1
dme-miR-1000-5p	21	2	dme-miR-10404-3p	22	1
dme-miR-1003-3p	22	2	dme-miR-184-5p	21	1
dme-miR-1004-5p	23	2	dme-miR-210-5p	23	1
dme-miR-1006-3p	23	2	dme-miR-2281-3p	21	1
dme-miR-1016-3p	21	2	dme-miR-2493-3p	23	1
dme-miR-10404-5p	22	2	dme-miR-252-5p	22	1
dme-miR-11-5p	22	2	dme-miR-263b-3p	22	1
dme-miR-125-5p	22	2	dme-miR-275-5p	23	1
dme-miR-133-3p	22	2	dme-miR-278-5p	23	1
dme-miR-13b-3p	22	2	dme-miR-286-3p	23	1
dme-miR-193-5p	22	2	dme-miR-303-3p	22	1

MiRNA	nt	Reads
dme-miR-306-3p	22	1
dme-miR-310-3p	22	1
dme-miR-3642-3p	22	1
dme-miR-3642-5p	22	1
dme-miR-3643-3p	22	1
dme-miR-4919-5p	21	1
dme-miR-4941-3p	24	1
dme-miR-4953-3p	23	1
dme-miR-4968-3p	22	1
dme-miR-4977-5p	21	1
dme-miR-4982-3p	22	1
dme-miR-6-3-5p	23	1
dme-miR-929-5p	22	1
dme-miR-92a-3p	22	1
dme-miR-9369-5p	23	1
dme-miR-9371-3p	22	1
dme-miR-9373-3p	21	1
dme-miR-9377-5p	22	1
dme-miR-9382-3p	22	1
dme-miR-960-5p	22	1
dme-miR-965-3p	22	1
dme-miR-967-3p	23	1
dme-miR-970-5p	24	1
dme-miR-971-5p	24	1
dme-miR-975-5p	23	1
dme-miR-977-3p	21	1
dme-miR-991-5p	22	1
dme-miR-994-3p	23	1
dme-miR-997-3p	21	1
dme-miR-998-3p	21	1

Replicate 2 S2 Extracellular Vesicles

MiRNA	nt	Reads	MiRNA	nt	Reads
dme-miR-184-3p	22	7323	dme-miR-980-5p	24	12
dme-miR-276a-3p	22	2037	dme-miR-1000-3p	22	11
dme-miR-9381-5p	20	1811	dme-miR-305-5p	23	11
dme-bantam-3p	23	559	dme-miR-252-5p	22	10
dme-miR-34-5p	24	490	dme-miR-92a-3p	22	10
dme-miR-11-3p	21	464	dme-miR-988-5p	22	10
dme-miR-2b-3p	23	406	dme-miR-9369-5p	23	9
dme-miR-33-5p	21	321	dme-miR-2c-3p	23	8
dme-miR-14-3p	22	300	dme-miR-310-3p	22	8
dme-miR-8-3p	23	279	dme-miR-988-3p	22	8
dme-miR-970-3p	21	236	dme-miR-996-5p	22	8
dme-miR-279-3p	22	201	dme-miR-263a-5p	24	7
dme-miR-9377-3p	21	179	dme-miR-4962-5p	24	7
dme-miR-995-3p	21	136	dme-miR-79-5p	23	7
dme-miR-275-3p	23	126	dme-miR-92b-3p	22	7
dme-miR-9b-5p	23	125	dme-miR-980-3p	22	7
dme-miR-277-3p	23	114	dme-miR-100-5p	22	6
dme-bantam-5p	23	108	dme-miR-263b-3p	22	6
dme-miR-4958-5p	22	88	dme-miR-310-5p	23	6
dme-miR-279-5p	26	82	dme-miR-278-3p	22	5
dme-miR-306-5p	22	75	dme-miR-281-3p	23	5
dme-miR-317-3p	24	70	dme-miR-4986-5p	23	5
dme-miR-303-3p	22	68	dme-miR-960-3p	22	5
dme-miR-14-5p	22	57	dme-miR-966-5p	21	5
dme-miR-13b-3p	22	56	dme-miR-9b-3p	22	5
dme-miR-9378-3p	22	47	dme-miR-1016-3p	21	4
dme-miR-8-5p	22	39	dme-miR-190-5p	24	4
dme-let-7-5p	21	28	dme-miR-281-2-5p	22	4
dme-miR-7-5p	23	28	dme-miR-4984-3p	22	4
dme-miR-313-5p	22	27	dme-miR-965-5p	23	4
dme-miR-4963-3p	22	27	dme-miR-995-5p	22	4
dme-miR-2b-2-5p	23	26	dme-miR-998-5p	22	4
dme-miR-305-3p	23	25	dme-miR-1002-5p	24	3
dme-miR-92a-5p	22	25	dme-miR-1007-3p	22	3
dme-miR-999-3p	22	22	dme-miR-2493-3p	23	3
dme-miR-990-3p	24	19	dme-miR-283-5p	22	3
dme-miR-4948-5p	22	15	dme-miR-2a-1-5p	22	3
dme-miR-979-5p	23	15	dme-miR-317-5p	22	3
dme-miR-289-5p	26	14	dme-miR-318-3p	22	3
dme-miR-996-3p	22	13	dme-miR-34-3p	23	3
dme-miR-11-5p	22	12	dme-miR-4948-3p	22	3
dme-miR-2a-2-5p	21	12	dme-miR-4958-3p	22	3
dme-miR-2a-3p	23	12	dme-miR-6-3p	22	3
dme-miR-4911-3p	22	12	dme-miR-9376-3p	21	3
dme-miR-960-5p	22	12	dme-miR-9380-3p	22	3

MiRNA	nt	Reads	MiRNA	nt	Reads
dme-miR-954-5p	21	3	dme-miR-2282-3p	22	1
dme-miR-133-3p	22	2	dme-miR-2492-3p	23	1
dme-miR-13a-5p	22	2	dme-miR-2493-5p	21	1
dme-miR-275-5p	23	2	dme-miR-2499-3p	24	1
dme-miR-281-1-5p	23	2	dme-miR-2499-5p	24	1
dme-miR-282-5p	24	2	dme-miR-2500-3p	22	1
dme-miR-306-3p	22	2	dme-miR-2501-5p	23	1
dme-miR-316-3p	22	2	dme-miR-277-5p	21	1
dme-miR-316-5p	22	2	dme-miR-286-3p	23	1
dme-miR-33-3p	22	2	dme-miR-286-5p	22	1
dme-miR-4-5p	24	2	dme-miR-2c-5p	25	1
dme-miR-4941-3p	24	2	dme-miR-307a-3p	23	1
dme-miR-4951-3p	23	2	dme-miR-308-5p	22	1
dme-miR-4951-5p	21	2	dme-miR-311-3p	22	1
dme-miR-4962-3p	23	2	dme-miR-312-3p	22	1
dme-miR-4965-3p	22	2	dme-miR-3642-5p	22	1
dme-miR-4966-3p	22	2	dme-miR-375-3p	22	1
dme-miR-4969-5p	24	2	dme-miR-4940-3p	22	1
dme-miR-4970-5p	22	2	dme-miR-4947-5p	23	1
dme-miR-4971-5p	22	2	dme-miR-4949-3p	22	1
dme-miR-4976-3p	20	2	dme-miR-4956-3p	22	1
dme-miR-4976-5p	22	2	dme-miR-4973-5p	21	1
dme-miR-6-3-5p	23	2	dme-miR-4977-3p	23	1
dme-miR-9388-3p	22	2	dme-miR-4981-3p	21	1
dme-miR-959-3p	22	2	dme-miR-4985-3p	22	1
dme-miR-965-3p	22	2	dme-miR-4986-3p	21	1
dme-miR-967-3p	23	2	dme-miR-6-2-5p	23	1
dme-miR-970-5p	24	2	dme-miR-79-3p	22	1
dme-miR-973-5p	25	2	dme-miR-929-3p	21	1
dme-miR-986-5p	22	2	dme-miR-9370-3p	22	1
dme-miR-989-3p	21	2	dme-miR-9371-5p	22	1
dme-miR-991-5p	22	2	dme-miR-9378-5p	24	1
dme-miR-9a-5p	23	2	dme-miR-9379-5p	21	1
dme-miR-9c-5p	22	2	dme-miR-9381-3p	22	1
dme-miR-1003-5p	21	1	dme-miR-9382-3p	22	1
dme-miR-100-3p	22	1	dme-miR-957-5p	23	1
dme-miR-1010-3p	24	1	dme-miR-958-3p	22	1
dme-miR-1015-3p	22	1	dme-miR-958-5p	23	1
dme-miR-1016-5p	20	1	dme-miR-968-5p	24	1
dme-miR-10-5p	22	1	dme-miR-971-5p	24	1
dme-miR-11182	22	1	dme-miR-975-3p	22	1
dme-miR-125-3p	21	1	dme-miR-984-5p	23	1
dme-miR-13b-1-5p	25	1	dme-miR-989-5p	23	1
dme-miR-184-5p	21	1	dme-miR-998-3p	21	1
dme-miR-210-3p	23	1			
dme-miR-219-3p	22	1			
dme-miR-2279-5p	22	1			

Replicate 3 S2 Extracellular Vesicles

MiRNA	nt	Reads	MiRNA	nt	Reads
dme-miR-184-3p	22	5907	dme-miR-980-3p	22	14
dme-miR-9381-5p	20	2754	dme-miR-2c-5p	25	13
dme-miR-276a-3p	22	1574	dme-miR-310-3p	22	13
dme-miR-14-3p	22	462	dme-miR-11-5p	22	12
dme-bantam-3p	23	354	dme-miR-282-5p	24	12
dme-miR-9377-3p	21	300	dme-miR-283-5p	22	12
dme-miR-11-3p	21	286	dme-miR-995-5p	22	12
dme-miR-33-5p	21	286	dme-miR-278-3p	22	11
dme-miR-2b-3p	23	279	dme-miR-996-3p	22	11
dme-miR-34-5p	24	261	dme-miR-305-5p	23	10
dme-miR-8-3p	23	247	dme-miR-310-5p	23	10
dme-miR-4958-5p	22	179	dme-miR-4986-5p	23	10
dme-miR-970-3p	21	155	dme-miR-6-3-5p	23	9
dme-miR-279-5p	26	139	dme-miR-79-5p	23	9
dme-miR-303-3p	22	136	dme-miR-92a-3p	22	9
dme-miR-275-3p	23	128	dme-miR-9380-3p	22	9
dme-miR-279-3p	22	111	dme-miR-9b-3p	22	9
dme-miR-9378-3p	22	110	dme-miR-252-5p	22	8
dme-miR-277-3p	23	90	dme-miR-263b-3p	22	8
dme-miR-306-5p	22	86	dme-miR-4951-3p	23	8
dme-miR-995-3p	21	86	dme-miR-100-5p	22	7
dme-bantam-5p	23	66	dme-miR-4962-3p	23	7
dme-miR-990-3p	24	66	dme-miR-4962-5p	24	7
dme-miR-289-5p	26	64	dme-miR-991-5p	22	7
dme-miR-317-3p	24	62	dme-miR-1002-5p	24	6
dme-miR-313-5p	22	60	dme-miR-1016-3p	21	6
dme-miR-9b-5p	23	57	dme-miR-2493-3p	23	6
dme-miR-92a-5p	22	37	dme-miR-4948-3p	22	6
dme-miR-979-5p	23	37	dme-miR-4970-5p	22	6
dme-miR-14-5p	22	36	dme-miR-133-3p	22	5
dme-miR-8-5p	22	30	dme-miR-1-3p	22	5
dme-miR-4963-3p	22	27	dme-miR-184-5p	21	5
dme-miR-960-5p	22	25	dme-miR-190-5p	24	5
dme-miR-305-3p	23	22	dme-miR-275-5p	23	5
dme-miR-4948-5p	22	22	dme-miR-277-5p	21	5
dme-miR-13b-3p	22	20	dme-miR-317-5p	22	5
dme-miR-2a-3p	23	19	dme-miR-92b-3p	22	5
dme-miR-4911-3p	22	19	dme-miR-988-3p	22	5
dme-miR-7-5p	23	19	dme-miR-996-5p	22	5
dme-let-7-5p	21	15	dme-miR-2496-5p	24	4
dme-miR-1000-3p	22	15	dme-miR-2a-2-5p	21	4
dme-miR-2b-2-5p	23	15	dme-miR-2c-3p	23	4
dme-miR-9369-5p	23	15	dme-miR-316-3p	22	4
dme-miR-960-3p	22	15	dme-miR-318-3p	22	4
dme-miR-999-3p	22	15	dme-miR-4965-3p	22	4

MiRNA	nt	Reads	MiRNA	nt	Reads
dme-miR-980-5p	24	4	dme-miR-1003-5p	21	1
dme-miR-988-5p	22	4	dme-miR-1007-3p	22	1
dme-miR-998-5p	22	4	dme-miR-10-3p	23	1
dme-miR-9c-5p	22	4	dme-miR-10404-3p	22	1
dme-miR-1012-3p	23	3	dme-miR-125-5p	22	1
dme-miR-281-2-5p	22	3	dme-miR-12-5p	23	1
dme-miR-307b-5p	22	3	dme-miR-1-5p	22	1
dme-miR-4951-5p	21	3	dme-miR-2281-3p	21	1
dme-miR-4958-3p	22	3	dme-miR-2281-5p	23	1
dme-miR-4968-3p	22	3	dme-miR-2492-3p	23	1
dme-miR-4973-5p	21	3	dme-miR-2494-5p	21	1
dme-miR-6-3p	22	3	dme-miR-252-3p	22	1
dme-miR-927-5p	22	3	dme-miR-2535b-3p	22	1
dme-miR-9370-3p	22	3	dme-miR-263a-3p	22	1
dme-miR-962-3p	22	3	dme-miR-276b-5p	23	1
dme-miR-965-5p	23	3	dme-miR-280-5p	27	1
dme-miR-973-5p	25	3	dme-miR-282-3p	22	1
dme-miR-976-5p	22	3	dme-miR-2a-1-5p	22	1
dme-miR-1000-5p	21	2	dme-miR-303-5p	23	1
dme-miR-1008-3p	21	2	dme-miR-306-3p	22	1
dme-miR-10404-5p	22	2	dme-miR-307a-3p	23	1
dme-miR-124-3p	23	2	dme-miR-308-5p	22	1
dme-miR-2491-3p	18	2	dme-miR-309-5p	22	1
dme-miR-2501-3p	22	2	dme-miR-311-3p	22	1
dme-miR-263a-5p	24	2	dme-miR-312-3p	22	1
dme-miR-276b-3p	22	2	dme-miR-314-5p	26	1
dme-miR-281-3p	23	2	dme-miR-31a-5p	23	1
dme-miR-34-3p	23	2	dme-miR-3-3p	22	1
dme-miR-3642-5p	22	2	dme-miR-3641-3p	22	1
dme-miR-3645-3p	21	2	dme-miR-4909-3p	23	1
dme-miR-4941-3p	24	2	dme-miR-4912-5p	23	1
dme-miR-4949-3p	22	2	dme-miR-4917-3p	22	1
dme-miR-4955-5p	22	2	dme-miR-4918-5p	24	1
dme-miR-4971-5p	22	2	dme-miR-4940-3p	22	1
dme-miR-4976-5p	22	2	dme-miR-4947-5p	23	1
dme-miR-4986-3p	21	2	dme-miR-4952-3p	21	1
dme-miR-9376-3p	21	2	dme-miR-4954-5p	22	1
dme-miR-9379-5p	21	2	dme-miR-4956-5p	22	1
dme-miR-9380-5p	22	2	dme-miR-4968-5p	22	1
dme-miR-9381-3p	22	2	dme-miR-4969-5p	24	1
dme-miR-954-5p	21	2	dme-miR-4973-3p	22	1
dme-miR-964-5p	22	2	dme-miR-4977-3p	23	1
dme-miR-965-3p	22	2	dme-miR-4980-3p	23	1
dme-miR-968-5p	24	2	dme-miR-4981-3p	21	1
dme-miR-985-5p	22	2	dme-miR-4982-5p	21	1
dme-miR-998-3p	21	2	dme-miR-4983-3p	22	1
dme-miR-9a-5p	23	2	dme-miR-4987-3p	21	1

MiRNA	nt	Reads
dme-miR-92b-5p	23	1
dme-miR-9373-3p	21	1
dme-miR-9379-3p	20	1
dme-miR-9382-5p	21	1
dme-miR-9385-5p	22	1
dme-miR-956-5p	24	1
dme-miR-959-3p	22	1
dme-miR-961-5p	22	1
dme-miR-966-5p	21	1
dme-miR-967-5p	21	1
dme-miR-978-5p	24	1
dme-miR-986-5p	22	1
dme-miR-987-3p	20	1
dme-miR-992-5p	22	1
dme-miR-999-5p	22	1
dme-miR-9a-3p	22	1

Supplementary Table Chapter 3

***L. migratoria* fifth nymphal haemolymph small RNA sequencing data.** Small RNA sequencing was executed on 3 and 4 biological replicates of high (N5 D6 and D7) and low (N5 D2 and D3) haemolymph ecdysteroid levels, respectively. Differential expression analysis was performed using edgeR. Amount of nucleotides (nt) and raw reads are included in the table.

Replicate 1 high haemolymph ecdysteroid level (N5 D7)

MiRNA	Reads	MiRNA	Reads
lmi-miR-276-3p	8545	ID607	42
lmi-miR-8-3p	1792	ID610	41
lmi-novel-miR-100	939	lmi-novel-miR-47	40
lmi-novel-miR-106	781	lmi-novel-miR-17	37
lmi-novel-miR-107	781	lmi-novel-miR-18	37
lmi-novel-miR-14	733	lmi-novel-miR-19	37
lmi-novel-miR-28	473	lmi-novel-miR-34	33
lmi-novel-miR-114	363	lmi-novel-miR-35	33
ID1725	325	lmi-novel-miR-36	33
lmi-miR-9a-5p	264	IM59	32
ID594	243	ID1580	30
lmi-novel-miR-121	195	ID903	30
lmi-novel-miR-112	179	lmi-novel-miR-67	30
lmi-novel-miR-50	127	lmi-novel-miR-68	30
lmi-novel-miR-51	127	lmi-novel-miR-69	30
ID1321	122	lmi-novel-miR-70	30
lmi-novel-miR-116	113	lmi-novel-miR-113	29
lmi-novel-miR-117	113	ID603	28
lmi-novel-miR-7	93	lmi-novel-miR-102	28
lmi-novel-miR-10	92	lmi-novel-miR-103	28
lmi-novel-miR-111	92	lmi-novel-miR-104	28
lmi-miR-8-5p	88	lmi-novel-miR-65	25
lmi-novel-miR-80	87	lmi-novel-miR-66	25
lmi-novel-miR-81	87	ID50	23
lmi-novel-miR-82	87	lmi-novel-miR-46	23
lmi-novel-miR-37	57	lmi-miR-10-5p	20
lmi-novel-miR-20	54	lmi-novel-miR-115	20
lmi-novel-miR-21	54	lmi-novel-miR-27	20
lmi-novel-miR-22	54	lmi-novel-miR-9	20
lmi-novel-miR-3	51	IM18	18
lmi-novel-miR-4	51	lmi-miR-307-3p	18
ID604	48	lmi-novel-miR-118	18
lmi-novel-miR-125	48	lmi-novel-miR-119	18
lmi-novel-miR-126	48	lmi-novel-miR-71	18
lmi-novel-miR-127	48	lmi-novel-miR-72	18
lmi-novel-miR-128	48	lmi-novel-miR-94	18
lmi-novel-miR-15	43	lmi-novel-miR-77	17

MiRNA	Reads	MiRNA	Reads
lmi-novel-miR-48	16	lmi-novel-miR-2	10
ID1454	15	lmi-novel-miR-25	10
ID1726	15	lmi-novel-miR-92	10
lmi-novel-miR-58	15	lmi-novel-miR-93	10
ID1728	14	lmi-novel-miR-76	9
lmi-novel-miR-120	14	lmi-novel-miR-8	9
ID592	13	lmi-novel-miR-30	8
lmi-miR-281-5p	11	lmi-novel-miR-31	8
lmi-novel-miR-1	10	lmi-novel-miR-63	8
lmi-novel-miR-2	10	lmi-novel-miR-64	8
lmi-novel-miR-25	10	lmi-novel-miR-52	7
lmi-novel-miR-92	10	lmi-novel-miR-53	7
lmi-novel-miR-93	10	lmi-novel-miR-59	7
lmi-novel-miR-76	9	lmi-novel-miR-60	7
lmi-novel-miR-8	9	lmi-novel-miR-61	7
lmi-novel-miR-30	8	lmi-novel-miR-78	7
lmi-novel-miR-31	8	lmi-novel-miR-79	7
lmi-novel-miR-63	8	lmi-novel-miR-86	7
lmi-novel-miR-64	8	lmi-novel-miR-38	6
lmi-novel-miR-52	7	lmi-novel-miR-39	6
lmi-novel-miR-53	7	lmi-novel-miR-40	6
lmi-novel-miR-59	7	lmi-novel-miR-41	6
lmi-novel-miR-60	7	lmi-novel-miR-83	6
lmi-novel-miR-61	7	lmi-novel-miR-84	6
lmi-novel-miR-78	7	lmi-novel-miR-88	6
lmi-novel-miR-79	7	lmi-novel-miR-90	6
lmi-novel-miR-86	7	lmi-novel-miR-91	6
lmi-novel-miR-38	6	ID1095	5
lmi-novel-miR-39	6	ID170	5
lmi-novel-miR-40	6	ID730	5
lmi-novel-miR-41	6	lmi-novel-miR-23	5
lmi-novel-miR-83	6	lmi-novel-miR-24	5
lmi-novel-miR-84	6	lmi-novel-miR-32	5
lmi-novel-miR-88	6	lmi-novel-miR-5	5
lmi-novel-miR-90	6	lmi-novel-miR-6	5
lmi-novel-miR-48	16	lmi-novel-miR-85	5
ID1454	15	lmi-novel-miR-87	5
ID1726	15	ID1794	4
lmi-novel-miR-58	15	lmi-miR-9a-3p	4
ID1728	14	ID1682	3
lmi-novel-miR-120	14	ID925	3
ID592	13	lmi-novel-miR-96	3
lmi-miR-281-5p	11	lmi-novel-miR-97	3
lmi-novel-miR-1	10	lmi-novel-miR-98	3

MiRNA	Reads	MiRNA	Reads
lmi-novel-miR-99	3	ID864	1
ID130	2	ID869	1
ID1327	2	ID877	1
ID1440	2	lmi-miR-276-5p	1
ID1668	2	lmi-miR-307-5p	1
ID1684	2	lmi-novel-miR-109	1
ID1795	2	lmi-novel-miR-11	1
ID23	2	lmi-novel-miR-110	1
ID231	2	lmi-novel-miR-12	1
ID424	2	lmi-novel-miR-122	1
ID425	2	lmi-novel-miR-123	1
ID568	2	lmi-novel-miR-124	1
ID609	2	lmi-novel-miR-129	1
ID893	2	lmi-novel-miR-13	1
IM23	2	lmi-novel-miR-42	1
lmi-miR-10-3p	2	lmi-novel-miR-43	1
lmi-miR-281-3p	2	lmi-novel-miR-44	1
lmi-novel-miR-105	2	lmi-novel-miR-54	1
lmi-novel-miR-45	2	lmi-novel-miR-55-0	1
lmi-novel-miR-73	2	lmi-novel-miR-56	1
lmi-novel-miR-74	2	lmi-novel-miR-57	1
lmi-novel-miR-75	2	lmi-novel-miR-89	1
lmi-novel-miR-95	2		
ID1142	1		
ID1330	1		
ID1332	1		
ID1538	1		
ID1576	1		
ID1621	1		
ID1663	1		
ID1666	1		
ID1691	1		
ID1711	1		
ID1714	1		
ID1752	1		
ID1802	1		
ID1805	1		
ID323	1		
ID593	1		
ID611	1		
ID712	1		
ID718	1		
ID724	1		
ID735	1		
ID863	1		

Replicate 2 high haemolymph ecdysteroid level (N5 D6_1)

MiRNA	Reads	MiRNA	Reads
lmi-miR-276-3p	9378	lmi-miR-8-5p	103
lmi-miR-8-3p	1940	ID1321	96
lmi-novel-miR-106	1361	lmi-novel-miR-46	86
lmi-novel-miR-107	1361	lmi-novel-miR-34	81
lmi-novel-miR-100	1078	lmi-novel-miR-35	81
lmi-novel-miR-14	647	lmi-novel-miR-36	81
lmi-novel-miR-28	524	lmi-novel-miR-3	81
lmi-novel-miR-114	421	lmi-novel-miR-4	81
lmi-novel-miR-112	288	ID607	74
ID1725	283	ID604	74
lmi-miR-9a-5p	219	lmi-novel-miR-20	71
lmi-novel-miR-50	202	lmi-novel-miR-21	71
lmi-novel-miR-51	202	lmi-novel-miR-22	71
lmi-novel-miR-121	197	lmi-novel-miR-113	62
lmi-novel-miR-116	116	lmi-novel-miR-7	62
lmi-novel-miR-117	116	ID603	59
lmi-miR-8-5p	103	lmi-novel-miR-80	54
ID1321	96	lmi-novel-miR-81	54
lmi-novel-miR-46	86	lmi-novel-miR-82	54
lmi-novel-miR-34	81	lmi-novel-miR-65	47
lmi-novel-miR-35	81	lmi-novel-miR-66	47
lmi-novel-miR-36	81	lmi-novel-miR-15	47
lmi-novel-miR-3	81	lmi-novel-miR-67	42
lmi-novel-miR-4	81	lmi-novel-miR-68	42
ID607	74	lmi-novel-miR-69	42
ID604	74	lmi-novel-miR-70	42
lmi-novel-miR-20	71	ID610	34
lmi-novel-miR-21	71	lmi-novel-miR-125	32
lmi-miR-276-3p	9378	lmi-novel-miR-126	32
lmi-miR-8-3p	1940	lmi-novel-miR-127	32
lmi-novel-miR-106	1361	lmi-novel-miR-128	32
lmi-novel-miR-107	1361	lmi-novel-miR-37	32
lmi-novel-miR-100	1078	ID594	32
lmi-novel-miR-14	647	lmi-novel-miR-77	30
lmi-novel-miR-28	524	lmi-novel-miR-9	30
lmi-novel-miR-114	421	ID50	27
lmi-novel-miR-112	288	lmi-novel-miR-86	22
ID1725	283	lmi-novel-miR-118	22
lmi-miR-9a-5p	219	lmi-novel-miR-119	22
lmi-novel-miR-50	202	lmi-novel-miR-115	22
lmi-novel-miR-51	202	lmi-novel-miR-27	22
lmi-novel-miR-121	197	lmi-novel-miR-76	20
lmi-novel-miR-116	116	ID1728	20
lmi-novel-miR-117	116	ID1726	20

MiRNA	Reads	MiRNA	Reads
ID903	20	lmi-novel-miR-60	7
lmi-novel-miR-17	20	lmi-novel-miR-61	7
lmi-novel-miR-18	20	lmi-novel-miR-78	7
lmi-novel-miR-19	20	lmi-novel-miR-79	7
lmi-novel-miR-8	17	lmi-novel-miR-30	7
lmi-novel-miR-1	17	lmi-novel-miR-31	7
lmi-novel-miR-2	17	lmi-novel-miR-120	7
lmi-novel-miR-71	17	lmi-miR-307-3p	7
lmi-novel-miR-72	17	IM59	7
lmi-novel-miR-63	15	ID167	5
lmi-novel-miR-64	15	lmi-novel-miR-90	5
lmi-novel-miR-47	15	lmi-novel-miR-91	5
lmi-novel-miR-16	12	ID592	5
lmi-novel-miR-87	12	lmi-novel-miR-58	5
lmi-novel-miR-92	12	lmi-novel-miR-94	5
lmi-novel-miR-93	12	ID1281	2
IM18	12	ID30	2
ID724	10	lmi-novel-miR-108-0	2
lmi-miR-9a-3p	10	ID1330	2
ID1454	10	ID1332	2
lmi-miR-10-5p	10	ID1663	2
lmi-novel-miR-102	10	ID1691	2
lmi-novel-miR-103	10	ID1714	2
lmi-novel-miR-104	10	ID1805	2
lmi-novel-miR-10	10	ID323	2
lmi-novel-miR-111	10	ID593	2
ID1666	7	ID869	2
ID877	7	lmi-novel-miR-11	2
lmi-novel-miR-42	7	lmi-novel-miR-12	2
lmi-novel-miR-96	7	lmi-novel-miR-129	2
lmi-novel-miR-97	7	lmi-novel-miR-13	2
lmi-novel-miR-98	7	lmi-novel-miR-44	2
lmi-novel-miR-99	7	lmi-novel-miR-54	2
ID170	7	lmi-novel-miR-55-0	2
lmi-novel-miR-23	7	lmi-novel-miR-56	2
lmi-novel-miR-24	7	lmi-novel-miR-57	2
lmi-novel-miR-85	7	lmi-novel-miR-89	2
lmi-novel-miR-38	7	ID1440	2
lmi-novel-miR-39	7	ID1668	2
lmi-novel-miR-40	7	ID23	2
lmi-novel-miR-83	7	ID424	2
lmi-novel-miR-84	7	ID609	2
lmi-novel-miR-52	7	lmi-miR-10-3p	2
lmi-novel-miR-53	7	lmi-novel-miR-45	2
lmi-novel-miR-59	7	lmi-novel-miR-73	2

MiRNA	Reads
lmi-novel-miR-74	2
lmi-novel-miR-75	2
ID1794	2
ID730	2
lmi-novel-miR-32	2
lmi-novel-miR-41	2
lmi-novel-miR-88	2
lmi-novel-miR-25	2

Replicate 3 high haemolymph ecdysteroid level (N5 D6_2)

MiRNA	Reads	MiRNA	Reads
lmi-miR-276-3p	9806	lmi-novel-miR-71	36
lmi-miR-8-3p	1504	lmi-novel-miR-72	36
lmi-novel-miR-106	1189	lmi-novel-miR-37	34
lmi-novel-miR-107	1189	lmi-novel-miR-63	34
lmi-novel-miR-100	1103	lmi-novel-miR-64	34
lmi-novel-miR-28	640	lmi-novel-miR-47	31
lmi-novel-miR-14	593	lmi-novel-miR-10	31
lmi-novel-miR-112	588	lmi-novel-miR-111	31
lmi-novel-miR-114	367	lmi-novel-miR-125	29
ID1725	286	lmi-novel-miR-126	29
lmi-novel-miR-50	226	lmi-novel-miR-127	29
lmi-novel-miR-51	226	lmi-novel-miR-128	29
lmi-miR-9a-5p	161	ID1726	23
lmi-novel-miR-121	154	lmi-novel-miR-16	23
lmi-miR-8-5p	120	lmi-novel-miR-76	21
ID594	109	ID1728	21
lmi-novel-miR-116	101	ID903	21
lmi-novel-miR-117	101	lmi-novel-miR-102	21
ID607	83	lmi-novel-miR-103	21
ID604	78	lmi-novel-miR-104	21
lmi-novel-miR-113	75	lmi-novel-miR-8	18
ID610	75	lmi-novel-miR-1	18
lmi-novel-miR-3	70	lmi-novel-miR-2	18
lmi-novel-miR-4	70	lmi-novel-miR-118	16
lmi-novel-miR-34	68	lmi-novel-miR-119	16
lmi-novel-miR-35	68	lmi-novel-miR-17	16
lmi-novel-miR-36	68	lmi-novel-miR-18	16
lmi-novel-miR-7	65	lmi-novel-miR-19	16
lmi-novel-miR-15	57	IM18	16
ID603	52	lmi-novel-miR-120	16
lmi-novel-miR-67	49	ID50	13
lmi-novel-miR-68	49	lmi-novel-miR-92	13
lmi-novel-miR-69	49	lmi-novel-miR-93	13
lmi-novel-miR-70	49	lmi-novel-miR-9	10
lmi-novel-miR-20	47	lmi-novel-miR-86	10
lmi-novel-miR-21	47	lmi-novel-miR-115	10
lmi-novel-miR-22	47	lmi-novel-miR-27	10
lmi-novel-miR-46	44	ID724	10
ID1321	39	lmi-miR-9a-3p	10
lmi-novel-miR-65	39	lmi-miR-307-3p	10
lmi-novel-miR-66	39	ID1795	10
lmi-novel-miR-80	36	lmi-miR-281-5p	10
lmi-novel-miR-81	36	lmi-novel-miR-42	8
lmi-novel-miR-82	36	lmi-novel-miR-38	8

MiRNA	Reads	MiRNA	Reads
lmi-novel-miR-39	8	ID30	3
lmi-novel-miR-40	8	ID1691	3
lmi-novel-miR-83	8	ID1714	3
lmi-novel-miR-84	8	ID323	3
ID592	8	lmi-novel-miR-54	3
lmi-novel-miR-58	8	lmi-novel-miR-55-0	3
ID1805	8	lmi-novel-miR-56	3
ID1794	8	lmi-novel-miR-57	3
lmi-novel-miR-41	8	lmi-novel-miR-89	3
ID1684	8	ID1440	3
lmi-novel-miR-77	5	lmi-novel-miR-73	3
lmi-novel-miR-87	5	lmi-novel-miR-74	3
ID1454	5	lmi-novel-miR-75	3
ID1666	5	ID730	3
ID877	5	lmi-novel-miR-32	3
lmi-novel-miR-23	5	lmi-novel-miR-25	3
lmi-novel-miR-24	5	ID1589	3
lmi-novel-miR-52	5	ID1764	3
lmi-novel-miR-53	5	ID863	3
lmi-novel-miR-59	5	ID130	3
lmi-novel-miR-60	5	ID231	3
lmi-novel-miR-61	5	ID425	3
lmi-novel-miR-78	5	lmi-novel-miR-105	3
lmi-novel-miR-79	5	ID925	3
lmi-novel-miR-90	5		
lmi-novel-miR-91	5		
lmi-novel-miR-129	5		
lmi-novel-miR-44	5		
ID23	5		
lmi-novel-miR-88	5		
ID1797	5		
ID1806	5		
ID611	5		
lmi-novel-miR-5	5		
lmi-novel-miR-6	5		
lmi-miR-10-5p	3		
lmi-novel-miR-96	3		
lmi-novel-miR-97	3		
lmi-novel-miR-98	3		
lmi-novel-miR-99	3		
lmi-novel-miR-30	3		
lmi-novel-miR-31	3		
IM59	3		
lmi-novel-miR-94	3		
ID1281	3		

Replicate 1 low haemolymph ecdysteroid level (N5 D2_2)

MiRNA	Reads	MiRNA	Reads
lmi-miR-276-3p	6783	lmi-novel-miR-22	49
lmi-miR-8-3p	3348	lmi-novel-miR-87	49
lmi-novel-miR-100	996	lmi-miR-8-5p	43
lmi-novel-miR-106	597	lmi-novel-miR-118	43
lmi-novel-miR-107	597	lmi-novel-miR-119	43
lmi-miR-9a-5p	480	IM18	38
lmi-novel-miR-14	392	ID603	37
lmi-novel-miR-114	297	lmi-novel-miR-102	36
lmi-novel-miR-121	293	lmi-novel-miR-103	36
ID1725	278	lmi-novel-miR-104	36
lmi-novel-miR-28	262	ID1580	30
lmi-novel-miR-80	197	lmi-novel-miR-76	28
lmi-novel-miR-81	197	lmi-novel-miR-120	27
lmi-novel-miR-82	197	lmi-novel-miR-77	27
ID1321	123	lmi-novel-miR-65	26
lmi-novel-miR-47	120	lmi-novel-miR-66	26
ID594	109	lmi-novel-miR-113	24
lmi-novel-miR-50	103	lmi-novel-miR-9	22
lmi-novel-miR-51	103	ID604	20
lmi-novel-miR-34	97	lmi-novel-miR-15	20
lmi-novel-miR-35	97	ID903	20
lmi-novel-miR-36	97	lmi-miR-307-3p	20
lmi-novel-miR-10	97	lmi-novel-miR-23	20
lmi-novel-miR-111	97	lmi-novel-miR-58	19
lmi-novel-miR-116	95	lmi-novel-miR-24	19
lmi-novel-miR-117	95	ID607	18
lmi-novel-miR-112	90	ID610	16
lmi-novel-miR-125	90	ID1726	16
lmi-novel-miR-126	90	lmi-miR-10-5p	16
lmi-novel-miR-127	90	lmi-novel-miR-46	15
lmi-novel-miR-128	90	lmi-novel-miR-8	15
IM59	86	ID1142	15
lmi-novel-miR-17	83	lmi-novel-miR-94	13
lmi-novel-miR-18	83	lmi-novel-miR-67	12
lmi-novel-miR-19	83	lmi-novel-miR-68	12
ID50	82	lmi-novel-miR-69	12
lmi-novel-miR-115	80	lmi-novel-miR-70	12
lmi-novel-miR-27	80	lmi-miR-9a-3p	12
lmi-novel-miR-3	64	lmi-novel-miR-90	12
lmi-novel-miR-4	64	lmi-novel-miR-91	12
lmi-novel-miR-37	60	lmi-novel-miR-129	12
lmi-novel-miR-7	50	lmi-novel-miR-88	11
lmi-novel-miR-20	49	ID170	11
lmi-novel-miR-21	49	lmi-novel-miR-38	10

MiRNA	Reads	MiRNA	Reads
lmi-novel-miR-39	10	lmi-novel-miR-83	2
lmi-novel-miR-40	10	lmi-novel-miR-84	2
ID1728	9	lmi-novel-miR-96	2
ID592	9	lmi-novel-miR-97	2
lmi-novel-miR-48	9	lmi-novel-miR-98	2
lmi-novel-miR-59	8	lmi-novel-miR-99	2
lmi-novel-miR-25	8	lmi-novel-miR-89	2
lmi-novel-miR-43	8	ID1440	2
lmi-novel-miR-71	7	lmi-novel-miR-73	2
lmi-novel-miR-72	7	lmi-novel-miR-74	2
lmi-novel-miR-1	7	lmi-novel-miR-75	2
lmi-novel-miR-2	7	ID1764	2
lmi-novel-miR-52	7	ID869	2
lmi-novel-miR-53	7	ID1582	2
lmi-novel-miR-60	7	ID272	2
lmi-novel-miR-61	7	ID1752	2
lmi-novel-miR-78	7	ID735	2
lmi-novel-miR-79	7	lmi-novel-miR-16	1
lmi-novel-miR-30	7	ID1795	1
lmi-novel-miR-31	7	lmi-novel-miR-41	1
lmi-novel-miR-54	7	ID877	1
lmi-novel-miR-55-0	7	ID1797	1
lmi-novel-miR-56	7	ID1806	1
lmi-novel-miR-57	7	ID611	1
lmi-novel-miR-29	7	ID30	1
lmi-novel-miR-92	6	ID425	1
lmi-novel-miR-93	6	ID925	1
ID724	6	lmi-novel-miR-108-0	1
ID1281	6	ID1330	1
ID323	4	ID1332	1
lmi-miR-10-3p	4	lmi-novel-miR-11	1
lmi-novel-miR-63	3	lmi-novel-miR-12	1
lmi-novel-miR-64	3	lmi-novel-miR-13	1
ID1454	3	ID1668	1
lmi-novel-miR-44	3	ID424	1
lmi-novel-miR-5	3	ID1333	1
lmi-novel-miR-6	3	ID1455	1
lmi-novel-miR-105	3	ID712	1
lmi-novel-miR-85	3	ID718	1
lmi-novel-miR-45	3	lmi-novel-miR-122	1
ID1326	3	lmi-novel-miR-123	1
ID864	3	lmi-novel-miR-124	1
lmi-novel-miR-86	2	IM23	1
lmi-miR-281-5p	2	lmi-miR-281-3p	1
lmi-novel-miR-42	2	lmi-novel-miR-95	1

MiRNA	Reads
ID1095	1

Replicate 2 low haemolymph ecdysteroid level (N5 D2_1)

MiRNA	Reads	MiRNA	Reads
lmi-miR-276-3p	9396	lmi-novel-miR-7	42
lmi-miR-8-3p	3075	lmi-novel-miR-87	42
lmi-novel-miR-100	1125	lmi-novel-miR-118	40
lmi-novel-miR-106	896	lmi-novel-miR-119	40
lmi-novel-miR-107	896	lmi-novel-miR-77	38
lmi-novel-miR-14	456	lmi-novel-miR-58	38
lmi-novel-miR-114	358	ID603	36
lmi-miR-9a-5p	349	lmi-novel-miR-65	35
ID1725	343	lmi-novel-miR-66	35
lmi-novel-miR-28	289	ID610	33
lmi-novel-miR-121	274	ID607	30
lmi-novel-miR-112	244	IM59	28
lmi-novel-miR-80	213	lmi-novel-miR-113	28
lmi-novel-miR-81	213	ID594	27
lmi-novel-miR-82	213	lmi-novel-miR-120	27
lmi-novel-miR-47	195	ID604	27
ID1321	167	lmi-novel-miR-15	27
lmi-novel-miR-50	135	lmi-novel-miR-102	26
lmi-novel-miR-51	135	lmi-novel-miR-103	26
lmi-novel-miR-37	129	lmi-novel-miR-104	26
lmi-novel-miR-17	103	lmi-miR-307-3p	26
lmi-novel-miR-18	103	ID1728	22
lmi-novel-miR-19	103	lmi-novel-miR-9	21
lmi-novel-miR-125	101	lmi-novel-miR-67	21
lmi-novel-miR-126	101	lmi-novel-miR-68	21
lmi-novel-miR-127	101	lmi-novel-miR-69	21
lmi-novel-miR-128	101	lmi-novel-miR-70	21
lmi-novel-miR-116	93	lmi-novel-miR-46	20
lmi-novel-miR-117	93	lmi-novel-miR-71	20
lmi-novel-miR-34	82	lmi-novel-miR-72	20
lmi-novel-miR-35	82	ID1726	19
lmi-novel-miR-36	82	lmi-novel-miR-23	18
lmi-novel-miR-3	75	ID903	17
lmi-novel-miR-4	75	lmi-miR-9a-3p	17
lmi-novel-miR-10	72	lmi-novel-miR-24	16
lmi-novel-miR-111	72	lmi-novel-miR-29	14
ID50	65	lmi-novel-miR-8	12
lmi-novel-miR-20	62	lmi-novel-miR-129	12
lmi-novel-miR-21	62	lmi-novel-miR-38	12
lmi-novel-miR-22	62	lmi-novel-miR-39	12
lmi-novel-miR-115	59	lmi-novel-miR-40	12
lmi-novel-miR-27	59	lmi-novel-miR-92	11
lmi-miR-8-5p	46	lmi-novel-miR-93	11
IM18	46	ID1580	9

MiRNA	Reads	MiRNA	Reads
lmi-novel-miR-76	9	lmi-novel-miR-41	3
lmi-novel-miR-59	8	ID23	3
lmi-novel-miR-45	8	ID1142	2
lmi-miR-10-5p	7	ID724	2
lmi-novel-miR-94	7	ID1454	2
lmi-novel-miR-1	7	lmi-novel-miR-105	2
lmi-novel-miR-2	7	ID272	2
lmi-novel-miR-52	7	ID609	2
lmi-novel-miR-53	7	ID323	1
lmi-novel-miR-60	7	lmi-miR-10-3p	1
lmi-novel-miR-61	7	lmi-novel-miR-85	1
lmi-novel-miR-78	7	lmi-miR-281-5p	1
lmi-novel-miR-79	7	lmi-novel-miR-96	1
lmi-novel-miR-54	7	lmi-novel-miR-97	1
lmi-novel-miR-55-0	7	lmi-novel-miR-98	1
lmi-novel-miR-56	7	lmi-novel-miR-99	1
lmi-novel-miR-57	7	lmi-novel-miR-73	1
lmi-novel-miR-83	7	lmi-novel-miR-74	1
lmi-novel-miR-84	7	lmi-novel-miR-75	1
lmi-novel-miR-88	6	ID1764	1
ID170	6	ID1795	1
lmi-novel-miR-30	6	ID1797	1
lmi-novel-miR-31	6	ID1806	1
lmi-novel-miR-63	6	ID611	1
lmi-novel-miR-64	6	ID30	1
lmi-novel-miR-48	5	ID925	1
lmi-novel-miR-25	5	ID1330	1
lmi-novel-miR-5	5	lmi-novel-miR-11	1
lmi-novel-miR-6	5	lmi-novel-miR-12	1
lmi-novel-miR-86	5	lmi-novel-miR-13	1
lmi-novel-miR-90	4	ID1668	1
lmi-novel-miR-91	4	ID424	1
ID1281	4	ID1455	1
lmi-novel-miR-42	4	lmi-novel-miR-122	1
lmi-novel-miR-89	4	lmi-novel-miR-123	1
ID735	4	lmi-novel-miR-124	1
lmi-novel-miR-108-0	4	IM23	1
ID1095	4	ID1805	1
ID730	4	ID1684	1
ID592	3	ID1666	1
lmi-novel-miR-43	3	ID1691	1
lmi-novel-miR-44	3	lmi-novel-miR-32	1
ID864	3	ID231	1
ID1440	3	ID167	1
ID869	3	ID1663	1

MiRNA	Reads
ID1134	1
ID868	1
ID1538	1
ID1576	1
ID1621	1
ID1802	1
lmi-miR-276-5p	1
lmi-novel-miR-109	1
lmi-novel-miR-110	1
ID1327	1
ID568	1
ID893	1

Replicate 3 low haemolymph ecdysteroid level (N5 D3_2)

MiRNA	Reads	MiRNA	Reads
lmi-miR-276-3p	8346	lmi-miR-8-5p	49
lmi-miR-8-3p	3365	lmi-novel-miR-102	45
lmi-novel-miR-100	1037	lmi-novel-miR-103	45
lmi-novel-miR-106	734	lmi-novel-miR-104	45
lmi-novel-miR-107	734	ID603	44
lmi-novel-miR-14	471	IM18	38
lmi-miR-9a-5p	430	lmi-novel-miR-77	38
lmi-novel-miR-114	353	ID594	35
ID1725	302	lmi-novel-miR-118	33
lmi-novel-miR-28	281	lmi-novel-miR-119	33
lmi-novel-miR-121	279	ID610	33
lmi-novel-miR-112	187	lmi-novel-miR-58	32
lmi-novel-miR-80	164	lmi-novel-miR-65	30
lmi-novel-miR-81	164	lmi-novel-miR-66	30
lmi-novel-miR-82	164	lmi-novel-miR-113	30
lmi-novel-miR-50	134	lmi-novel-miR-120	30
lmi-novel-miR-51	134	ID604	30
lmi-novel-miR-47	131	ID607	29
ID1321	115	lmi-novel-miR-46	29
lmi-novel-miR-116	101	lmi-novel-miR-71	29
lmi-novel-miR-117	101	lmi-novel-miR-72	29
lmi-novel-miR-10	101	lmi-novel-miR-15	28
lmi-novel-miR-111	101	lmi-novel-miR-87	25
lmi-novel-miR-17	100	lmi-miR-307-3p	25
lmi-novel-miR-18	100	lmi-novel-miR-76	25
lmi-novel-miR-19	100	lmi-novel-miR-67	24
lmi-novel-miR-125	100	lmi-novel-miR-68	24
lmi-novel-miR-126	100	lmi-novel-miR-69	24
lmi-novel-miR-127	100	lmi-novel-miR-70	24
lmi-novel-miR-128	100	ID1580	23
lmi-novel-miR-34	75	ID1728	20
lmi-novel-miR-35	75	ID1726	19
lmi-novel-miR-36	75	lmi-novel-miR-8	19
IM59	73	lmi-novel-miR-23	18
lmi-novel-miR-37	64	ID903	18
lmi-novel-miR-20	59	lmi-novel-miR-9	17
lmi-novel-miR-21	59	lmi-novel-miR-24	17
lmi-novel-miR-22	59	lmi-miR-9a-3p	16
lmi-novel-miR-3	57	lmi-miR-10-5p	16
lmi-novel-miR-4	57	lmi-novel-miR-25	16
ID50	55	lmi-novel-miR-38	12
lmi-novel-miR-115	51	lmi-novel-miR-39	12
lmi-novel-miR-27	51	lmi-novel-miR-40	12
lmi-novel-miR-7	51	lmi-novel-miR-45	12

MiRNA	Reads	MiRNA	Reads
lmi-novel-miR-48	11	lmi-novel-miR-97	3
lmi-novel-miR-92	9	lmi-novel-miR-98	3
lmi-novel-miR-93	9	lmi-novel-miR-99	3
lmi-novel-miR-129	8	ID1764	3
lmi-novel-miR-55-0	8	lmi-novel-miR-108-0	2
ID170	8	ID1095	2
ID1281	8	lmi-novel-miR-43	2
ID1142	8	lmi-miR-10-3p	2
lmi-novel-miR-29	7	lmi-novel-miR-73	2
lmi-novel-miR-54	7	lmi-novel-miR-74	2
lmi-novel-miR-56	7	lmi-novel-miR-75	2
lmi-novel-miR-57	7	lmi-miR-281-3p	2
lmi-novel-miR-86	7	ID130	2
lmi-novel-miR-59	6	lmi-novel-miR-94	1
lmi-novel-miR-52	6	lmi-novel-miR-89	1
lmi-novel-miR-53	6	ID735	1
lmi-novel-miR-60	6	lmi-novel-miR-44	1
lmi-novel-miR-61	6	ID864	1
lmi-novel-miR-78	6	ID1440	1
lmi-novel-miR-79	6	lmi-novel-miR-41	1
lmi-novel-miR-83	6	ID272	1
lmi-novel-miR-84	6	ID609	1
lmi-novel-miR-63	6	lmi-novel-miR-85	1
lmi-novel-miR-64	6	ID611	1
lmi-novel-miR-5	6	ID925	1
lmi-novel-miR-6	6	lmi-novel-miR-11	1
lmi-novel-miR-90	6	lmi-novel-miR-12	1
lmi-novel-miR-91	6	lmi-novel-miR-13	1
ID592	6	ID1668	1
ID724	6	ID1455	1
ID1582	6	ID1805	1
lmi-novel-miR-1	5	ID1684	1
lmi-novel-miR-2	5	ID1666	1
lmi-miR-281-5p	5	ID167	1
lmi-novel-miR-88	4	ID1134	1
ID730	4	ID868	1
ID23	4	ID1538	1
ID1454	4	ID1576	1
lmi-novel-miR-105	4	ID1621	1
IM23	4	lmi-miR-276-5p	1
lmi-novel-miR-30	3	lmi-novel-miR-109	1
lmi-novel-miR-31	3	lmi-novel-miR-110	1
lmi-novel-miR-42	3	ID1327	1
ID869	3	ID568	1
lmi-novel-miR-96	3	ID1326	1

MiRNA	Reads
ID1752	1
lmi-novel-miR-16	1
ID425	1
ID1333	1
ID1714	1
ID1589	1
ID593	1
ID1711	1
lmi-miR-307-5p	1
ID1682	1

Replicate 4 low haemolymph ecdysteroid level (N5 D3_1)

MiRNA	Reads	MiRNA	Reads
lmi-miR-276-3p	8783	lmi-novel-miR-115	52
lmi-miR-8-3p	3203	lmi-novel-miR-27	52
lmi-novel-miR-100	1287	ID50	51
lmi-novel-miR-106	1275	ID594	49
lmi-novel-miR-107	1275	lmi-novel-miR-118	46
lmi-novel-miR-14	557	lmi-novel-miR-119	46
lmi-miR-9a-5p	394	IM59	43
lmi-novel-miR-114	356	lmi-novel-miR-15	38
lmi-novel-miR-28	315	ID607	35
ID1725	300	ID603	34
lmi-novel-miR-121	291	lmi-novel-miR-102	33
lmi-novel-miR-112	284	lmi-novel-miR-103	33
lmi-novel-miR-80	194	lmi-novel-miR-104	33
lmi-novel-miR-81	194	lmi-novel-miR-77	31
lmi-novel-miR-82	194	ID604	30
lmi-novel-miR-47	146	lmi-novel-miR-58	28
lmi-novel-miR-50	143	lmi-novel-miR-65	28
lmi-novel-miR-51	143	lmi-novel-miR-66	28
lmi-novel-miR-116	130	lmi-novel-miR-113	28
lmi-novel-miR-117	130	lmi-novel-miR-87	27
ID1321	127	lmi-novel-miR-120	26
lmi-novel-miR-17	97	ID610	24
lmi-novel-miR-18	97	lmi-novel-miR-9	24
lmi-novel-miR-19	97	lmi-novel-miR-67	23
lmi-novel-miR-125	97	lmi-novel-miR-68	23
lmi-novel-miR-126	97	lmi-novel-miR-69	23
lmi-novel-miR-127	97	lmi-novel-miR-70	23
lmi-novel-miR-128	97	lmi-miR-307-3p	21
lmi-novel-miR-37	89	lmi-novel-miR-8	21
lmi-novel-miR-34	88	lmi-novel-miR-46	18
lmi-novel-miR-35	88	lmi-novel-miR-23	18
lmi-novel-miR-36	88	ID1728	17
lmi-novel-miR-10	79	lmi-novel-miR-38	16
lmi-novel-miR-111	79	lmi-novel-miR-39	16
lmi-novel-miR-71	76	lmi-novel-miR-40	16
lmi-novel-miR-72	76	lmi-novel-miR-48	16
lmi-novel-miR-20	66	lmi-novel-miR-5	16
lmi-novel-miR-21	66	lmi-novel-miR-6	16
lmi-novel-miR-22	66	lmi-miR-9a-3p	14
lmi-novel-miR-3	61	lmi-miR-10-5p	14
lmi-novel-miR-4	61	lmi-novel-miR-76	13
lmi-miR-8-5p	58	ID903	13
lmi-novel-miR-7	54	lmi-novel-miR-24	13
IM18	53	lmi-novel-miR-29	13

MiRNA	Reads	MiRNA	Reads
ID1726	12	lmi-novel-miR-43	2
ID1580	9	ID724	1
lmi-novel-miR-63	9	ID730	1
lmi-novel-miR-64	9	ID23	1
ID1281	8	lmi-novel-miR-105	1
lmi-novel-miR-88	8	IM23	1
lmi-novel-miR-30	8	lmi-novel-miR-42	1
lmi-novel-miR-31	8	lmi-novel-miR-96	1
lmi-novel-miR-25	7	lmi-novel-miR-97	1
lmi-novel-miR-45	7	lmi-novel-miR-98	1
ID1142	6	lmi-novel-miR-99	1
lmi-novel-miR-59	6	ID1764	1
lmi-novel-miR-52	6	lmi-miR-10-3p	1
lmi-novel-miR-53	6	lmi-miR-281-3p	1
lmi-novel-miR-60	6	ID735	1
lmi-novel-miR-61	6	ID864	1
lmi-novel-miR-78	6	ID1440	1
lmi-novel-miR-79	6	ID925	1
lmi-novel-miR-83	6	lmi-novel-miR-11	1
lmi-novel-miR-84	6	lmi-novel-miR-12	1
lmi-novel-miR-92	5	lmi-novel-miR-13	1
lmi-novel-miR-93	5	ID1668	1
lmi-novel-miR-129	5	ID1455	1
lmi-novel-miR-55-0	5	ID1805	1
lmi-novel-miR-54	5	ID1666	1
lmi-novel-miR-56	5	ID1134	1
lmi-novel-miR-57	5	ID868	1
lmi-novel-miR-90	5	ID1576	1
lmi-novel-miR-91	5	ID1621	1
ID170	4	lmi-miR-276-5p	1
lmi-novel-miR-86	4	lmi-novel-miR-109	1
ID592	4	lmi-novel-miR-110	1
lmi-novel-miR-1	4	ID1327	1
lmi-novel-miR-2	4	ID568	1
lmi-novel-miR-108-0	4	ID1326	1
lmi-novel-miR-89	4	ID1752	1
lmi-novel-miR-41	4	lmi-novel-miR-16	1
ID1582	3	ID1333	1
lmi-miR-281-5p	3	ID1714	1
ID1454	3	ID1589	1
ID869	3	ID1711	1
ID1095	3	lmi-miR-307-5p	1
lmi-novel-miR-94	3	ID1682	1
lmi-novel-miR-44	3	ID323	1
lmi-novel-miR-85	3	ID1795	1

MiRNA	Reads
ID1806	1
ID1330	1
ID424	1
lmi-novel-miR-122	1
lmi-novel-miR-123	1
lmi-novel-miR-124	1
ID1691	1
ID231	1
ID1802	1
ID893	1
ID877	1
ID1332	1
ID712	1
ID718	1
lmi-novel-miR-95	1
ID1794	1
ID863	1